Keele University

An *in vitro* investigation of the effects of factors secreted by mesenchymal stem cells on skin-wound healing

Merlin Nathaniel Mark Walter

Submitted for the degree of Doctor of Philosophy

October 2014

Keele University

SUBMISSION OF THESIS FOR A RESEARCH DEGREE

Degree for which thesis being submitted: Ph.D.

Title of thesis: An in vitro investigation of the effects of factors secreted by mesenchymal stem cells on skin-wound healing

Date of submission   Original registration date   30-07-2007

(Date of submission must comply with Regulation 2D)

Name of candidate   Merlin Nathaniel Mark Walter

Research Institute   ISTM

Name of Lead Supervisor   Dr. Eustace Johnson

DECLARATION by the candidate for a research degree

I certify that:

(a)   the decision to submit this thesis has been taken following consultation with, and having received advice from, my academic and (where appropriate) non-academic (e.g. industrial) supervisor(s)

(b)   The thesis being submitted for examination is my own account of my own research

(c)   My research has been conducted ethically. Where relevant a letter from the approving body confirming that ethical approval has been given has been bound in the thesis as an Annex

(d)   The data and results presented are the genuine data and results actually obtained by me during the conduct of the research

(e)   Where I have drawn on the work, ideas and results of others this has been appropriately acknowledged in the thesis

(f)   Where any collaboration has taken place with one or more other researchers, I have included within an 'Acknowledgments' section in the thesis a clear statement of their contributions, in line with the relevant statement in the Code of Practice (see Note overleaf).

(g)   The greater portion of the work described in the thesis has been undertaken subsequent to my registration for the higher degree for which I am submitting for examination

(h)   Where part of the work described in the thesis has previously been incorporated in another thesis submitted by me for a higher degree (if any), this has been identified and acknowledged in the thesis

(i)   The thesis submitted is within the required word limit as specified in the Regulations

Total words in submitted thesis (including the text and footnotes, but excluding references and appendices) 39000

Signature of candidate   …………………………………Date   …………………

I have read the thesis*/I have read part of the thesis*/I have not read the thesis*, and I am aware that the student intends to submit.

Signature of lead supervisor ………………………………   **Date   …………………**

Please print name...

Cc: Director of Postgraduate Research

Table of contents

Abstract

Mesenchymal stem cells (MSC) have been used clinically to treat a range of conditions, and have been shown to enhance skin wound healing *in vivo*. There is evidence suggesting that the beneficial effects of MSC transplantation may be mediated more through their paracrine activity than through their differentiation into mature cell types.

This thesis has sought to examine the effects of MSC secreted factors on dermal fibroblasts, keratinocytes, and endothelial cells, using an *in vitro* wound healing model. The results presented demonstrate that mesenchymal stem cell-conditioned culture medium (MSC-CM) enhances wound closure by dermal fibroblasts and keratinocytes through increased skin cell migration. MSC-CM was similarly shown to enhance wound closure by endothelial cells. The contents of MSC-CM were analysed by immunological techniques and mass spectrometry to reveal targets for further investigation. These included cytokines, notably interleukin-6 (IL-6), interleukin-8 (IL-8) and transforming growth factor-beta one (TGF-β1); and extracellular matrix (ECM) components, notably collagen type I, fibronectin and decorin. Examining these factors individually or in combination with each other or MSC-CM demonstrated differential and interdependent effects. Fibronectin was generally stimulatory to wound closure, whilst decorin was inhibitory. The cytokines studied had variable effects, e.g. TGF-β1 was stimulatory to fibroblast migration in combination with collagen type I, elicited no effect in combination with fibronectin, and was inhibitory to keratinocyte migration in both conditions.

This study has thereby progressed our understanding of how MSC secreted factors influence skin wound healing and suggests that further investigation of MSC activity is needed in order to inform the eventual clinical use of MSC to treat severe or chronic skin wounds. With further work, MSC-related therapy, using MSC transplantation or the delivery

of MSC secreted products, might provide a preferable alternative to current treatment strategies for these wounds, either in terms of patient benefit or clinical cost reduction.

<u>Acknowledgements</u>

I would like to thank;

Abbreviations

ANOVA	Analysis of variance
BMP	Bone morphogenic protein
BSE	Bovine spongiform encephalitis
CAM	Chorioallantoic membrane
CD	Cluster of differentiation
CHCA	Cyano-hydroxycinnamic acid
CM	Conditioned medium
COMP	Cartilage oligomeric matrix protein
DED	De-epidermalised dermis
DMEM	Dulbecco's Modified Eagle's Medium
DMSO	Dimethyl sulphoxide
DNA	Deoxyribonucleic acid
ECM	Extracellular matrix
EDTA	Ethylendiamine tetra-acetic acid
ELISA	Enzyme-linked immunosorbent sssay
FCS	Foetal calf serum
FISH	Fluorescence in situ hybridisation
GRO	Growth regulated oncogene
GM-CSF	Granulocyte-macrophage colony-stimulating factor
HGF	Hepatocyte growth factor
HSPG	Heparan sulphate proteoglycan
IFN	Interferon
IGF	Insulin-like growth factor
IGFBP	Insulin-like growth factor binding protein
IL	Interleukin
IPA	Isopropyl alcohol
ITS	Insulin Transferrin Selenium
KGF	keratinocyte growth factor
MALDI	Matrix-assisted laser desorption/ionization
MCP	Monocyte chemotactic protein
MAPK	Mitogen associated protein kinase
MRSA	Methicillin-resistant *Staphylococcus aureus*
MSC	Mesenchymal stem cell
MTS	Dimethylthiazol-yl-carboxymethoxyphenyl-sulfophenyl-tetrazolium
NHS	National Health Service
PBS	Phosphate buffered saline
PCR	Polymerase chain reaction
PDGF	Platelet-derived growth factor
PG	Proteoglycan
PGE	Prostaglandin-E
PHSRN	Proline-Histidine-Serine-Arginine-Asparagine
PPAR	Peroxisome proliferator-activated receptor

RANTES	Regulated upon activation, normal T-cell expressed, and secreted
RGD	Arginine-Glycine-Aspartic acid
RNA	Ribonucleic acid
SEM	Standard error of the mean
SLRP	Small leucine rich proteoglycan
SMA	Smooth muscle actin
SPARC	Secreted protein acidic and rich in cysteine
TFA	Trifluoroacetic acid
TGF	Transforming growth factor
TNF	Tumour necrosis factor
TOF	Time of flight
UV	Ultra-violet light
VEGF	Vascular endothelial growth factor

List of figures

List of tables

<u>Dedication</u>

This thesis is dedicated to my mother Susan Teresa Walter, my brother Kieran John Walter, and my friend Adam John Kesterton, without the support of whom I would never have been writing it in the first place, and to the memory of my father Christopher Mark Walter.

Chapter 1

Introduction

1.1 Skin structure and function.

The largest organ of the vertebrate body, skin is comprised of three layers, the epidermis, dermis and hypodermis, or subcutaneous layer (Stevens & Lowe 1997, Metcalfe & Ferguson 2007) (Figure 1.1). These layers contribute individually and in combination to skin function and maintenance. Skin provides barrier protection against chemicals, micro-organisms, and ultra-violet (UV) light (MacNeil 2007, Metcalfe & Ferguson 2007, Stevens & Lowe 1997), as well as protecting the body from mechanical damage (Metcalfe & Ferguson 2007), and also contributes to the maintenance of homeostasis by transducing external stimuli and effecting thermoregulatory actions via sweat glands, follicles and vasculature (Stevens & Lowe 1997).

Epidermis: The outermost of the three layers, the epidermis, is responsible for barrier function (Metcalfe & Ferguson 2007) and contributes to homeostasis. The epidermis is mostly cellular, composed mainly of keratinocytes (Hoath & Leahy 2003, Metcalfe & Ferguson 2007, Stevens & Lowe 1997) and organised into two principal strata: A basal layer, from which all keratinocytes of the epidermis are derived, and the stratum corneum, a layer of keratinizing cornifying cells which are displaced outwards and shed desquamously once terminally differentiated (Stevens & Lowe 1997). As well as keratinocytes the epidermis contains melanocytes and Langerhans cells (Hoath & Leahy 2003, Stevens & Lowe 1997), both interacting with local keratinocytes to form functional epidermal units (Hoath & Leahy 2003). The ratio of both melanocytes and Langerhans cells to nucleated keratinocytes is maintained at a markedly constant level (1:36 ratio of melanocytes: keratinocytes and 1:53 Langerhans cells: keratinocytes) (Hoath & Leahy 2003). Melanocytes are dendritic cells responsible for skin

pigmentation and protection from damage from UV radiation (Stevens & Lowe 1997), by interacting with adjacent keratinocytes to comprise epidermal melanin units of one melanocyte and ≈36 viable keratinocytes (Hoath & Leahy 2003). Langerhans cells are responsible for the immune surveillance of the other cells of the epidermis (Hoath & Leahy 2003). The extracellular matrix of the epidermis consists of small amounts of intercellular proteoglycans, and constitutes a vastly smaller portion of the epidermis than the cellular components. Between the epidermis and underlying dermis is the dermal-epidermal junction, or basement membrane zone, responsible for the mechanical support of the epidermis and the adherence between the two layers, as well as maintaining the compartmentalisation of the skin strata). The basement membrane zone is comprised of the plasma membrane of the basal keratinocytes, and the Lamina Lucida and Lamina Densa, and is permeated by anchoring fibrils secreted by epidermal keratinocytes either terminating in the Lamina Densa, or extending into the dermis (Stevens & Lowe 1997).

Dermis and hypodermis: The dermis is the thickest layer of the skin, and makes up the bulk of its mass. It is much less cellular than the epidermis, consisting mainly of extracellular matrix components; collagen and elastic fibres embedded in proteoglycans and glycoproteins (Metcalfe & Ferguson 2007). Eighty five percent to ninety percent of the collagen present in the dermis is type I collagen, with type III (8%-11%), type V (2%-4%), and very small amounts of type VI, type XII, type XIII and type XIV making up the rest. The major proteoglycan (PG) component of the dermal extracellular matrix is decorin, a Small Leucine Rich Proteoglycan (SLRP). Another SLRP, biglycan, is also present in smaller amounts. In addition, a network of elastic fibres within the dermis contributes to skin resilience and elasticity. The cellular component of the dermis is comprised mostly of fibroblasts (Sorrell & Caplan

2004). These cells are responsible for the formation of the extracellular matrix which comprises the larger portion of the skin, and the regulation of the skin physiology through communication with other cell types. Fibroblasts also differentiate in response to injury, adopting a migratory phonotype (myofibroblast). Myofibroblasts contribute to the closure of cutaneous wounds by contracting the wound area. As well as the fibroblast population the dermis is inhabited by neural and vascular cells that make up the nervous and circulatory system supporting the skin. Fibroblasts can be divided spatially and physiologically into three distinct subpopulations. Two of these form the papillary and reticular layers of the dermis, whilst the third is associated specifically with hair follicles embedded within the dermal papillary region (Sorrell & Caplan, 2004). The papillary dermis is that portion of the dermal layer directly adjacent to the basement membrane (Figure 1.2), and is involved in the sustenance of the epidermis, containing the neural and vascular components required to maintain viable keratinocytes. These components are extended towards the basement membrane zone within the dermal papillae - folds in the papillary surface that increase the surface area available for delivery of soluble molecules into the epidermis. The extracellular matrix of papillary dermal tissue is made up of thin, poorly organised bundles of primarily type I and type III collagens, and large quantities of the proteoglycan, decorin. A vascular plexus, the rete subpapillaire, lies between the papillary dermis and the reticular dermis. The extracellular matrix of the reticular layer is made up of thicker and more organised collagen bundles than the papillary dermis, and has a higher proportion of type III to type I collagen (Sorrell & Caplan, 2004). This reticular layer extends from below the rete subpapillaire to another vascular plexus, the rete cutaneum, which marks the lower limit of the dermis and lies adjacent to the hypodermal layer (Sorrell & Caplan 2004). The hypodermis,

or subcutis, is made up of adipose tissue and loose connective tissues, and contains the major nerves and blood vessels from which the overlying layers are supplied. The hypodermis is permeated by fibrous bands growing out from the dermis, dividing the hypodermal layer into lobules and anchoring the skin by extending into the underlying periosteum or facia.
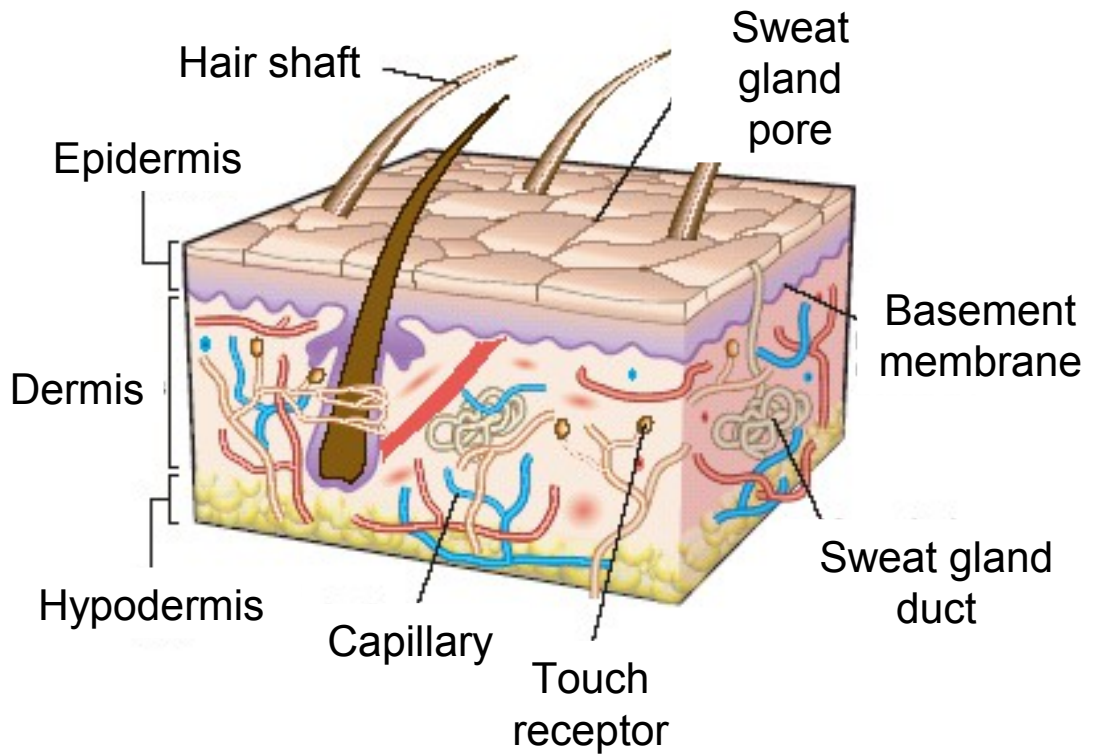
Figure 1.1. The structure of human skin. The horizontal organisation of the dermal, epidermal, and subcutaneous layers comprising human skin, as well as major skin appendages (*adapted from MacNeil, 2007*).
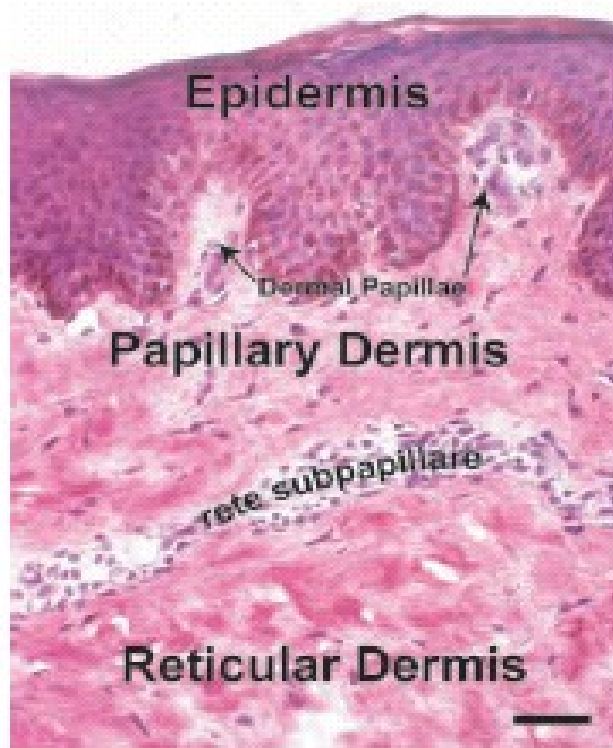
Figure 1.2. The Papillary and Reticular dermis. The organisation of the dermal lamina, divided by the rete subpapillaire, and also dermal papillae extending into the epidermis. Bar = 45μm. (*Image taken from Sorrell and Caplan, 2004).*

1.2 Skin damage and repair.

Skin damage can occur as a result of burns, cuts/incisions, abrasions, ulcers, and various other causes, to varying degrees of severity. Any breach in the skin can compromise its barrier function and expose the body's tissues to microbial infections and mechanical damage, and affect the maintenance of homeostasis if left unrepaired. The process of tissue regeneration and repair is generally considered in terms of three overlapping phases; inflammation, proliferation, and remodelling (Figure 1.3). These processes all require complex interactions between the dermal and epidermal cells, the extracellular matrix components and the nervous and vascular components of the damaged and surrounding skin (Yamada and Clark, 1996, Harding *et al,* 2002).

Inflammation; Immediately following a common or minor skin injury, thrombus formation maintains haemostasis and triggers an inflammatory response by releasing vasodilators from platelets within the clot, and triggering complement activation (Metcalfe & Ferguson 2007). Recruited on initiation of an inflammatory response, neutrophils are the initial immune entity responsible for removal of foreign material and potential pathogens from the wound site, by phagocytosis and the secretion of extracellular enzymes, until macrophages replace them in this role (Cooper *et al* 1994). Macrophages also initiate progression to the next phase of repair, the proliferation stage, by secreting the various growth factors and cytokines that recruit keratinocytes and fibroblasts to the wound site.

Proliferation: Keratinocytes migrate into the wound area from the basal population around the wound edge before contact inhibition triggers their resumption of a basal phenotype, and subsequent differentiation into stratified squamous keratinizing

epidermis, reepithelialising the wound and restoring the barrier function of the damaged skin. Fibroblasts are of major significance in cutaneous wound healing as they contribute to wound contraction, secrete new extracellular matrix materials and produce matrix metalloproteinases, enzymes required to remodel the extracellular matrix. Initially migrating to the site along with sprouting vasculature, fibroblasts differentiate into specialised myofibroblast cells (Sorrell & Caplan 2004). These cells respond to macrophage derived factors to provide a provisional wound matrix made up of fibronectin and hyaluronan, and provide the motive force required for skin wound contraction. These myofibroblasts die off by apoptosis and are replaced by a second wave of fibroblasts from the surrounding dermis.

Remodelling: Fibroblasts produce new extracellular matrix material, and also matrix metalloproteinases, a group of zinc dependant endopeptidases that cleave the extracellular matrix material around the margins of the wound site. Remodelling follows wound closure, and can take place over months or years as matrix metalloproteinases cleave old collagen and new collagen is formed (Harding *et al,* 2002) (Bayat *et al,* 2003)). The formation of an acellular collagenous scar, combined with wound contraction and re-epithelialisation leads to the complete closure of the wound (Sorrell & Caplan 2004).
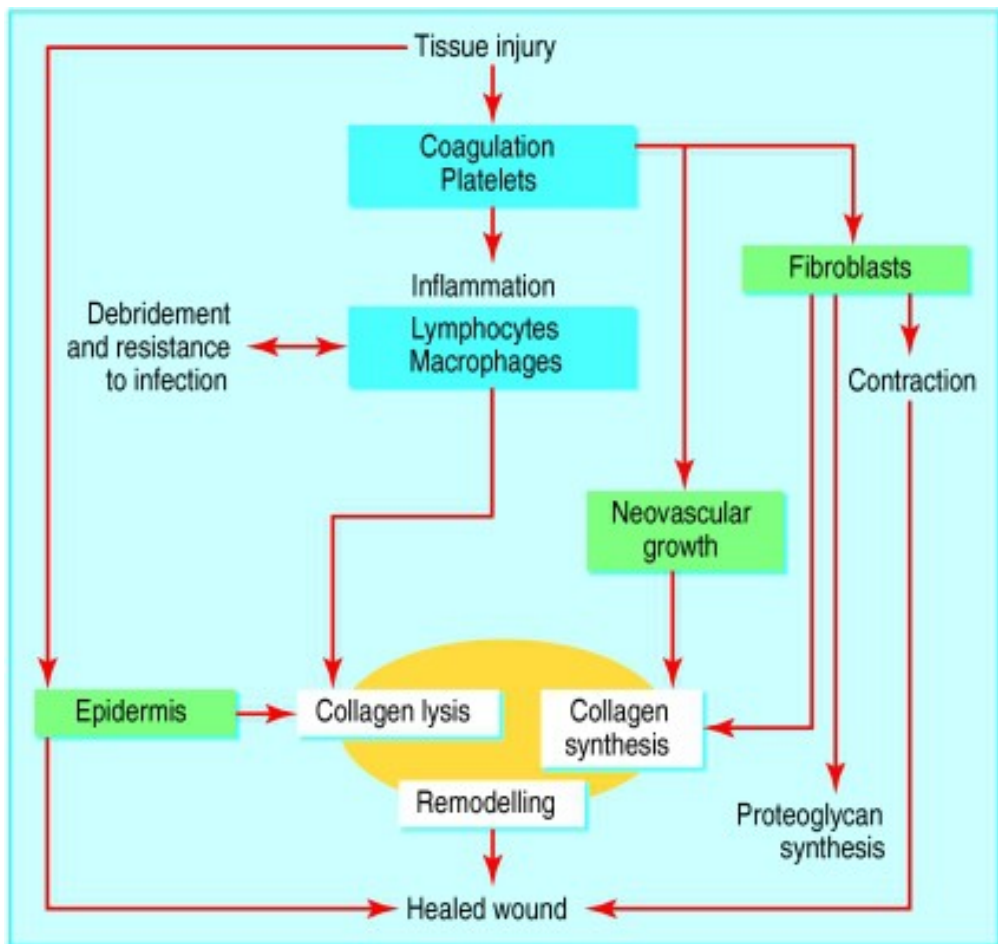
Figure 1.3. Phases of wound healing. Numerous processes contribute to cutaneous wound healing including the actions of both circulatory and local cells. These can be broadly divided into three overlapping phases as represented above: Inflammation in blue, Proliferation in green and Remodelling in yellow (image taken from *Harding et al 2002*).

Scarring: Scarring can manifest as multiple varieties including normal fine lines, widespread scars, contracting scars, and atrophic, hypertrophic or keloid scar types (Figure 1.4) (Bayat *et al,* 2003). Often the balance between new and old collagen determines the final characteristics of the scar. Wide spread scars are flat pale scars occurring when fine lines become stretched or widened, often occurring after knee or shoulder surgery. The abdominal striae seen after pregnancy are a variant of widespread scar in which there is damage to the dermal and hypodermal layers, but without breach in the epidermis. Atrophic scars are flat and depressed, often small and rounded, usually occurring due to acne or chickenpox. Hypertrophic and keloid scars are characterised by being raised above the surrounding skin. Hypertrophic scars are associated with burns on the trunk and extremities and are often red, itchy and inflamed, and sometimes even painful. Keloid scars are invasive, spreading beyond the original wound into surrounding skin. Keloid scars do not spontaneously regress and have a 50%-80% chance of recurrence after excision. These tend to occur in the ear lobe following piercing, the deltoid after vaccination and on the sternum after acne, chickenpox, or trauma/surgery. Predisposing factors to the occurrence of keloid scars include age, with 10-30 year-olds being predominantly afflicted, and race, with dark skinned populations being more prone. Puberty and pregnancy are also associated with increased incidence of keloid scarring. Interestingly, keloid scars are a uniquely human condition (Bayat*, et al,* 2003). Scar contractures can occur when a scar is formed perpendicular to skin creases or joints (Figure 1.5). Contracture generally takes place before the scar has matured, and is common following severe burns across joints. These scars can be hypertrophic, and are often disabling and/or dysfunctional.
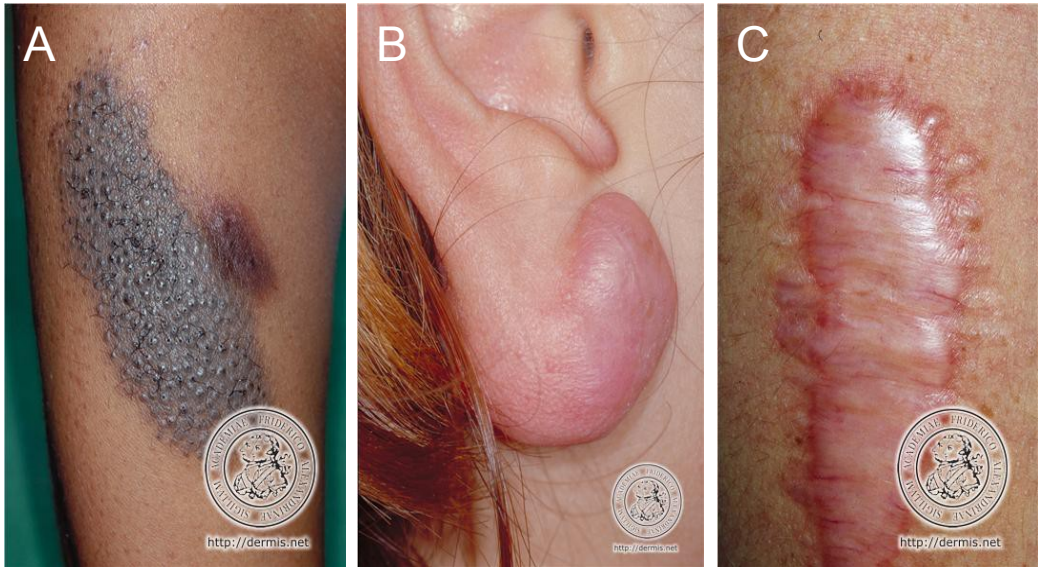
Figure 1.4. Scar types. Examples of abnormal scarring: (a) Atrophic, (b) Keloid, and (c) Hypertrophic scars (*images taken from www.dermis.net*).

Figure 1.5. Scar contracture. An example of scar contracture across the forearm and wrist following a burn injury (*image taken from Bayat et al, 2003*).

Foetal wound healing: During the first third of the gestational period, damage to foetal skin results in scarless healing and the complete regeneration of functional skin, indistinguishable from that present prior to being damaged, including regularly distributed appendages and appropriate vasculature (reviewed in Metcalfe & Ferguson 2007, Ferguson and O'Kane, 2004). Studies have shown this process of tissue regeneration to be dependant upon the degree of differentiation of the skin tissues and the magnitude of the inflammatory response. The correct deposition of collagens and hyaluronan is essential to the absence of scarring in foetal wound repair and is regulated by the cytokine environment of the wound site (Whitby & Ferguson 1991a,b, Lindblad, 1998). The lack of fibrin clots and platelet degranulation, and the significantly reduced inflammatory responses that characterise foetal regeneration result in a growth factor profile markedly different from that found in adult wound repair, featuring reduced levels of growth factors released by platelets and inflammatory cells, such as TGF- β1, TGF-β2 and platelet derived growth factor (PDGF), and elevated TGF- β3. Exogenous addition of TGF-β3 or the neutralisation of TGF-β1, TGF-β2, PDGF etc have been shown experimentally to reduce or eliminate scarring in adult rodents (Shah *et al*, 1994, Shah *et al*, 1995).

Factors influencing wound healing.

Growth factors/cytokines

Cell signalling molecules such as cytokines and growth factors are essential mediators of wound healing, necessary for the initiation of each phase of the wound healing response and its orderly resolution as one phase progresses to the next. These signalling molecules recruit circulating cells such as neutrophils to the wound site, coordinate the proliferation of cells needed for effective reepithelialisation and neo-angiogenesis, and stimulate the synthesis of both the matrix metalloproteinases (MMPs) and also new extracellular matrix components required for the remodelling of repaired tissue.

Platelet-derived growth factor (PDGF). Released by platelets and secreted by activated macrophages, PDGF is an essential mediator the early phases of the wound healing response acting as a chemoattractant for neutrophils and monocytes (Werner and Grose, 2003). PDGF also influences the later stages of wound healing, recruiting fibroblasts to the wound site and stimulating the production of new extracellular matrix proteins, as well as promoting myofibroblast differentiation leading to the contraction of the wound area (Heldin and Westermark, 1999). Additionally PDGF has a role in the inhibition of apoptosis required for effective progression through the sequential phases of wound healing (Ching *et al.,* 2011, Greenhalgh, 1998).

Fibroblast growth factors (FGF). FGF is expressed strongly in the central area of skin wounds, decreasing towards the periphery and almost absent in uninjured skin (Gu *et al.,* 2000). FGFs have a broad pectrum of effects (Werner and Grose, 2003, Ching *et al.,* 2011), stimulating both the proliferation and migration of numerous cell types involved in wound healing and angiogenesis including keratinocytes, fibroblasts and

endothelial cells (Werner and Grose 2003, Nissen *et al.,* 1996, Montesano *et al.,* 1986). Additionally, members of the FGF protein family have been demonstrated to contribute to the macrophage activation and the production of new ECM (Ching *et al.,* 2011, Greenhalgh, 1996). Keratinocyte growth factors (KGF) are members of the FGF family that promote reepithelialisation by stimulating the migration and proliferation of keratinocytes, as well as stimulation of the formation of granulation tissue and the deposition of collagen within the wound (Soler *et al.,* 1999, Ching *et al.,* 2011, Xia *et al.,* 1999). KGF also plays a role in protecting cells from the harmful effects of oxidative stress. In the earliest stages of wound healing, the disruption of normal blood supply through damage to blood vessels and vasoconstriction results in localised hypoxia and an increase in reactive oxygen species (ROS) within the wound environment (Gorlach *et al.,* 2000, Schremi *et al.,* 2010). In normal wound healing this increase results in the release of enzymes capable of detoxifying ROS, mediated by the actions of appropriate cytokines. Keratinocyte growth factor stimulates the expression of the intracellular enzyme peroxiredoxin-6, protecting keratinocytes from ROS-induced oxidative damage (Kumin *et al.,* 2007). The impairment of this protective response is associated with chronic wounds, with the resulting imbalance of oxidants and antioxidants causing the healing process to stall in a persistent state of inflammation (Soneja *et al.,* 2005, Schafer and Werner, 2008).

Epidermal growth factors (EGF) EGFs are another family of mitogenic factors involved in wound healing. Expressed by macrophages, epidermal keratinocytes and hair follicle epithelial cells (Rappolee *et al.,* 1988, Cribbs *et al.,* 2002), EGF stimulate the proliferation of epithelial and endothelial cells as well as accelerating reepithelialisation and increasing the tensile strength of healed dermis (Alemdaroglu *et al.,* 2006, Alemdaroglu *et al.,* 2008, Brown *et al.,* 1989).

Vascular endothelial growth factor (VEGF). VEGF are cytokine mediators of angiogenesis that stimulate the proliferation and migration of endothelial cells (Nissen *et al.,* 1998, Papapetropoulos *et al.,* 2009), as well as promoting reepithelialisation and collagen deposition with in the wound (Bao *et al.,* 2009). There is evidence to suggest that the application of exogenous VEGF through a variety of means results in the acceleration or enhancement of wound healing (Romano *et al.,* 2002, Dedato *et al.,* 2002, Galeano *et al.,* 2003, Muhlhauser *et al.,* 1995).

Insulin like growth factor (IGF). IGF has well characterised systemic anabolic effects and contributes to wound healing by promoting the migration of fibroblasts and keratinocytes as well as inhibiting apoptosis and stimulating the deposition of new ECM (Martin 1997, Steenfos 1994, Dasu *et al.,* 2003, Spies *et al.,* 2001). IGF also mediates the production of pro and anti-inflammatory cytokines (Ching *et al.,* 2011).

Transforming Growth Factor-Beta (TGF-β). The mammalian TGF-β family consists of three structurally and functionally similar isoforms: TGF-β1, TGF-β2 and TGF-β3, and affects every phase of the wound healing process. TGF-β stimulates the deposition of collagen and other matrix components by fibroblasts, inhibits collagenase, enhances angiogenesis, and is chemotactic for fibroblasts, monocytes and macrophages. TGF-β induces alpha-smooth muscle actin expression in fibroblasts, providing the motive force for contraction of the wound margins (Barnard *et al.,* 1990, Sporn and Roberts 1992, Desmouliere *et al.,* 1993). Additionally TGF-β, and specifically the relative expression of the different isoforms, is strongly implicated in the process of scar formation (Shah *et al.,* 1994, Shah *et al.,* 1995).

Additional factors. Further growth factors have been experimentally implicated in the process of cutaneous wound healing. Exogenous nerve growth factor (NGF) has been

shown to accelerate the healing of chronic wounds in both mice (Li *et al.,* 1980, Matsuda *et al.,* 1998) and humans (Bernabei *et al.,* 1999). Hepatocyte growth factor (HGF) stimulates migration, proliferation (Matsumoto *et al.,* 1991), and matrix metalloproteinase (Dunsmore *et al.,* 1996) production by keratinocytes, as well as neo-angiogenesis (Bussolino *et al.,* 1992), and so has been suggested to play a role in cutaneous wound repair (Werner and Grose 2002). BMP-6 may play a role in the reepithelialisation of cutaneous wounds. BMP-6 is highly expressed in the keratinocytes at the leading edge of the wound margin as well as in granulation tissue fibroblasts, before accumulating throughout the supra-basal layers of the newly formed epidermis upon completion of wound closure (Kaiser *et al.,* 1998). BMP-6 has also been shown to induce keratinocyte differentiation *in vitro* (D'Souza *et al.,* 2001, McDonnell *et al.,* 2001).

Extracellular matrix components

The behaviour of cells both *in vitro* and *in vivo* is influenced by the nature and composition of the local extracellular matrix (ECM). Specifically relevant to the investigations presented within this thesis are three ECM proteins: Type I collagen, fibronectin and decorin.

Collagen I. Collagens are the most abundant fibrous proteins in ECM. The most common of these, and the most common protein found in the human body (Di Lullo *et al.,* 2002), Type I collagen is a heterotrimeric ECM protein comprised of three alpha chains (two α1 chains and one α2) in a triple helix conformation (Gordon and Hahn 2010). The polypeptide precursors to these chains are synthesised by fibroblasts, as well as osteoblasts and odontoblasts, and trimerise within the

endoplasmic reticulum before being secreted into the extracellular space. Within the extracellular space multiple triple helices associate in a 'quarter-stagger' pattern to form thick bundles or fibrils which become the major component of the ECM found in skin, tendon, vascular ligature, organs, and the organic portion of bone. (Ghosh 2002, Myllyharju and Kivirikko 2001, Byers 2000).

Fibronectin. Usually existing as a dimer of two subunits of approximately 250 kDa, fibronectin mediates a wide variety of cellular interactions with the extracellular matrix (ECM) and plays important roles in cell adhesion, migration, growth and differentiation (Pankov and Yamada 2002). Each of the two subunits is made up of three different repeating domains that between them comprise 90% of the gene sequence (Patel *et al.,* 1987). Multiple forms of the protein can arise from alternative splicing of pre-mRNA (French-Constant 1995, Kosmehl *et al.,* 1996). Of these variants, the most significant sub-division is between the soluble fibronectin abundant within plasma and other bodily fluids and the insoluble fibronectin of the ECM (Pankov and Yamada 2002). Fibronectin is involved in a broad range of biological processes mediated by its ability to ligate numerous integrin receptors (Plow *et al.,* 2000), binding to a number of biologically important molecules including heparin, collagen and fibrin (Yamada and Clark 1996, Pankov and Yamada, 2002) and its aggregation into fibrils (Geiger *et al.,* 2001).

Decorin. Decorin is a small proteoglycan comprised of a leucine-rich core protein (approximately 40 kDa) and associated dermatan sulphate/chondroitin sulphate side chains (Heinegard and Oldberg, 1989). Decorin associates with other protein components of the ECM including fibronectin and collagen types I and II (Hardingham and Fosang, 1992), modulating the formation of collagen fibres (Scott and Haigh, 1988), and also sequesters TGF-β effectively neutralising the effects of the

growth factor (Markmann et al., 2000). As TGF-β stimulates the synthesis of decorin core protein and its glycosaminoglycan side chain, the resulting inhibition of growth factor function suggests a role for decorin in the negative feedback control of TGF-β (Ruoslahti and Yamaguchi 1991).

Cytoskeletal biology and cell migration

The directional migration of cells occurs in response to a variety of extracellular stimuli including gradients in the concentration of growth factors and cytokines (chemokines), mechanical forces, and extracellular matrix composition. Driven by the polymerisation of actin filaments, protrusions of the cell membrane extend in the direction of migration and are subsequently stabilised by adhesions linking the actin cytoskeleton of the cell to the underlying ECM. The contraction of actomyosin generates a mechanical force upon the cell whilst simultaneously stimulating the disassembly of adhesions towards the rear of the cell, resulting in a forward motion (Kaverina and Straube, 2011).

Cytoskeletal components. The cytoskeleton of eukaryotic cells, required to provide structure and shape to the cell membrane as well as the apparatus for cell migration and division, is mainly comprised of three types of structural filaments. Actin filaments, the finest of the cytoskeletal structures, are made up of actin polymers organised into polarised molecules possessing fast-growing 'barbed-ends' and slow-growing 'pointed-ends'. (Fuchs and Cleveland, 1998) The difference between the rates of growth between these ends generates a motive force utilising energy provided by ATP hydrolysis, transporting the filament in the direction of the 'barbed-end'. Intermediate filaments are a larger component of the cellular cytoskeleton involved in the maintenance of the three dimensional shape and support of the cell membrane as

well as anchoring various organelles within the cytoplasm. These can be made up of a variety of protein components, such as vimentin, common to mesenchymal lineage cells, keratins that make up intermediate filaments in the cytoplasm of epithelial cells, or lamins that provide structure within the nucleus. Microtubules, polymers of dimeric α and β tubulin, are the largest filaments in the cytoskeleton. These hollow tube structures are highly polarised, similar to actin filaments, with a stable (-) end capped by a third tubulin isotype (γ-tubulin) and dynamic (+) end capable of GTP/GDP dependent growth and shrinkage in response to the local concentrations of soluble α and β tubulin (Kaverina and Straube, 2011, Fuchs and Cleveland, 1998).

Cytoskeletal changes in migrating cells. The polymerisation of actin filaments towards the leading edge of a migrating cell results in the extensions of the cell membrane termed lamellipodia (broad 'sheet-like' protusions) or filopodia (narrow 'spike-like' protrusions) (Pollard and Borisy, 2003). Cells express a range of surface adhesion receptors, of which the best characterised are the integrin family receptors. Integrin extracellular domains bind to specific sequence motifs present in ECM proteins such as fibronectin and collagen. The binding of integrins to these extracellular ligands induces a conformational change that results in their attachment to the actin cytoskeleton (Puklin-Faucher and Sheetz, 2009, Vicente-Manzanares *et al.,* 2009, Hynes 2002).

The initial adhesions formed between the cellular cytoskeleton at the leading edge of lamellipodia and the ECM are small and relatively short lived 'nascent' adhesions that will persist for approximately a minute before either breaking down or maturing to form larger points of adhesion termed 'focal complexes'. These focal complexes exist further away from the leading edge of the protruding membrane than the nascent adhesions, and will persist for longer before potentially maturing further into larger

focal adhesions. The focal adhesions associate with the ends of large actin bundles extending towards the centre and rear of the cytoplasmic body of the cell. As traction forces move the cell forwards, the rearmost focal adhesions are disassembled (Zimerman *et al.,* 2004, Parsons *et al.,* 2010).

The breakdown of adhesions between the cytoskeleton and the ECM occurs both towards the rear of the cell and at those areas of lamellipodia undergoing retraction, in a tension-dependent manner, from the periphery of the adhesion inwards towards the centre resulting in the eventual dispersal of the adhesion structures (Broussard *et al.,* 2008, Ballestrem *et al.,* 2001).

1.3 Chronic wounds and impaired repair.

Chronic or non-healing wounds occur when the normal processes of tissue regeneration fail to achieve closure re-epithelialisation of the damaged skin, instead appearing to become arrested in a state of prolonged inflammation. This can occur as a result of foreign bodies present in the wound site, ischemia, infection, or tissue maceration. Common chronic wounds include diabetic leg and foot ulcers, decubitus ulcers (pressure sores) and venous ulcers. Malnutrition, advanced age, impaired renal function and diabetes are all potential contributing factors to the development of a chronic wound, as well as reduced growth factor expression and imbalance in proteinases and proteinase inhibitors (Harding *et al*, 2002). Effects of platelet derived growth factor, basic fibroblast growth factor, epidermal growth factor, vascular endothelial growth factor and TGF-β have all been shown to be reduced in chronic ulcers , and it is thought that they may be trapped by extracellular matrix molecules or excessively degraded by proteases involved in matrix remodelling. Studies have shown reduced levels of matrix metalloproteinase 9 and elevated matrix metalloproteinase 2 in human diabetic chronic wound fluid compared to fluid from acute wounds (). These proteinase enzymes are thought to contribute to the degradation of the growth factors involved in normal tissue regeneration and to cause excessive degradation of the extracellular matrix, resulting in non-closure. Vascular endothelial growth factor has been shown to exhibit increased levels of expression in chronic wounds, but suffer rapid degradation due to the increased proteolytic activity associated with the wound environment. This impairs angiogenesis and results in the absence of new capillaries, a characteristic feature of venous, diabetic, and decubitus ulcers (Lauer *et al,* 2000). As the formation of new vasculature is essential for the

formation of granulation tissue, the breakdown of vascular endothelial growth factor due to increased protease activity may be a direct cause of the failure to heal chronic wounds. Age related senescence in dermal fibroblasts might also contribute to the development of chronic wounds, by reducing the degree of the cellular response to growth factors (Agren *et al,* 1999, Hasan *et al,* 1997, Stanley *et al,* 1997). The effect of these wounds on the quality of life for those afflicted can be severe and often debilitating, due to the intense pain resulting from the damage to tissues and nerve cells. Estimates suggest that up to 63% of chronic wound patients may suffer from depression as a result of their ailment.

Infection of chronic wounds: Infection is another important aspect of non-healing wounds. The compromised barrier function of the damaged epidermis exposes the tissue to bacterial colonisation, and prior to debridement any necrotic material present provides an ideal growth medium for bacteria. Despite prevention strategies such as surgical removal of necrotic tissue and cleansing the wound with saline, chronic wounds tend to become infected, often through contact with surrounding skin, the local environment and healthcare providers, and endogenous patient sources. Secondary bacteraemia and septicaemia are potential complications of these infections and are both associated with increased mortality of chronic wound patients. Organisms known to infect chronic wounds include *Staphylococcus aureus* (including MRSA), Pseudomonas species such as *Pseudomonas aeruginosa*, β-haemolytic streptococci, vancomycin-resistant enterococci as well as Gram negative coliforms and anaerobes. Most chronic wound infections progress through three characteristic stages: colonisation, critical colonisation, and infection. Colonisation is thought to begin with aerobic species, Staphylococci, *Pseudomonas aeruginosa* and β-haemolytic streptococci, with these species being predominant in wounds less than

one month old. Over time, as the ulcer fails to heal, the spectrum of organisms broadens, and Gram negative species also become established. Critical colonisation follows, causing increased friability and drainage of the wound, and contributing to the degradation of granulation tissue, hindering tissue regeneration. Some of the organisms above may produce a biofilm on the wound bed, protecting themselves from immune detection and challenge. Once the host immune response is overcome full infection ensues, leading to erythema, increased tissue damage and further friability, as well as purulent drainage, these signs sometimes spreading beyond wound margins in deep infections. These deep infections can lead to increased wound size and secondary ulceration, and in sufficiently severe or long term ulcers can extend to the bone, causing osteomyelitis. This is particularly common in diabetic ulcer patients. Infections of this nature are treated with both topical and systemic antibiotics as necessary (Reviewed in Frank *et al*, 2005).

Pressure ulcers: Pressure ulcers are an area of localised damage to the skin and underlying tissue, caused by shear forces, pressure, and friction, over prolonged periods of time resulting in ischemia and reperfusion. This leads to necrosis of muscle, subcutaneous tissue and of the dermis and epidermis. Pressure ulcers are a significant cause of increased morbidity and mortality in elderly patients, and are commonly associated with spinal injuries as well as impaired sensation and mobility. The prevalence of pressure ulcers in hospitals is between 1% and 5%, rising to up to 8% amongst patients confined to bed or a wheelchair for just one week. Amongst spinal injury patients pressure ulcer incidence lies between 20% and 30%, and can be as high as 70% in elderly patients suffering orthopaedic problems. Pressure ulcers in elderly patients are associated with a five-fold increase in mortality. The annual cost to the NHS of treating these wounds has been estimated to be anywhere between

£180million and almost £2billion (Grey *et al*, 2006). Pressure ulcers occur most often upon areas of the body where prolonged pressure is common, and will usually centre over bony prominences, where the effects of the body's weight, in terms of pressure, friction and shear force generated, are most profound (Figure 1.6) or over points of prolonged contact between a wheelchair and wheelchair user (Figure 1.7). It has been suggested that pressure ulcers originate within the muscle rather than the skin, as muscle is softer and more vulnerable to the ischemia and reperfusion related damage responsible for the tissue death that leads to ulcer formation. As muscle requires more oxygen than skin it seems likely that muscle would suffer greater damage from the occlusion of capillaries caused by prolonged pressure (Consortium for spinal cord medicine, 2007, Grey *et al*, 2006, Reddy e*t al*, 2006).

Pressure ulcer grading: Pressure ulcers are graded from I to IV according to presentation, giving an indication of the severity of the wound (Figure 1.8), although they do not progress sequentially from grade I to IV, nor necessarily heal in the reverse order (Consortium for spinal cord medicine, 2007, Grey *et al*, 2006). Consequences of pressure ulcers include the prolongation of rehabilitation following injury, severe pain, and impaired psychological and social well being, as well as potentially giving rise to local and systemic infections, septicaemia, bacteraemia and osteomyelitis (Grey *et al*, 2006). In severe cases these infections can necessitate amputation of ulcerated limbs, leading to impaired mobility, with social and psychological implications and reduced quality of life for patients.
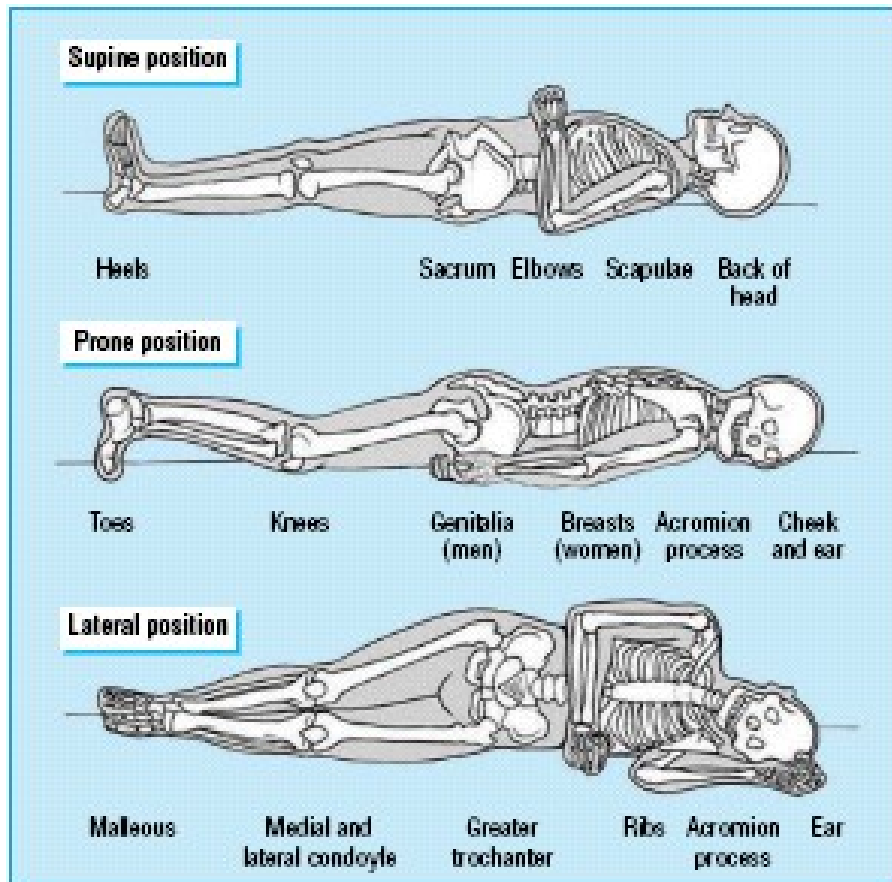
Figure 1.6. Areas of the body commonly associated with pressure ulcer incidence. Bony prominences and areas of prolonged contact in different positions contributing to pressure ulceration (*Image taken from Grey et al 2006).*
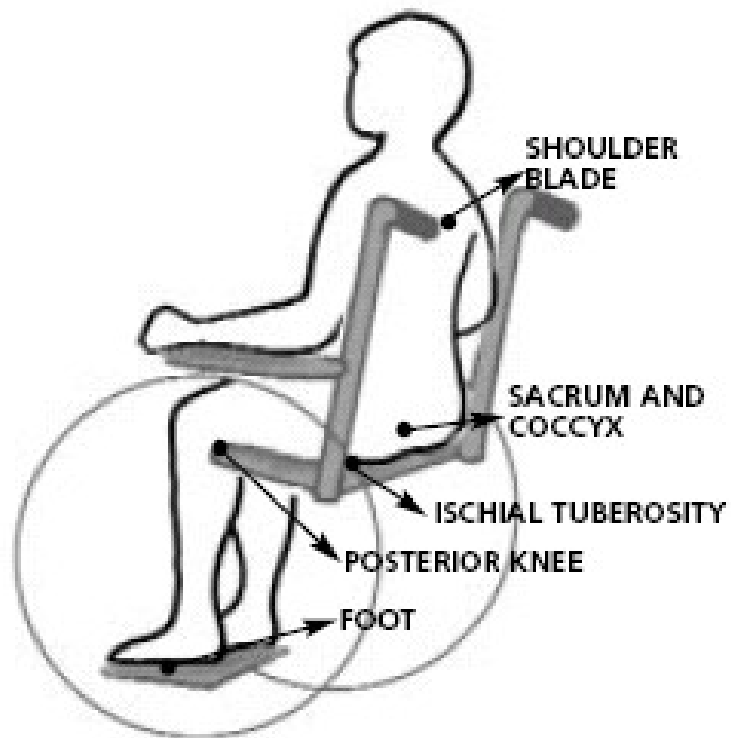
Figure 1.7. Areas commonly associated with pressure ulcer incidence in wheelchair users. Areas of prolonged contact between patient and wheelchair, contributing to pressure ulceration (*Consortium for spinal cord medicine, Clinical Practical Guidelines, 2007*).
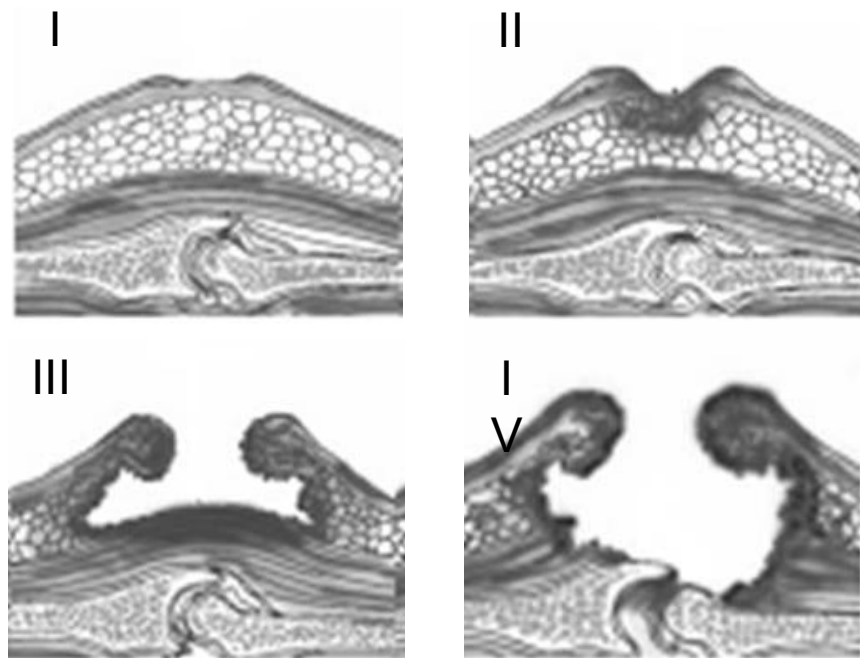
Figure 1.8. Classification of pressure ulcers by grade.

I: Observable difference in intact skin, potentially including temperature, redness, pain, itching or tissue consistency.

II: Partial-thickness skin loss, involving epidermis, dermis or both, and presenting superficially as an abrasion or blister.

III: Full-thickness skin loss, and damage to or necrosis of underlying tissue, extending down to but not through the underlying facia.

IV: Extensive destruction, tissue necrosis, or damage to muscle, bone or supporting structures, with or without full-thickness skin loss. (*Adapted from Consortium for spinal cord medicine, Clinical Practical Guidelines, 2007*)

Treatment of pressure ulcers: Currently much of pressure ulcer care is focused on the prevention of ulcer formation. Recommended prevention strategies are based around regular skin inspections, focused on but not confined to the areas most likely to develop pressure ulcers, (Ischii, Sacrum, Coccyx, Trochanters, Heels, Etc) and on management of pressure upon these areas. Regular turning of patients confined to bed is essential to relieve built up pressure, especially over bony prominences, and it is recommended that in moving patients care staff endeavour to avoid stretching or folding skin, or inducing shear forces whilst moving patients. Pressure reducing support surfaces are available to protect soft tissues from injury, and care should be taken whilst positioning immobile patients, avoiding loads upon the trochanter, and contact between knees and ankles if lying in the lateral position. In some cases, often with patients considered to be high risk, or when contact between commonly afflicted areas and support surfaces is unavoidable, Dynamic mattresses and overlays can be used to provided cyclical pressure relief. Moisture accumulation at the skin-support surface interface is also to be avoided. Individually prescribed wheelchairs with pressure reducing seating systems can reduce pressure ulcer incidence in wheelchair users. Where feasible it is recommended to have an ongoing exercise regime for patients to maintain skin and muscle integrity and to avoid atrophy. Appropriate nutrition is also an important factor in pressure ulcer prevention, and aggressive nutritional support may be required for nutritionally compromised patients. Once developed, the current methods for pressure ulcer treatment and care are somewhat limited. Regular wound cleansing is required, using saline and avoiding antiseptics. Care must be taken when cleaning and irrigating to avoid causing further trauma to the wound site. Surgical debridement of eschar and necrotic or devitalised tissue

should be undertaken where appropriate to the ulcer's progression and the patient's condition/goals. Appropriate dressing is also necessary to pressure ulcer care. Dressing should keep the wound bed continually moist and the surrounding intact skin dry. Materials that macerate surrounding tissue should be avoided. Ulcer cavities should be filled with dressing material but over packing is to be avoided. The placement of dressing materials should be monitored and dressings changes regularly. Grade III and IV pressure ulcers may benefit from electrical stimulation to promote wound closure (Reviewed in Consortium for spinal cord medicine, 2007, Reddy *et al,* 2006, Grey *et al,* 2006). Postoperative care is often of paramount importance to promote wound healing and prevent recurrence, and should include continued pressure management, manually moving the patient's lying or sitting position every two hours if immobile, and avoiding direct pressure to the wound site when possible and monitoring the ulcer's progress regularly. Patients lying down should be progressively mobilised to a sitting position, where possible, over 4 to 8 weeks following surgery to prevent any re-injury of the wound site. Topical growth factors have shown some potential for the healing of chronic wounds. Platelet derived growth factor is currently licensed for use on non-infected diabetic foot ulcers, and has shown some value in treating pressure ulcers, as has fibroblast growth factor. There is a strong theoretical basis in support of the development of proteinase inhibitors as agents to treat chronic wounds such as pressure ulcers, and alternatives such as occlusive dressings and negative pressure therapy have potential applications in this area. To date, however, there does not appear to be sufficient evidence from clinical trials supporting these methods to justify their use in the treatment of pressure ulcers (Reviewed in Consortium for spinal cord medicine, 2007, Reddy *et al,* 2006, Grey *et al,* 2006).

Spinal injury and pressure ulcers: As previously mentioned spinal injury patients show an increased incidence of pressure ulceration. (20% to 30% compared to 1% to 5% in the general hospitalised population). Not only do spinal injuries often result in prolonged periods of immobility, wheelchair use or loss of sensation that contribute to pressure ulcer formation, but spinal injury can affect the physical properties of the skin, rendering it more prone to damage. Sufficiently severe spinal injury can impair the thermoregulatory processes necessary to maintain skin temperature, causing the skin to overheat. Neurologically impaired skin also undergoes distinct metabolic changes that often do not stabilize for years following injury. Increased collagen catabolism, combined with decreased activity of lysyl hydroxylase, an enzyme involved in collagen biosynthesis, reduces the tensile strength of the skin, and renders it more fragile below the level of injury. Increased excretion of glycosaminoglycans reduces the elasticity of the skin, leaving it ill equipped to deal with the mechanical forces of pressure, shear and friction associated with immobility. A decrease in adrenergic receptors in neurologically impaired skin leads to unusual vascular reactions, and it has been reported that this can dramatically reduce the skin's ability to withstand ischemia. The reduced blood supply associated with spinal injury contributes to this, leaving tissues at risk of severe hypoxia. Spinal injury also results in a reduced proportion of type I collagen, compared to type III. As type III collagen forms thinner, weaker fibrils than type I, this contributes to the increased fragility seen in neurologically impaired skin, which leaves patients at significantly increased risk of pressure ulceration. It has also been shown that blood reflow rates immediately following occlusion are reduced in spinal injury sufferers compared with able bodied individuals. The muscular atrophy caused by paralysis originating from spinal injuries leads to the loss of muscle mass in the affected areas. This reduced muscle mass

results in less padding between prominences and support surfaces, further increasing the risk of pressure ulcer development. The combination periods of prolonged immobility, sensory impairment, or wheelchair use, and the physiological, mechanical, and biochemical factors outlined above goes a long way to explain the increased incidence of pressure ulcers associated with spinal injuries (Reviewed in Consortium for spinal cord medicine 2007).

1.4 Model systems for the investigation of chronic wounds and skin wound healing.

Systems used to investigate pressure ulcers, and skin damage or repair in general can be divided broadly into *in vitro* and *in vivo* models.

In vivo models: The majority of *in vivo* studies have utilised animal models, as pressure ulcers are too hazardous and expensive to induce in the clinical environment, thus limiting human studies to patients with already existing ulcers. Individual variations in the intrinsic (anaemia, lean body mass, neurological impairment etc) and extrinsic factors (shear, friction, immobility, pressure) as well as co-morbid conditions between patients also limit the reliability of the results of human studies. Animal models have traditionally utilised rats, mice, and swine, as there skin types are considered similar to that of humans. The use of rats and mice in particular avoids the impediments and expenditure associated with bigger bodied animals in large scale experiment. Experimentally induced pressure ulcers have been used to determine the degree of external pressure that will consistently lead to tissue damage. Animal studies have involved the application of standardised pressures or shear forces to soft tissue, followed by histological observation of the resulting breakdown. Work using pigs in the 1970s, for example, featured paraplegic and normal swine, and utilised light and electron microscopy of tissue biopsies. These studies showed pressure ulcers to be caused by two main factors, friction and ischemic pressure, and demonstrated that friction did not contribute to ischemia in pressure ulcer development (Dinsdale *et al,* 1973). Both rat and swine models have been used to demonstrate the role of myofibroblasts in cutaneous wound contraction (Salcido *et al,* 2006). The Diabetes mouse has been used as a model for impaired dermal wound healing to investigate the

expression of matrix metalloproteinases (Wall *et al,* 2002). In addition, other mammals such as rabbits and greyhounds have also been used as models for mammalian wound healing (Salcido *et al,* 2006). These models do not however accurately represent normal human skin conditions. Pigs skin is covered in hair much coarser than that found in humans, and the porcine dermis is only moderately vascularised compared to our own. Pigs also lack the epidermal stratum lucidum, a layer of flat keratinocytes immediately below the cornified surface cells in thick skin, and this may influence the regeneration of the outer layer. Rat skin is much less cellular than human skin, and derives its circulation directly from large blood vessels such as the cutaneous arteries, as opposed to human skin, which is sustained by a more complex system of smaller blood vessels, derived from the musculocutaneous arteries. The use of animal models in research as a whole has been in decline since the 1970s as a combined effect of the animal rights movement, increased public and scientific sympathy towards ethical issues, and the development of biotechnological alternatives that reduce the need for animal testing (Salcido *et al,* 2006).

In vitro models: In vitro models used in pressure ulcers tend to be tissue cultured skin substitutes, or donor skin tissue. Keratinocytes cultures, either primary keratinocytes or cell lines, can be used to represent the epidermis,). Fibroblasts seeded in extracellular matrix proteins, such as collagen gels), or de-epidermalised human dermis (Haddow *et al,* 2001) have been used to represent the dermis. Organotypic co-cultures, incorporating both a dermal and epidermal equivalent can be used to represent whole or living skin (Marionnet *et al,* 2006). The growing of keratinocytes at an air-liquid interface leads to nearly complete differentiation and the formation of an organised stratified epidermal substitute similar to living skin (Marionnet *et al*, 2006). An example of a reconstructed human skin equivalent, Episkin, consists of

primary human keratinocytes grown upon an acellular dermal substitute of type I and III collagens covered by a film of collagen type IV and is being investigated for its use in skin irritation studies. Models such as these contain primary cells, which are known to demonstrate inter-individual variations. In order to develop more reproducible skin equivalents work has been done regarding the incorporation of cell lines into living skin models). Sterile acellular de-epidermalised human dermis (DED) is used as a wound bed model and has been used in the study of the transfer of cultured cells from tissue engineered dressings to the model wound bed (Haddow *et al,* 2001). Although these models are used to represent human skin to a degree, they do not have common skin appendages such as follicles or sweat glands, do not incorporate immune or circulatory responses, nor contain cells such as Langerhans cells, melanocytes, or macrophages and so do not exactly reproduce *in vivo* conditions (Metcalfe & Ferguson 2007).

2 dimensional (2D) models of cell migration (scratch assays)

In vivo, most cell migration occurs in three dimensions (3D) or at least in a laminar manner. Whilst assays are being developed for the assessment of cell migration in 3D conditions, the use of such model systems is made difficult and limited compared to 2D cell migration assays by their relative degree of complexity in set up and analysis, high expense in time and resource, and by being markedly less well characterised and established within the current literature. Of the 2D cell migration assays in common use, the most widely utilised is the scratch assay (as described in the methods section of this thesis) (Ashby and Zilastra, 2012). The scratch assay is advantageous as a model system of cell migration mostly due to its simplicity and versatility, allowing migration to be assessed under a variety of culture conditions and in relatively high numbers of replicates whilst requiring no specialised equipment outside of that

commonly present within a culture laboratory (Nikolic *et al.,* 2006). In addition, the scratch assay has value as an established model of re-epithelialisation especially, where the migrating keratinocytes move across the surface of an ECM, much as occurs in scratch assays involving a pre-prepared substrata of ECM molecules. The main disadvantages of scratch assays arise from the difficulty in determining the degree of damage to both the cells and the underlying matrix material done by the mechanical means of scratching, and the possible effects of this upon cell migration in to the scratch area. Additionally, the high density of cells required for these assays may result in the modification of an exogenous substrate of interest by the cell population as they migrate (Ashby and Zilastra, 2012).

1.5 Cell therapies for skin wound healing.

Extensive wounds require barrier protection to prevent infection and desiccation, and the loss of full thickness skin over an area exceeding 4cm diameter will not heal well without a graft (Reviewed in MacNeil, 2007). As far back as 1871 the transplantation of either full thickness or split thickness skin from elsewhere on the patient's body has been the standard surgical treatment for wounds of this severity; as the patient will re-grow skin over the source site, provided sufficient epidermal cells remain within the dermal surface. In many wounds however, especially severe burns, there is not enough skin available on the patient's body for transplantation, without causing further damage. This has led to the development of engineered skin substitutes for use as biological dressings. These dressings not only achieve the initial closure of the wound but can also promote regeneration, and reduce healing time. Current strategies include the engineering of substitute dermis, epidermis or both, and often include an artificial extracellular matrix (Metcalfe & Ferguson 2007, Horch *et al,* 2005). No substitute yet developed accurately replicates the full properties of uninjured skin, but the numerous criteria that an ideal skin substitute should fulfil are listed below:

Engineered skin substitutes should demonstrate:

- Absence of antigenicity
- Tissue compatible
- No local or systemic toxicity
- Impermeability to exogenous micro-organisms
- Transmission of water vapour similar to normal skin
- Rapid and sustained adherence to the wound bed
- Conformation to surface irregularities
- Elasticity to permit motion of underlying tissue
- Resistance to linear and shear stresses
- Sufficient tensile strength to resist fragmentation
- Inhibition of wound surface flora and bacteria
- Long shelf life, minimal storage requirements
- Low cost
- Minimised nursing care of wound
- Minimised patient discomfort
- Translucent properties to allow direct observation of healing
- Reduced healing time
- Non increased rate of infection
- Patient acceptance

(Ehrenreich and Ruszczak, 2006)

Generally, tissue engineered skin is created by expanding skin cells in the laboratory, at a rate far exceeding that which would occur *in vivo*. Utilising the rapid growth of cells in culture, enough skin to cover almost the entire surface area of the body can potentially be grown within three weeks (MacNeil 2007).

Epidermal repair: Cultured keratinocytes are widely used to provide an engineered epidermis, to restore skin barrier function, and to promote regeneration. This can be achieved using a range of methods. Integrated sheets of autologous keratinocytes can be grown from a biopsy of patient's cells, and enzymatically removed from culture for direct application to the wound site (Epicel, Genzyme Tissue Repair). Alternatively, a subconfluent population of cells can be delivered to the patient on a chemically defined carrier dressing (Myskin, CellTran). Keratinocytes in suspension can also be applied to the wound bed as a spray, sometimes also containing fibrin (CellSpray, Clinical Cell Culture). Small sheets of keratinocytes can be cultured from patient's hair follicles (Epidex, Modex Therapeutics) (Metcalfe & Ferguson 2007, Horch *et al*, 2005) . As yet, there has been little direct comparison of the relative effectiveness of these methods.

Dermal repair: Epidermal replacements will generally fail to take in the absence of a vascularised dermis, and in the case of chronic wounds the replacement of the dermal layer is important to promote healing. Allografts of human donor skin can be used as a temporary cover for full thickness wounds, before removing the non-immune compatible epidermal layer. This leaves behind a donor dermis with sufficient vasculature to support subsequent skin grafts or engineered epidermal substitutes (Metcalfe & Ferguson 2007). Integra, an alternative dermal substitute, consists of bovine collagen and shark chondroitin sulphate and a silicone membrane. When grafted onto a wound bed, this forms a temporary barrier, and stimulates vasculogenesis. Once vascularised, the silicone membrane can be removed and a subsequent graft, either split thickness autologous skin or an engineered epidermal substitute can be applied (MacNeil 2007). Synthetic materials seeded with cultured or

donor fibroblasts (Dermagraft and Transcyte, Advanced Biohealing) have also been used to generate a vascularised dermis prior to epidermal replacements.

Whole skin repair: Problems with adherence between replacement epidermis and prepared dermal wound beds led to the development of composite skin replacement materials, such as Apligraf, Orcel and Permaderm, incorporating both dermal and epidermal components. Apligraf (Organogenesis) and OrCel (Ortec international) use allogeneic keratinocytes and fibroblasts in a bovine collagen matrix, and are suitable for use in the treatment of chronic wounds. Permaderm utilises autologous keratinocytes and fibroblasts in reconstructed skin with bovine collagen, and is used to treat burns patients (Metcalfe & Ferguson 2007).

Issues with engineered skin substitutes: The range of currently available skin substitutes still has certain aspects which require address or improvement. The use of animal products such as bovine collagen, animal serums and enzymes in culture medium has potential health implications for patients, centred on the transfer of viruses or prion disease proteins. Work has been done to develop xenobiotic free protocols for tissue engineering and the bovine serums and collagens currently used are sourced from herds known to be free of bovine spongiform encephalitis (BSE) (Bullock *et al*, 2006). Wound infection is a major cause of graft loss, and cultured skin is more susceptible to damage from bacterial infection than conventional grafts due to the fragility of the non-cornified epithelium and the incomplete development of the dermal-epidermal junction (Horch *et al,* 2005). Given the very high incidence of infection amongst chronic wounds this is potentially a very serious failing. Scarring at the margins of grafts is a problem common to conventional and tissue engineered skin grafts. As well as some degree of mechanical impairment, pronounced scarring is an aesthetic defect that may be of more concern to patients than physicians. The study of

foetal scar free regeneration has lead to the experimental manipulation of growth factors in adult wounds, resulting in the reduction and prevention of scarring (reviewed in Ferguson and O'Kane, 2004). The timescale involved in skin culture is an area for potential improvement. Although cells grow much more rapidly in culture than they do *in vivo*, the time taken to grow autologous skin equivalents is still quite significant, around two to three weeks (Metcalfe & Ferguson 2007), especially when compared to the ability of allogeneic products to be produced and stored ready for use (Mansbridge 2006), or the immediate availability of patient's skin for conventional grafting. Dermagraft for example can be cryopreserved for a shelf life of up to six months, although this process may have an effect on the efficacy of the product.

Immune rejection of allogeneic cells also limits the effectiveness of some engineered skin substitutes. Although there are reports of immunogenic tolerance to allogeneic fibroblasts permitting their survival for weeks and even months within a host (Coulomb et al., 1998, reviewed in Shevchenko et al., 2010), there are also studies that suggest that these cells do not persist for longer than seven days in either human or porcine hosts (Price *et al.,* 2004, Kolokol'chikova *et al*., 2001), Similarly allogeneic keratinocytes are reported to suffer immune rejection within weeks (Strande et al., 1997, Clark *et al.,* 2007).

Failure of integration is a common problem associated artificial skin substitutes. Vascularisation of grafts is essential if the replacement skin is to take and survive long term, successfully integrating with host tissues. Often the vascularisation of cultured skin grafts (in those that do allow angiogenesis to occur) is too slow or insufficient to allow the construct to take, resulting in cell death and ultimately the sloughing off of the skin graft. The recent observation of the origins of vascularisation occurring within the central area of the graft suggests that engineered skin substitutes

which incorporate prefabricated vessels may vascularise more rapidly, increasing the success rate of these grafts (Metcalfe & Ferguson 2007). Cultured skin substitutes generally consist of keratinocytes, fibroblasts, or co-cultures of both, and as such do not contain many of the appendages and functional structures found in skin. A lack of follicles means that the grafts lack hair, and combined with the absence of sweat glands may result in some impairment of thermoregulation over the graft area. The absence of dendritic cells and macrophages in engineered skin grafts leaves the graft area potentially devoid of immune surveillance, although this is thought to benefit allografts by preventing rejection. Studies have, however, experimented with the incorporation of these structures, as well as melanocytes for pigmentation, into engineered skin tissue, with some success. In a case described by Zheng and co-workers the injection of dermal cells and epidermal aggregates into the dermis of nude mice resulted in normal hair morphogenesis, giving rise to hair follicles within 8-12 days (Zheng *et al*, 2005).

Commercial considerations: Commercially, those tissue engineered products licensed for clinical use have fallen short of promoters expectations (Ehrenreich & Ruszczak 2006), receiving less of the market share than anticipated. This short fall is, in part, due to the extensive differences between the laboratory environment in which these products are developed, and the requirements for high quality and cost effective manufacturing. Allogeneic cells are well suited to commercial scale up, whilst autologous cells inherently are not, and so it is the allogeneic products (Apligraf, Dermagraft etc) that have met with a greater degree of commercial success. For example, Dermagraft has been developed to incorporate several beneficial features for commercial production- through the design of an aseptic bioreactor suitable for use in automated systems, being capable of preservation by cryofreezing, and the inclusion

of translucent and ink accepting surfaces allowing wound outlines to be traced upon the packaged tissue pocket, dermagraft was designed to provide optimal end-user convenience (Mansbridge 2006).

1.6 Mesenchymal Stem Cells

Background: Over 100 years ago Conheim, a German pathologist, proposed that fibroblastic cells present with adult bone marrow could contribute to the repair of damaged peripheral tissues (Prokop, 1997). Subsequently in the 1970s Friedenstein and colleagues demonstrated the clonogenic potential of fibroblast-like cells isolated from rodent bone marrow (Friedenstein *et al,* 1970, Friedenstein *et al,* 1976, Friedenstein, 1980). Friedenstein's method of flushing whole bone marrow into plastic culture vessels and discarding the non adherent population gave rise to a heterogeneous population of plastic adherent fibroblastic colony forming cells, and has formed the basis for the isolation of MSC from bone and bone marrow to this day. Friedenstein also demonstrated that these cells possessed a capacity for self-renewal, as well as the potential to form bone. Since Friedenstein's initial experiments, numerous groups have expanded upon these findings, demonstrating that an equivalent cell population was present in human bone marrow, and that cells isolated by methods similar to Friedenstein's could be sub-passaged *in vitro* and differentiated into other cells of the mesenchymal lineage such as osteoblasts, chondrocytes and adipocytes (reviewed in Caplan, 2007, Bianco *et al,* 2008).

Characteristics and definition of MSC: There are currently no single markers or receptors considered to be unique to MSC (Rastegar *et al,* 2010) but established criteria dictates that in order to be considered to be MSC, a population of cells must be plastic adherent, capable of differentiation into osteoblasts, chondrocytes and adipocytes, and to express cluster of differentiation (CD) markers CD105, CD73 and CD90 whilst not expressing CD34, CD45, or CD14 (Dominici *et al,* 2006). This profile is consistent between cell populations isolated from a range of tissues that are considered to be MSC, but the expression of other cell surface molecules can differ

quite markedly between MSC isolated from different sources (Table 1.1) (Cao *et al*, 2005, Pittenger *et al*, 1999, Jörn *et al*, 2010, Schaffler *et al*, 2007, De Ugarte *et al*, 2003, Zuk *et al,* 2002, Tondreau *et al,* 2005).

	Bone marrow-MSC	Adipose tissue-MSC	Peripheral blood-MSC
Positive	CD13 CD44 CD73 CD90 CD105 CD166 STRO-1	CD9 CD13 CD29 CD44 CD54 CD73 CD90 CD105 CD106 CD146 CD166 HLA STRO-1	CD44 CD54 CD90 CD105 CD166
Negative	CD14 CD34 CD45	CD11B CD14 CD19 CD31 CD34 CD45 CD79α CD133 CD144 HLA-DR	CD14 CD34 CD45 CD31

Table 1.1. Differential expression of cluster of differentiation (CD) markers between MSC isolated from different source tissues.

Sources of MSC: Whilst the majority of MSC used for experimental investigation are isolated from bone marrow, and these are generally regarded as being the 'gold standard' (Hass *et al,* 2011), MSC have been isolated from numerous other tissues including adipose tissue, peripheral and umbilical cord blood, bone, placenta and amniotic membrane (Kern *et al*, 2006, Miao *et al*, 2006, Tsai *et al*, 2007). Whilst bone marrow derived MSC are often considered to be preferable, the process of harvesting bone marrow aspirate from patient donors is invasive, often painful and carries an associated risk of infection (Hass *et al,* 2011, Malgieri *et al*, 2010). Conversely, Adipose tissue suitable for the isolation of MSC can be easily obtained through elective procedures such as liposuction or lipoplasty. The low cost of isolation and ease of accessibility of adipose derived MSC establishes them as an attractive alternative to bone marrow derived cells (Romanov *et al,* 2005), especially as the capacity of adipose tissue derived MSC to differentiate along the mesodermal lineage is equal to that of bone marrow MSC (Baglioni *et al,* 2009). Birth-associated tissues such as umbilical cord and umbilical cord blood are often considered as medical waste in delivery rooms and can be collected and utilised in a non-invasive manner (Malgieri *et al*, 2010). Cells isolated from umbilical cord are also more primitive than bone marrow MSC (Lu *et al,* 2006, Can and Karahuseyinoglu 2007, Sarugaser *et al*, 2005, Wu *et al*, 2007). Disadvantageously, the isolation of MSC form umbilical cord blood is markedly less regularly successful than from bone marrow (Kern *et al*, 2006).

MSC differentiation: As well as being isolated from numerous tissue sources, MSC have been successfully differentiated into numerous cell types from multiple lineages both *in vitro* and *in vivo* (Arthur *et al*, 2009, Deans *et al,* 2000, Bianco *et al,* 2000) (Figure 1.9), including the aforementioned cells of mesodermal origin; osteoblasts,

chondrocytes and adipocytes, as well as skeletal and cardiac muscle, (Bianco *et al*, 2000, Tokcaer-Keskin *et al*, 2009, Moscoso *et al,* 2005) and cells derived from both the ectodermal and endodermal lines, (Figure 1.10) e.g. astrocytes (Kopen *et al,* 1999) neurons (Sanchez-Ramos *et al*, 2000, Woodbury *et al,* 2000) and pancreatic islet cells (Chen *et al,* 2004). Of these potential MSC progeny, their differentiation into osteoblasts, chondrocytes and adipocytes are relatively well understood. MSC have been differentiated into osteoblasts *in vitro* using a range of methods. Exposure to bone morphogenic proteins (BMP) such as BMP-2, BMP-4, BMP-6 , BMP-7 and BMP-9 have been shown to induce osteogenic differentiation of MSC (Cei *et al*, 2006, Chen *et al,* 2004, Fujii *et al*, 1999, Gu *et al*, 2004, Katagiri *et al*, 1994, Yeh *et al*, 2002, Zachos *et al*, 2006, Zhu *et al*, 2006). BMP signal though serine/threonine kinase receptors, signalling via mitogen associated protein kinase (MAPK) components to trigger the transcription of genes associated with osteoblasts cells within the nucleus (Chen *et al,* 2004, Fujii *et al*, 1999). Transcription factors such as Runx2 (Arthur *et al,* 2009, Fujita *et al,* 2004) and oseterix (Tominaga *et al*, 2009) are also known to promote osteogenic differentiation, as well as *ex vivo* culture in osteogenic media supplemented with dexamethasone and ascorbate (Choi *et al,* 2010, Oreffo *et al,* 1999). MSC differentiation into chondrocytes can be induced by the aggregation of cells in culture into alginate beads or cell pellets, and by exposure to BMP and TGF-β (Shen *et al*, 2009, Mehlhorn *et al*, 2006). MSC have also been shown to differentiate into chondrocytes when cultured in the presence of cartilage or nucleus pulposus tissues (Rastegar *et al*, 2010). The differentiation of MSC into adipocytes is controlled by peroxisome proliferator-activated receptor γ (PPARγ), a nuclear receptor and transcription factor that regulates the expression of adipocytes associated genes (Michalik *et al,* 2006, Rosen and Spiegelman, 2000). *In vitro*, MSC

can be differentiated into adipocytes by culture in media containing insulin and dexamethasone (Yin *et al,* 2010, Oishi *et al*, 2009). Numerous reports have suggested that MSC are capable of neural trans-differentiation, induced by a variety of methods, for example exposure to retinoic acid and brain-derived neurotrophic factors (Sanchez-Ramos, *et al*, 2000), growth factors EGF and HGF (Bae *et al*, 2011) or antioxidant compounds such as β-mercaptoethanol, dimethyl sulfoxide, and butylated hydroxyanisole (Woodbury *et al,* 2000). Recently however, it has been shown that many of the markers used to demonstrate neural differentiation can be expressed in the undifferentiated MSC population (Montzka *et al*, 2009). This considered along with the failure of some reports (e.g. Sanchez-Ramos *et al*, 2000, Fu *et al*, 2008) to demonstrate the absence of neuronal markers in the MSC population prior to the application of their neural differentiation protocols, and the variable degrees of success reported by some groups when attempting to differentiate MSC into neural cells (Montzka *et al*, 2009), should inform future investigation into the neural differentiation potential of MSC. This said, both human and rodent MSC have been successfully and robustly differentiated into functional neurons that effectively improve the symptoms of neurodegenerative disorders following transplantation into animal models (Dezawa *et al*, 2005).
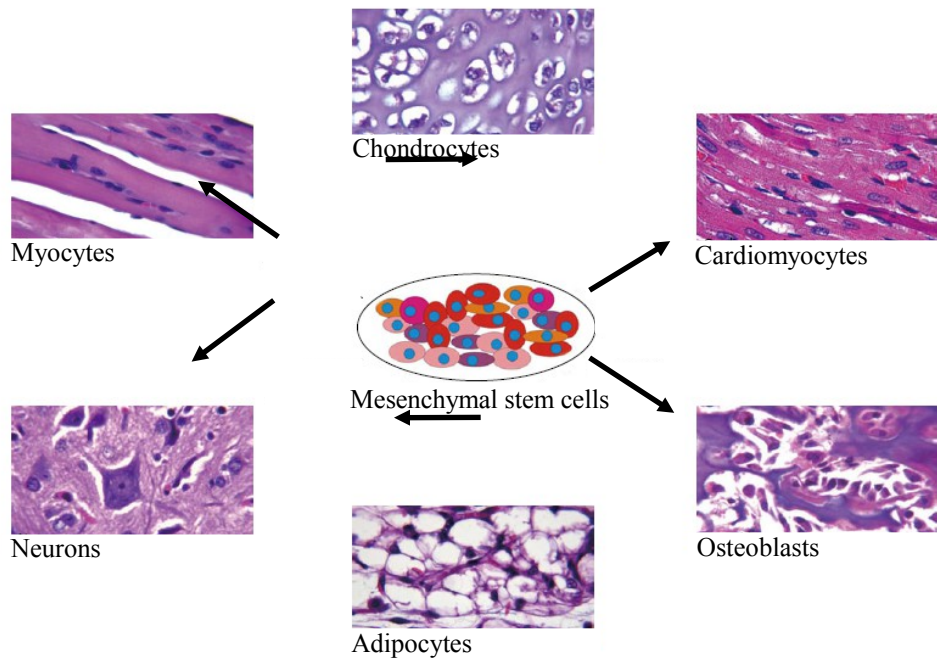
Figure 1.9. The differentiation potential of MSC. Mesenchymal stem cells have been shown to be capable of differentiation into cells of the mesenchymal lineage; osteoblasts, chondrocytes and adipocytes as well as other cell types such as neurons (*Image adapted from Rastegar et al, 2010*)
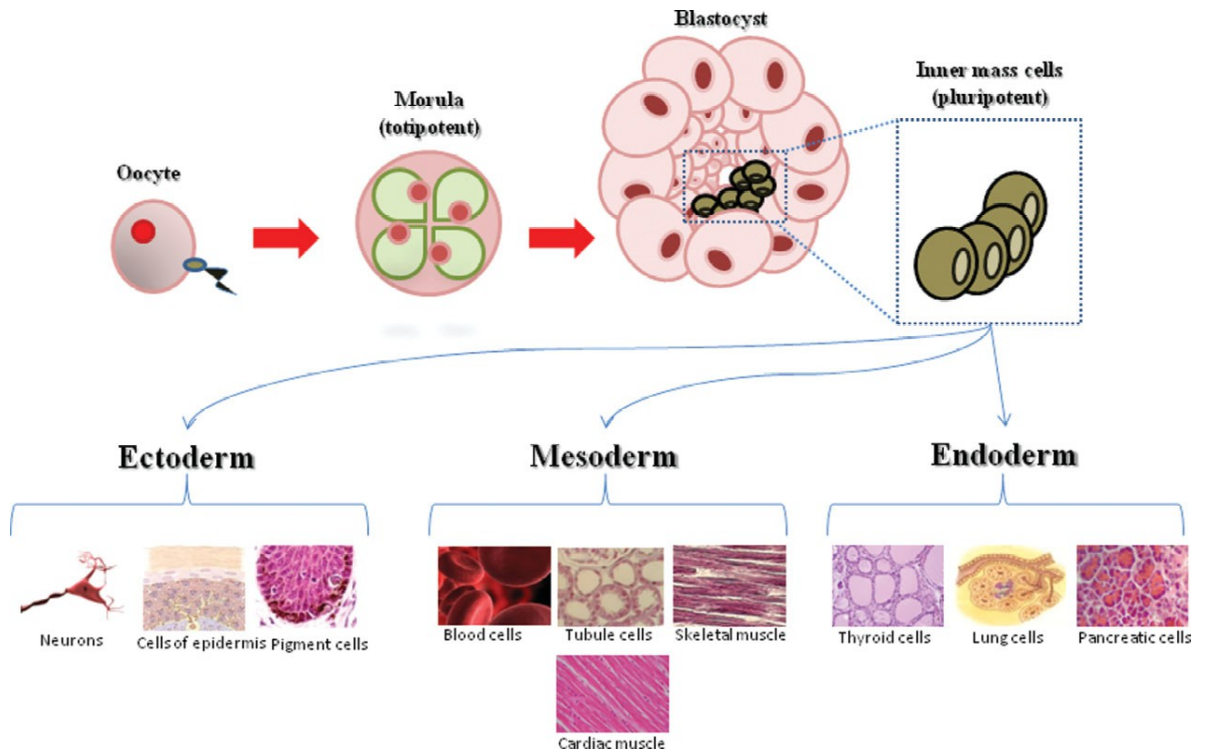
Figure 1.10. The Hierarchy of stem cells (*Image taken from Salem and Thiemermann, 2010*)

Clinical applications and therapeutic potential: MSC have shown potential as a therapeutic agent for the treatment of a wide range of disorders, and have recently become the subject of numerous clinical trials (Table 1.2). Following transplantation in humans, MSC have been reported to have therapeutic potential for the treatment of, for example; osteogenesis imperfecta (Horwitz *et al,* 2002), bone fracture (Bajada *et al,* 2007), traumatic brain injury (Zhang *et al,* 2008), stroke (Honmou *et al,* 2011, Bang *et al,* 2005), and myocardial infarction (Tendera *et al,* 2009, Hare *et al,* 2009).

The ability of MSC to differentiate into osteoblasts and chondrocytes has rendered them an attractive treatment option for orthopaedic complaints such as fracture non-union and critical sized bone defects, as well as for cartilage regeneration and the treatment of osteogenesis imperfecta (Horwitz *et al,* 2002). For example, Bajada *et al* showed that an application of MSC delivered with calcium sulphate resulted in enhanced repair of fracture non-union compared to calcium sulphate alone (Bajada *et al,* 2007) Similarly, reporting on a seven year pilot study, Marcacci and co-workers showed that MSC in a bio-ceramic carrier significantly enhanced the healing of critical sized defects in long bones (Marcacci *et al*, 2007). These findings show that MSC represent a potential alternative to autologous bone grafting, which despite being the standard treatment for such conditions is associated with significant donor site morbidity and limited by the availability of appropriate donor tissue (Marsh, 1998, Einhorn 1996). MSC have also been used in numerous cases to successfully regenerate damaged cartilage in both injury associated defects and osteoarthritis (Wakitani *et al,* 2002, Wakitani *et al,* 2004, Kuroda *et al,* 2007, Wakitani *et al,* 2007).

Clinical trial	Disease	Cell Source	Location/Sponsor
Mesenchymal Stem Cells in Multiple Sclerosis	Multiple sclerosis	BM-derived autologous MSC	University of Cambridge, UK
Safety Study of Allogeneic Mesenchymal Precursor Cells (MPCs) in Subjects With recent Acute Myocardial Infarction	Myocardial infarction	BM-derived allogenic MSC	Angioblast Systems, U.S
Mesenchymal Stem Cells and Subclinical Rejection	Organ Transplantation	BM-derived allogenic MSC	Leiden Universitary Medical Center, Netherlands
Use of Autograft Mesenchymal Stem Cells Differentiated Into Progenitor of Hepatocytes for Treatment of Patients With End-Stage Liver Disease	Cirrhosis, liver failure	Hepatocyte drived autologous MSC	Shaheed Beheshti Medical University, Iran
A Phase II Dose-Escalation Study to Assess the Feasibility and Safety of Transendocardial Delivery of Three Different Doses of Allogeneic Mesenchymal Precursor Cells (MPCs) in Subjects With Heart Failure	Heart failure	BM-derived allogenic MSC	Angioblast Systems, U.S
Mesenchymal Stem Cells Under Basiliximab/Low Dose RATG to Induce Renal Transplant Tolerance	Kidney transplant	BM-derived autologous MSC	Mario Negri Institute for Pharmacological Research, Italy
Safety and Efficacy Study of Adult Human Mesenchymal Stem Cells to Treat Acute GvHD.	Graft versus host disease	BM derived allogenic MSC (Prochymal)	Osiris Therapeutics, U.S.
Autologous Implantation of Mesenchymal Stem Cells for the Treatment of Distal Tibial Fractures	Tibial fracture	BM-derived autologous MSC	Hadassah Medical Organization, Israel
Prospective Randomized Study of Mesenchymal Stem Cell Therapy in Patients Undergoing Cardiac Surgery (PROMETHEUS)	Left ventricular dysfunction	BM-derived autologous MSC	National Heart, Lung, and Blood Institute, U.S.
Cord Blood Expansion on Mesenchymal Stem Cells	Myelodysplastic syndrome; leukemia	CB-derived allogenic MSC	U.T.M.D. Anderson Cancer Center, U.S
Mesenchymal Stem Cell Infusion as Prevention for Graft Rejection and Graft-Versus-Host Disease	Hematological malignancies	BM-derived allogenic MSC co-infusion with either HLA-mismatched PBSC or cord blood	University Hospital of Liege, Belgium

Clinical trial	Disease	Cell Source	Location/Sponsor
Extended Evaluation of Prochymal Adult Human Stem Cells for Treatment-Resistant Moderate-to-Severe Crohn's Disease	Crohn's disease	BM derived allogenic MSC (Prochymal)	Osiris Therapeutics, U.S.
Efficacy and Safety of Adult Human Mesenchymal Stem Cells to Treat Patients Who Have Failed to Respond to Steroid Treatment for Acute Graft Versus Host Disease (GvHD)	Graft-versus-host disease	BM-derived allogenic MSC (Prochymal)	Osiris Therapeutics, U.S.
Prochymal (Human Adult Stem Cells) for the Treatment of Recently Diagnosed Type 1 Diabetes Mellitus T1DM)	Type 1 diabetes mellitus	BM-derived allogenic MSC (Prochymal)	Osiris Therapeutics, U.S.
Prochymal (Human Adult Stem Cells) for the Treatment of Moderate to Severe Chronic Obstructive Pulmonary Disease (COPD)	Chronic obstructive pulmonary disease	BM-derived allogenic MSC (Prochymal)	Osiris Therapeutics, U.S.
Mesenchymal Stem Cell Transplantation in the Treatment of Chronic Allograft Nephropathy	Chronic allograft nephropathy, kidney transplant	BM-derived MSC	Fuzhou General Hospital, China
Autologous Mesenchymal Stromal Cell Therapy in Heart Failure	Congestive heart failure	BM-derived autologous MSC	Rigshospitalet University Hospital, Copenhagen, Denmark
Marrow Mesenchymal Cell Therapy for Osteogenesis Imperfecta: A Pilot Study	Osteogenesis imperfecta	BM-derived allogenic MSC	St. Jude Children's Research Hospital, Memphis

Abbreviations: BM, bone marrow; CB, cord blood; MSC, mesenchymal stromal cells.

Table 1.2. Clinical trials using mesenchymal stem cells. *(adapted from Salem and Thiemermann, 2010)*

Having been shown to be capable of differentiating into cardiomyocytes *in vitro* (Makino *et al,* 1999, Shiota *et al,* 2007), and following successful *in vivo* utilisation treating post-myocardial infarction rats (Miyahara *et al,* 2006) and pigs (Schuleri *et al,* 2008), MSC have been trialled clinically to treat damaged cardiac tissue following myocardial infarction with contradictory results; reporting upon one randomised multi-centre trial, Tendera and co-workers concluded that no significant improvement was observed in patients treated with MSC compared to the control group (Tendera *et al,* 2009), whereas Hare *et al* report a significant improvement in global symptom score and left ventricular ejection fraction in all MSC-treated compared to the placebo group patients (Hare *et al,* 2009).

Smaller initial trials have also produced promising results using MSC to treat traumatic brain injury (Zhang *et al*, 2008), Parkinson's disease (Venkataramana *et al,* 2009) and stroke (Honmou *et al,* 2011, Bang *et al,* 2005) and their findings reinforce the need for randomised, blinded and placebo controlled trials on a larger scale to rigorously investigate the efficacy of MSC treatments for these conditions.

Immunological activity of MSC: A large and increasing body of work demonstrates an immunoregulatory function for MSC in both *in vitro* and *in vivo* studies, suggesting that MSC can suppress immune function both locally by inhibiting the proliferation of immune cells in the immediate vicinity of the MSC, and systemically through their effects upon T cells and the generation of regulatory T cells (Ghannam *et al*, 2010). This immunosuppressive effect occurs as a response to an initial stimulation of MSC by immune cell secreted pro-inflammatory cytokines such as Interferon-gamma (IFN-γ), Tumour necrosis factor-alpha (TNF-α), IL1-α, and IL1-β (Krampera *et al*, 2006, Ren *et al*, 2008). In response to this initial stimulation, MSC secrete a range of soluble

factors that, in combination, inhibit a range of cellular functions involved in an effective immune response (Trento and Dazzi, 2010, Ghannam *et al*, 2010). (Figure 1.11).

The immunoregulatory properties of MSC have shown potential to be exploited clinically, most notably in the prevention of graft versus host disease (Tisato *et al,* 2007) but also in the treatment of autoimmune diseases such as collagen induced arthritis (Augello *et al*, 2007) and experimental autoimmune encephalomyelitis (Zappia *et al,* 2005, Gerdoni *et al,* 2007) and in systemic lupus erythematosus (Sun *et al,* 2009). MSC immunoregulation has also been investigated for its potential to improve engraftment and survival of transplantations of skin (Bartholomew *et al,* 2001) and cardiac tissue (Casiraghi *et al,* 2008), as well as hematopoietic stem cell transplants (Koc *et al,* 2000). Importantly, clinical trials performed to date have shown MSC transplantation to be safe for patients and not associated with any major side effects (Ghannam *et al,* 2010, Centeno *et al,* 2009, Tarte *et al,* 2009).
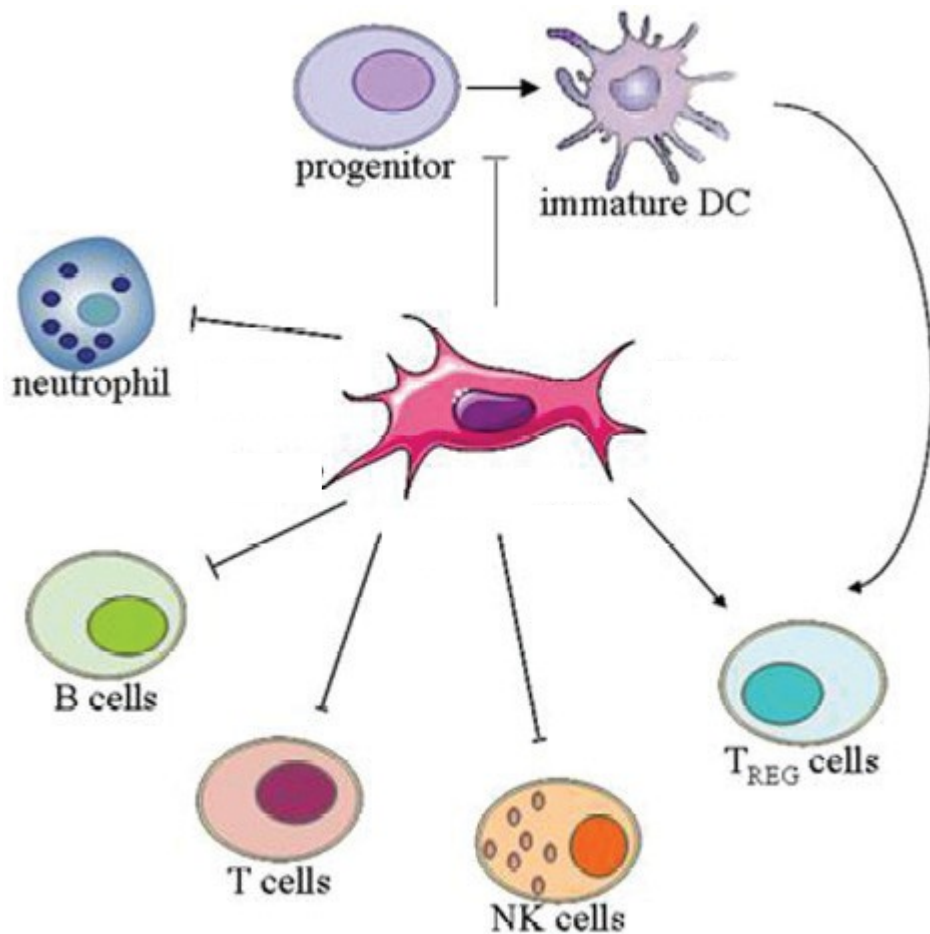
Figure 1.11. Immunoregulatory action of MSC. Mesenchymal stem cells inhibit T cell proliferation and function and prevent the maturation of dendritic cells, whilst suppressing natural killer cell proliferation and function and inhibiting the migration of neutrophils into tissues. MSC may also inhibit B cell differentiation and proliferation and drive the generation of T_{REG} cells (*adapted from Ghannam et al, 2010).*

1.7 MSC and skin wound healing

As previously described, MSC have the potential to facilitate the repair of numerous damaged tissues. Amongst the many possible clinical applications for MSC, there is an emerging body of work that suggests that these cells may be able to enhance the rate of healing of wounded skin. Pre-clinical animal studies have shown that MSC transplantation enhances wound healing (Sasaki *et al,* 2008), and reports have shown that increased wound healing also occurs when MSC are applied to humans with acute wounds (after treatment for skin cancer) or with lower extremity chronic skin wounds (Falanga *et al,* 2007, Vojtassák *et al,* 2006). The mechanisms responsible for the enhancement of skin wound healing by MSC are poorly understood but can be broadly divided into the cellular engraftment and differentiation of MSC into new skin tissue, and the paracrine activity of MSC secreted trophic factors stimulating wound healing activity of the endogenous cell population, as well as a possible supportive role for MSC, stimulating angiogenesis and promoting wound healing indirectly by facilitating the formation of new vasculature within the wound area.

MSC engraftment and differentiation into skin cells: Bone marrow derived MSC have been previously shown to accumulate in the dermis of both uninjured skin and cutaneous wounds (Fathke *et al*, 2006, Deng *et al*, 2005), supporting the possibility that they might facilitate skin wound healing by their engraftment into regenerated tissue. In an investigation carried out by Wu and co-workers, MSC used to treat full thickness *in vivo* wounds in mice have been shown to significantly enhance the rate of wound closure compared to dermal fibroblasts or an acellular carrier. Histological examination of the wound showed a large number of MSC were present in the newly formed dermal tissue as well as the regenerated epidermis, with MSC present in the

epidermis expressing markers of differentiation into keratinocytes (Wu *et al*, 2007). Similarly, Sasaki and co-workers showed that MSC were capable of keratinocyte differentiation *in vitro* and, when applied *in vivo* to wounded mice, that MSC undergo differentiation into a range of cell types present in skin including keratinocytes, and again induced a significant enhancement to the rate of skin wound healing (Sasaki *et al*, 2008). It has been suggested that the co-localisation of MSC and keratinocyte markers observed might be due to the fusion of exogenous MSC with cells of the endogenous keratinocyte population (Wu *et al*, 2010), and this phenomena has been observed by *in vitro* investigations (Baxter *et al*, 2004), but in the afore mentioned studies, fluorescence in situ hybridisation (FISH) analysis of the X and Y chromosomes of engrafted MSC indicates that this is not the case *in vivo* (Sasaki *et al*, 2008, Wu *et al*, 2007, Wu *et al*, 2010).

Paracrine activity of MSC secreted factors: MSC are known to secrete a range of factors which are involved in one or more stages of normal cutaneous wound healing (Chen *et al*, 2008). This, along with the relatively low degree of MSC engraftment observed in a range of repaired tissues (Prockop, 2007) suggests that MSC may contribute to wound healing by paracrine signalling, enhancing the wound healing response of the endogenous cell population. This is supported by studies in which the growth media from MSC cultures (MSC-CM) has been used to stimulate wound healing-associated responses of skin cells (Chen *et al*, 2008, Jeon *et al*, 2010), and in which co-cultures of skin cells with MSC were divided by culture inserts, showing comparable results (Smith *et al*, 2010). Specifically, MSC-CM has been shown to promote both proliferation and migration of human keratinocytes *in vitro* as well as enhancing *in vivo* wound healing in mice (Chen *et al*, 2008) and the survival, proliferation and migration of human dermal fibroblasts *in vitro* as well as increasing

the production of the ECM components collagen, fibronectin and elastin. Similarly, MSC were shown to enhance *in vivo* wound healing in rats (Jeon *et al*, 2010). MSC grown in co-culture with human dermal fibroblasts but divided by cell culture inserts have also been shown to promote their proliferation and migration, as well as enhancing the rate at which human dermal fibroblasts close wounds in an *in vitro* model (Smith *et al*, 2010).

Stimulation of angiogenesis by MSC: Mesenchymal stem cells may also contribute to cutaneous wound healing by stimulating angiogenesis. *In vivo*, the injection of MSC into wounded mice resulted in markedly accelerated formation of new vasculature within the wound sites compared to the injection of either fibroblasts or the vehicle medium alone. This enhancement may occur though paracrine mechanisms, as MSC have been shown to secrete factors known to be pro-angiogenic such as vascular endothelial growth factor (VEGF) (Chen *et al*, 2008, Wu *et al*, 2007), and MSC-CM has been shown to promote the formation of new vasculature *in vitro,* enhancing tubule formation by vascular endothelial cells, and to promote the recruitment of endothelial cells to wound sites *in vivo*. However, exogenous MSC may also be involved in the formation of new vascular tissue *in vivo*. Bone marrow derived MSC have been shown to be capable of differentiation into endothelial cells when introduced intravenously to an *in vivo* wound environment (Sasaki *et al*, 2008).

1. 8 Experimental cell lines.

The cell lines used to represent the cellular components of skin were: L929 Fibroblasts, HaCaT keratinocytes, and EaHy-926 endothelial cells. The advantages of using these cell lines instead of the corresponding primary cells include their comparative consistency from culture to culture and across numerous passages when compared to the inter-donor variability and passage-induced changes common to primary cells. This allows for a consistent model system with which to examine the potentially variable effects of different MSC-CM without additional confounding factors. It is also advantageous that these cell lines are highly proliferative, allowing for the high numbers of cells required for culture experiments dependent upon confluent monolayers (i.e. the scratch assays) to be regularly available. However, these cells are limited in that they may differ in certain aspects of their behaviour to that observed in primary cells either in culture or i*n vivo.* This may manifest as reduced responsiveness to stimulatory factors such as those secreted by MSCs (although as is apparent from data presented later in this thesis, it was evident that these cells do respond to MSC conditioned medium). In the case of L292 fibroblasts, which are of murine origin, there is also an issue of cross species differences as this thesis has sought to examine the effects of human MSC secreted factors on these cells, as well as co-cultures of L929 cells with HaCaT cells. However, L929 cells have been shown to respond to growth factors and cytokines, including human recombinant proteins, in a manner that is similar to human dermal fibroblasts. The limitations associated with the use of cell lines, combined with the profound differences between a culture system and the *in vivo* wound healing environment, limits the extent to which this model system accurately represents the processes involved in the natural healing of a living wounded organism. Nonetheless, the model

does allow for a reductionist approach to be taken in a controlled test environment in which it is possible to examine individual aspects of the wound healing process in relative isolation.

Table 1.3. Properties of cell lines.

	[1,2] L929 Fibroblast cell line	[3] HaCaT Keratinocyte cell line	[4,5] EaHy-926 Endothelial cell line
Species	Murine	Human	Human
Cell type	Fibroblast	Keratinocyte	Endothelial
Tissue of origin	Adipose/areolar	Normal skin	Umbilical vein/lung carcinoma cell hybrid
Morphology	Fibroblastic, smaller than normal human fibroblast	Similar to normal human keratinocytes	endothelial
Growth in culture	Adherent	Adherent/monolayer	Adherent
Differentiation potential	Osteogenic Adipogenic	Organotypic keratinization to terminally differentiated keratinocytes	Angiogenic phenotype Mature vascular structures
Doubling time	14 hours	21 hours	12 hours
Established	1943	1988	1983

([1]Earle *et al.,* 1943, [2]Theerakittayakorn and Bunprasert 2011, [3]Boucamp et al., 1988, 1997, [4]Edgell *et al.,* 1983, [5]Ribatti et al., 1999).

1.9 Aim and Objective

Mesenchymal stem cells have been shown to promote skin wound healing *in vivo* in animal models and in humans (Sasaki *et al,* 2008, Falanga *et al,* 2007, Vojtassák *et al,* 2006). Furthermore, MSC can be readily isolated from the bone marrow (amongst other tissues) of patient donors, culture-expanded *in vitro* and then returned to the patients after such culture expansion (Ghannam *et al,* 2010, Centeno *et al,* 2009, Tarte *et al,* 2009). Thus, MSC represent an attractive option for autologous cell therapies, and have been trialled for the treatment of a range of conditions in humans (Horwitz *et al,* 2002, Bajada *et al,* 2007, (Zhang *et al,* 2008, Tendera *et al,* 2009, Hare *et al,* 2009). Whilst some data suggests that MSC can differentiate into skin cell types, including dermal fibroblasts and keratinocytes (Sasaki *et al,* 2008, Wu *et al,* 2007), it is evident that MSC secrete factors that are capable of stimulating an improved wound healing response in the endogenous cells already present (Chen *et al,* 2007, Kim *et al,* 2008). Relatively low numbers of MSC have been found to persist within repaired tissues following cell transplantation (Prockop *et al,* 2007, Caplan and Dennis, 2006) and thus it seems likely that the paracrine activity of MSC may be responsible for their enhancement of skin wound healing, rather than their differentiation to form mature skin cells.

Therefore, the overriding aim of this thesis was to examine the potential role of MSC secreted factors in skin wound healing. In order to address this aim, a number of specific objectives were determined, as follows:

- To develop and characterise an *in vitro* model of skin wound healing based upon the scratch-assay and utilising the cell lines, L929 and HaCaT, to represent the cellular components of normal skin.

- To utilise this model system to examine the effects of culture medium in which MSC have been grown (MSC conditioned medium; MSC-CM) upon wound healing and L929 dermal fibroblast and HaCaT keratinocyte cell behaviour. This study has been presented in Chapter 3.

- To identify factors present in MSC-CM that may influence skin wound healing (via immunological techniques and mass spectrometry) and to assess their relative contribution. This study has been presented in Chapters 3 and 4.

- To further investigate the effects of factors present within the MSC secretome that were found to contribute to the enhancement of skin wound healing by assessing their effects singly and in combination, and by comparison with the effects of 'whole' MSC-CM. This study has been presented in Chapter 5.

- To investigate the potential angiogenic effects of MSC-CM, and individual or combined components therein, again using the scratch assay and an endothelial cell line, EaHy-926. This study has been presented in Chapter 6.

- To consider how these experiments may inform our understanding of whether and how MSC secreted factors may influence skin wound healing, with discussion presented throughout the thesis and especially in Chapter 7.

Chapter 2

Methods

2.1 Maintenance of cells.

2.1.1. Tissue culture of the tumour derived murine fibroblast cell line, L929:

L929, a dermal fibroblast cell line (Earle, 1943, Sanford *et al*, 1948), was maintained under exponential growth in $25cm^2$ and $75cm^2$ tissue culture flasks (Fisher Scientific, Leicestershire, UK) in Dulbecco's Modified Eagle's Medium (DMEM)/F12 culture medium (Invitrogen, Paisley, UK) supplemented with 10% (v/v) foetal calf serum (FCS) (Invitrogen) and 1% (v/v) penicillin and streptomycin (Invitrogen). Tissue culture flasks were incubated at 37°C and in a humidified atmosphere containing 5% (v/v) CO_2. Passaging was performed at ≈90% confluence by trypsinisation, and cells were routinely re-seeded at 1×10^4 cells per cm^2. L929-Conditioned medium (CM) was generated by initially washing serum-containing cultures in phosphate buffered saline (PBS, Invitrogen) prior to incubating the cultures at ≈90% confluence in serum-free DMEM/F12 supplemented with 1% penicillin/streptomycin and 1% ITS-X (Insulin, transferrin and selenium, Sigma-Aldrich, Dorset, UK) for 72 hours. The CM was then removed and filtered through a 0.2 micron filter (supplier) to remove any debris before being stored at -20°C. The L929 cells were then trypsinised (see 2.1.4) and a viable cell count performed using trypan blue exclusion (see 2.1.5) to determine the number of cells present at the end of the conditioning process.

2.1.2. Tissue culture of the human keratinocyte cell line, HaCaT.

HaCaT, a keratinocyte cell line (Boukamp *et al*, 1988), was maintained and conditioned medium generated in much the same way as L929 cells. Hence HaCaT cells were routinely kept under exponential growth in $25cm^2$ and $75cm^2$ tissue culture flasks in Dulbecco's Modified Eagle's Medium (DMEM)/F12 culture medium supplemented with 10% (v/v) (FCS) and 1% (v/v) penicillin and streptomycin. Tissue culture flasks were incubated at 37°C and in a humidified atmosphere containing 5% (v/v) CO_2. Passaging was performed at ≈90% confluence by trypsinisation and cells were routinely re-seeded at 1×10^4 cells per cm^2. HaCaT-CM was generated by incubating PBS washed cells at ≈90% confluence in serum-free DMEM/F12 supplemented with 1% penicillin/streptomycin and 1% ITS-X for 72 hours. The CM was removed and filtered before being stored at -20°C. The HaCaT cells were then trypsinised and a viable cell count performed, as for the L929 cultures, to determine the number of cells present at the end of the conditioning process.

2.1.3. Tissue culture of the endothelial cell line, EaHy-926:

Similar to L929 fibroblasts and HaCaT keratinocytes, EaHy-926 endothelial cells (Edgell *et al,* 1983) were maintained at 37°C and in a humidified atmosphere containing 5% (v/v) CO_2 in under exponential growth in $25cm^2$ and $75cm^2$ tissue culture flasks (Fisher Scientific) in DMEM/F12 culture medium (Invitrogen,) supplemented with 10% (v/v) FCS (Invitrogen) and 1% (v/v) penicillin and streptomycin (Invitrogen). Passaging was performed at ≈90% confluence by trypsinisation, and cells were routinely re-seeded at 2×10^3 cells per cm^2.

2.1.4. Isolation and tissue culture of primary human mesenchymal stem cells (MSC):

MSC were isolated from bone marrow harvested from the iliac crest of donor patients aged between 20-80 years (average approx. 47 years) , or from femoral heads excised during total hip replacements, following local research ethical committee approval and the patient's informed consent. The iliac crest bone marrow was removed from iliac crests as aspirates using a Jamshedi needle and heparin coated syringe (Becton Dickenson Medical Supplies, Oxford, UK). These aspirates were approximately 5-10ml in volume and were then mixed with 10ml PBS and half of the resultant mix layered over each of two 10ml Lymphoprep (Fresenius Kabi Norge, AS) aliquots in 50ml Falcon Blue Max tubes (Becton Dickenson Medical Supplies). Mononuclear cells present within the bone marrow aspirates were isolated by density gradient centrifugation of both tubes (20 minutes at 900g), resulting in the formation of a 'buffy coat', a distinct layer of mononuclear cells within the tubes that is separated from fat and erythrocytes. The buffy coats from each tube were collected using 19 gauge needles and 5ml syringes (Becton Dickenson Medical Supplies) before being pooled and added to 20ml of DMEM/F12 supplemented with 20% (v/v) FCS and 1% (v/v) penicillin and streptomycin. The resulting cell suspension was once more centrifuged (10 minutes at 750g) and the supernatant discarded to produce a cell pellet that was subsequently re-suspended in 2ml of DMEM/F12 supplemented with 20% (v/v) FCS and 1% (v/v) penicillin and streptomycin. A viable cell count was performed using trypan blue exclusion and the cells were seeded into 75cm^2 tissue culture flasks in 20ml of the same 20% serum containing culture medium at a density of 2 x 10^7 cells/flask. The mononuclear cell-seeded flasks were then incubated for 24

hours at 37°C in a humidified atmosphere containing 5% (v/v) CO_2 before any non-adherent cells were removed by removing the medium and washing the flasks with PBS. The remaining adherent cell population was then culture expanded in DMEM/F12 supplemented with 10% (v/v) FCS and 1% (v/v) penicillin and streptomycin at 37°C in a humidified atmosphere containing 5% (v/v) CO_2. As the cells reached ≈70% confluence they were passed by trypsinisation and re-seeded at 5 x 10^3 cells per cm^2 up to a maximum of passage 8. It has previously been shown in our group that the cell population obtained by this method of isolation (due to plastic adherence) and monolayer culture expansion is consistent with the characteristics expected of mesenchymal stem cells, as laid out by the International Society for Cellular Therapy (Dominici *et al*, 2006); they were adherent, fibroblastic in appearance, capable of adipogenic, chondrocytic and osteoblastic differentiation, as well as being immunopositive for CD105 and immunonegative for CD34 and CD45 (Wright *et al*, 2008). Conditioned media was generated as described for cell lines.

2.1.5. Trypsinisation of cells for passaging.

Adherent cell lines required removing from the surface of tissue culture flasks in order to be used experimentally or seeded into new flasks, to avoid contact inhibition and hence kept in exponential growth. This was achieved using a serine endopeptidase proteolytic enzyme, trypsin, to dissociate adherent cells from the culture surface. Culture medium was removed from flasks and the cells were rinsed with PBS before being incubated for 5 minutes at 37°C in 0.25% (w/v) trypsin-ethylendiamine tetra-acetic acid (trypsin-EDTA, Sigma-Aldrich). An equal volume of culture medium containing 10% (v/v) FCS was then added to stop the trypsin activity and the resulting cell suspension was centrifuged at 1000rpm for 10 minutes to pellet the cells. The supernatant was discarded and the cell pellet re-suspended in

DMEM/F12 supplemented with 10% (v/v) FCS and 1% (v/v) penicillin and streptomycin. A viable cell count was performed by trypan blue exclusion before seeding cells into fresh culture flasks at a seeding density of 1 x 10^4 cells per cm^2, or their use experimentally.

2.1.6. Viable cell counting by trypan blue exclusion

Trypan blue is a coloured dye that cannot pass through an intact cell membrane. This property allows its use to selectively stain dead or membrane-damaged cells a distinguishing blue colour (Altman *et al*, 1993). A 20µl sample of a cell suspension was taken and mixed in a small eppendorf tube (Fisher Scientific, Loughborough, UK) with 20µl of trypan blue solution (Sigma-Aldrich), before the resulting mixture was loaded into a standard improved Neubauer haemocytometer (Fisher Scientific). Using the 10 x objective, cells were visible as either unstained and phase-bright (trypan blue negative), i.e. viable, or stained dark blue (trypan blue positive), i.e. non viable. The numbers of both types of cells within an area corresponding to a volume of 1 x 10^{-4} cm^3 (Figure 2.1) were counted to give a ratio of viable to non-viable cells. The concentration of viable cells per ml in the original cell suspension was calculated by multiplying the viable cell count by 2 x 10^4.
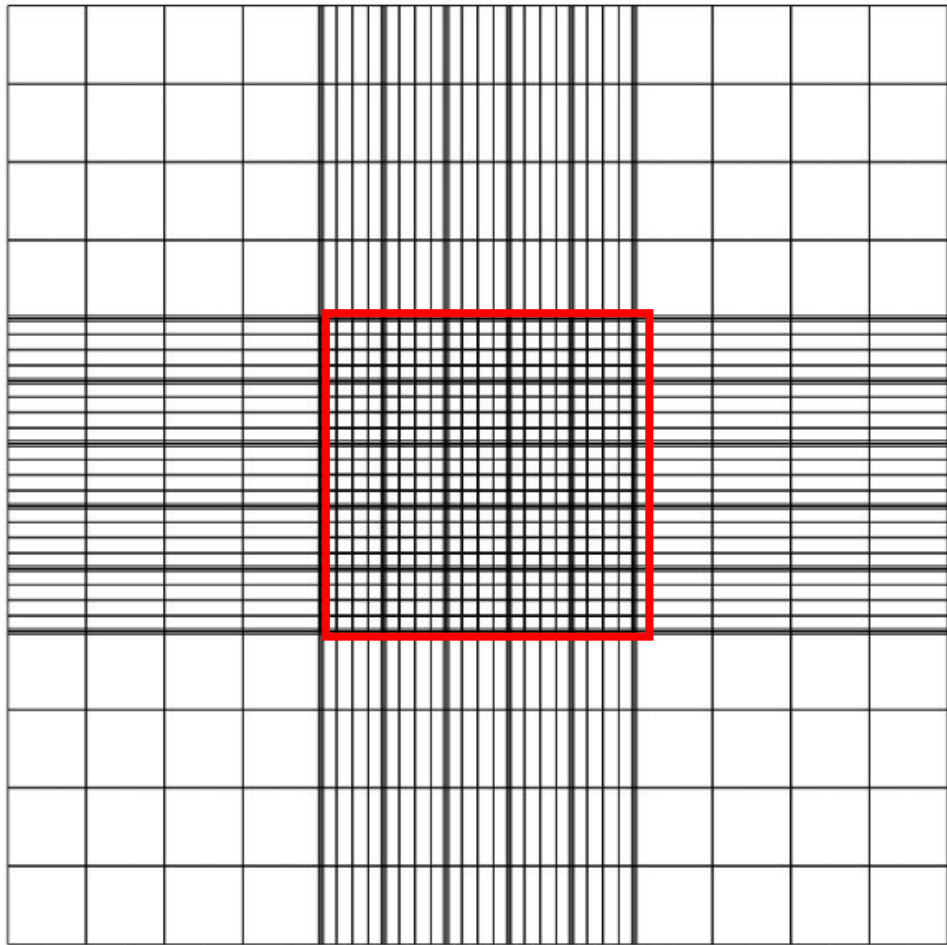
Figure 2.1. Standard Haemocytometer: A counting grid as seen through a microscope on a standard haemocytometer. The area bordered in red represents a volume of 1 x 10^{-4} cm^2. The number of cells within this area represents 1/1 x 10^4 of the cells present in 1ml of a cell suspension.

2.1.7 Screening of cells for mycoplasma.

Mycoplasma are a large group of micro-organisms that can contaminate cell cultures, thereby potentially affecting experimental data, but that are difficult to readily discern visibly as they are intracellular. Their lack of a cell wall renders them unaffected by β-Lactam antibiotics such as penicillin and its derivatives, as these agents target bacterial cell wall synthesis. Mycoplasma contamination can not only induce significant changes in cell behaviour, if sufficiently severe it can destroy a cell culture. (Drexler *et al,* 2002). In response to this potential problem, cell cultures were screened for contamination with mycoplasma whenever a new cell line was acquired and then routinely in all cell lines within the laboratory every 3-6 months. An adapted EZ-PCR mycoplasma test kit protocol (Biological Industries, Israel Biet Haemek Ltd, Israel) was used to screen cell cultures. For each culture tested, 0.5-1ml of culture medium was centrifuged for 60 seconds at 250g to pellet cellular debris. The supernatants were transferred to fresh tubes and centrifuged once more for 10 minutes at 15,000-20,000g to pellet any mycoplasma present. Supernatants were discarded and the pellets re-suspended in 50ul of Polymerase chain reaction (PCR) buffer and incubated for 3 minutes at 95°C (Hybaid PCR sprint authorised thermal cycler, Thermo Life Sciences, Basingstoke, UK). Reaction mixtures were prepared in PCR tubes by combining 43µl of RNAse free water (Qiagen Ltd, Crawley, UK) with 5µl of reaction test kit and 2µl of test sample. These were placed into the thermal cycler along with positive and negative controls (Qiagen) and held for 30 seconds at 94°C before undergoing 36 cycles of denaturation (94°C for 30 seconds), annealing (60°C for 120 seconds) and elongation (72°C for 60 seconds). The final cycle ended with an elongation temperature hold of 72°C for 5 minutes. 2% (w/v) agarose gels containing

1μl/ml SYBR safe DNA gel stain in 0.5 x TBE buffer (89mM TRIS-borate, 2.5mM EDTA, pH 8.3) (Sigma-Aldrich) were prepared to separate PCR products by electrophoresis. A 1kb commercial DNA ladder (Cambio, Cambridge, UK) was used to determine the size of PCR products. This ladder was diluted to 100μl/ml in RNAse free water along with an equal concentration of tracking dye (blue juice, Invitrogen). Agarose gels were run at 100 Volts for 1 hour and then visualised under UV light and digitised images taken. The positive control for mycoplasma infection gave a visible band at 270bp. No cell cultures demonstrated a matching band and thus all tested negative for mycoplasma infection.

2.2 Storage of cells.

2.2.1 Cryopreservation of cells

Cells kept for long periods were stored in liquid nitrogen. Cells were trypsinised and centrifuged for 10 minutes at 1000rpm to form a cell pellet, which was subsequently re-suspended in 1ml aliquots in cold 10% (v/v) dimethyl sulphoxide (DMSO, Sigma-Aldrich) in FCS at 1×10^6 cells/ml and transferred into 1.5ml cryovials (Fisher Scientific). Cryovials were then frozen overnight at -80°C in a designated cryofreezing container, 'Mr Frosty' (Genta Medical, York, UK) containing isopropyl alcohol (IPA) before transfer to liquid nitrogen storage.

2.2.2 Recovery of cells from liquid nitrogen:

Cryovials recovered from liquid nitrogen were rapidly thawed by placing under a hot running tap. 1ml of ice cold DMEM/F12 supplemented with 10% (v/v) FCS and 1% (v/v) penicillin and streptomycin was added to the thawed cell suspension drop wise over one minute and then the resultant diluted suspension was left to stand for a further one minute. After this, a further 10ml of cold culture medium was added drop wise over ten minutes and then the resulting cell suspension was centrifuged for ten minutes at 1000rpm. The cell pellet was then re-suspended in a further 10ml of culture medium and centrifuged once again as before to remove any remaining DMSO. Finally, the cell pellet was re-suspended, counted, and the cells seeded into tissue culture flasks at a seeding density of either 1×10^4 cells per cm^2 (L929 and HaCaT cells) or 5×10^3 cells per cm^2 (MSC).

2.3 Experimental procedures.

2.3.1 Coating of culture plates:

Tissue culture plates (24-well and 96-well, Fisher Scientific) were coated with a range of commercially available ECM protein solutions, i.e. type-I collagen, decorin, or fibronectin (all from Sigma-Aldrich). The stock protein solutions were diluted in PBS to the required concentration (0.2mg/ml) and an amount sufficient to cover the bottom surface was added to each well (50µl for 96-well plates, 500µl for 24-well plates). These plates were then refrigerated at 1-5°C for 24 hours before being rinsed three times with PBS immediately prior to use. In later experiments, plates were also coated with undiluted MSC-CM using the same method.

2.3.2 Fluorescence labelling of L929 and HaCaT cells for co-culture experiments:

In co-culture experiments, different cell types were distinguished by fluorescently tagging them different colours, using green and red linker kits (PKH26 or PKH67 Fluorescent cell linker kit for general membrane labelling, Sigma-Aldrich) according to the manufacturers methods. In brief, cells were removed from culture flasks by trypsinisation and re-suspended in serum-free DMEM/F12 then centrifuged for 10 minutes at 1000rpm and the supernatant discarded. This step was repeated in order to remove all traces of serum from the original culture medium before re-suspending the final cell pellet in 1ml of Linker kit diluent-C at 2x the required concentration. 2µl-4µl of PKH26 or PKH67 dye was then added to a separate 1ml of diluent-C immediately before use. This solution was added to the cell suspension and incubated for five minutes at room temperature, inverting regularly to ensure a homogeneous mix, before an equal volume of culture medium with serum was added to stop the staining reaction. Labelled cells were then washed three times and checked to make sure they were fluorescently stained prior to experimental use.

2.3.3 Scratch-wound assays:

The scratch-wound assay is a 2D model of cells migrating to heal a wound (Morley *et al*, 2003, Firth *et al*, 2008, Smith *et al*, 2010), wherein confluent cell monolayers are scored with a sterile point to leave an acellular strip, the 'wound area', and then observed as they repopulate the wound area; the rate at which they do this "wound healing" activity is quantified by image analysis. Prior to performing scratch assays, tissue culture plates were protein-coated as described above. Cells were removed from culture flasks by trypsinisation and rinsed to remove any traces of FCS by centrifugation at 1000rpm for 10 minutes and re-suspension in DMEM/F12 supplemented with 10% (v/v) FCS and 1% (v/v) penicillin and streptomycin. The number of viable cells was determined by trypan blue exclusion before cells were seeded into each well to a final density of 2×10^5 viable cells per well in 1ml of medium. In co-cultures, where L929 and HaCaT cells had been pre-labelled by fluorescently tagging in order to distinguish them, equal numbers of each cell type were used to give this final cell number of 2×10^5 viable cells per well. Seeded plates were maintained at 37°C and 5% CO_2 for 24 hours to permit cell adhesion and the formation of a confluent monolayer. After 24 hours, the culture medium was removed from these confluent monolayers, the back of the wells was marked with a horizontal guideline and the cell surface was then scored vertically with a sterile 200μl pipette tip to leave a scratch of approximately 0.4mm-0.8mm in width, and then the culture medium was immediately removed along with any dislodged cells or debris. All wells were then gently rinsed with 0.5ml of PBS, with care taken to avoid forcibly jetting the liquid directly onto the cell monolayers. The PBS was removed and replaced with either:

(i) fresh serum-supplemented culture medium (10% FCS)

(ii) with fresh serum-free culture medium

(iii) serum-free culture medium supplemented with either TGF-β1, IL-6, or IL-8,

 (iv) with conditioned medium which had been generated from L929, HaCaT or MSC,   cultures under serum free conditions, as described above.

Scratch-wound closure was monitored by collecting digitised images at 3 hour intervals after the scratch was performed until closure was either complete or no longer progressing. Digitised images were captured with an inverted microscope (Inverso TC100, Medline scientific LTD, Oxfordshire, UK) and digital camera (ProgRes CF, Jenoptik, Jena, Thuringia, Germany) under phase or fluorescence by aligning the wells in the tissue culture plate such that the horizontal marker line ran tangentially across the uppermost point of the field of view seen through the microscope (Figure 2.2). This ensured that images would be taken of the same point along the scratch length at each subsequent time point.
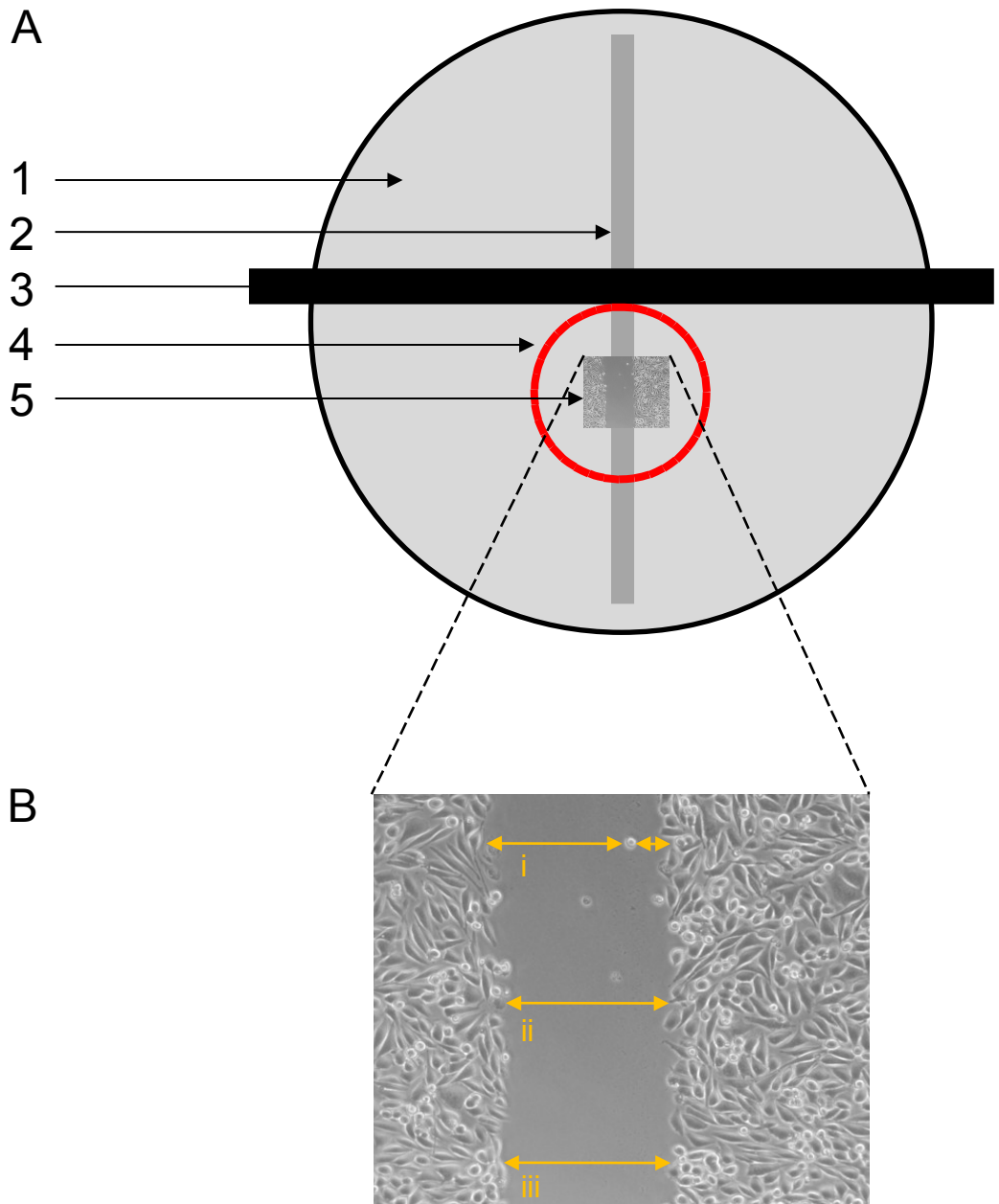
Figure 2.2. Orientation of scratch assay: A, 1) A confluent monolayer of cells within a 24 well plate. 2) An acellular scratch-wound running from top to bottom through the well. 3) A horizontal marker line running from right to left across the well. 4) The entire field of view seen through the microscope at 10 x magnification. 5) The area of image capture taken by the digital camera. B, The image captured during a scratch assay. The scratch width is the mean of the size of the acellular area at three points corresponding to the top (i), middle (ii), and bottom (iii) of the image.

2.3.4 MALDI-TOF/TOF mass spectrometry: Mass spectrometry is a method of identifying the chemical structures of large molecules such as peptides by ionising the molecules of interest to generate charged particles and measuring the mass to charge ratios of these charged molecular fragments. In the case of MALDI-TOF/TOF mass spectrometry, ions are generated using a laser, whilst protected by a matrix (comprised of a solution of crystalline molecules) to prevent the destruction of the molecule of interest, and accelerated towards a detector by an electric field (MALDI: Matrix Assisted Laser Desorption/Ionisation). The mass of the ions determined from the time taken for the ions to arrive at the detector (TOF: Time of Flight). TOF/TOF is a tandem mass spectrometry method where two time-of-flight mass spectrometers are used consecutively (Vestal *et al,* 2005). Media conditioned by MSC n=4 different patient donors were each analysed once.

Two ml of MSC-CM was incubated with 40µl of Strataclean resin for 30mins at room temperature. Unbound supernatant was removed and 1µl of trypsin (porcine sequencing grade – Promega, Southampton, UK) was added to the resin/bound proteins and incubated overnight at 37°C. The sample was centrifuged at 13000rpm for 5mins to recover the tryptic peptides. The tryptic peptides (20µl) were first separated by liquid chromatography (Dionex Ultimate 3000, Dionex, Leeds, UK) on a Pepmap C18 column, 200µm x 15cm (Dionex) at a flow rate of 3µl/minute. The eluants used were: A. 0.05% Trifluoroacetic acid (TFA) in water and B. 0.05% TFA in 100% acetonitrile. The gradient was run as follows: 5 minutes isocratic pre-run at 100% A, followed by a linear gradient from 2-50% B over 40 minutes. The column was then washed in 100% B for a further 10 minutes. During the elution gradient, a sample was spotted at 10 second intervals using a Probot (Dionex) with α-cyano-4-

hydroxycinnamic acid (CHCA) at 3mg/ml (70% MeCN, 0.1% TFA) at a flow rate of 1.2ul/min. Both MS and Tandem MS (MS/MS) analysis was performed on the fractionated peptides using an Applied Biosystems 4800 MALDI-TOF/TOF mass spectrometer (Applied Biosystems Inc., Foster City, CA, USA). The mass spectrometer was operated under control of 4000 Series Explorer v3.5.2 software (Applied Biosystems). Peak lists of MS and MS/MS spectra were generated using 4000 Series Explorer v3.5.2 software after selective labelling of monoisotopic mass peaks. An automated database search was run using GPS Explorer v3.6 (Applied Biosystems). MASCOT was used as the search engine to search NCBInr database using the following search parameters: precursor ion mass tolerance of 50ppm, fragment ion mass tolerance of 0.3Da, the taxonomy was selected as human and oxidation of methionine residues were allowed as variable modifications. The identification criterion was at least 2 peptides by MS/MS with total ion score confidence intervals of at least 95%.

2.3.5 Cell adherence/spreading:

Twenty four well tissue culture plates were coated in either recombinant or purified ECM proteins (type I collagen, decorin or fibronectin) or MSC-CM as described above (section 2.3.1). L929 fibroblasts and HaCaT keratinocytes were seeded at a density of 2×10^5 cells per well in serum-free DMEM/F12 supplemented with 1% penicillin/streptomycin (Sigma-Aldrich) and 1% ITS-X (Sigma-Aldrich). Plates were then incubated for 2 hours at 37°C and 5% CO_2 and digitised images were captured with an inverted microscope (Inverso TC100, Medline Scientific LTD) and digital camera (ProgRes CF, Jenoptik).

2.3.6 Cell proliferation:

L929 and HaCaT cell proliferation was investigated using the MTS (3-(4, 5-dimethylthiazol-2-yl)-5-(3-carboxymethoxyphenyl)-2-(4-sulfophenyl)-2H-tetrazolium) assay. This assay determines cell number by measuring the degree of cellular metabolism within a sample as mitochondrial reductases convert MTS into a coloured formazan product (Cory *et al.* 1991). Cells were seeded into 96 well plates in 100µl DMEM/F12 culture medium containing 10% FCS and 1% penicillin and streptomycin at a seeding density of 1×10^4 cells per well, incubated for 2 hours at 37°C and 5% CO_2 (to permit cell adhesion) and then washed repeatedly by centrifugation at 1000rpm for 10 minutes and re-suspension in serum free unconditioned medium. Cells were then maintained in either serum free unconditioned medium or in each of three separate samples of MSC-CM (i.e. from 3 different donor MSC cultures). The relative number of viable cells present at the 24, 48 and 72 hours time-points following this treatment was subsequently determined by adding the MTS solution for 3 hours, after which time the absorbance was read at

490nm. The values obtained were compared to a 'standard curve' of absorbance values for a range of known cell populations to determine the number of viable cells present in each experimental well.

2.3.7 Multi-array ELISA

Detection of cytokines within MSC-CM was carried out using an ELISArray kit (SA Bioscience, Maryland USA) according to the manufacturer's instructions: Samples of MSC-CM were prepared by centrifugation for 10 minutes at $1000 \times g$ to remove any particulate material that might be present. The ELISArray kit reagents: wash buffer concentrate, assay buffer stock, sample dilution buffer stock and the ELISArray plate were thawed and maintained at room temperature whilst the 10% BSA and donkey serum were thawed at room temperature and kept on ice until required.

The wash buffer concentrate was shaken to suspend any precipitate and 50ml of wash buffer concentrate was diluted into distilled water to a final volume of 500ml. Assay buffer was prepared by diluting 0.6ml of 10% BSA into a final volume of 30ml with assay buffer stock, and sample dilution buffer was prepared by dilute 2ml of 10% BSA into a final volume of 20ml with sample dilution buffer stock.

An antigen standard cocktail was generated by thawing antigen standards on ice for 20 minutes and mixed by gentle vortexing. A concentrated antigen standard cocktail containing all 12 of the antigen standards was prepared in a single tube pipetting 10μl of each antigen standard into the same 880μl volume of the appropriate sample dilution buffer to yield 1ml of a concentrated antigen standard cocktail. 200μl of the concentrated standard antigen cocktail was then diluted into 800μl of the sample dilution buffer to form the final antigen standard cocktail. 50μl of assay buffer was added each well of the ELISArray plate using a multi-channel pipettor and 50μl of the sample dilution buffer into each well of row A in the ELISArray plate to set up

the negative control, followed by 50µl of MSC-CM into each well of rows B through G. 50µl of the final antigen standard cocktail was added into each well of row H to set up the positive control. Thus prepared, the ELISArray plate was gently shaken for 10 seconds to ensure the complete mixing of the reagents before being allowed to stand for 2 hours at room temperature.

Meanwhile, the development solution and stop solution were allowed to warm to room temperature in lab bench drawer protected from light, whilst the detection antibodies were thawed on ice for 30 minutes, 855µl of assay buffer was added to each tube of detection antibody and the resulting solutions were gently mixed before being transferred to the appropriate tube of the detection antibody tube strip.

After 2 hours at room temperature, the contents of the ELISArray plate were removed form the wells and discarded before washing each well with 350µl of wash buffer, gently shaking the plate for 10 seconds and then removing the wash buffer from each well and blotting the plate upside down on absorbent paper to remove any residual buffer. This wash process was then repeated a further two times for a total of three washes before transferring 100µl of the dilute detection antibodies from the dilution tube strip to the appropriate rows of the ELISArray plate and again gently shaking the plate for 10 seconds to mix the reagents and allowing the plate to stand for a further 60 minutes at room temperature.

Whilst the plate was left to stand, avidin-HRP conjugate was thawed on ice for 20 minutes, mixed gently and then 11µl of the avidin-HRP conjugate added to 11ml of assay buffer before removing the contents of the ELISArray plate and again washing the plate as before: rinsing each well with 350µl of wash buffer, gently shaking the plate for 10 seconds and then removing the wash buffer and blotting the plate upside down on absorbent paper. 100µl of avidin-HRP was then added to all

wells and the plate again shaken for 10 seconds to mix before being allowed to stand for 30 minutes at room temperature in the dark and then washed four times as previously described.

Finally, 100μl of development solution were added to each well, the plate left for 15 minutes at room temperature in the dark and then 100μl of stop solution added to each well. The absorbance of each well was read at 450nm and 570 nm immediately after the addition of the stop solution, and the latter subtracted from the former to give the final absorbance, ranging from 0.00 to 2.50, for each well.

2.4 Data analysis

2.4.1 Image analysis:

Digitised images of scratch-wounds were analysed using Image-J software (Collins, 2007) to measure the width of the scratch at previously defined points along its length equating to the top, middle and bottom of the field of view (Figure 2.3.1-B). Images of cell adherence/spreading were analysed using the same software to measure the area of the imaged cells (Figure 2.3.2).

2.4.2 Statistical analysis and experimental replicates:

Data has been presented in all Figures as means with error bars to represent standard errors of the mean (SEM) derived from the standard deviation (σ) using the formula

$sem = \frac{\sigma}{\sqrt{n-1}}$ presented as means (± SEM) in text. Statistical analysis of experimental data was performed using the Mann-Whitney U test and, when comparing more than two means, a non-parametric analysis of variance (ANOVA), i.e. the Kruskal-Wallis test, where significant differences between individual means were determined by *post-hoc* analysis using Tukeys HSD (honest significant difference) test. In all cases, a 95% confidence interval ($p < 0.05$) was considered to be significant, indicated by an asterisk within Figures. Experimental procedures using MSC-CM were performed as a single independent experiment using CM generated from MSC cultures derived from each of three individual donors, i.e. n=3. All data from experiments examining the effects of cytokines and ECM components on L929, HaCaT, or Ea-Hy926 cell lines were pooled from two independent experiments, i.e. n=2, normalised to percentage wound closure to account for variability in the values (though not their relative magnitudes) observed between these independent experiments; the means ± SEM were calculated and statistical analysis performed using this pooled data. Studies performed using L929, HaCaT, or Ea-Hy926-CM were also performed twice i.e. through two independent experiments where data was similarly pooled and analysed. Each independent experiment consisted of at least n=4 internal replicates (i.e. wells). All images shown of cells in culture were drawn from single representative experiments.
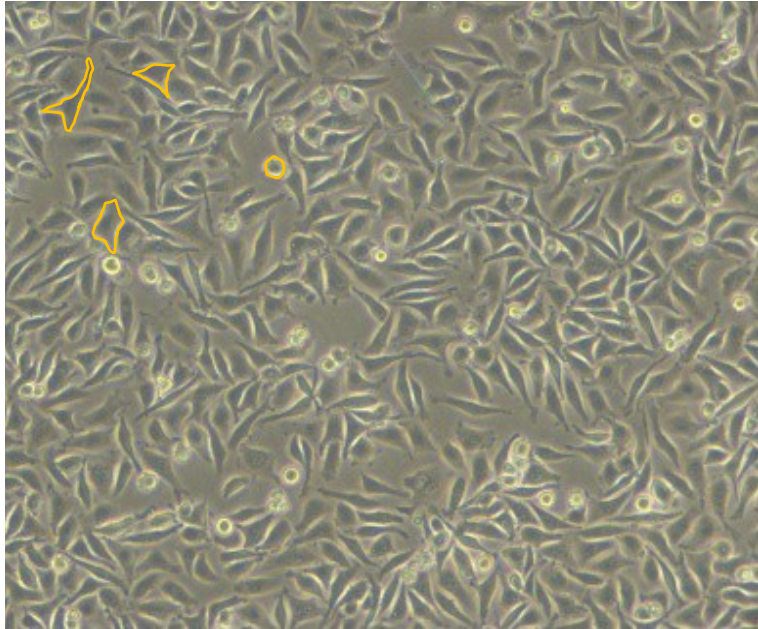
Figure 2.3. Cell area outlining: An example of the outlines (yellow) used to determine the area of cells from digital images.

Chapter 3

An *in vitro* investigation of the paracrine activity of mesenchymal stem cells on skin wounds using the scratch assay.

3.1 Aims and Background.

The healing of cutaneous wounds requires complex interactions between the dermal and epidermal cells, the extracellular matrix (ECM), and the nervous and vascular components of the damaged and surrounding skin (Harding *et al,* 2002, Metcalf and Ferguson, 2007). The precise involvement of many of these various factors has been identified by a combination of *in vitro* and *in vivo* studies. As described in the Introduction, MSC have been observed to promote skin wound healing *in vivo*; however the mechanisms responsible for such MSC-enhanced wound healing are currently unclear. Despite evidence supporting the capacity of MSC to differentiate or trans-differentiate along a variety of dermal and epidermal cell lineages (Sasaki *et al,* 2008, Wu *et al,* 2007; Liu *et al,* 2007), it has been suggested that the low levels of MSC engraftment after transplantation indicate that their beneficial effects are more likely mediated through the secretion of soluble factors rather than through their long-term presence as cellular components of subsequently repaired tissue (Prockop 2007).

This thesis has sought to elucidate, in part, how MSC may influence skin wound healing by affecting the behaviour of resident skin cells. The initial stages of this investigation involved the establishment and characterisation of an *in vitro* skin wound model, the scratch assay. A confluent monolayer of cells is grown on a defined surface substrate, in this case type I collagen-coated tissue culture plastic, and then scored with a sterile point, i.e. a pipette tip. The remaining adherent cells are then observed as they repopulate the scratched area, effectively "healing the wound". A tumour-derived dermal fibroblast cell line, L929 (Earle *et al,* 1943), and an immortalised human keratinocyte cell line, HaCaT (Boucamp *et al,* 1988) were used to conduct scratch assays. These skin cell lines were used both because their behaviour was considered likely to be relatively consistent from experiment to

experiment, and also due to difficulties in obtaining sufficient numbers of primary skin cells.

The aim of the first part of this study was to compare how the two skin cell types brought about closure of the scratch assay, as single cell type cultures and co-cultures. In particular, the study compared scratch assays of L929 and HaCaT cultures, and L929: HaCaT co-cultures, in the presence and absence of supplementary serum. Subsequently, experiments were performed to examine the influence of MSC-secreted factors on L929 and HaCaT cells, both as single cell and co-culture scratch assays. These latter studies tested the effects of serum-free culture conditioned medium which had been derived from primary cultures of human MSC. Finally, the contents of the MSC conditioned medium (MSC-CM) were analysed by a combination of ELISA and mass spectrometry.

3.2: L929 fibroblast and HaCaT keratinocyte wound models.

In the presence of serum, confluent monolayers of L929 fibroblasts appeared to respond to the scratch injury and migrate into the scratched area to bring about wound closure more rapidly than monolayers of HaCaT keratinocytes (Figure 3.1). This was also true in L929: HaCaT co-cultures, where the fibroblasts again appeared to respond to the injury and migrate faster than the keratinocytes, such that at wound closure the scratched areas were filled almost exclusively with L929 cells (Figure 3.2). There was no obvious loss of cell adhesion or viability during the wound closure of either of the single cell type scratch assays or in the co-cultures. It was also apparent that the L929 cells and HaCaT keratinocytes in co-culture were compatible, with no evidence of repulsion upon cell-cell contact.

The increased response of L929 cells to scratch injuries was marked and significant. Hence, 12 hours after scratching, the extent of wound closure was in L929 cultures was 49% (±5%), compared to only 15% (±3%) in HaCaT cultures (p<0.05, *Mann Whitney U test*). At this 12 hour time point, the extent of wound closure in L929: HaCaT co-cultures was also significantly greater (56% ±4%), than that seen in HaCaT cultures (p<0.05 *Mann Whitney U test*) (Figure 3.3). There was no significant difference in wound closure at the 12 hour time point between L929 and co-cultures.

In similarly designed scratch assays performed in serum free conditions L929 fibroblasts again appeared to respond to the scratch injury and close scratch wounds more rapidly than HaCaT keratinocytes (Figure 3.4). Furthermore, in L929: HaCaT co-cultures the L929 fibroblasts also filled the scratched area to the apparent exclusion of HaCaT keratinocytes (Figure 3.5). In serum free conditions, the extent of wound closure 12 afters after scratching was 47% (±7%) for L929 cells compared with only 15% (±4%) for HaCaT cells (p<0.05 *Mann Whitney U test*), whilst the

extent of closure in co-cultures at the same time point was 56% (±9%) (Figure 3.6). There was no significant difference in wound closure at the 12 hour time point between L929 and co-cultures in serum free conditions, although there was an observable difference compared to those scratches performed in the presence of exogenous serum.

Although the extent of wound closure was similar in serum versus serum free conditions at earlier time points (i.e. 12 hours), at later time points it was apparent that L929 fibroblasts effected wound closure more rapidly in the presence of serum than the absence of serum. Hence in the presence of serum all scratches of L929 fibroblasts exceeded 90% wound closure within 21 hours of scratching in all instances, whereas this level of wound closure was only seen after 42 hours in serum free conditions. In contrast, serum deprivation did not significantly influence the later stages of wound closure in HaCaT scratch assays, which achieved >90% wound closure after 48 hours in both serum and serum free conditions in all instances. There was no clear loss of cell adhesion or decreased cell viability in L929, HaCaT or co-cultures throughout the time course.

	L929	HaCaT
0 hr		
12 hr		
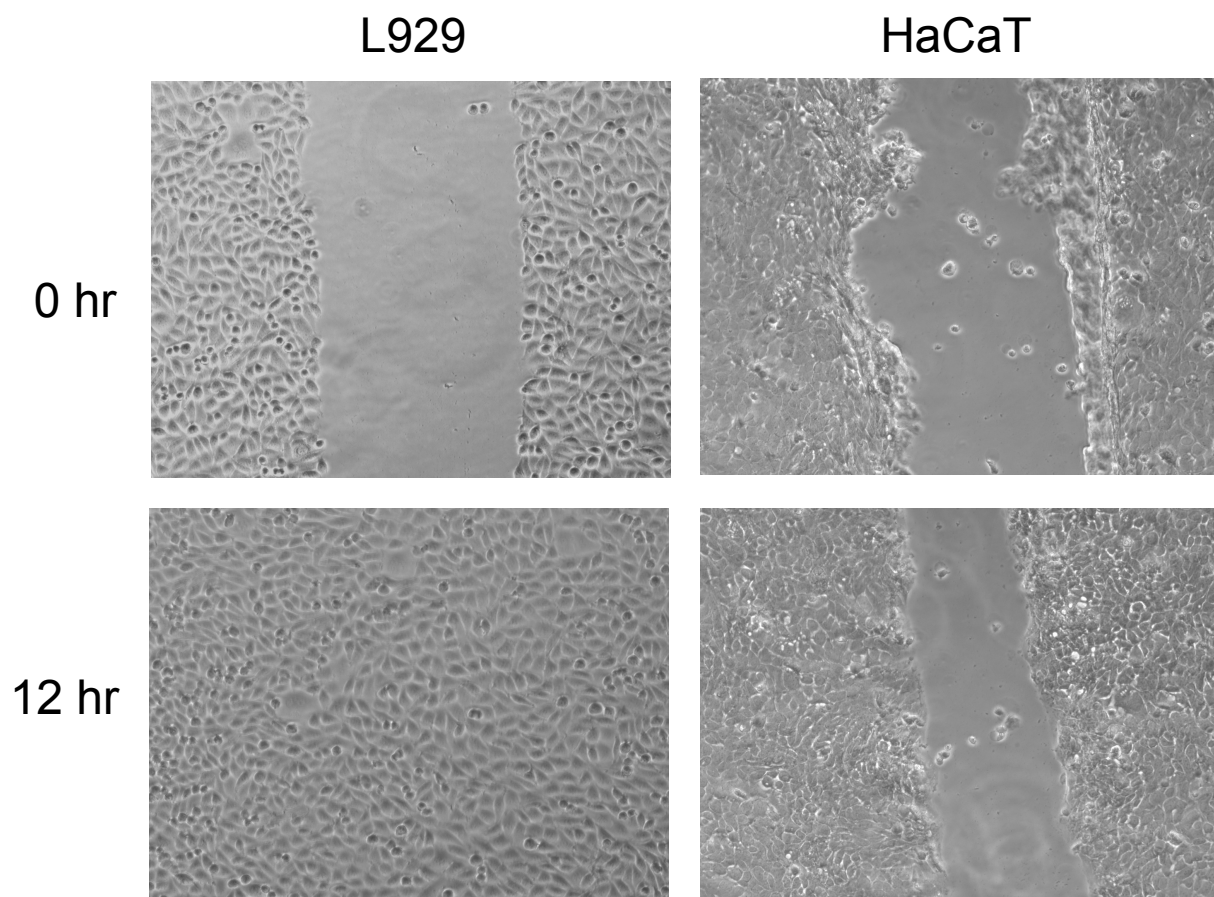
Figure 3.1 L929 fibroblasts closed scratch wounds faster than HaCaT keratinocytes. Representative phase contrast images are shown of single cell type (L929 or HaCaT) scratch assays immediately following the scratch and 12 hours thereafter. Original magnification is x10.
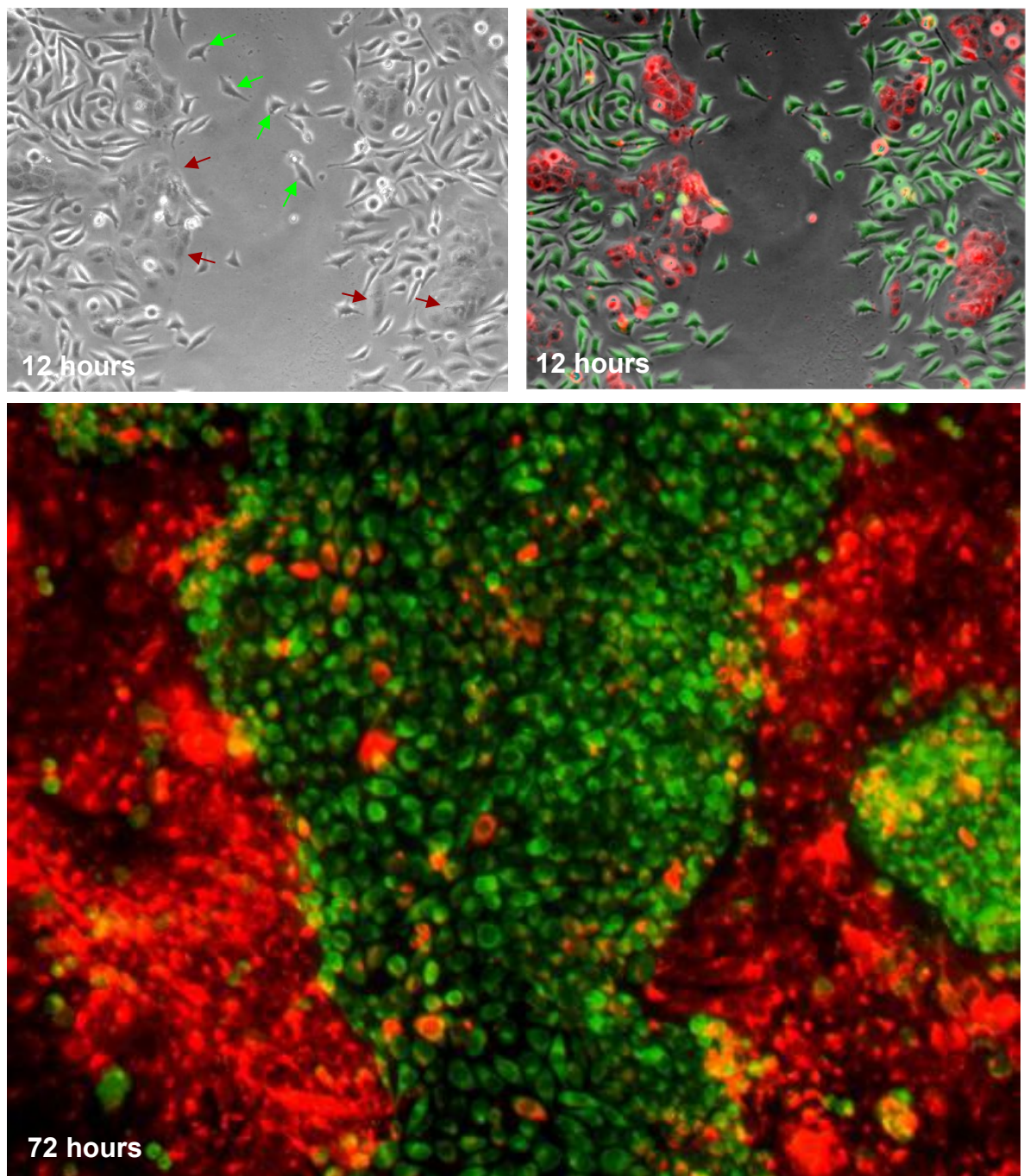
Figure 3.2 In co-cultures, L929 fibroblasts closed scratch wounds faster than HaCaT keratinocytes. In co-cultures of L929 fibroblasts and HaCaT keratinocytes, the L929 fibroblasts (fluorescently tagged green) appeared to migrate faster than the HaCaT keratinocytes (fluorescently tagged red) to close scratch wounds, thereby filling the scratch area almost to the exclusion of HaCaT cells. Representative digitised images are shown of phase constrast microscopy (top left) with green and red fluorescence images overlaid at 12 hours after the scratch was formed, along with green and red fluorescence images overlaid at wound closure (72 hours in this instance. All images were collected at original magnification of x10.
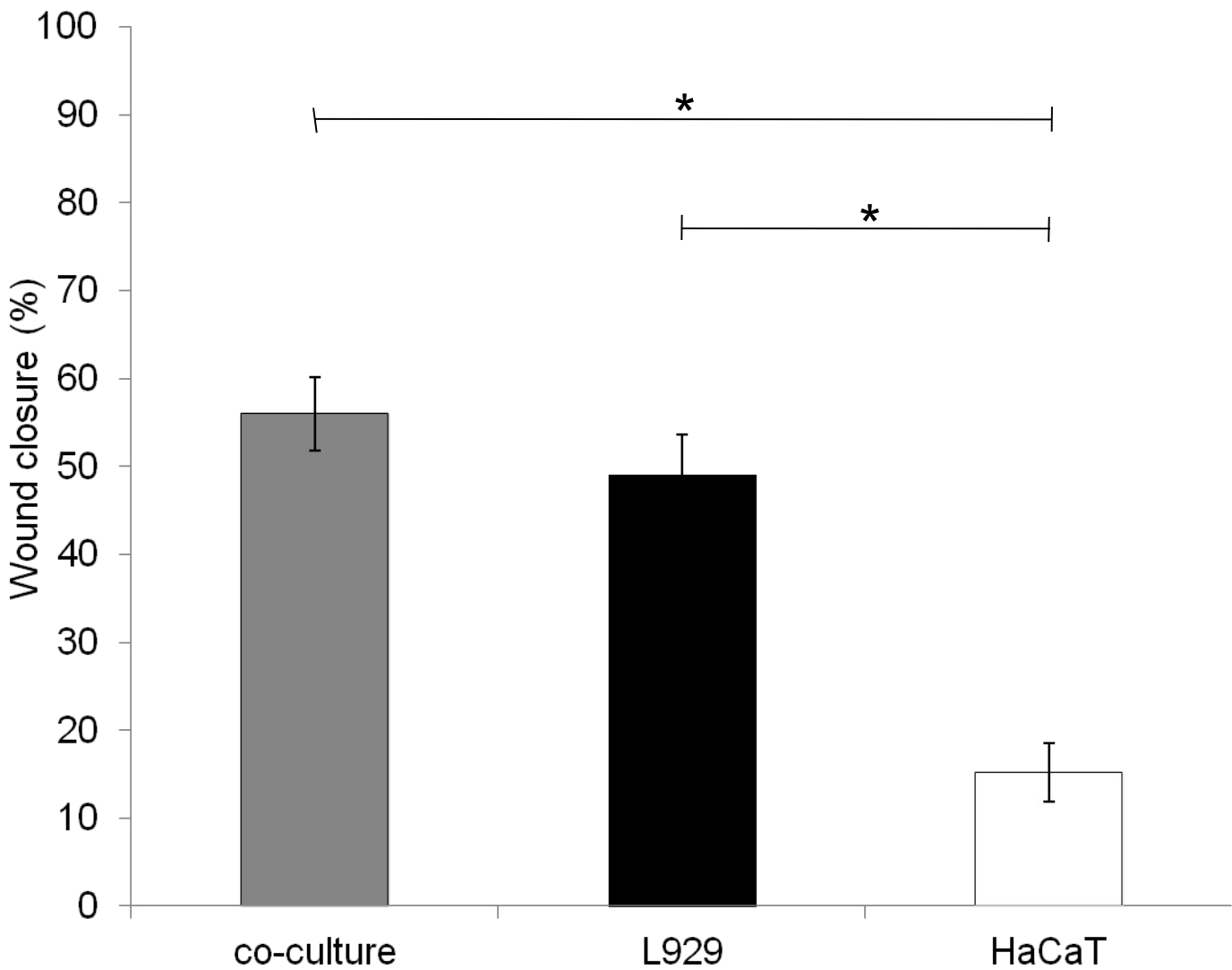
Figure 3.3 Scratch wound closure by L929 fibroblasts and HaCaT keratinocytes. Twelve hours post-scratch, the extent of wound closure was 49% (±4.6%) for L929 cells, 15% (±3.4%) for HaCaT and was 56% (±4%) for L929:HaCaT co-cultures. Data shown are means ± SEM There was a significant difference by ANOVA (p<0.05). (* denotes significance by Tukey's HSD).
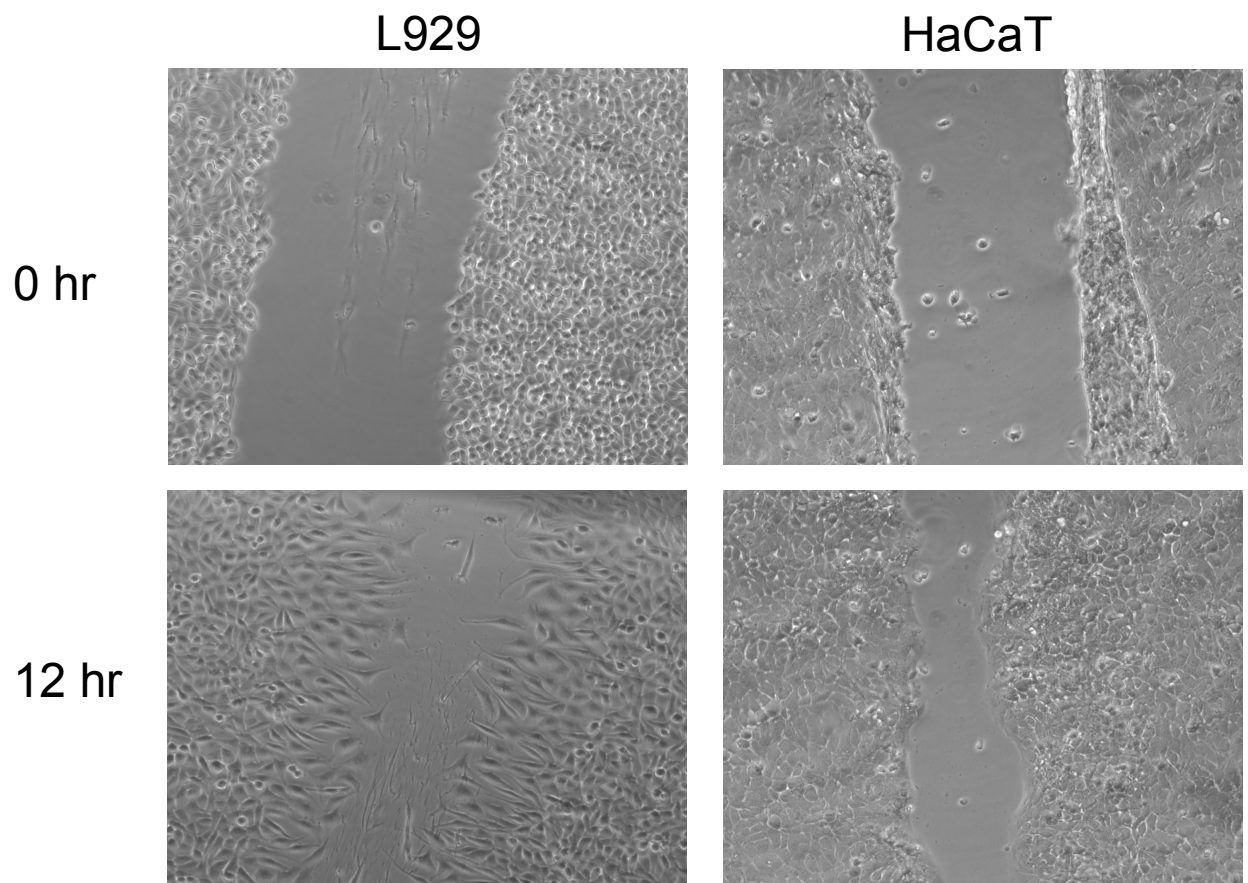
Figure 3.4 In serum free conditions L929 fibroblasts closed scratch wounds faster than HaCaT keratinocytes. Representative phase contrast images are shown of single cell type (L929 or HaCaT) scratch assays immediately following the scratch and 12 hours thereafter. Original magnification is x10.

Figure 3.5 In serum free co-cultures L929 fibroblasts closed scratch wounds faster than HaCaT keratinocytes. In serum free conditions L929 fibroblasts (fluorescently tagged green) appeared to migrate faster than HaCaT keratinocytes (fluorescently tagged red) in co-cultures of both cell types, thereby filling the scratch area almost to the exclusion of HaCaT cells. Representative digitised fluorescent and phase contrast images are shown of co-culture (both L929 and HaCaT) scratch assays immediately following the scratch and representative phase contrast images are shown of successive time points thereafter. Original magnification is x10.
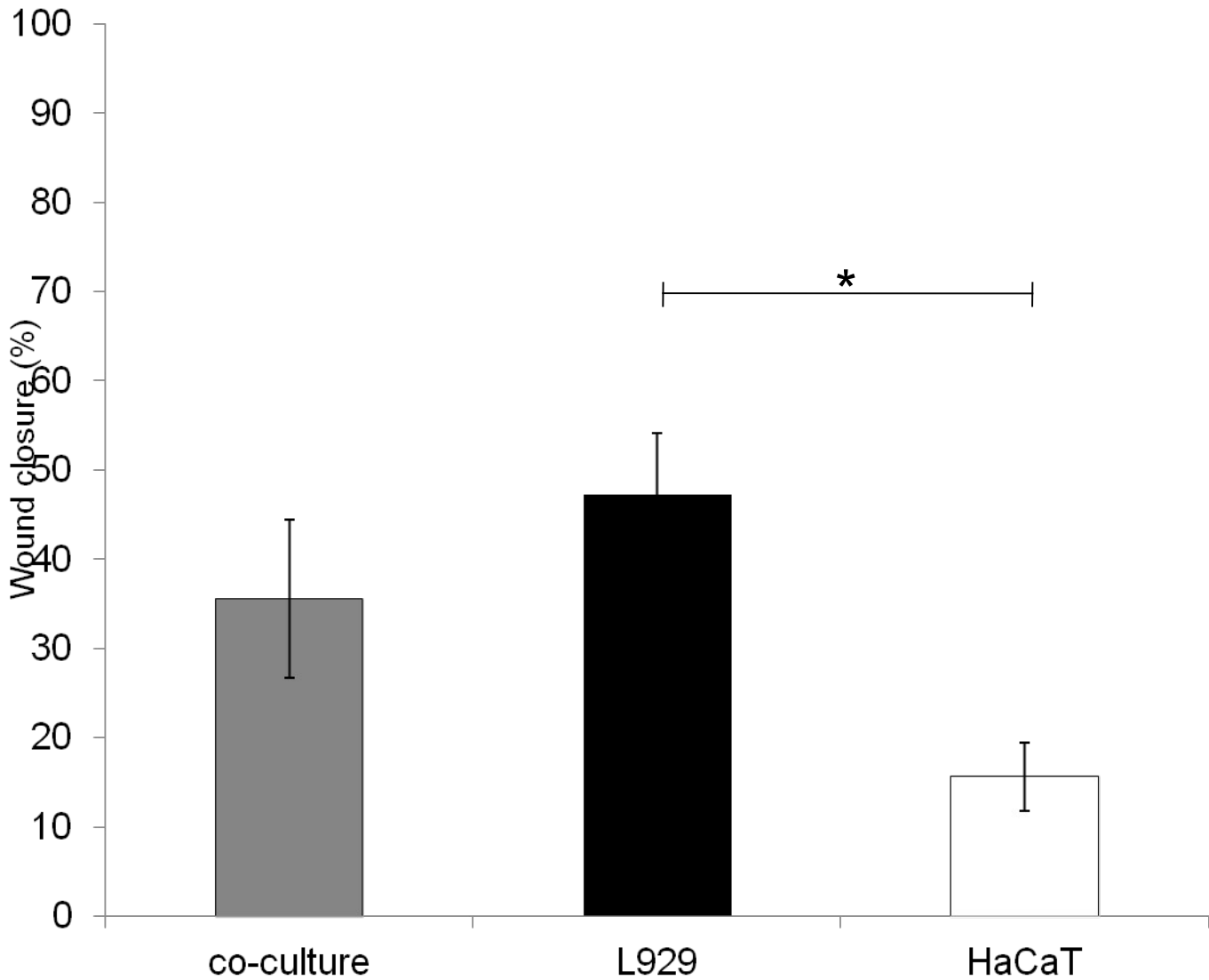
Figure 3.6 Scratch wound closure by L929 fibroblasts and HaCaT keratinocytes in serum free conditions. Twelve hours post-scratch, the extent of wound closure in serum free conditions was 47% (±6.9%) for L929 cells, 15% (±3.8%) for HaCaT and was 56% (±8.8%) for L929:HaCaT co-cultures. There was a significant difference by ANOVA ($p<0.05$). (* denotes significance by Tukey's HSD).

3.3: MSC-CM enhances L929 fibroblast and HaCaT keratinocyte scratch wound closure *in vitro.*

MSC-CM significantly enhanced the rate of wound closure in single cell L929 fibroblast scratch assays in serum-free conditions (Figure 3.7). Hence, 9 hours after scratches, all L929 cultures had closed in the presence of serum free MSC-CM (100% ±0% closure), while those in unconditioned serum free media had only closed by 51% (±10%) (p<0.05 *Mann Whitney U test*) (Figure 3.8). Similarly, serum free MSC-CM significantly enhanced the closure of HaCaT keratinocyte scratch assays (Figure 3.9), although these remained slower than L929 scratch assays. After 27 hours, those HaCaT scratch assays performed in serum free MSC-CM were closed by 95% (±3%), whereas those performed in unconditioned serum free media had only closed by 57% (±8%) (p<0.05 *Mann Whitney U test*) (Figure 3.10). Scratch assays in co-cultures of L929 fibroblasts and HaCaT keratinocytes were also seen to close faster in the presence of serum free MSC-CM than in unconditioned serum free media. In contrast to the co-culture scratch assays in serum free unconditioned media, L929 and HaCaT cells both appeared to fill the scratch area in the presence of MSC-CM (Figure 3.11). In the L929: HaCaT co-cultures, the scratches in serum free MSC-CM had closed by 76% (±6%) after 12 hours compared to 35% (±13%) in unconditioned serum free media (p<0.05 *Mann Whitney U test*) at the same time point (Figure 3.12).

There was no clear loss of cell adhesion or decreased cell viability in L929, HaCaT or co-cultures throughout the time course of these experiments. In addition, L929 fibroblasts and HaCaT keratinocytes also appeared compatible in co-culture in serum free MSC-CM. To address whether serum free MSC-CM may have stimulated cell proliferation (and to further test that cells remained viable) in addition to cell

migration during wound closure, L929 fibroblast and HaCaT keratinocyte cultures were established in 96 well plates in serum free MSC-CM versus serum free unconditioned media. The MTS assay was then performed to ascertain the relative number of viable cells. There was a non-significant, but marked increase in the number of both L929 and HaCaT cells present at 72 hours in serum free MSC-CM compared to serum free unconditioned media. However, no marked increases in viable cell number were seen for either cell type over the first 48 hours of incubation, i.e. within the time frame of L929 and HaCaT wound closure in serum-free MSC-CM (Figure 3.13).

In contrast to serum free MSC-CM, neither serum free L929-CM nor serum free HaCaT-CM affected the rate of wound closure in scratch assays of either cell type at any time during the wound healing process. For example, when wound closure of single cell L929 scratch assays was 48% (±7%) in serum free control media (at 12 hours in this set of experiments), wound closure was only 43% (±8%) in serum free L929-CM and only 42% (±17%) in serum free HaCaT-CM at the same time point. Similarly, when wound closure of single cell HaCaT scratch assays was 15% (±4%) in serum free control media (also at 12 hours), it was only 14% (±8%) in serum free L929-CM and 20% (±5%) in serum free HaCaT-CM (Figure 3.14)

	MSC-CM	control
0 hr		
9 hr		
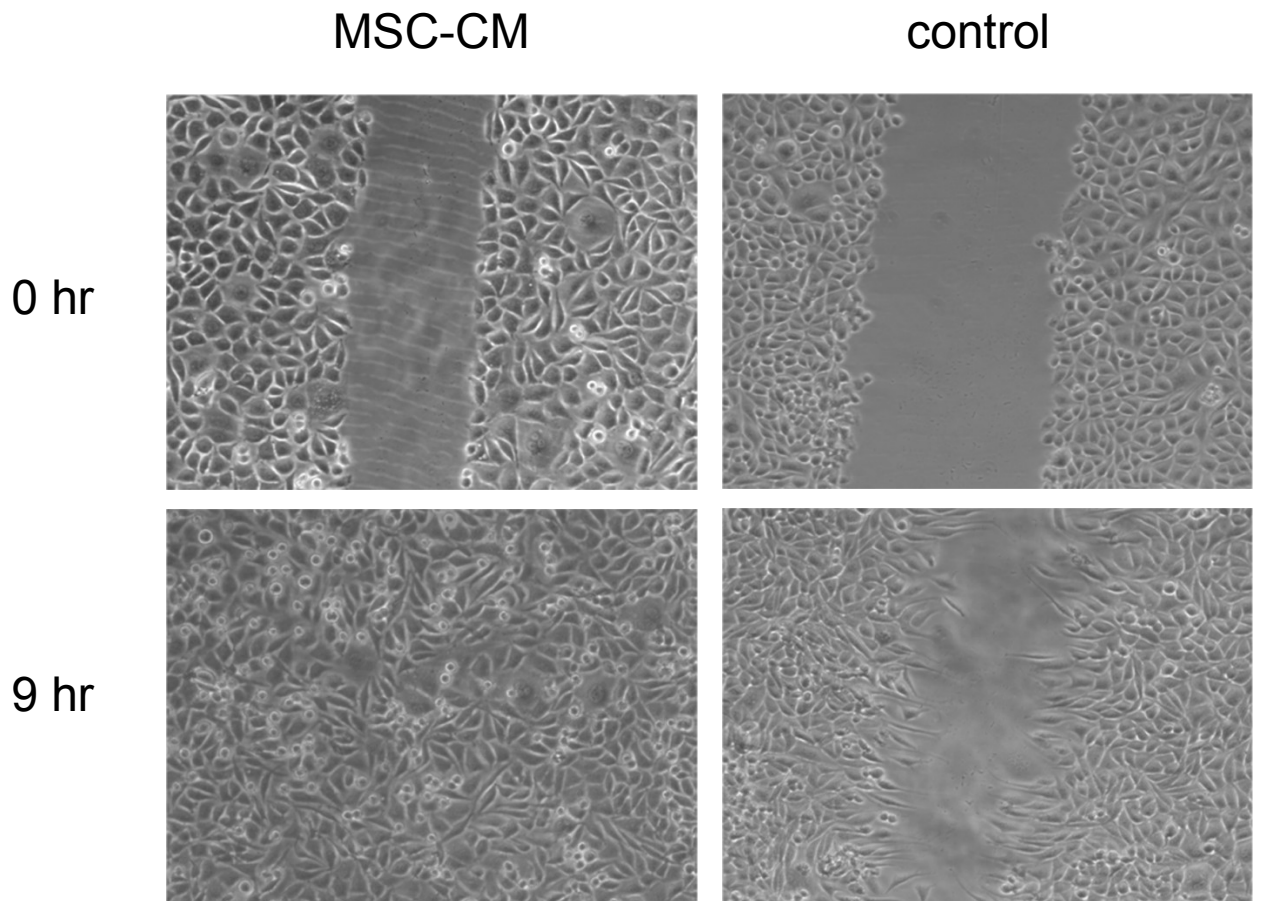
Figure 3.7 L929 fibroblasts closed scratch wounds faster in the presence of MSC-CM than in unconditioned control media. Representative phase contrast images are shown of single cell type (L929) scratch assays immediately following the scratch and 9 hours thereafter. Original magnification is x10.
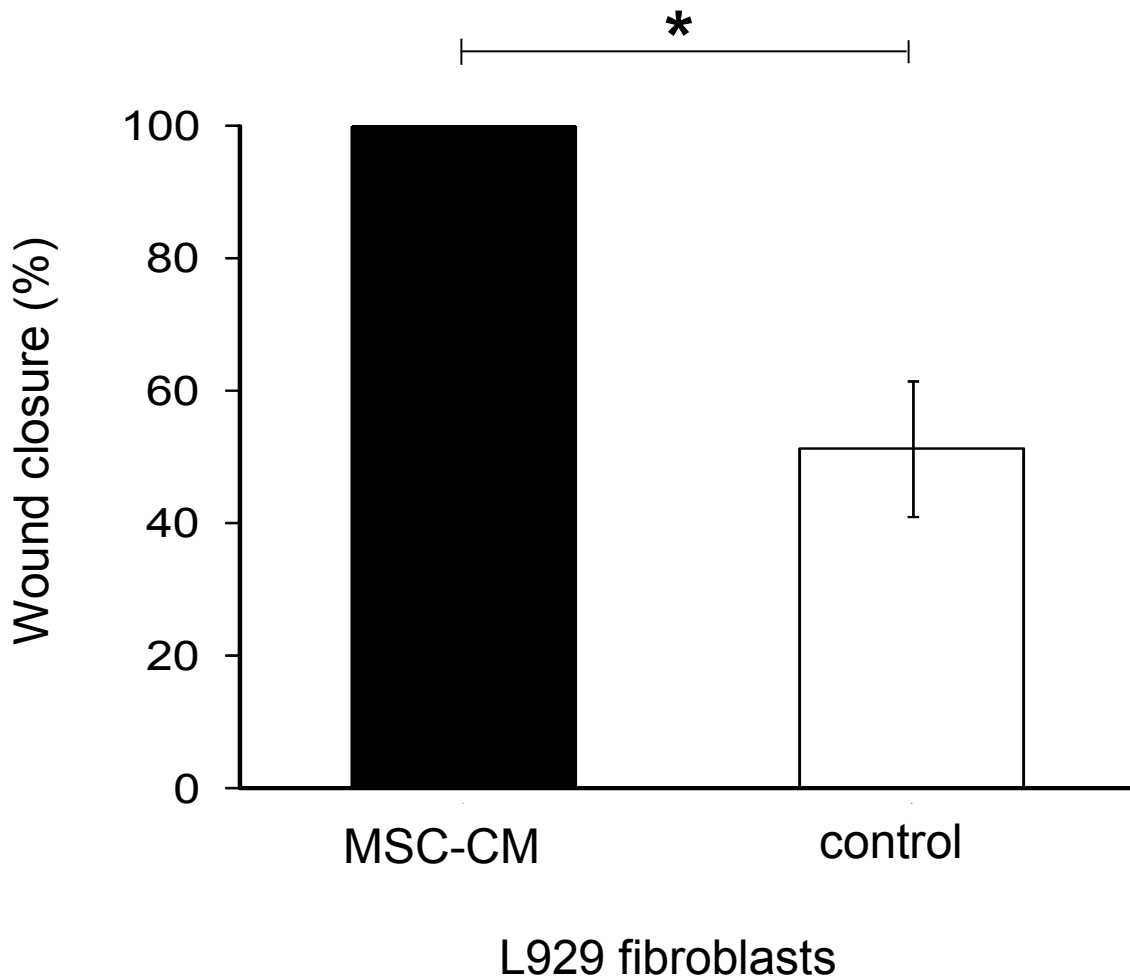
Figure 3.8 Scratch wound closure by L929 fibroblasts in MSC-CM. Nine hours post scratch, L929 fibroblasts had achieved 100% (±0%) wound closure in the presence of MCS-CM, while those in unconditioned media had only closed by 51% (±10.2%). Data shown are means ± SEM (*= $p < 0.05$ Mann Whitney U test).
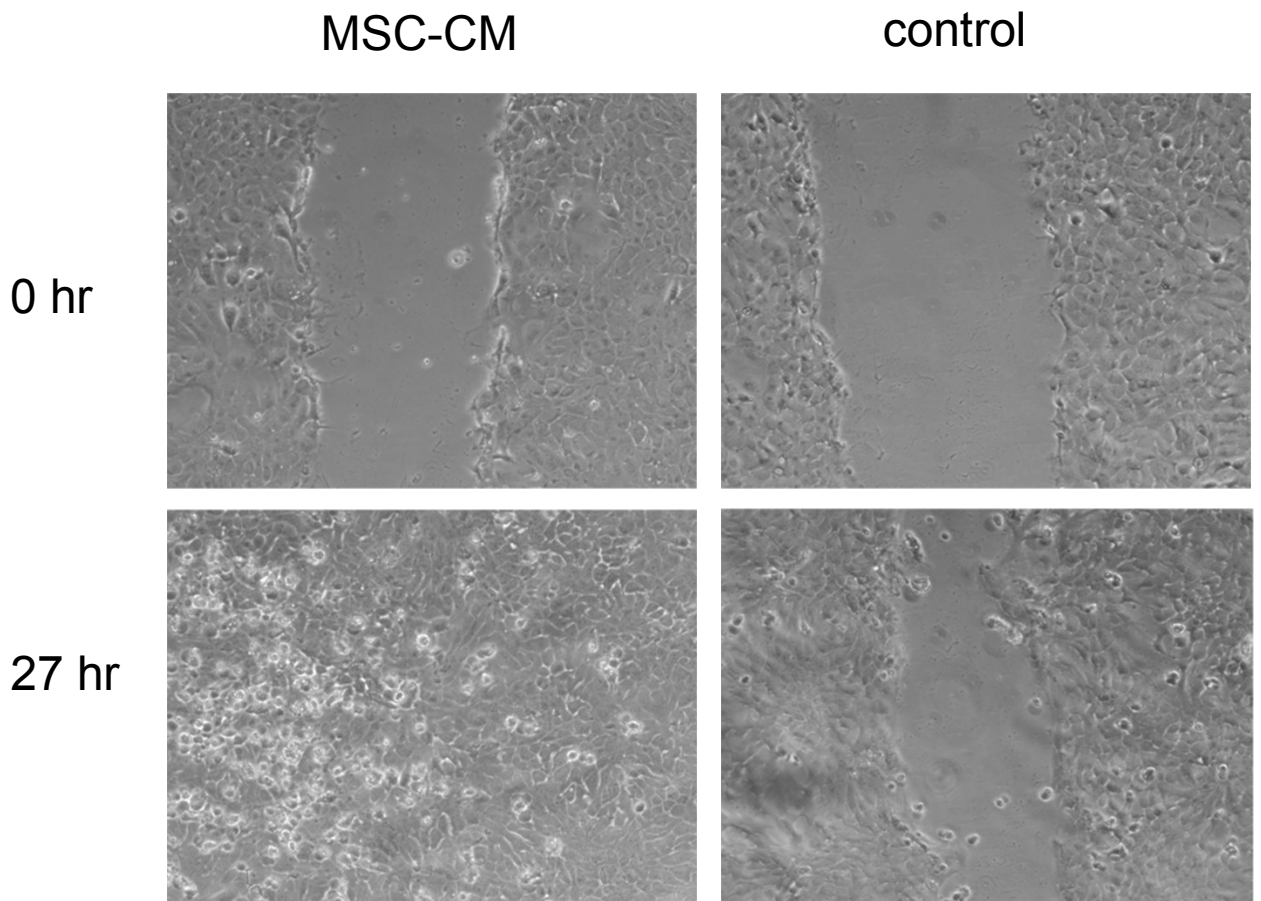
Figure 3.9 HaCaT keratinocytes closed scratch wounds faster in the presence of MSC-CM than in unconditioned control media. Representative phase contrast images are shown of single cell type (HaCaT) scratch assays immediately following the scratch and 27 hours thereafter. Original magnification is x10.
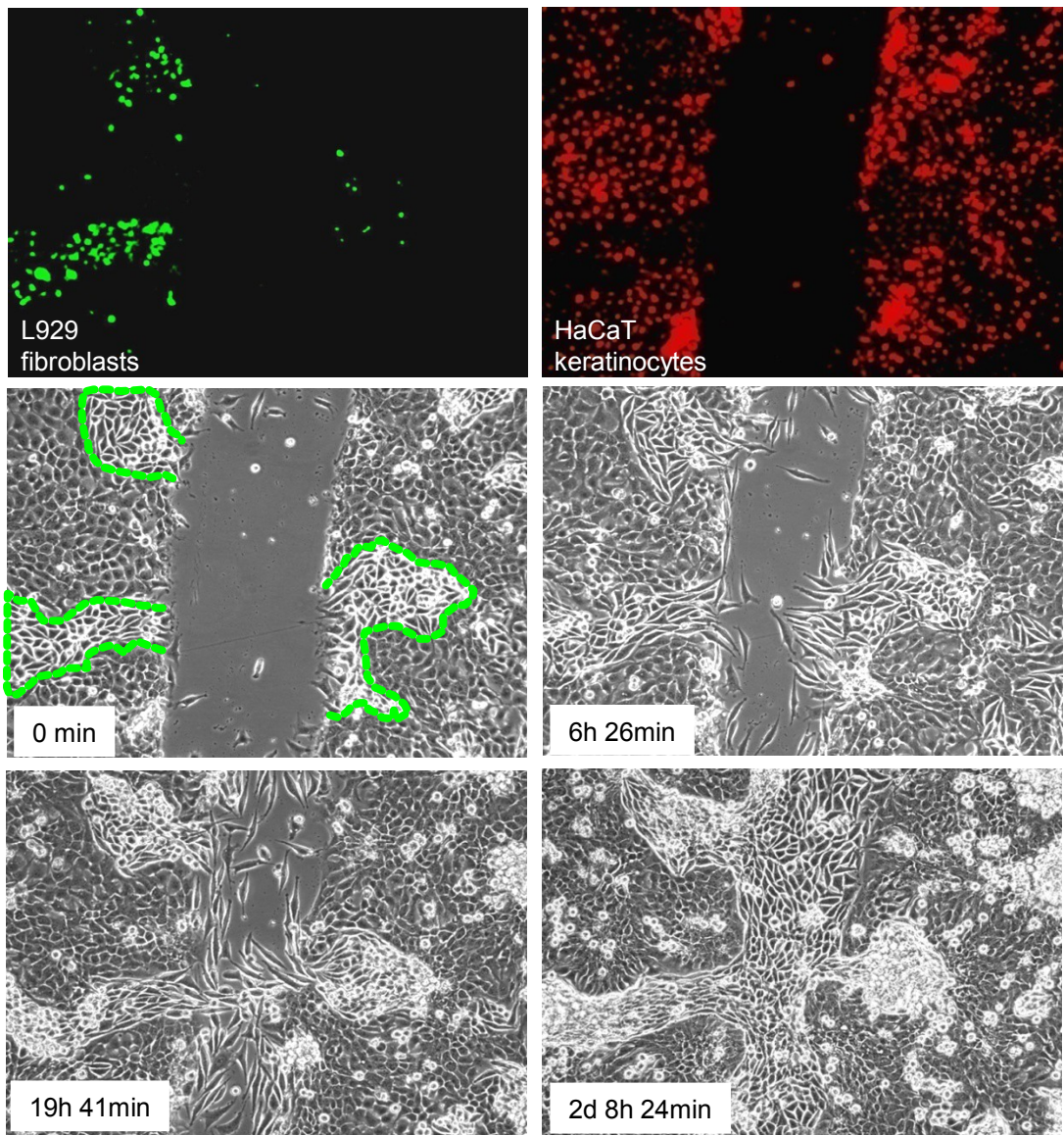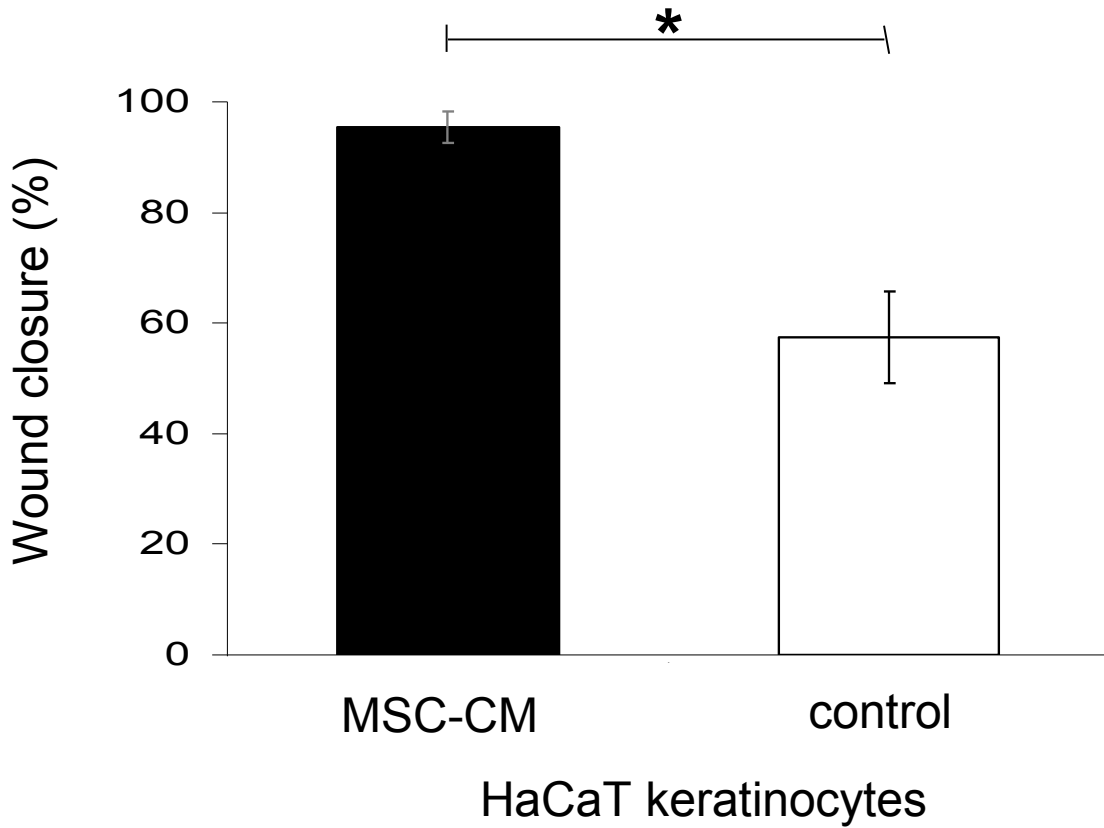
Figure 3.10 Scratch wound closure HaCaT keratinocytes in MSC-CM. Twenty seven hours post scratch, HaCaT keratinocytes had achieved 95% (±2.8%) wound closure in the presence of MCS-CM, while those in unconditioned media had only closed by 57% (±8.3%). Data shown are means ± SEM (*= p<0.05 Mann Whitney U test).
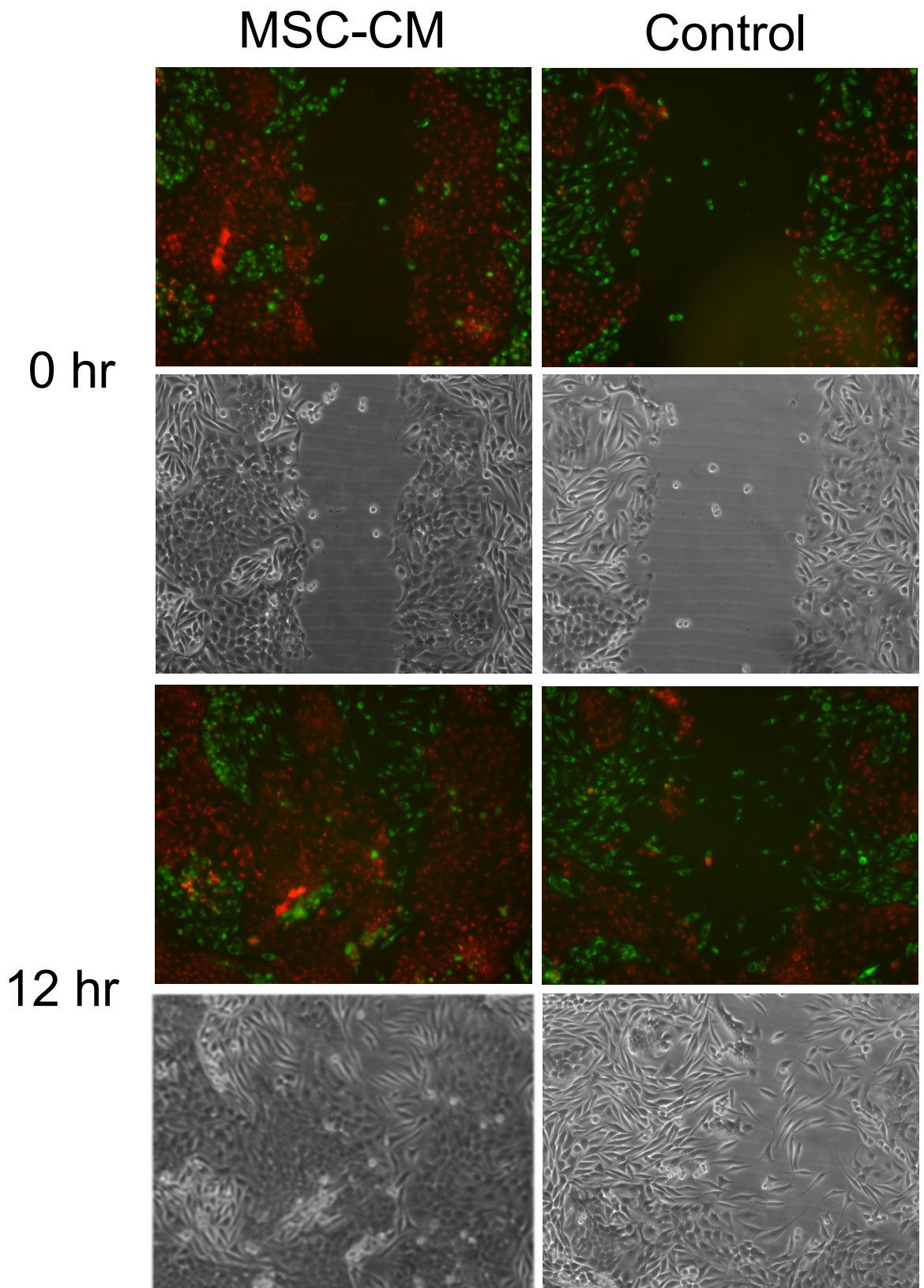
Figure 3.11 L929 fibroblast and HaCaT keratonocyte co-cultures close scratch-wounds more rapidly in MSC-CM than in unconditioned media. In co-cultures of L929 fibroblasts and HaCaT keratinocytes, the L929 fibroblasts (fluorescently tagged green) and the HaCaT keratinocytes (fluorescently tagged red) appeared to close scratch wounds more rapidly in the presence of MSC-CM than in unconditioned control media. Representative digitised images are shown of both phase constrast microscopy and digitied images with green and red fluorescence overlaid immediately following the scratch and 12 hours thereafter. All images were collected at original magnification of x10.
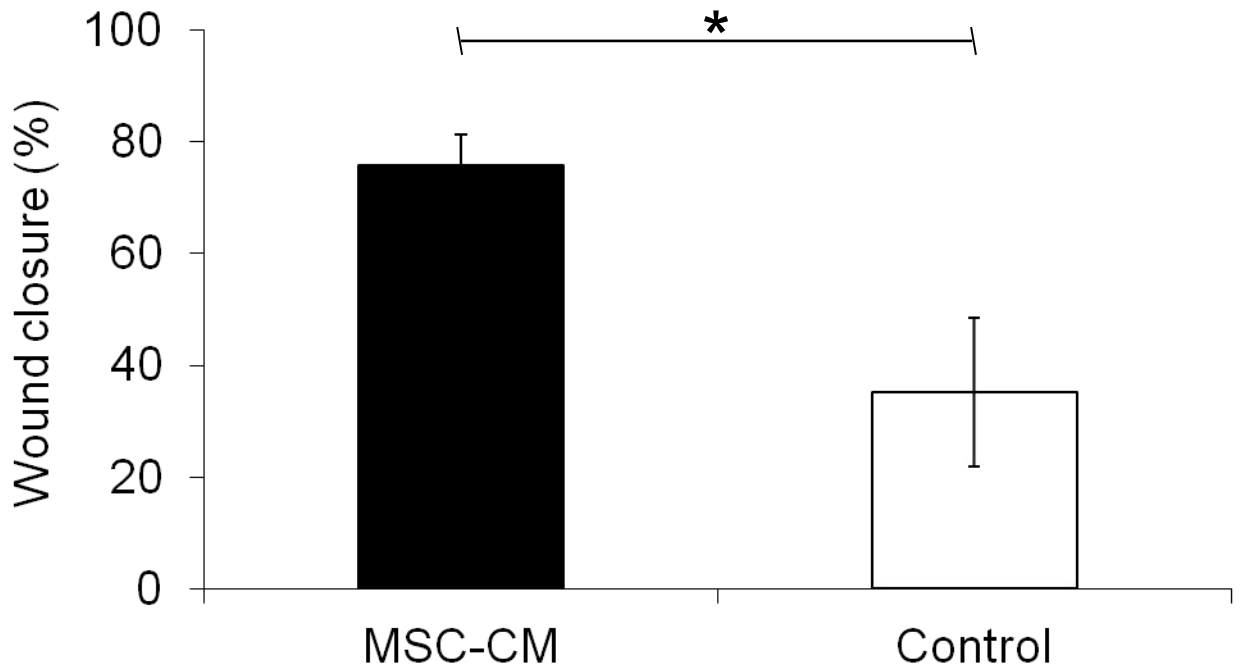
Figure 3.12 Scratch-wound closure by L929 fibroblasts and HaCaT keratinocyte co-cultures in MSC-CM. Twelve hours post scratch, L929:HaCaT co-cultures had achieved 76% (±5.7%) wound closure in the presence of MCS-CM, while those in unconditioned media had only closed by 35% (±13.3%). Data shown are means ± SEM (*= $p < 0.05$ Mann Whitney U test).

A

L929 fibroblasts

V bä ℓ eℓ slℓ DQ a t094mm (

2
1.8
1.6
1.4
1.2
1
0.8
0.6

24 hr   48 hr   72 hr

B

HaCaT keratinocytes

0.4

0.35

0.3

0.25

0.2

24 hr   48 hr   72 hr
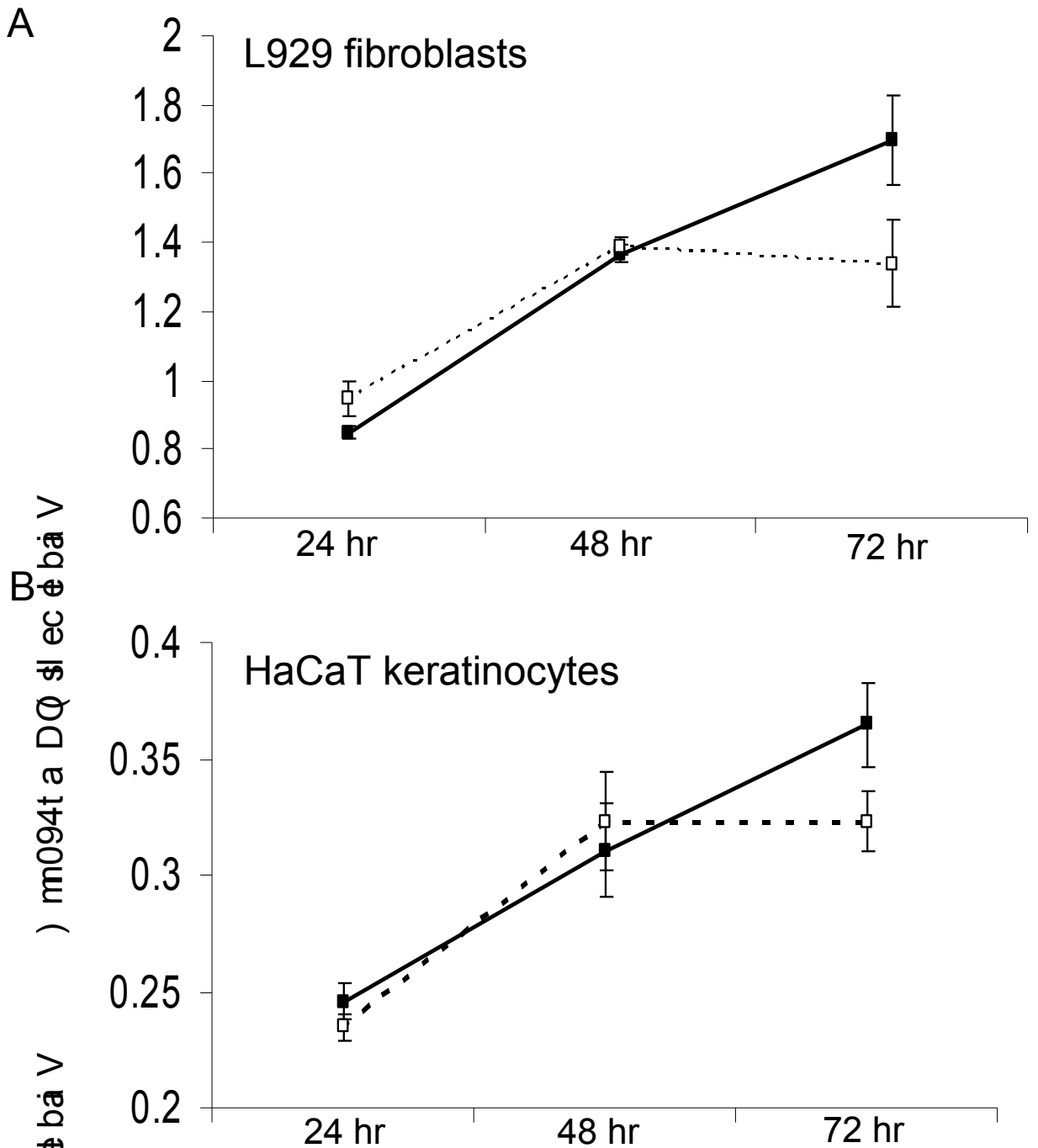
Figure 3.13 MSC-CM did not significantly increase cell number over 72 hours. Over 48 hours there was no significant difference in either L929 fibroblast or HaCaT keratinocyte cell number between cultures in MSC-CM (solid line) and those in unconditioned control media (broken line). After 72 hours there was a marked but not statistically significant difference. Data shown are means ± SEM (p>0.05 Mann Whitney U test).
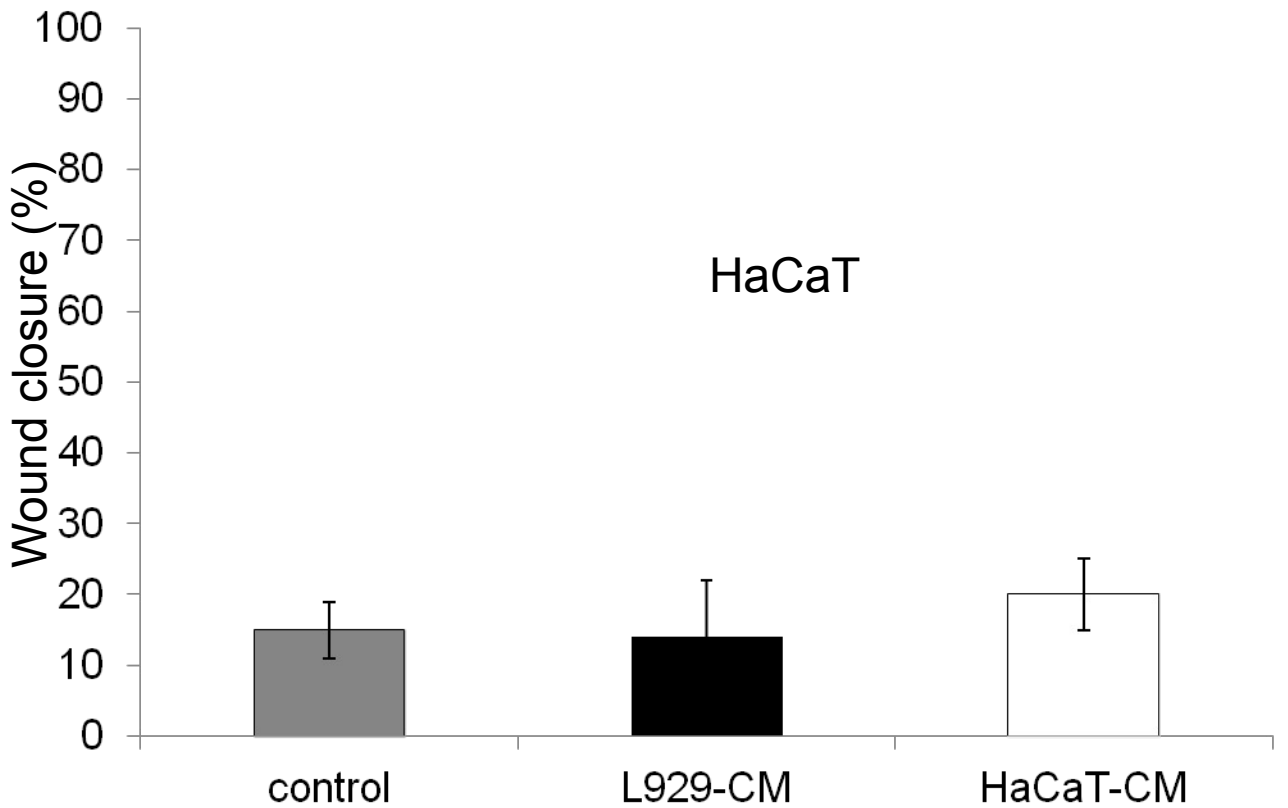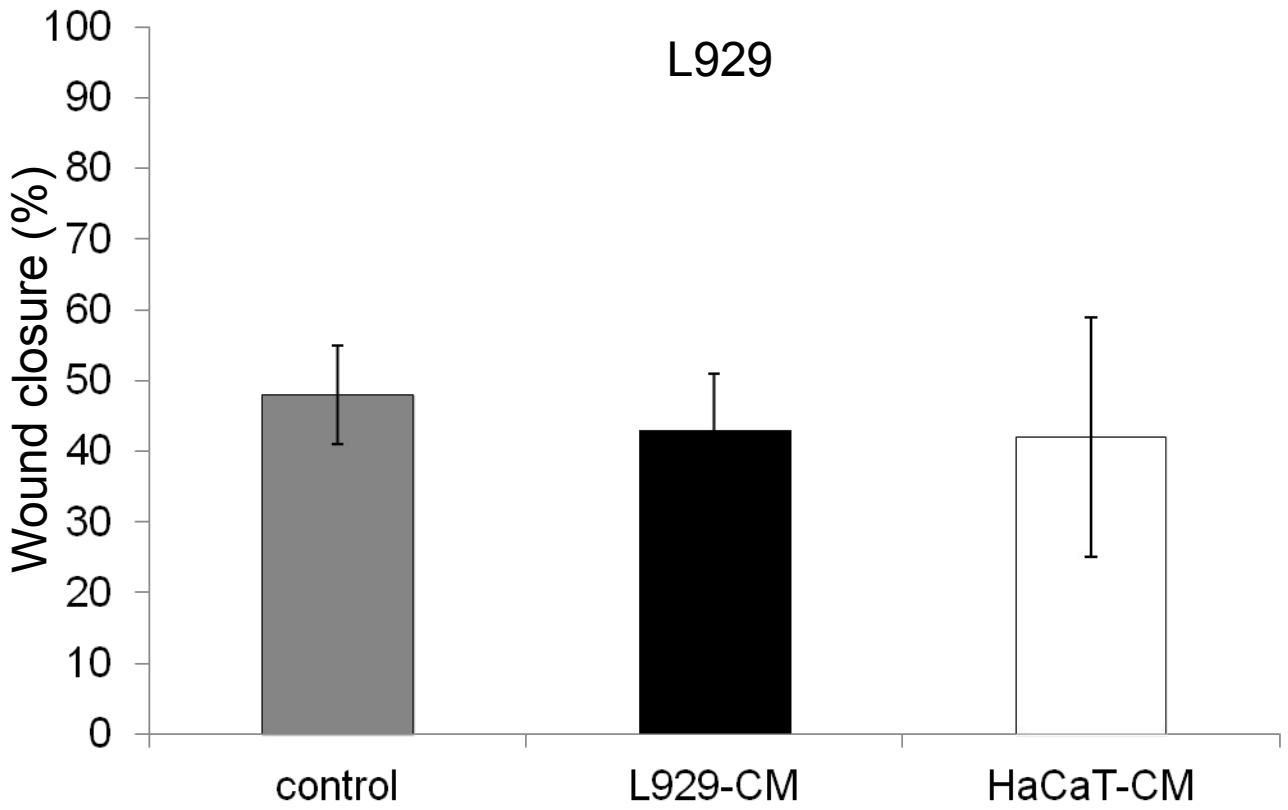
Figure 3.14 Twelve hours post-scratch, neither L929-CM or HaCaT-CM enhanced wound closure in cultures of either cell type compared to unconditioned media. Data shown are means ± SEM (p>0.05 ANOVAt).

3.4: The secretome of MSC-CM

Serum free MSC-CM was assayed to determine the presence of secreted cytokines or ECM components that may have influenced L929 fibroblast or HaCaT keratinocyte cell growth, migration and/or wound closure. Detectable levels of interleukin (IL)-6, IL-8, transforming growth factor-β1 (TGF-β1), monocyte chemotactic protein-1 (MCP-1) and RANTES (Regulated upon Activation, Normal T-cell Expressed, and Secreted) were found in the MSC-CM by ELISA (Figure 3.15). In contrast, IL-1a, IL-1b, IL-4, IL-10, IFN-γ, TNF-α, and growth regulated oncogene-α (GRO-A) were not detected. In addition, the ECM components collagen types I, V, VI and XII and fibronectin were detected in serum free MSC-CM by MALDI-TOF/TOF mass spectrometry, along with secreted protein acidic and rich in cysteine (SPARC) and insulin-like growth factor binding protein-7 (IGFBP-7) (Table 3.1).
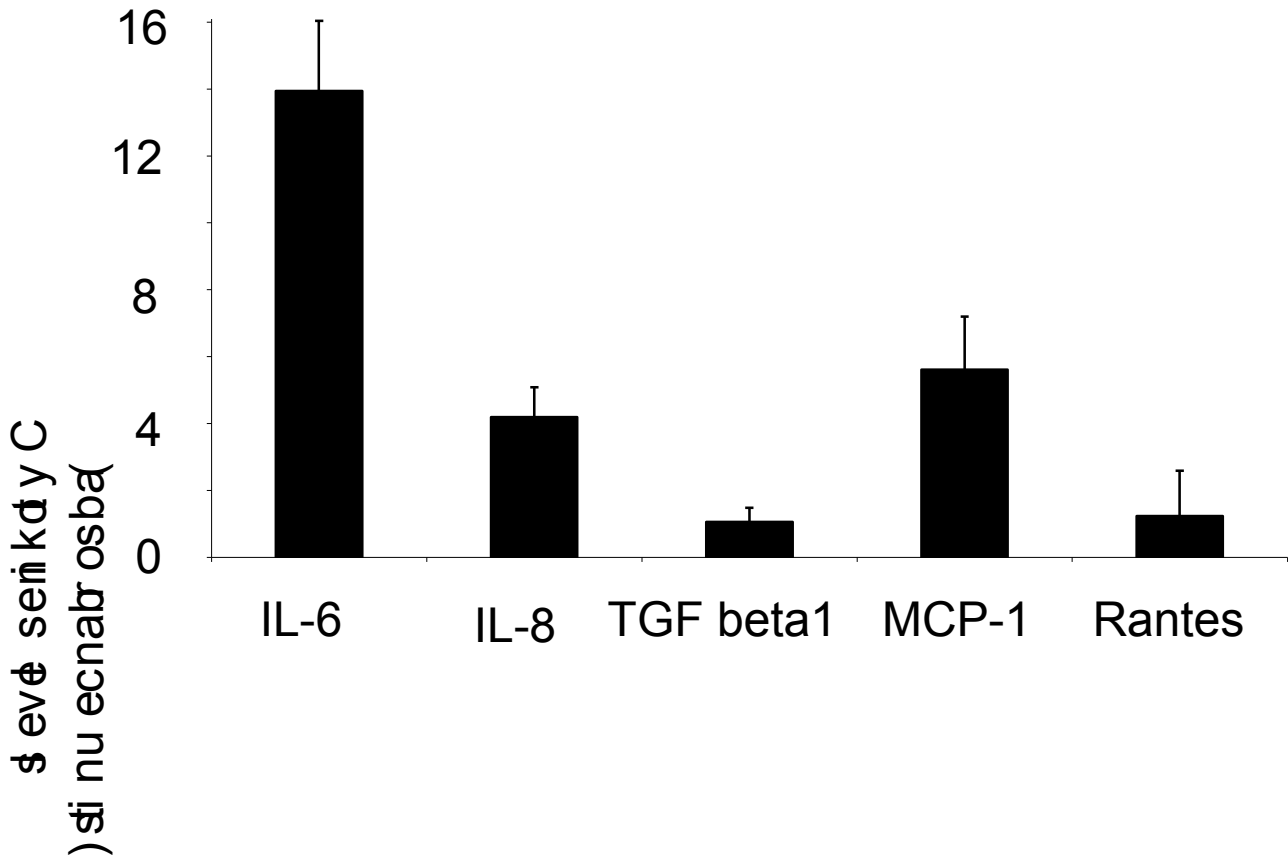
Figure 3.15 Cytokines present in the MSC secretome. ELISA analysis of MSC-CM showed detectable levels of interleukin (IL)-6, IL-8, transforming growth factor-β1 (TGF-β1), monocyte chemotactic protein-1 (MCP-1) and Rantes. IL-1a, IL-1b, IL-4, IL-10, interferon-γ (IFN-γ), tumour necrosis factor-α (TNF-α), and growth regulated oncogene-α (Gro-A) were not detected. Data shown are means ± SEM.

TABLE 1:   PROTEINS DETECTED IN MSC CONDITIONED MEDIUM VIA MASS SPECTROMETRY (MALDI TOF/TOF)

Protein Name	Accession Number	Peptide Count	Total Ion Score C.I.%
Collagen type I (alpha 1 chain)	gi22328092	16	100
Collagen type I (alpha 2 chain)	gi48762934	27	100
Collagen type V (alpha 2 chain)	gi16197600	3	100
Collagen type VI (alpha 1 chain)	gi87196339	10	100
Collagen type XII (alpha 1 long isoform)	gi93141047	6	99.999
Fibronectin	gi4204943	8	99.999
Fibronectin (type III domain)	gi55667857	2	96.825
SPARC	gi2624793	3	96.613
Insulin-like growth factor binding protein 7	gi4504619	4	100

Table 3.1 Mass spectrometry of MSC-CM. MALDI-TOF/TOF mass spectrometry of MSC-CM detected collagen types I, V, VI and XII, fibronectin, secreted protein acidic and rich in cysteine (SPARC) and insulin-like growth factor binding protein-7 (IGFBP-7).

3.5: Discussion

Cell migration is a rate limiting event in skin wound healing. Hence, the study of factors that influence dermal fibroblast and epidermal keratinocyte migration may help target therapies for improved cutaneous wound healing. In this set of *in vitro* investigations, the scratch assay was used to show that L929 fibroblasts migrated to effect wound closure more rapidly than HaCaT keratinocytes. In co-culture, the L929 fibroblasts were seen to fill the closed scratch almost entirely to the exclusion of the HaCaT keratinocytes, both in the presence or absence of serum supplementation. The chronology of cell migration into human cutaneous wounds is currently unclear. However, a recent study has suggested that dermal fibroblasts along with dermal microvascular endothelial cells may migrate into the wounded area prior to keratinocytes (Kehe *et al*, 1999). It was further suggested that dermal fibroblast migration is then halted as keratinocytes migrate to initiate re-epithelialisation, after which a further wave of fibroblast migration occurs during the tissue remodelling stage of wound healing. If this order of skin cell migration is correct, then the novel co-culture scratch assay reported here using L929 and HaCaT cell lines may prove useful in identifying factors that influence cutaneous wound healing. The interaction of dermal fibroblasts and epidermal keratinocytes plays an important role in the healing process. Hence, the incorporation of both cell types in this co-culture model may be more representative of *in vivo* skin wound healing than the use of either cell type alone.

The differences in healing rates seen in scratch assays of L929 or HaCaT cells as single cell types may simply be due to the fact that the L929 fibroblasts were murine in origin, whilst the HaCaT keratinocytes were human. Furthermore, L929 is

derived from a tumour (Earle *et al,* 1943) whilst HaCaT is an immortalised cell line (Boukamp *et al,* 1988). As such, these cells may differ in their behaviour from normal human cells *in vivo*. However, the use of cell lines in this study eliminates potential donor variations in primary skin cell cultures, which has thereby allowed for the development of a consistent model to assay the effects of MSC derived factors from a number of separate MSC isolates.

The stimulatory activity of MSC-CM was established in serum free conditions. Hence, it was possible to identify a number of MSC secreted factors in MSC- CM, including factors that are known to promote cutaneous wound healing. TGF-β1 has diverse roles in cutaneous wound healing, including a stimulatory activity on re-epithelialisation, wound contracture, angiogenesis, scar formation and ECM deposition (Barrientos *et al,* 2008). In particular, TGF-β1 stimulates increased cell migration in dermal fibroblasts (Postlethwaite *et al,* 1987) and keratinocytes (Li *et al,* 2006). Studies of knock-out mice have suggested that IL-6 forms an essential element of the normal cutaneous wound healing process by influencing dermal fibroblast migration (Luckett-Chastain & Gallucci, 2009), and has also been shown to influence keratinocyte migration (Gallucci *et al,*2004) and proliferation (Sato *et al,* 1999), whilst IL-8 similarly promotes skin re-epithelialisation by increasing keratinocyte migration (Michel *et al,* 1992) and proliferation (Tuschil *et al,* 1992). MCP-1 and RANTES may also function to promote dermal wound healing as a chemoattractant to cells of the immune system, particularly macrophages (Dipietro *et al,* 2001)

The increase in L929 and HaCaT cell number over the course of wound closure in co-culture scratch assays was non-significant for either cell type; both in serum free unconditioned media or in serum free MSC-CM. This overall lack of an

increase in cell number may not preclude some localised proliferation, or indeed enhanced cell survival, around the scratch wound margins contributing to an enhancement in wound closure; nonetheless, the lack of any change in overall cell number does seem to support the assertion that increased cell migration may have been the main contributing factor. In addition, serum free MSC-CM was found to have little effect on L929 or HaCaT cell proliferation or survival, as assessed via the MTS assay. The moderate difference seen in the viable cell number present in serum free MSC-CM compared with serum free unconditioned media at 72 hours was at a time point outside of the time course of scratch wound closure in the presence of serum free MSC-CM. Furthermore, there were no obvious differences in the adherence of L929 or HaCaT cells in serum free MSC-CM or serum free unconditioned media in the scratch assays themselves. Therefore, the activity of serum free MSC-CM on scratch wound closure may be more readily attributed to stimulation of increased fibroblast and keratinocyte cell migration, rather than increased cell proliferation or survival. As described above, several of the MSC secreted growth factors and chemokines are likely targets for this stimulatory activity of cell migration in L929 and HaCaT scratch assays. The composition of the ECM plays a major role in regulating cell migration (Lauffenburger & Horwitz 1996) and a number of ECM components in serum free MSC-CM were identified by mass spectrometry (non of the cytokines found to be present using ELISA were detected by this method). Prominent amongst these were collagen type I and fibronectin, which are well-characterised stimulatory factors of fibroblast and keratinocyte cell adhesion and migration. The potential involvement of TGF beta, fibronectin, along with decorin, in enhancing wound closure by L929 and HaCaT cells has been investigated in Chapter 4.

Also detected was the extracellular glycoprotein SPARC (osteonectin). Elevated levels of SPARC expression have been observed in cells at wound sites (Reed *et al,* 1993) and it has been demonstrated that the absence of SPARC is associated with impaired fibroblast migration (Basu *et al,* 2001). Conversely, the absence of SPARC has also been shown to accelerate wound closure in SPARC-null mice (Bradshaw *et al,* 2002), but this study suggested that this effect may have been due to an associated reduction in collagen content in skin, which in turn lead to increased wound contractibility. Insulin-like growth factor binding proteins (IGFBP) play an important role in skin homeostasis, modulating IGF-mediated enhancement of dermal and epidermal cell migration, survival and proliferation (Edmonson *et al,* 2003). In particular, IGFBP-7 has been shown to regulate the proliferation and survival of both HaCaT and primary human keratinocytes *in vitro* (Nousbeck *et al,* 2009). This suggests that IGFBP-7 in serum free MSC-CM may have contributed to the increased wound closure seen in HaCaT keratinocyte scratch assays. However, further experiments that specifically target IGFBP-7 in MSC-CM are required to confirm such activity.

Chapter 4

An *in vitro* investigation of the role of individual MSC-CM components on wound healing.

4.1. Aims and Background

Mesenchymal stem cells (MSCs) have been suggested to stimulate wound healing via paracrine effects on skin cells. In the previous chapter, ELISA and MALDI-TOF/TOF Mass spectrometry were used to show that MSCs secrete the ECM proteins fibronectin, decorin and collagen type I as well as cytokines such as IL-6, IL-8 and TGF- β, amongst other factors. Here, we have investigated the differential effects of these factors on wound healing. Previous studies have investigated the effects of certain of these factors, e.g. a topical application of fibronectin has been shown to enhance *in vivo* wound healing in rats (Kwon *et al,* 2007) and TGF-β1 has been shown to promote human keratinocyte migration (Nam *et al*, 2010). As healing progresses through inflammatory and remodeling phases, levels of cytokine expression alters as does ECM composition, changing from a matrix rich in fibronectin to one containing more collagen type I and decorin. Therefore possible temporal and constituent variations in the effects of wound healing mediators resulting from different ECM composition may be of interest when considering the potential clinical application of MSC-CM or MSC derived factors to enhance cutaneous wound healing.

This chapter has sought to identify the different factors secreted by MSC that contribute to the enhancement of scratch wound healing seen in the presence of MSC-CM. As in the previous chapter the primary investigative technique employed was the scratch assay, incorporating the L929 fibroblast cell line and the HaCaT keratinocyte cell line. In addition to the effects of various factors on *in vitro* wound healing, their influence on cell adhesion was observed by quantifying the relative degree of cell spreading after two hours in culture. These experiments were conducted in the

absence of supplementary FCS, as the effects of MSC-CM were observed in serum-free conditions.

4.2. The effects of MSC secreted cytokines on L929 fibroblasts and HaCaT keratinocytes.

Transforming Growth Factor-β1; TGF-β1 supplemented (serum free) media had little effect on the rate of scratch wound closure by L929 fibroblasts on collagen (Figure 4.1). After 12 hours post-scratch l929 fibroblasts had achieved 62% (±9%) closure in unsupplemented medium compared to 71% (±8%) in 2ng/ml TGF-β1 supplemented medium and 71% (±9%) in 8ng/ml TGF-β1 supplemented medium (Figure 4.2). ($p > 0.05$ by ANOVA).

However, the rate of closure of scratches of HaCaT keratinocytes on collagen was slightly inhibited by TGF-β1 supplemented (serum free) medium at both 2ng/ml and 8ng/ml concentrations (Figure 4.3) such that after 12 hours post-scratch the HaCaT keratinocytes in unsupplemented medium had reached 81% (±6%) closure compared to 68% (±11%) closure in 2ng/ml TGF-β1 supplemented medium and 65 % (±15%) closure in 8ng/ml TGF-β1 supplemented medium (Figure 4.4). ($p > 0.05$ by ANOVA).
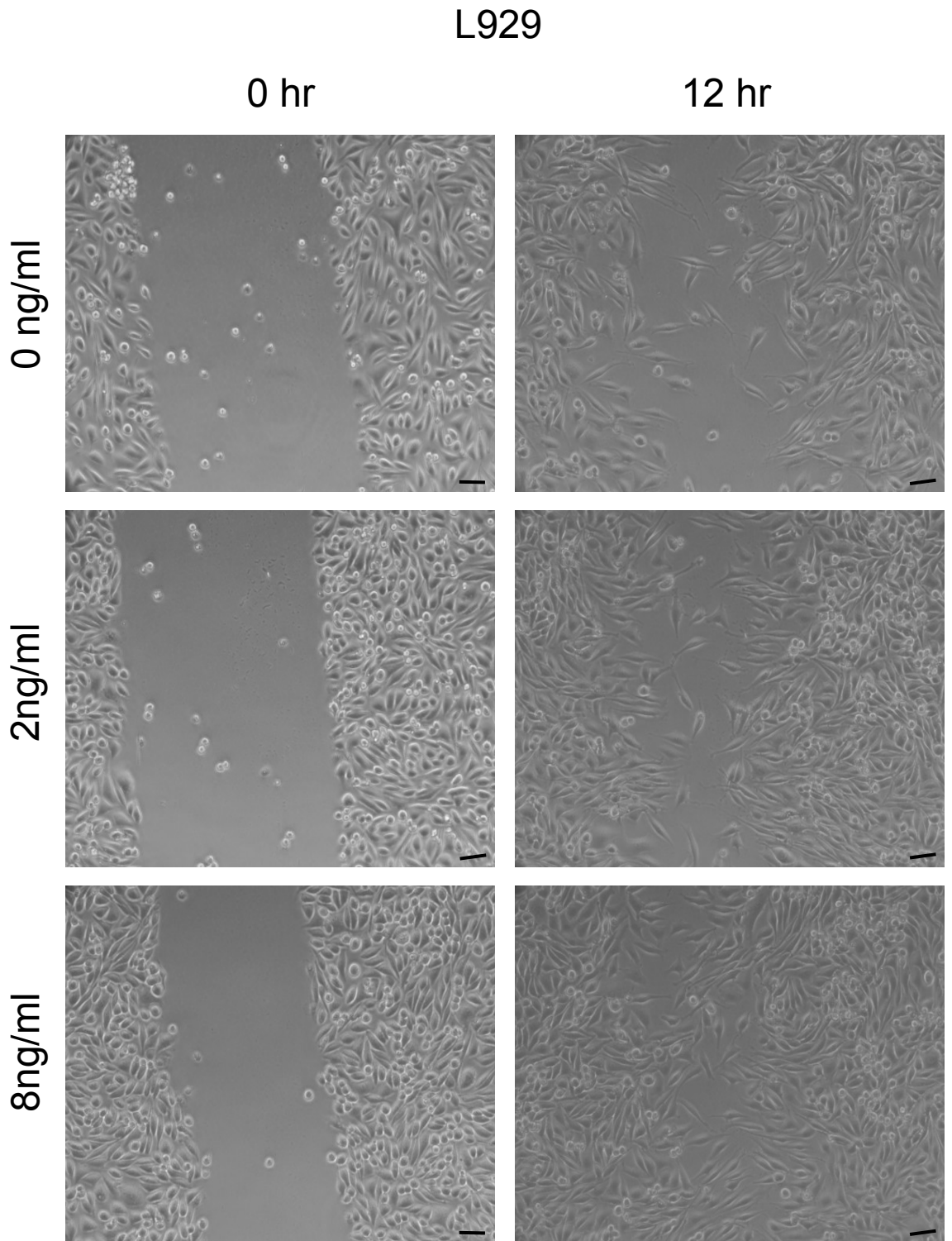
Figure 4.1 L929 fibroblasts closed scratch wounds marginally faster in TGF-β1 supplemented medium than in unsupplemented medium. There was no apparent difference between a lower concentration and a higher concentration of TGF-β1 Representative phase contrast images are shown of single cell type (L929) scratch assays immediately following the scratch and 12 hours thereafter. Original magnification is x10 (bar = 10μm).
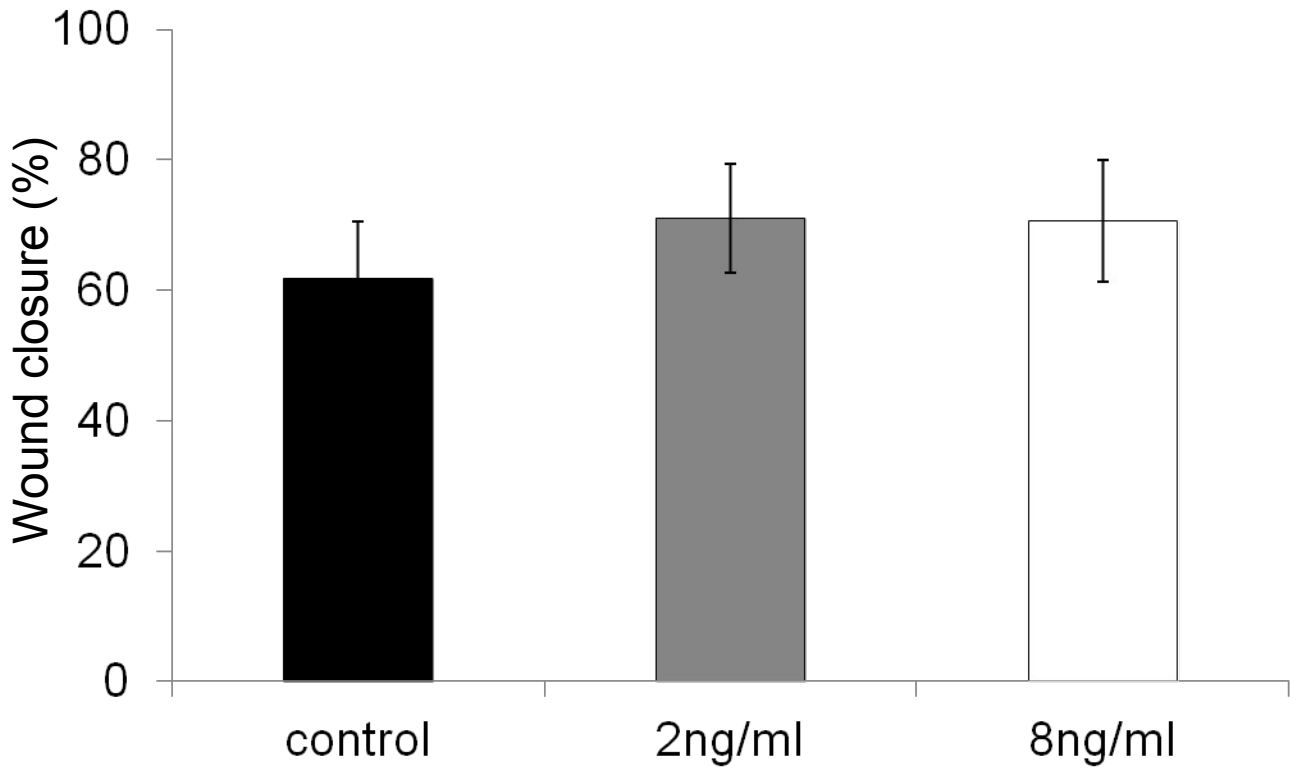
Figure 4.2 Scratch wound closure by L929 fibroblasts in TGF-β1. Twelve hours post-scratch, the extent of wound closure was 62% (±9%) for L929 fibroblasts in unsupplemented medium, 71% (±8%) for L929 fibroblasts in 2ng/ml TGF-β1 supplemented medium and 71% (±9%) for L929 fibroblasts cells in 8ng/ml TGF-β1 supplemented medium . Data shown are means ± SEM. No significant differences were found between results (p>0.05 by ANOVA)
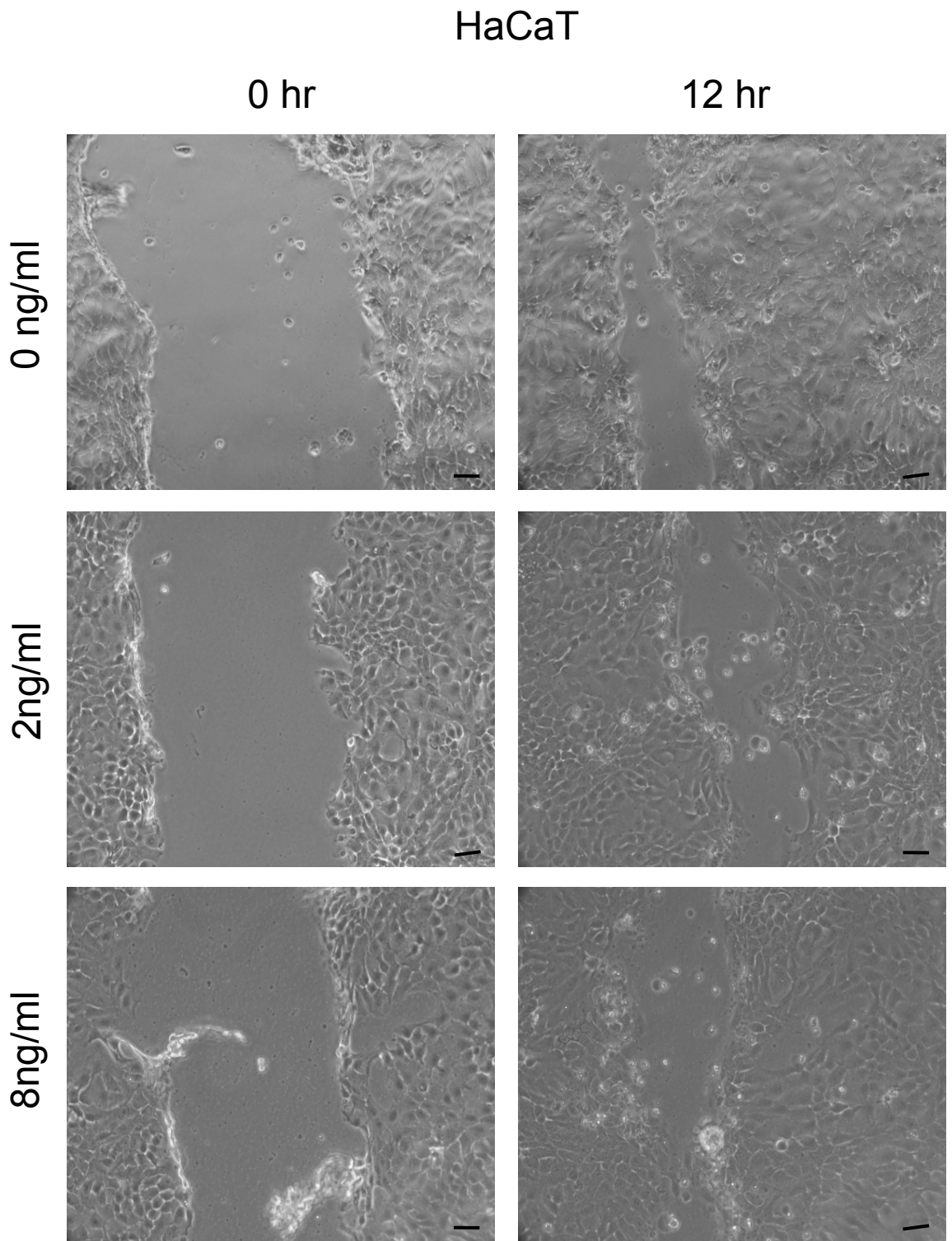
Figure 4.3 HaCaT keratinocytes closed scratch wounds slower in TGF-β1 supplemented medium than in unsupplemented medium. There was no apparent difference between a lower concentration and a higher concentration of TGF-β1 Representative phase contrast images are shown of single cell type (HaCaT) scratch assays immediately following the scratch and 12 hours thereafter. Original magnification is x10 (bar = 10μm).
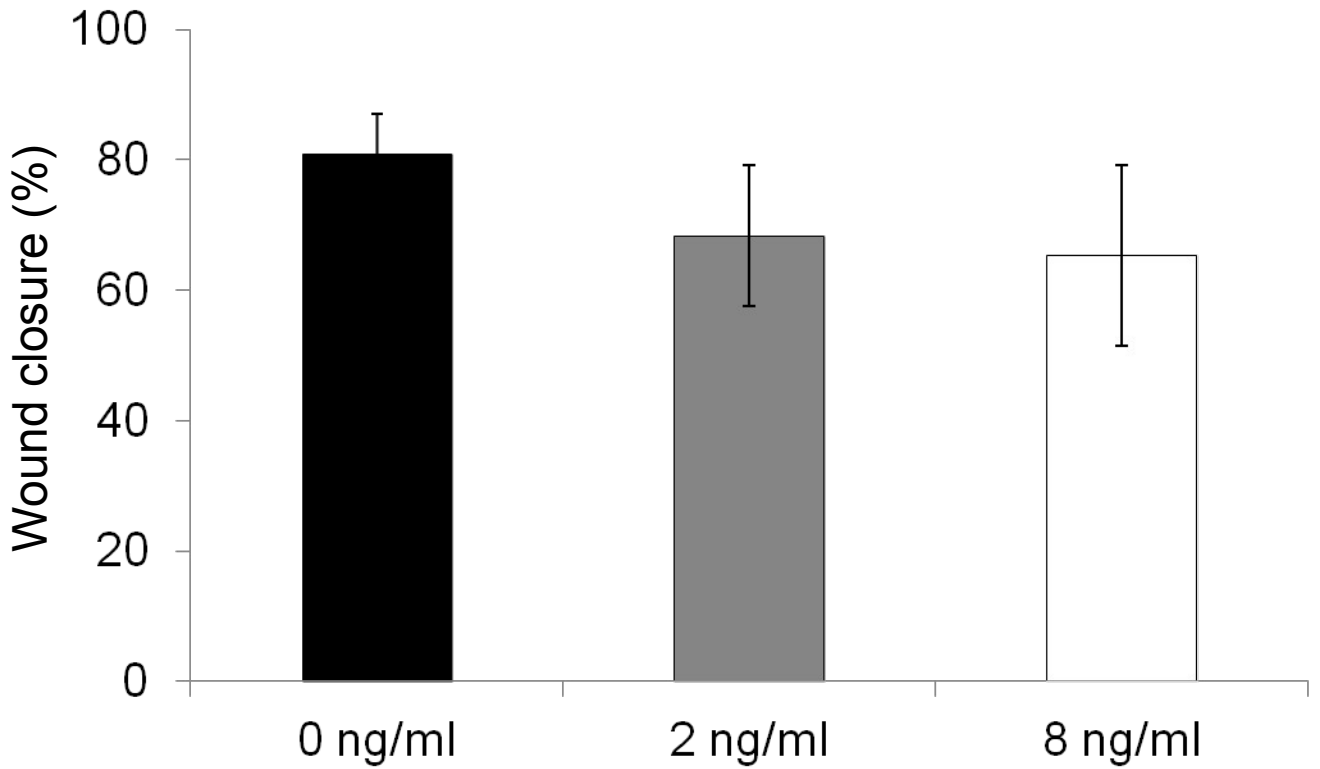
Figure 4.4 Scratch wound closure by HaCaT keratinocytes in TGF-β1 supplemented media. Twelve hours post-scratch, the extent of wound closure was 81% (±6%) for HaCaT keratinocytes in unsupplemented medium, Whereas scratches in 2ng/ml TGF-β1 supplemented medium and in 8ng/ml TGF-β1 supplemented medium had reached 68% (±11%) closure and 65% (±15%) respectively. Data shown are means ± SEM. No significant differences were found between results (p>0.05 by ANOVA).

Interleukin-6; L929 fibroblast scratch wounds closed at a similar rate in unsupplemented serum free medium or (serum free) media supplemented with either a low or a high concentration of IL-6 (Figure 4.5). 6 hours after scratching, L929 fibroblasts in unsupplemented medium had reached 66% (±4%) closure, rising to 98% (±1%) by 12 hours post scratch. In comparison, L929 fibroblasts in 10ng/ml IL-6 had closed by 80% (±6%) after 6 hours and 99% (±1%) at 12 hours post scratch whilst those in 100ng/ml had closed by 63% (±8%) at 6 hours and 93% (±4%) after 12 hours (figure 4.6). (p<0.05 by ANOVA). Similarly, HaCaT keratinocyte scratch wounds also closed at a similar rate in unsupplemented medium or IL-6 supplemented media (Figure 4.7). Six hours after scratching, HaCaT keratinocytes in unsupplemented medium had reached 75% (±13%) closure, rising to 90% (±9%) by 12 hours post scratch. In comparison, HaCaT keratinocytes in 10ng/ml IL-6 had closed by 62% (±13%) after 6 hours and 93% (±7%) at 12 hours post scratch whilst those in 100ng/ml had closed by 78% (±18%) at 6 hours and 91% (±11%) after 12 hours (Figure 4.8). (p>0.05 by ANOVA).

L929
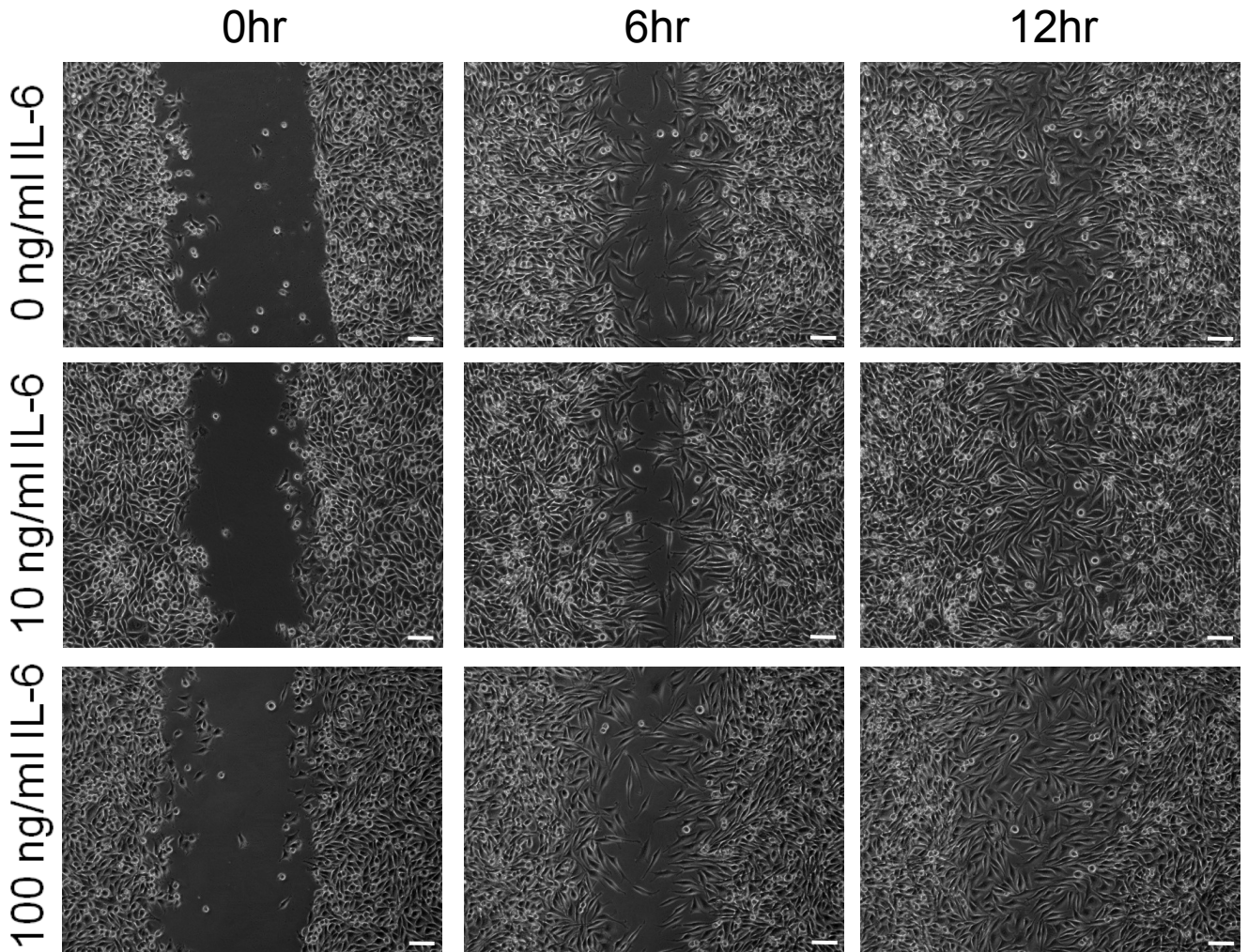
Figure 4.5 L929 fibroblasts closed scratch wounds at a similar rate in IL-6 supplemented medium than in unsupplemented medium. This was consistent for both a lower concentration and a higher concentration of IL-6. Representative phase contrast images are shown of single cell type (L929) scratch assays immediately following the scratch and 6 and 12 hours thereafter. Original magnification is x10 (bar = 10μm).
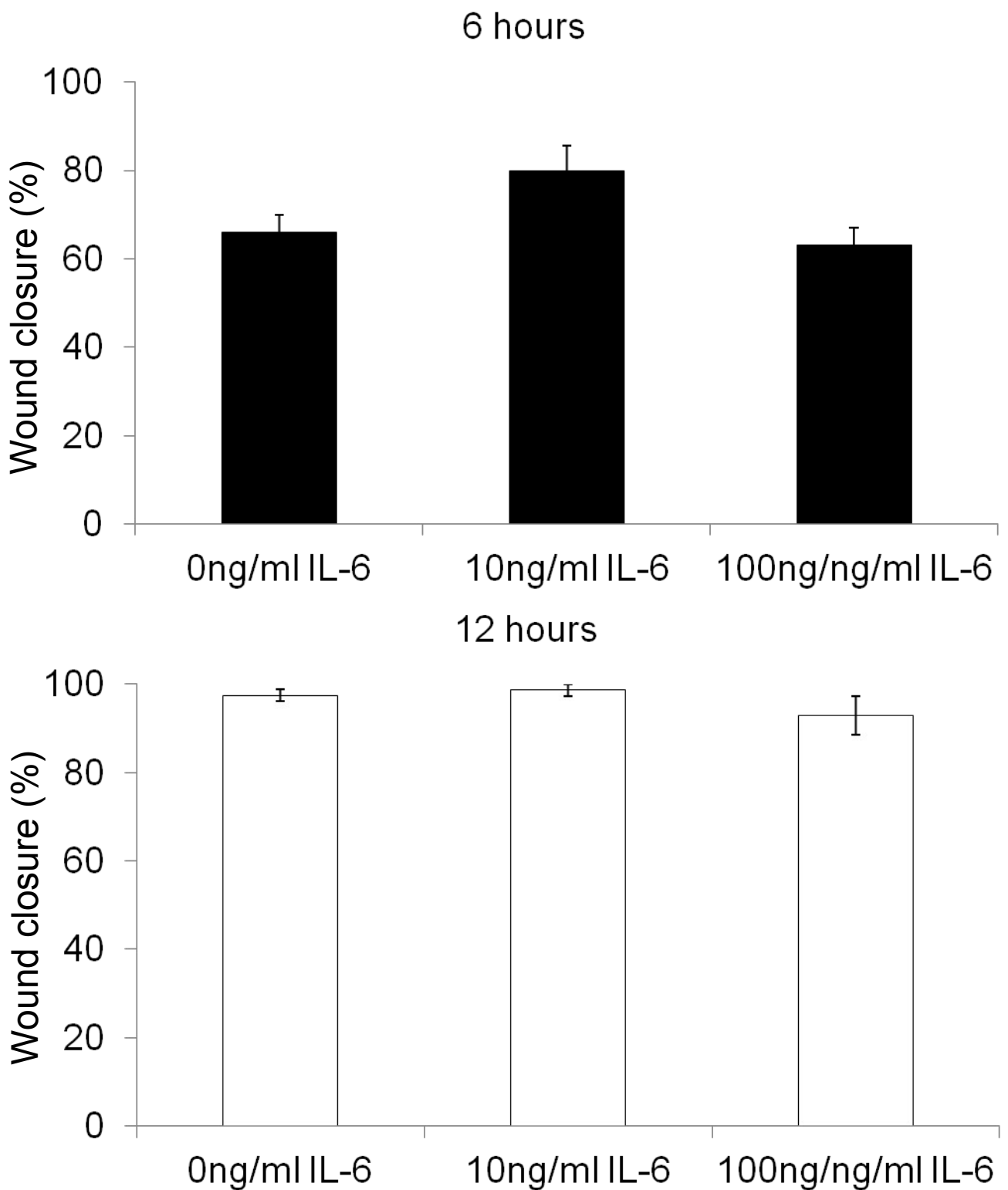
Figure 4.6 Scratch-wound closure by L929 fibroblasts in IL-6 supplemented media. Six hours post-scratch, the extent of wound closure was 66% (±4%) for L929 Fibroblasts in unsupplemented medium, 80% (±6%) for L929 Fibroblasts in 10ng/ml IL-6 supplemented medium and 63% (±8%) for L929 Fibroblasts in 100ng/ml IL-6 supplemented medium. Twelve hours post-scratch, the extent of wound closure was 98% (±1%) for L929 Fibroblasts in unsupplemented medium, 99% (±1%) for L929 Fibroblasts in 10ng/ml IL-6 supplemented medium and 93% (±4%) for L929 Fibroblasts in 100ng/ml IL-6 supplemented medium . Data shown are means ± SEM. No significant differences were found between results (p>0.05 by ANOVA).

HaCaT
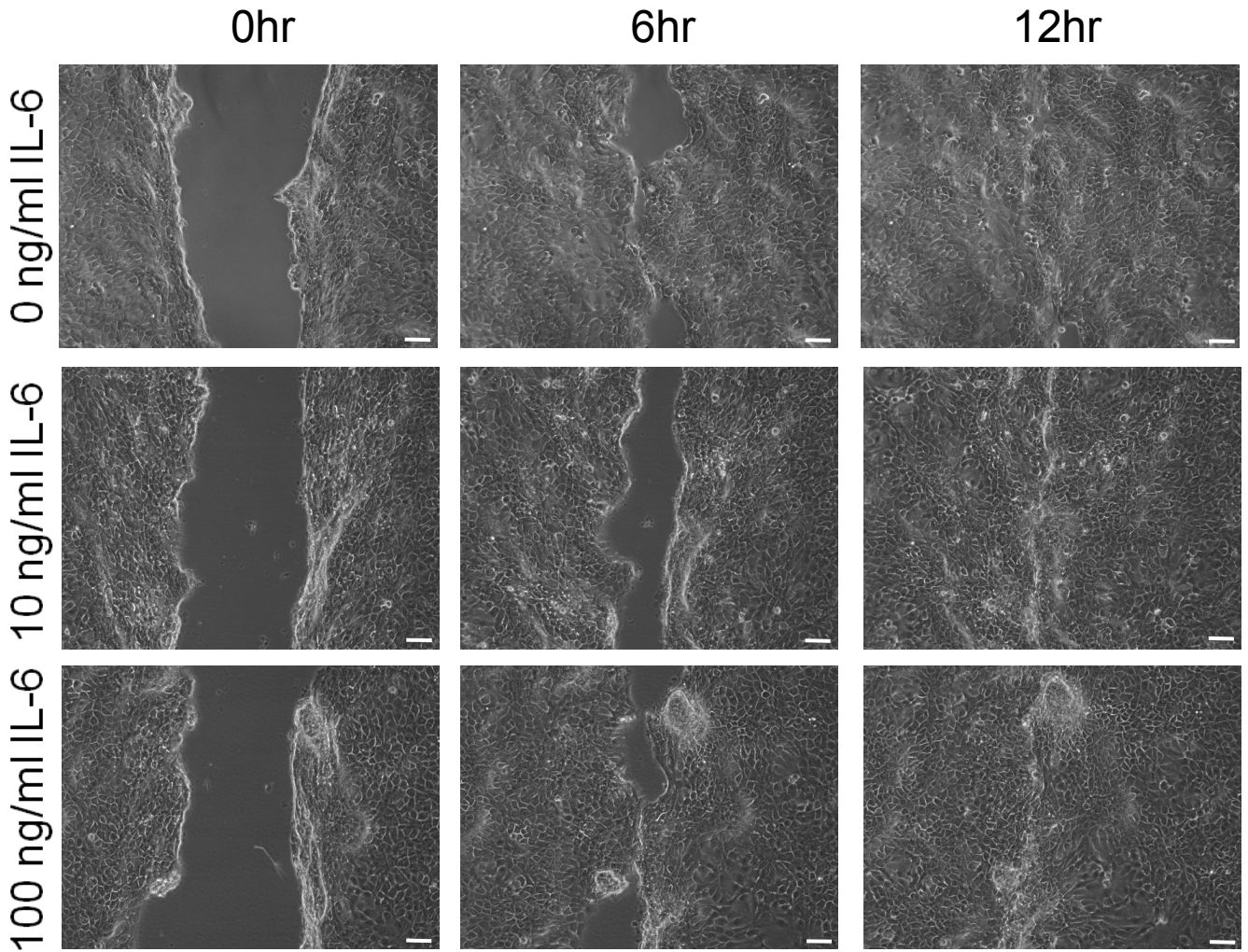
Figure 4.7 HaCaT keratinocytes closed scratch wounds at a similar rate in IL-6 supplemented medium than in unsupplemented medium. This was consistent for both a lower concentration and a higher concentration of IL-6. Representative phase contrast images are shown of single cell type (HaCaT) scratch assays immediately following the scratch and 6 and 12 hours thereafter. Original magnification is x10 (bar = 10μm).
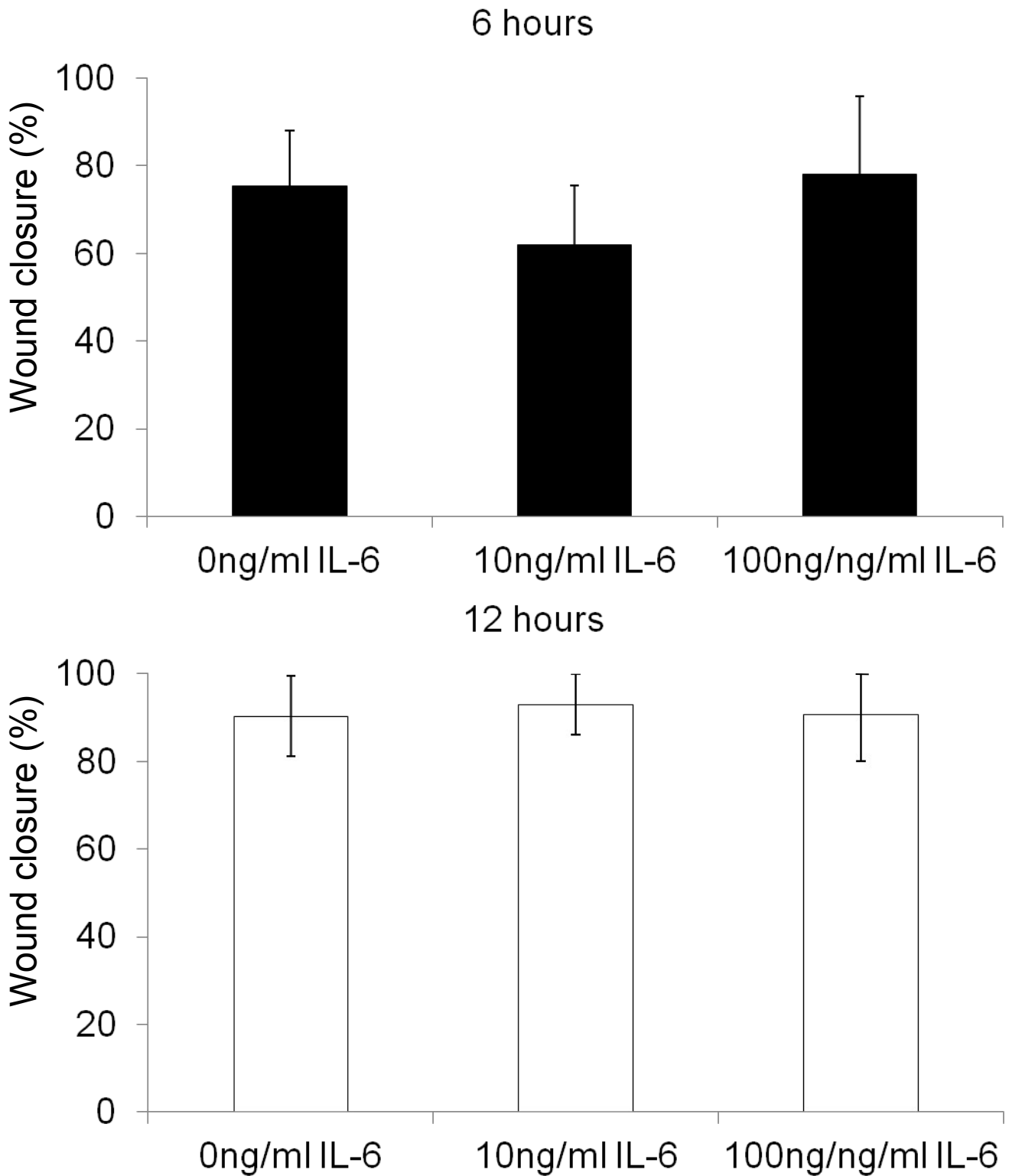
Figure 4.8 Scratch-wound closure by HaCaT keratinocytes in IL-6 supplemented media.
Six hours post-scratch, the extent of wound closure was 75% (±13%) for HaCaT keratinocytes in unsupplemented medium, 62% (±13%) for HaCaT keratinocytes in 10ng/ml IL-6 supplemented medium and 78% (±18%) for HaCaT keratinocytes in 100ng/ml IL-6 supplemented medium. Twelve hours post-scratch, the extent of wound closure was 90% (±9%) for HaCaT keratinocytes in unsupplemented medium, 93% (±7%) for HaCaT keratinocytes in 10ng/ml IL-6 supplemented medium and 91% (±11%) for HaCaT keratinocytes in 100ng/ml IL-6 supplemented medium . Data shown are means ± SEM. No significant differences were found between results (p>0.05 by ANOVA).

Interleukin-8; IL-8 appeared to have a transient inhibitory effect on scratch wound closure by L929 fibroblasts. Over the first 6 hours, L929 fibroblast scratches in IL-8 supplemented medium closed more slowly than those in unsupplemented medium, in an IL-8 concetration dependant manner. However, this difference was not observed after 12 hours (Figure 4.9). At 6 hours post scratch the degree of closure was 97% (±2%) in unsupplemented medium, 87% (±5%) in 10ng/ml IL-8 and 69% (±9%) in 100ng/ml IL-8. After 12 hours the degree of closure had reached 100% (±0%) for both unsupplemented and 10ng/ml IL-8 supplemented media, and 99% (±1%) for 100ng/ml medium (Figure 4.10). This inhibitory effect of IL-8 was statistically significant at 6 hours, but not at 12 hours ($p < 0.05$ by ANOVA).

HaCaT keratinocytes also closed scratch wounds more slowly in both 10ng/ml and 100ng/ml IL-8 supplemented media than in unsupplemented medium (Figure 4.11), But this effect was not significant ($p > 0.05$ by ANOVA). After 6 hours, those scratches in unsupplemented medium had reached 63% (±16%) closure, rising to 95% (±4%) closure by 12 hours, whereas scratches in 10ngml IL-8 had reached 56% (±20%) closure by 6 hours and 81% (±23%) closure after 12 hours. In 100ng/ml IL-8 the scratches had reached 57% (±20%) closure by 6 hours and 85% (±23%) closure by 12 hours (figure 4.12).
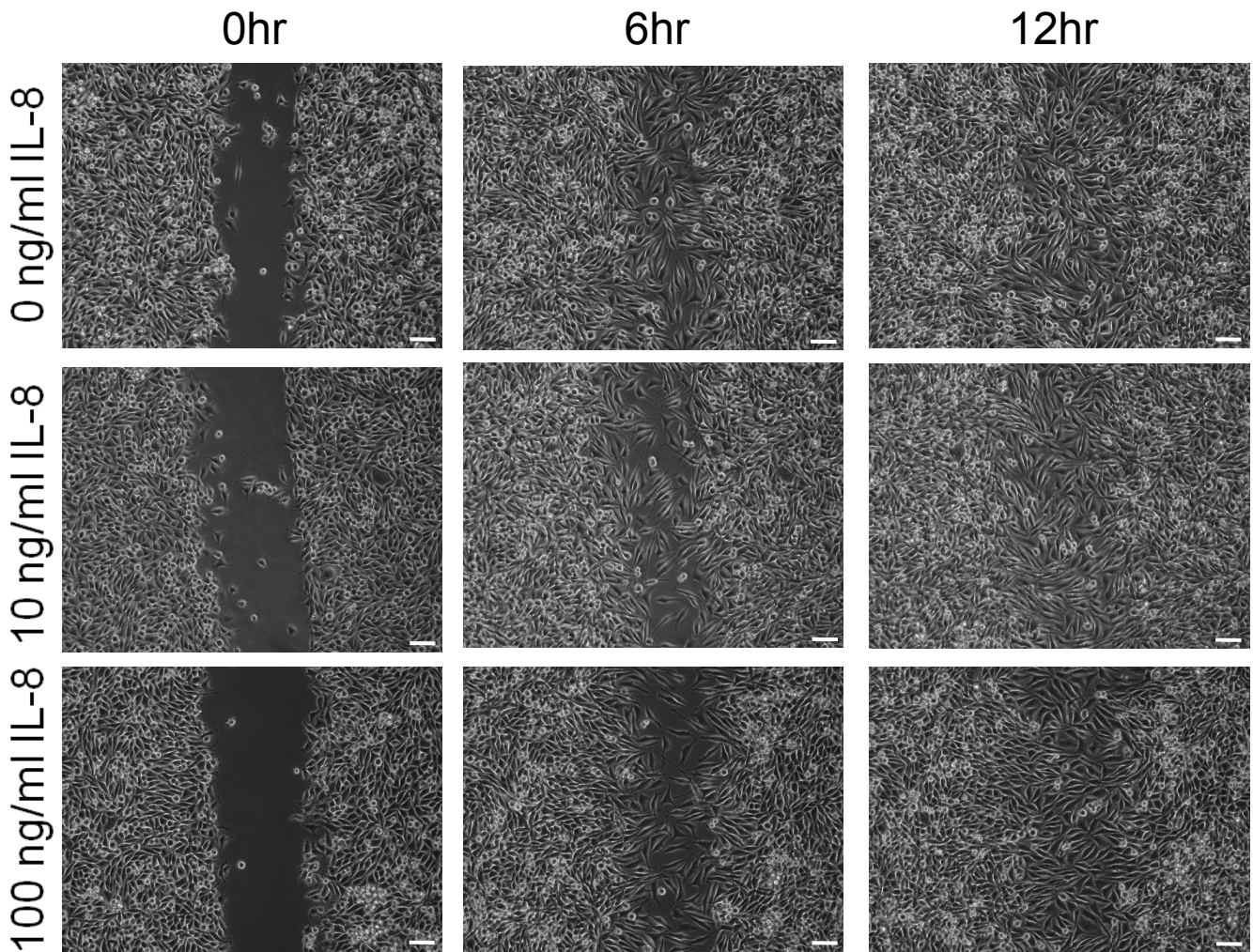
Figure 4.9 L929 fibroblasts closed scratch wounds more slowly in IL-8 supplemented medium than in unsupplemented medium over 6 hours. By 12 hours there was no difference between IL-8 supplemented and unsupplemented medium. This was consistent for both a lower concentration and a higher concentration of IL-8. Representative phase contrast images are shown of single cell type (L929) scratch assays immediately following the scratch and 6 and 12 hours thereafter. Original magnification is x10 (bar = 10μm).
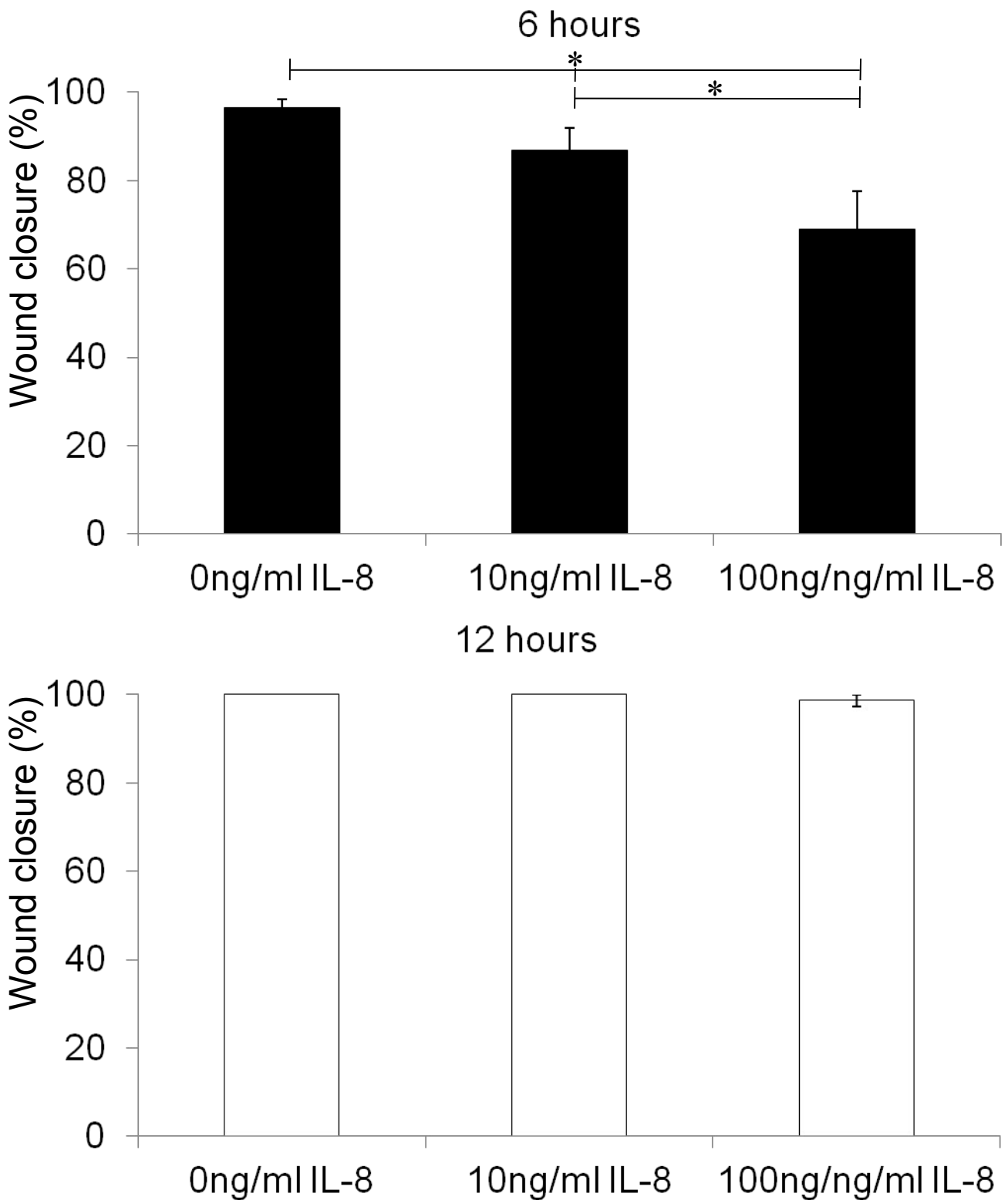
Figure 4.10 Scratch-wound closure by L929 fibroblasts in IL-8 supplemented media. Six hours post-scratch, the extent of wound closure was 97% (±2%) for L929 fibroblasts in unsupplemented medium, compared to 87% (±5%) in 10ng/ml IL-8 supplemented medium and 69% (±9%) in 100ng/ml IL-8 supplemented medium. This was a significant dose dependent inhibition of L929 scratch wound closure in response to IL-8 over the initial 6 hours. Twelve hours post-scratch, the extent of wound closure was very similar in all conditions; 100% (±0%) in unsupplemented medium, 100% (±0%) in 10ng/ml IL-8 supplemented medium and 99% (±1%) in 100ng/ml IL-8 supplemented medium. Data shown are means ± SEM. Six hour differences were significant (p<0.05 by ANOVA) specifically between both 0mg/ml vs 100mg/ml and 10mg/ml vs 100mg/ml IL-8 (Tukey's HSD) whilst no significant differences were observed at 12 hours (p>0.05 by ANOVA).
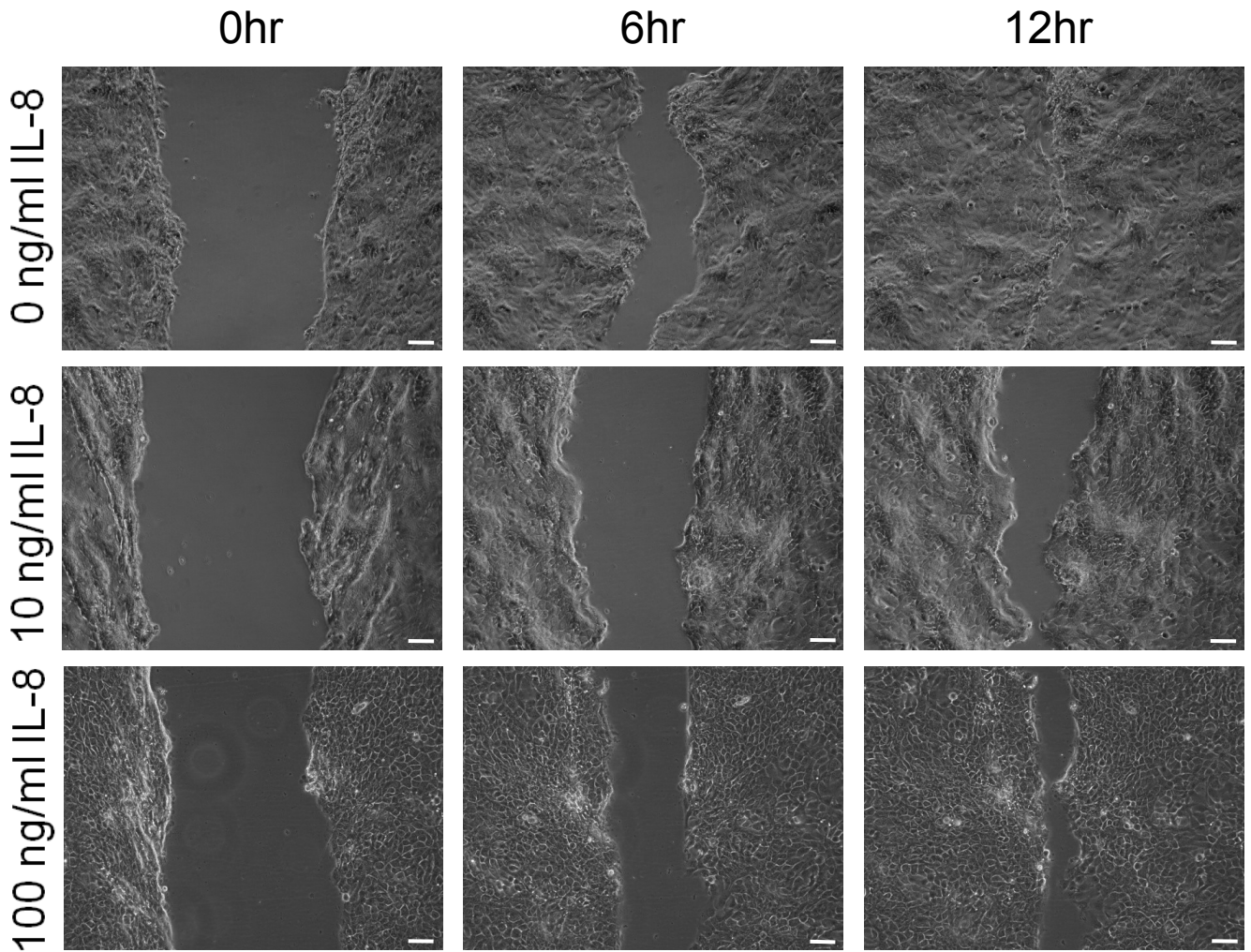
Figure 4.11 HaCaT keratinocytes closed scratch wounds more slowly in IL-8 supplemented medium than in unsupplemented medium. This was consistent for both a lower concentration and a higher concentration of IL-8. Representative phase contrast images are shown of single cell type (HaCaT) scratch assays immediately following the scratch and 6 and 12 hours thereafter. Original magnification is x10 (bar = 10µm).
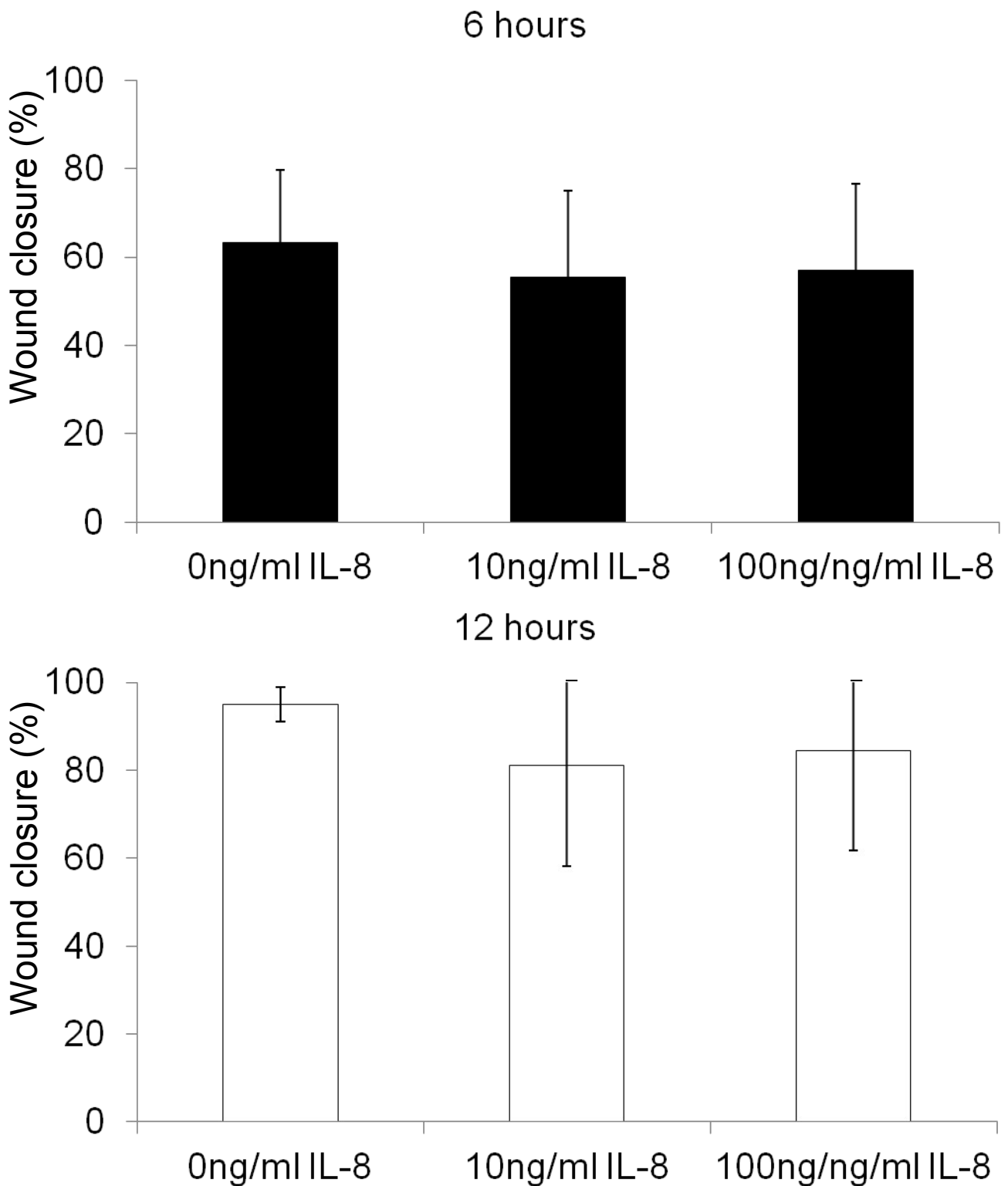
Figure 4.12 Scratch-wound closure by HaCaT keratinocytes in IL-8 supplemented media. Six hours post-scratch, the extent of wound closure was 63% (±16%) for HaCaT keratinocytes in unsupplemented medium, 56% (±20%) for HaCaT keratinocytes in 10ng/ml IL-8 supplemented medium and 57% (±20%) for HaCaT keratinocytes in 100ng/ml IL-8 supplemented medium. Twelve hours post-scratch, the extent of wound closure was 95% (±4%) for HaCaT keratinocytes in unsupplemented medium, 81% (±23%) for HaCaT keratinocytes in 10ng/ml IL-8 supplemented medium and 85% (±23%) for HaCaT keratinocytes in 100ng/ml IL-8 supplemented medium . Data shown are means ± SEM. No significant differences were found between results at either 6 hours or 12 hours (p>0.05 by ANOVA).

Figure 4.13 Summary of cytokine effects upon scratch-wound closure by skin cell lines. (* = p<0.05)

4.3: The effects of MSC secreted extracellular matrix proteins on L929 fibroblasts and HaCaT keratinocytes

L929 fibroblasts and HaCaT keratinocytes adhered to 0.2mg/ml type I collagen coated tissue culture plastic after 2 hours in culture. In serum free conditions, coating tissue culture plastic with 0.2mg/ml fibronectin instead of type I collagen resulted in significantly enhanced adherence of both cell types after 2 hours, observable as a greater degree of cell spreading (Figure 4.14). In contrast, coating tissue culture plastic with 0.2ng/ml decorin significantly inhibited the adherence of both cell types compared to either collagen or fibronectin. (Figure 4.15) ($p < 0.05$ *by ANOVA*).

The closure of scratch wounds by L929 fibroblasts was significantly faster on 0.2mg/ml fibronectin than on 0.2mg/ml type I collagen (figure 4.16) such that after 12 hours those scratches performed on fibronectin had reached 88% (±5%) closure whereas scratches on type I collagen had only reached 62% (±9%) closure. ($p < 0.05$ *Mann Whitney U test*) (Figure 4.17). Closure of scratch wounds by HaCaT keratinocytes was also marginally faster on fibronectin than on collagen and scratch wounds on either type I collagen or fibronectin closed faster than those on Decorin (Figure 4.18). After 12 hours, scratch wounds on fibronectin had closed by 98% (±3%) whereas those on type I collagen had closed by 81% (±9%) and those on decorin only 63% (±8) (Figure 4.19) ($p < 0.05$ between decorin and fibronectin by *ANOVA*). These assays were all performed in the absence of serum.
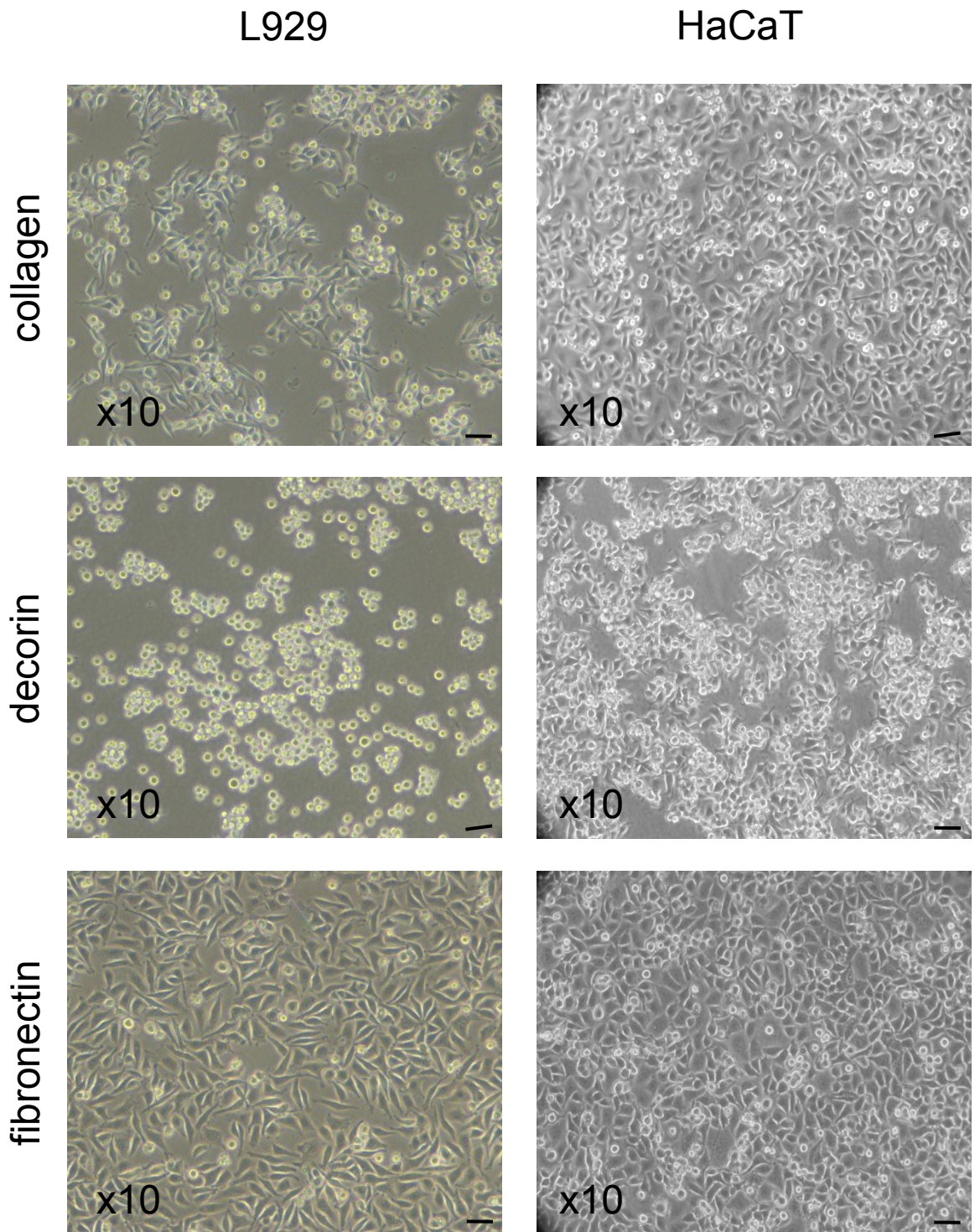
Figure 4.14 Cell spreading on ECM proteins. After 2 hours in culture, both L929 and HaCaT cells were observably more spread on fibronectin than on type I collagen and on type I collagen than on decorin. Representative phase contrast images are shown of single cell type (L929 or HaCaT) . Original magnifications are x10 (bar = 10μm).
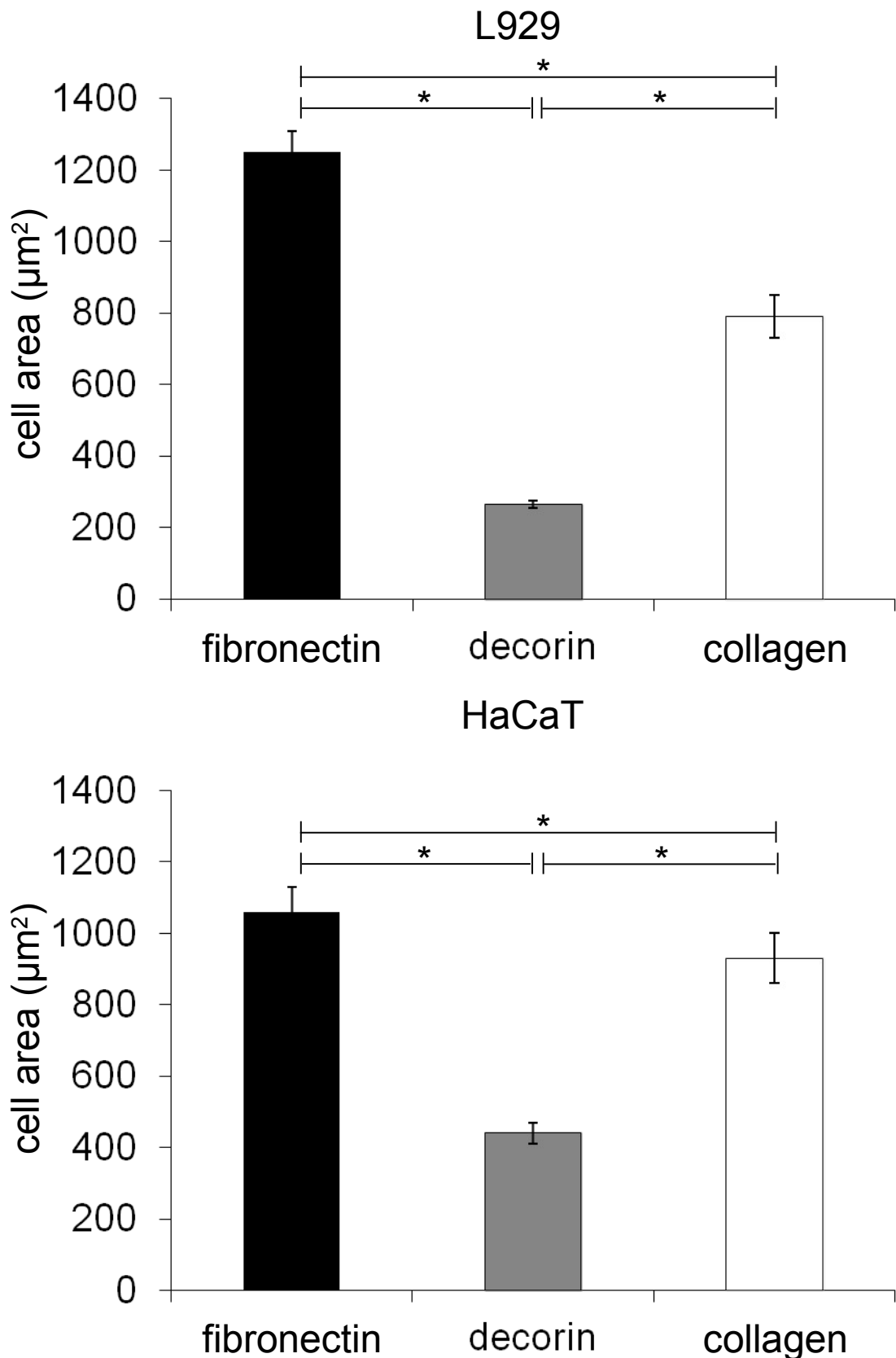
Figure 4.15 Cell areas on ECM proteins. After 2 hours in culture the average cell area was 1250μm² (±60μm²), for L929 fibroblasts on fibronectin, 790μm² (±60μm²), for L929 fibroblasts on decorin and 265μm² (±10μm²), for L929 fibroblasts on type I collagen. The average cell area for HaCaT keratinocytes on fibronectin was 1060μm² (±70μm²), 440μm² (±30μm²) for HaCaT keratinocytes on decorin and 930μm² (±70μm²) for HaCaT keratinocytes on type I collagen. Data shown are means ± SEM. There was a significant difference by ANOVA (p<0.05). (* denotes significance by Tukey's HSD).
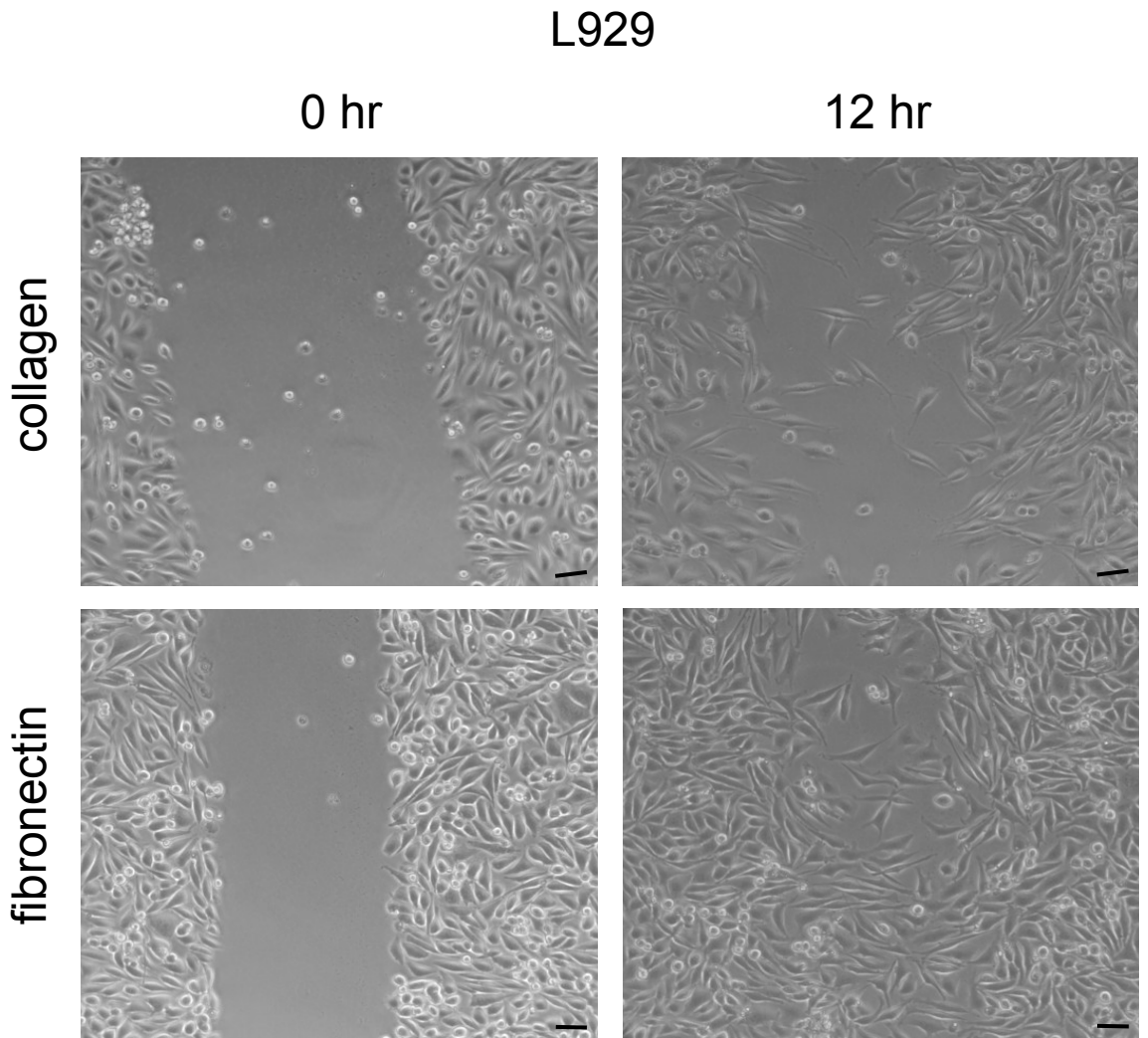
Figure 4.16 L929 fibroblasts closed scratch wounds faster on fibronectin coated plates than on type I collagen coated plates. Representative phase contrast images are shown of single cell type (L929) scratch assays immediately following the scratch and 12 hours thereafter. Original magnification is x10 (bar = 10μm).
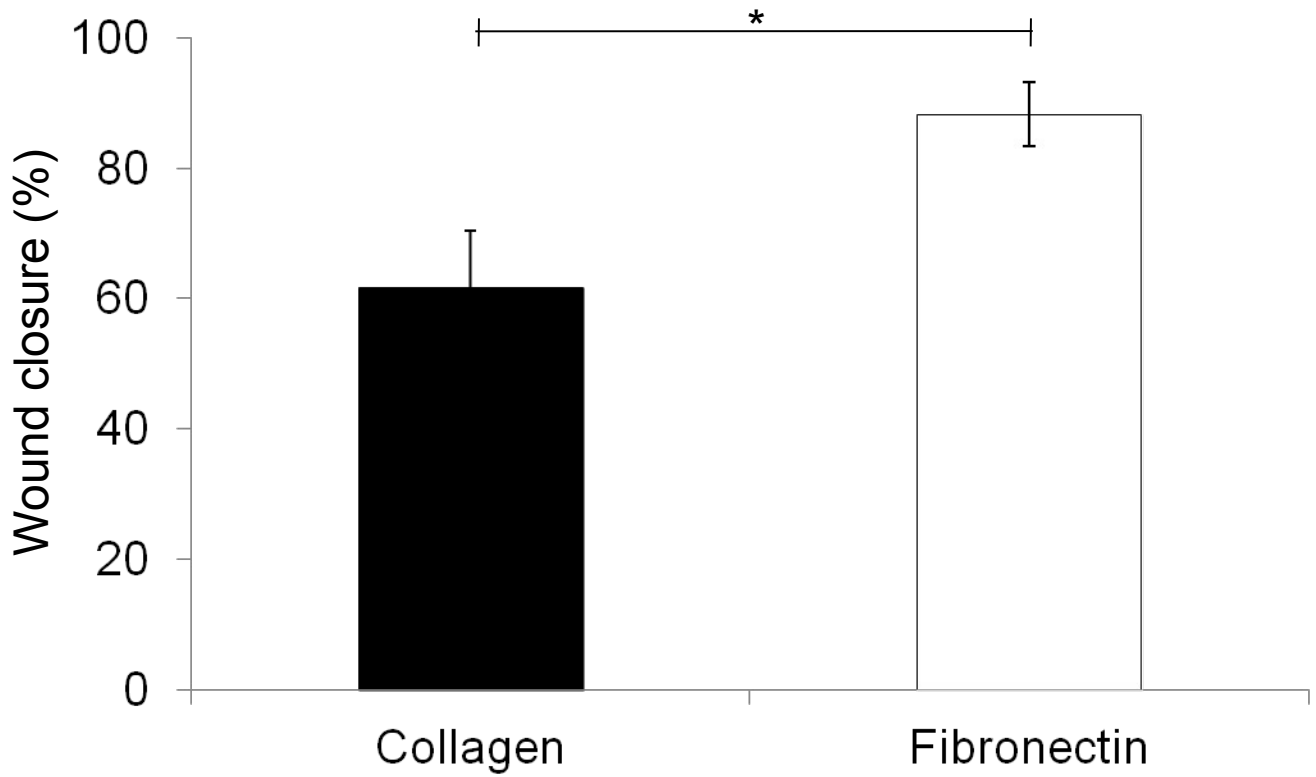
Figure 4.17 Scratch-wound closure by L929 fibroblasts on type I collagen and fibronectin. Twelve hours post-scratch, the extent of wound closure was 62% (±9%) for L929 cells on collagen and 88% (±5%) for L929 fibroblasts on fibronectin. Data shown are means ± SEM (*=p<0.05 Mann Whitney U test).
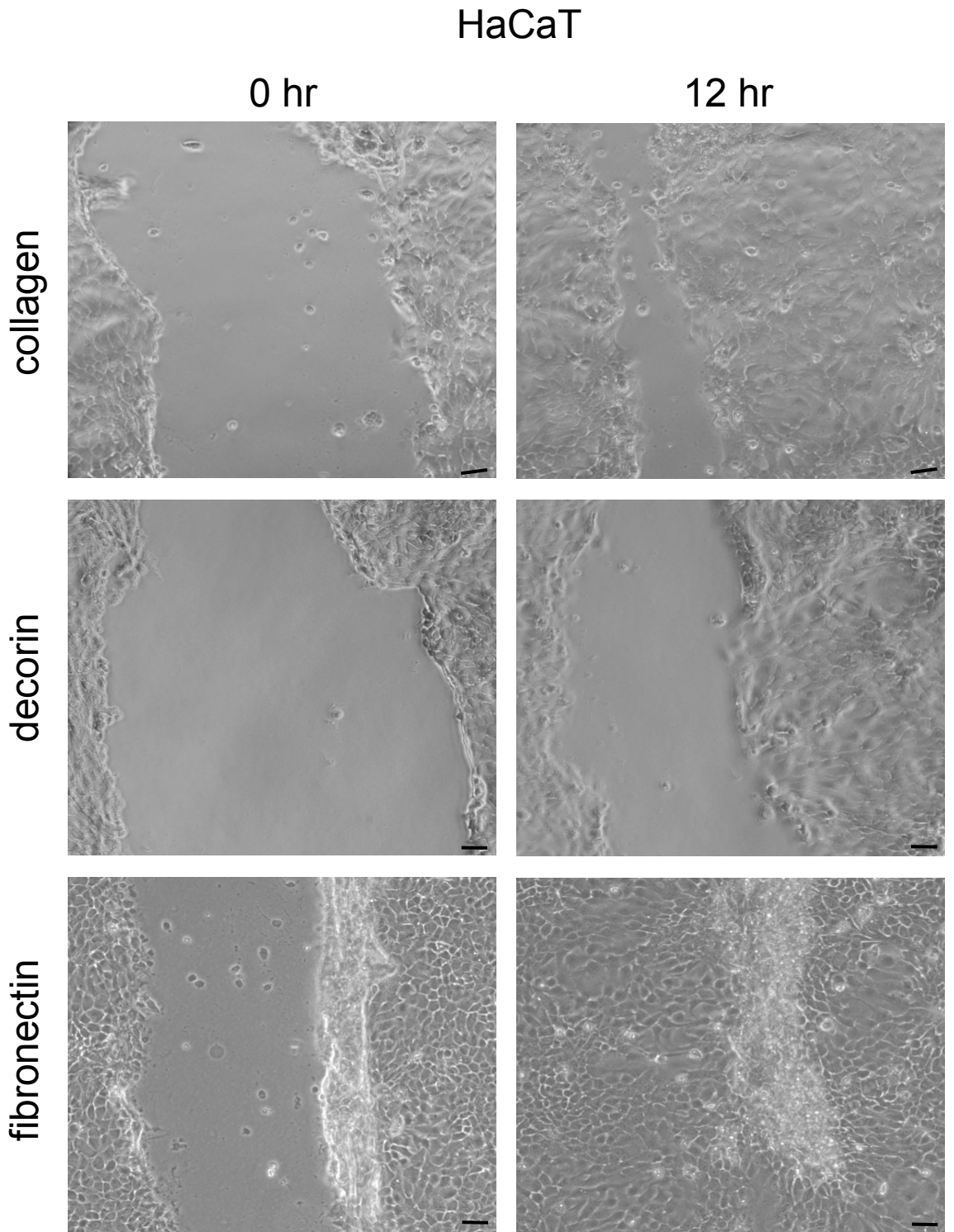
Figure 4.18 HaCaT keratinocytes closed scratch wounds faster on fibronectin coated plates than on collagen coated plates, and faster on both fibronectin and type I collagen coated plates than on decorin coated plates. Representative phase contrast images are shown of single cell type (HaCaT) scratch assays immediately following the scratch and 12 hours thereafter. Original magnification is x10 (bar = 10μm).
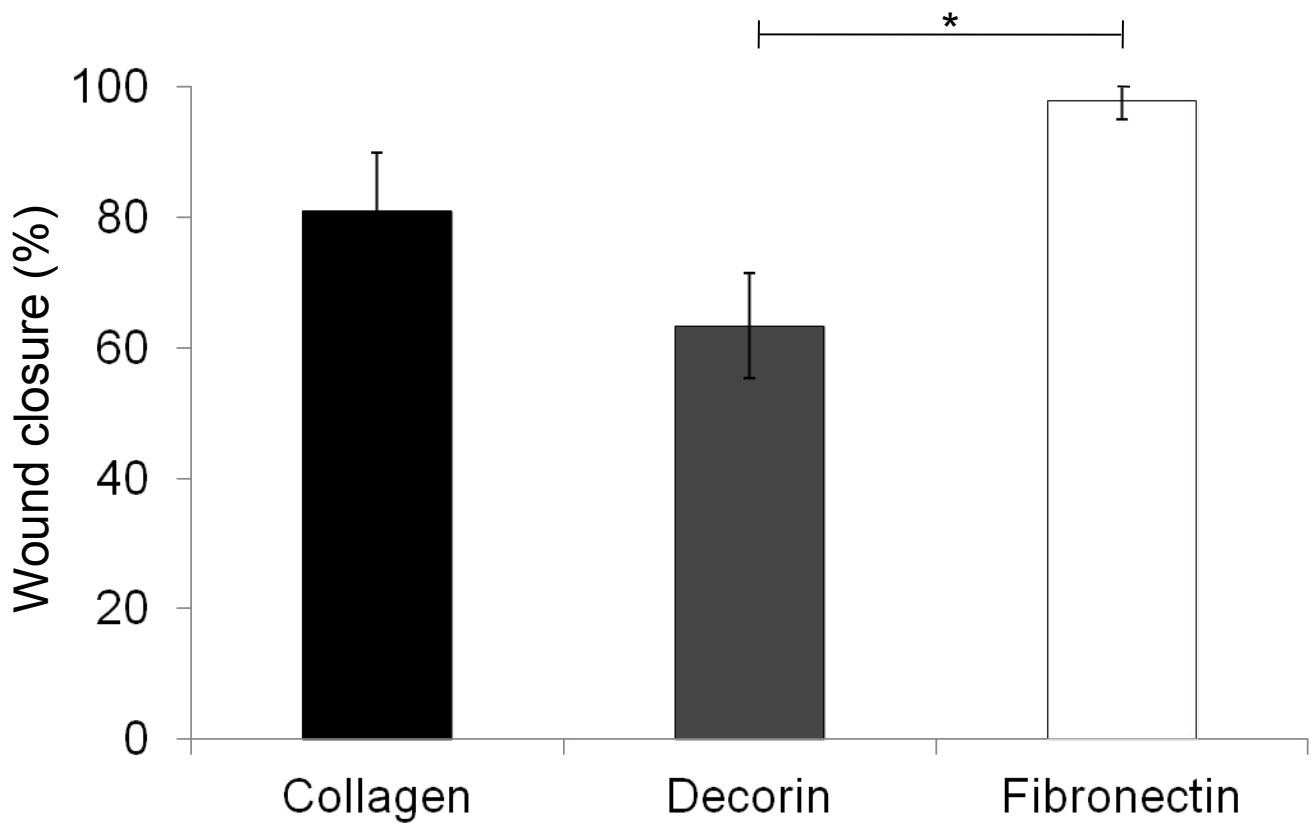
Figure 4.19 Scratch-wound closure by HaCaT keratinocytes on ECM proteins.
Twelve hours post-scratch, the extent of wound closure was 81% (±9%) for HaCaT
keratinocytes on type I collagen, 63% (±8%) for HaCaT keratinocytes on decorin and
98% (±3%) for HaCaT keratinocytes cells on fibronectin. Data shown are means ± SEM.
There was a significant difference by ANOVA (p<0.05); (* denotes significance by
Tukey's HSD).

Figure 4.20 Summary of decorin and fibronectin effects upon scratch-wound closure by skin cell lines compared to type I collagen.

4.4: Discussion

The previous chapter showed MSC secreted factors that enhanced L929 fibroblast and HaCaT keratinocyte scratch wound closure, and identified a range of cytokines and ECM proteins present in the MSC secretome. This chapter has investigated the effects of certain of those factors on L929 fibroblast and HaCaT keratinocyte behaviour *in vitro.*

Amongst the cytokines found to be present in MSC-CM were the interleukins; IL-6 and IL-8, as well as TGF-β1. In these experiments, IL-6 was shown to have little observable effect upon the rate of scratch wound closure by L929 fibroblasts. However, *in vivo* experiments involving IL-6 knock out mice have shown a significant delay in cutaneous wound healing in the absence of IL-6 associated with reduced expression of α-SMA (smooth muscle actin), a marker of myofibroblast differentiation. (Gallucci *et al,* 2006). It is not known whether or not L929 fibroblasts undergo myofibroblastic differentiation when migrating into scratch wounds in our *in vitro* model of wound healing. If they do not, then the absence of this migratory phenotype may go some way towards explaining the lack of an observable cellular response to IL-6. Immunostaining of IL-6 treated and untreated L929 fibroblast cultures with an antibody for α-SMA would potentially further elucidate the mechanisms involved in this phenomenon. This possibility is further discussed below.

Similarly, IL-6 did not appear to have any effect upon the rate of scratch wound closure by HaCaT keratinocytes. This mirrors observations made by another group using primary keratinocytes isolated form IL-6 knock-out mice in which, despite the role of IL-6 in *in vivo* wound healing mentioned above, the *in vitro* treatment of cultured keratinocytes with recombinant IL-6 failed to induce a direct enhancement of either keratinocyte migration or proliferation. Instead IL-6 was

shown to indirectly enhance keratinocyte migration by the inducing the production of stimulatory factors by fibroblasts (Gallucci *et al,* 2004). Whether or not exogenous IL-6 would stimulate scratch-wound healing in L929 fibroblast and HaCaT keratinocyte co-cultures, despite having no observable effect upon either cell type individually, or whether L929-CM from L929 fibroblasts cultured in the presence of IL-6 might stimulate HaCaT keratinocyte migration and/or proliferation may be a question worthy of further investigation chapters. IL6 does not appear to account fot the effects of MSC-CM

TGF-β1 is involved in numerous aspects of cutaneous wound healing *in vivo*, including inflammation, re-epithelialisation and ECM regeneration (reviewed in Barrientos *et al,* 2008). The importance of TGF-β1 in successful wound healing is demonstrated by its relative up-regulation in normal 'acute' wounds (Kane *et al,* 1991), compared to its down-regulation in non-healing 'chronic' wounds (Robson, 1997). In this chapter's experiments, TGF-β1 was associated with a non-significant increase in the rate of scratch wound closure by L929 fibroblasts. TGF-β1 has long been known to stimulate fibroblast migration *in vitro* (Postlethwaite *et al,* 1987) and is involved in the differentiation of normal fibroblasts into myofibroblasts, a migratory and contractile phenotype associated with wound healing (Serini *et al,* 1998). As mentioned previously, the question of whether or not L929 fibroblasts undergo myofibroblast differentiation in *in vitro* scratch-wounds, either spontaneously or in response to either MSC-CM or exogenous TFG-β1 may be the subject of further investigation. In addition to enhancing fibroblast migration *in vitro*, TFG-β1 is known to increase the ability of myofibroblasts to contract wounds *in vivo.* Hence the secretion of TFG-β1 by MSC may be potentially beneficial in the healing of chronic wounds that show down-regulated TFG-β1 expression.

TFG-β1 was shown to slightly inhibit the rate of *in vitro* scratch wound closure by HaCaT keratinocytes in these experiments. This seems contrary to previously published studies that show TFG-β1 to stimulatory to keratinocyte migration (Sutherland *et al,* 2005). This may be due to the difference between the HaCaT cell line in our experiments and the primary keratinocytes used by Sutherland *et al*. It is known that TFG-β1 drives HaCaT keratinocytes towards terminal differentiation (Bushke *et al,* 2011) and this enhanced differentiation status may account for the absence of a migratory response by these cells to TFG-β1. The expression of various keratins could be investigated to determine the differentiation status of HaCaT keratinocytes exposed to either TFG-β1 or MSC-CM. Recent studies have shown that co-treatment of HaCaT keratinocytes with TGF-β1 and hepatocyte growth factor (HGF) results in enhanced keratinocyte migration (Nam *et al,* 2010). As HGF is produced by fibroblast *in vivo* (Zarnegar and Michalopoulos, 1995) this suggests that the effects of MSC-secreted TGF-β1 may differ in an *in vivo* wound healing context to those observed in single cell cultues. TFG-β1 has also been shown to alter keratinocyte integrin expression towards a more migratory phenotype (Barrientos *et al,* 2008) and up regulates the expression of the integrin receptors for fibronectin (α5β1 and αVβ6), vitronectin (αVβ1) and collagens, including type I collagen (α2β1), stimulating keratinocyte migration towards both collagen and Fibronectin (Zambruno *et al*, 1995, Stepp *et al*, 2007). It is interesting to note that of these ECM components, both type I collagen and fibronectin are strongly and consistently present in the MSC secretome. TGF-β1 does not seem to cause the effects of MSC-CM observed in vitro.

IL-8 supplemented medium significantly reduced the rate of scratch wound closure by L929 fibroblasts, suggesting that the presence of IL-8 in the MSC secretome does not contribute to the associated enhancement of scratch wound

closure in this model system. Whilst it has been previously demonstrated that IL-8 may enhance fibroblast migration *in vitro* by reducing the ability of cells to form focal adhesions (Dunlevy and Couchman 1995), and IL-8 has also been shown to be chemo-attractant to keratinocytes (Michel *et al,* 1992), in some chronic wounds, elevated levels of IL-8 are associated with impaired wound healing (Ghazarian *et al,* 2000) and IL-8 has also been associated with a loss of fibroblast contractile ability in wound healing. This may have unwelcome implications for *in vivo* wound healing, howver IL-8 is also known to promote angiogenesis (Waugh and Wilson, 2008). As poor vascularisation of wound beds is a major cause of the failure of tissue engineered skin substitutes in wound healing, the secretion of angiogenic factors by MSC may have potential use in improving this method of treating difficult wounds.

There is a possibility that MSC secreted factors could enhance the differentiation of L929 fibroblasts by stimulating their differentiation to a migratory myofibroblastic phenotype. One study (Joseph *et* al., 2013) has recently shown that L929 fibroblast can express alpha SMA and hence it appears these cells may be capable of such differentiation. If MSC secreted factors can stimulate myofibroblast differentiation, this might reasonably be expected to enhance the rate of wound closure *in vivo,* if the same effect applies to normal human fibroblasts. Within this hypothetical mechanism, however, there may be some cause for concern that this might lead to excessive contracture of wound margins, leading to a range of possible complications as discussed previously within this thesis. An alternative scenario, in which L929 are incapable of true myofibroblast differentiation, calls into question the capacity of these cells to accurately represent normal dermal fibroblasts within this model. Normal dermal fibroblasts are known to be capable of myofibroblast differentiation in response to factors found in MSC-CM (i.e. TGF-Beta) and this may affect their

behaviour in a wound healing context. In order to investigate these hypotheses in future, immunostaining of L929 cultures during or following scratch-wound healing could be undertaken and the results of these investigations might further elucidate the effects of MSC-secreted factors within this model of skin wound healing.

The variable effects of the cytokine portion of the MSC secretome implies that although MSC-CM enhances the rate of scratch-wound closure by skin cells not all of the factors produced by MSC directly contribute to this effect and indeed some may be inhibitory to scratch wound closure. Further understanding of those MSC-derived factors that are of benefit in a wound healing context compared to those that are not may inform more effective use of MSC as a potential therapy for cutaneous wounds, perhaps via screening of MSC for favourable secretory profiles or the formulation of pharmaceutical treatments based upon an optimal combination of MSC derived factors.

As well as cytokines, MSC secrete a range of ECM proteins including type I collagen, fibronectin and decorin, which are all major ECM components deposited during wound healing (Chen and Abatangelo 1999). Fibronectin is a large dimeric glycoprotein involved in cutaneous wound healing, cellular adhesion and migration (Yamada, 1991) as well as the induction of fibroblast-myofibroblast differentiation by TGF-β1 (Serini *et al,* 1998). This chapter's experiments showed fibronectin to be a better substrate for both L929 fibroblast and HaCaT keratinocyte adhesion and scratch wound closure compared to either type I collagen or decorin. This implies that fibronectin is amongst the MSC-secreted factors that contribute to the enhanced *in vitro* wound healing observed in Chapter 3. Indeed, previous studies have shown that a topical application of plasma fibronectin can enhance the rate of wound healing *in vivo* (Kwon *et al,* 2007).

Also present in MSC-CM was the small leucine rich proteoglycan, decorin. Decorin is usually associated with type one collagen fibres in normal skin, but is also deposited in granulation tissue during wound healing and further up regulated towards the later stages (Yeo *et al,* 1991). This chapter's experiments found decorin to be inhibitory to adherence and wound closure by HaCaT keratinocytes and prohibitively so to L929 fibroblasts. This, along with the observations made using growth factors discussed above, confirms that whilst MSC-CM is beneficial to *in vitro* wound healing overall, it is made up of components with both beneficial and inhibitory effects. Decorin is known to be anti-adherent to both human and mouse fibroblasts (Merle *et al,* 1997, Schmidt *et al,* 1987) suggesting that decorin would inhibit wound closure. However, delayed wound healing was reported in decorin knock out mice compared to wild type animals (Järveläinen *et al,* 2006) and furthermore a tripeptide copper complex that was shown to upregulate *in vivo* decorin expression (Siméon *et al,* 2000) also enhanced both acute (Downey *et al,* 1985) and chronic (Mulder *et al,* 1994) wound closure *in vivo*. The role of decorin in wound healing is variable and perhaps requires further study, but despite the presence of decorin in the MSC secretome, MSC-CM enhances scratch-wound healing by L929 fibroblasts and HaCaT keratinocytes.

The presence of various growth factors and ECM proteins in the MSC secretome prompted this investigation into the relative contribution of the individual factors to the 'net' effect of MSC-CM. However, the cytokines involved in *in vivo* wound healing act in a complex and combinatorial fashion to influence cell behaviour, for example: IL-6 has been shown to regulate the expression of TGF-β1, which was also present in MSC-CM (Luckett-Chastain and Gallucci, 2009). Thus the effect of cytokines in isolation may differ significantly from that in the presence of one or more other MSC-secreted factors. Similarly, type I collagen, fibronectin and

decorin are capable of interaction both with each other and with cytokines, e.g. decorin binds to type one collagen fibres as well as sequestering TGF-β1 (Kresse and Schönherr 2001). Additionally, the effects of surface-bound ECM proteins may not equate to the effects of those same proteins when in solution, as in MSC-CM. This necessitates the investigation of the actions of these components in combination in order to further assess their relative involvement in MSC-CM mediated enhancement of scratch wound healing. Informed by the results presented herein, the next chapter will attempt to elucidate some of these interactions.

Chapter 5

The potential role of MSC-secreted fibronectin, during *in vitro* scratch wound healing.

5.1: Aims and Background

The previous chapter demonstrated variable effects of individual components of the MSC secretome on *in vitro* scratch-wound closure and the adherence and spreading of skin cells in culture. Of the soluble factors investigated, neither IL-6 nor IL-8 enhanced scratch wound closure in either L929 fibroblasts or HaCaT keratinocytes used in these experiments. The ECM proteoglycan, decorin, was inhibitory to the adherence and scratch wound closure of both cell types. Conversely, the MSC secreted ECM component fibronectin, was shown to have a stimulatory effect upon both L929 fibroblasts and HaCaT keratinocytes, which is similar to the overall stimulatory effect of MSC CM reported in Chapter 3. Therefore, in this chapter, the role of fibronectin, and that of the MSC secretome when presented specifically as an ECM substratum, has been investigated in more depth. Firstly, the influence of fibronectin-coating of cultures plates was tested in combination with TGF-β1 (which was seen in Chapter 4 to be stimulatory to L929 fibroblast scratch wound healing, but inhibitory to HaCaT keratinocytes when collagen type I was used as a culture substrate). Secondly, the effects of MSC-CM on L929 and HaCaT cells on fibronectin-coated plates were examined. Finally, the effects of MSC-CM as a matrix substratum were examined directly, by comparing scratch wound closure by L929 and HaCaT cells on culture plates that had been coated either with MSC-CM or with unconditioned (control) medium.

5.2: The combined effects of fibronectin-coating tissue culture plates and TGF-β1 treatment on L929 fibroblasts and HaCaT keratinocytes.

TGF-β1 supplemented growth medium had no observable effect upon the rate of L929 fibroblast scratch-wound closure on fibronectin-coated tissue culture plates at either a lower or a higher concentration of TGF-β1 compared to unsupplemented medium (Figure 5.1). After 12 hours post-scratching, the degree of scratch wound closure had reached 88% (±5%) for L929 fibroblasts in unsupplemented medium, 93% (±4%) for L929 fibroblasts in 2ng/ml TGF-β1 supplemented medium and 84% (±7%) for L929 fibroblasts in 8ng/ml TGF-β1 supplemented medium, respectively (Figure 5.2). No significant differences were found between these results ($p > 0.05$ by ANOVA).

In contrast, TGF-β1 had a concentration-dependent inhibitory effect on the rate of scratch wound closure of HaCaT keratinocytes on fibronectin-coated plates (Figure 5.3). After 12 hours post-scratching, scratch wounds in unsupplemented medium had closed by 98% (±3%), whereas scratch wounds in 2ng/ml TGF-β1 supplemented medium had closed by 77% (±23%), and scratch wounds in 8ng/ml TGF-β1 had only achieved 53% (±5%) of wound closure (Figure 5.4). This concentration-dependent inhibitory effect of TGF-β1 treatment was statistically significant ($p < 0.05$ by ANOVA).
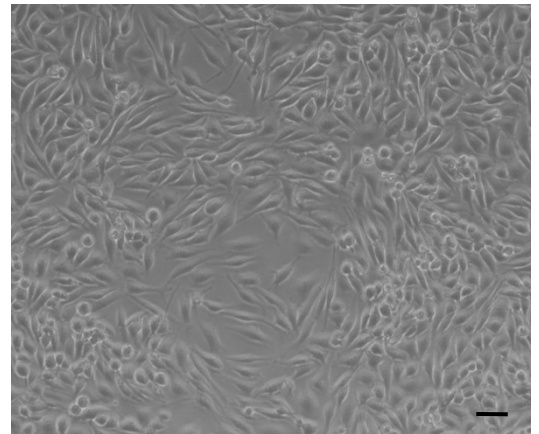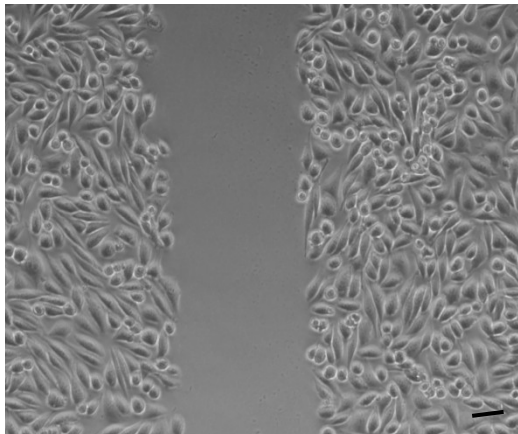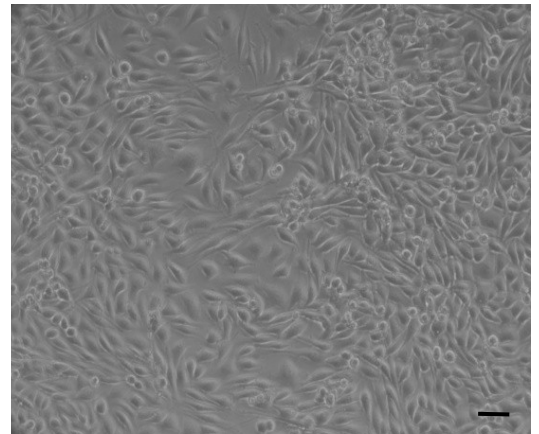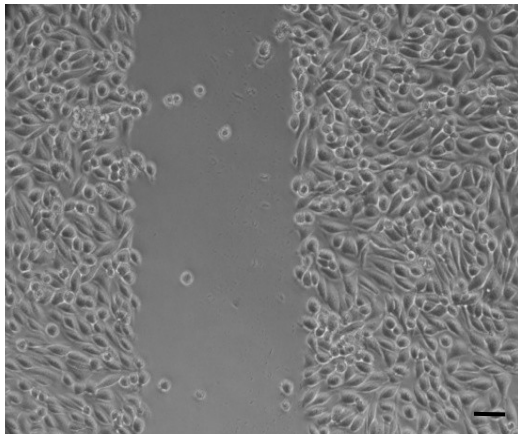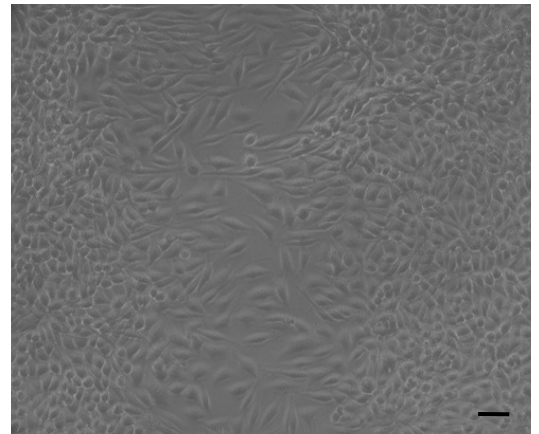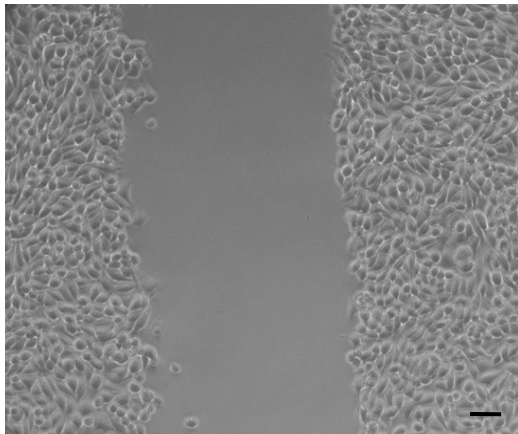
Figure 5.1 L929 fibroblasts on fibronectin closed close scratch wounds at a similar rate in TGF-β1 supplemented medium to that in unsupplemented medium. There was little apparent difference between a lower concentration and a higher concentration of TGF-β1 Representative phase contrast images are shown of single cell type (L929) scratch assays immediately following the scratch and 12 hours thereafter. Original magnification is x10 (bar = 10μm).
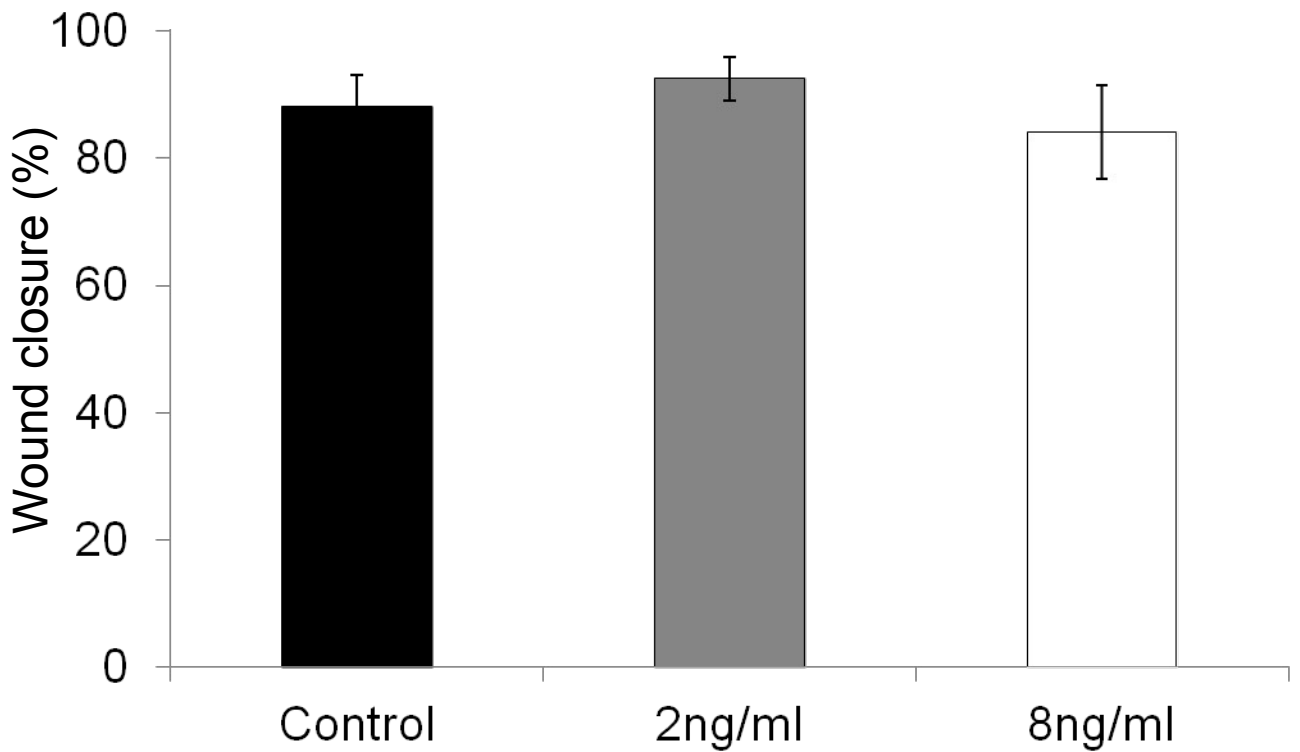
Figure 5.2 Scratch-wound closure by l929 fibroblasts in TGF-β1 supplemented media on fibronectin. Twelve hours post-scratch, the extent of wound closure was 88% (±5%) for L929 fibroblasts in unsupplemented medium, 93% (±4%) for L929 fibroblasts in 2ng/ml TGF-β1 supplemented medium and 84% (±7%) for L929 fibroblasts in 8ng/ml TGF-β1 supplemented medium . Data shown are means ± SEM. No significant differences were found between results (p>0.05 by ANOVA).
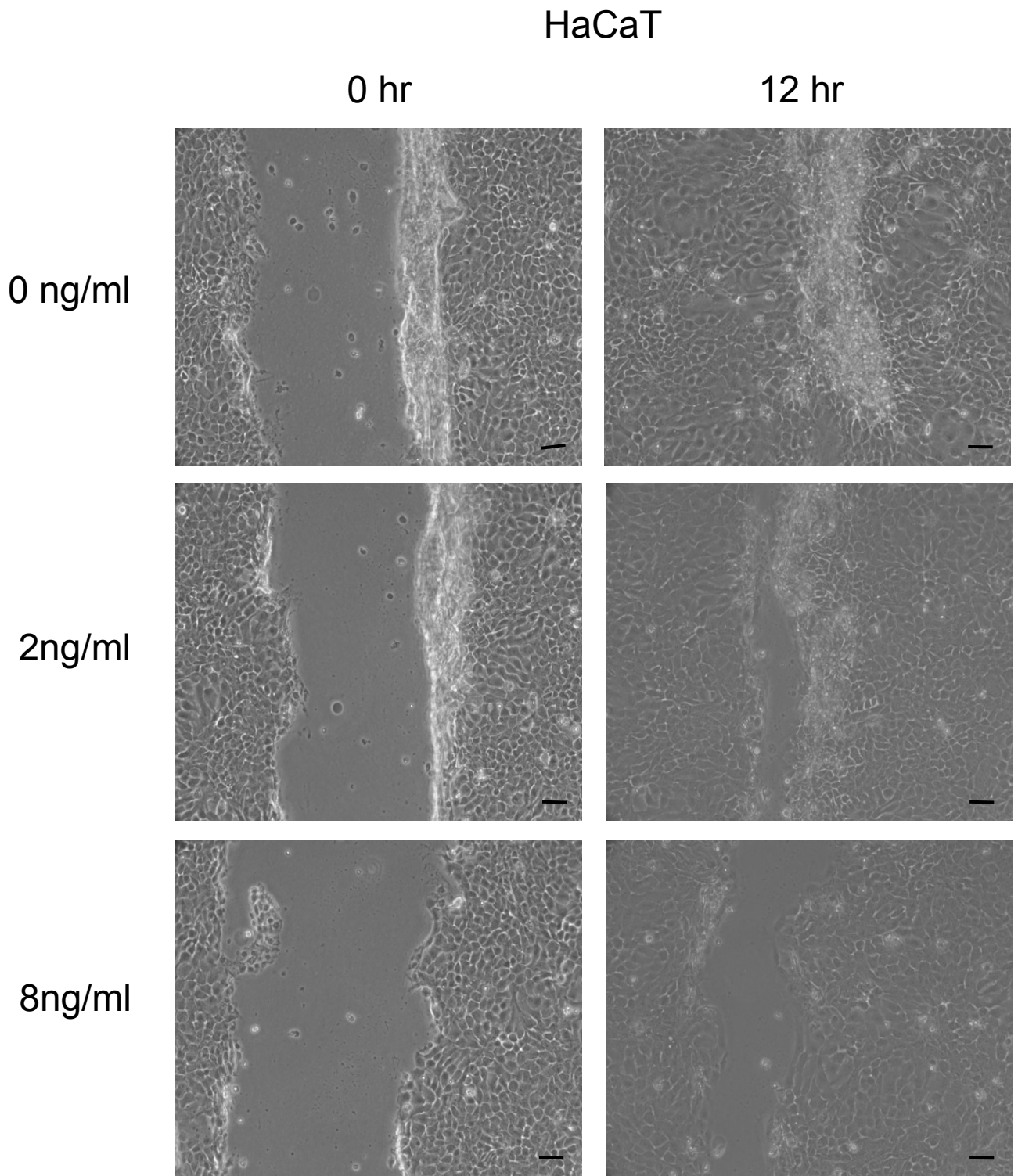
Figure 5.3 HaCaT keratinocytes on fibronectin closed scratch wounds slower in TGF-β1 supplemented medium than in unsupplemented medium. A lower concentration of TGF-β1 seemed to be less inhibitory to scratch wound closure than a higher concentration of TGF-β1 Representative phase contrast images are shown of single cell type (HaCaT) scratch assays immediately following the scratch and 12 hours thereafter. Original magnification is x10 (bar = 10μm).
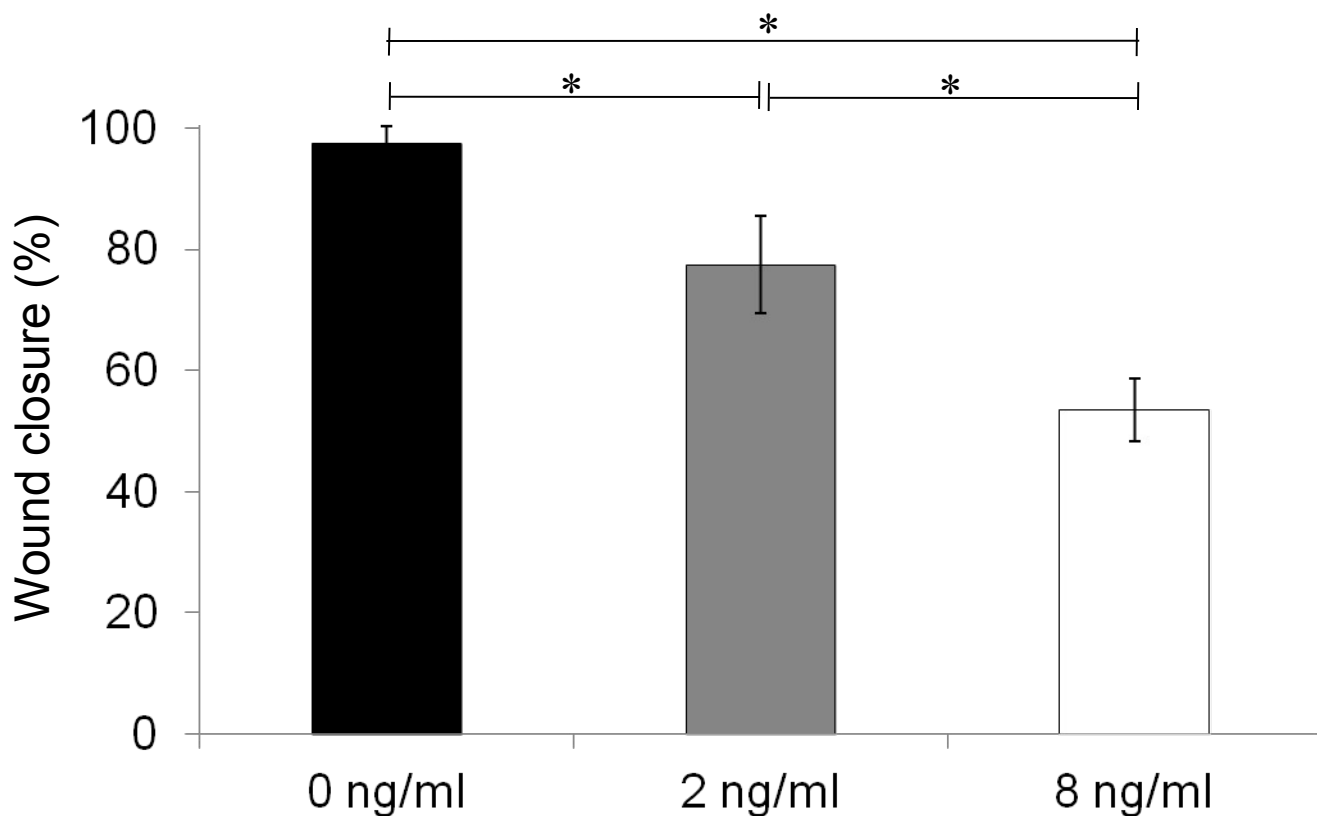
Figure 5.4 Scratch-wound closure by HaCaT keratinocytes in TGF-β1 supplemented media on fibronectin. Twelve hours post-scratch, the extent of wound closure was 98% (±3%) for HaCaT keratinocytes in unsupplemented medium, 77% (±23%) for HaCaT keratinocytes in 2ng/ml TGF-β1 supplemented medium and 53% (±5%) for HaCaT keratinocytes in 8ng/ml TGF-β1 supplemented medium . Data shown are means ± SEM. There was a significant difference by ANOVA ($p < 0.05$); (* denotes significance by Tukey's HSD).

5.3: The combined effects of fibronectin-coating culture plates and treatment with MSC-CM on L929 fibroblasts and HaCaT keratinocytes.

There was a marginal increase if the rate of L929 fibroblast scratch-wound closure in the presence of MSC-CM compared to unconditioned medium on fibronectin-coated plates (Figure 5.5). Hence, after 12 hours post-scratching the degree of scratch wound closure by L929 fibroblasts in unconditioned medium had reached 88% (±5%) compared to 99% (±2%) for scratch wound closure in MSC-CM (Figure 5.6). However, this marginal difference was not   statistically significant (p>0.05 *Mann Whitney U test*).

There was also little observable difference between the rate of scratch wound closure by HaCaT keratinocytes in unconditioned medium versus MSC-CM on fibronectin-coated culture plates (Figure 5.7). Hence, after 12 hours post-scratching wound closure by HaCaT keratinocytes on fibronectin had reached 98% (±2) in unconditioned medium compared to 94% (±6) in MSC-CM (Figure 5.8). No significant differences were found between these values (p>0.05 *Mann Whitney U test*).
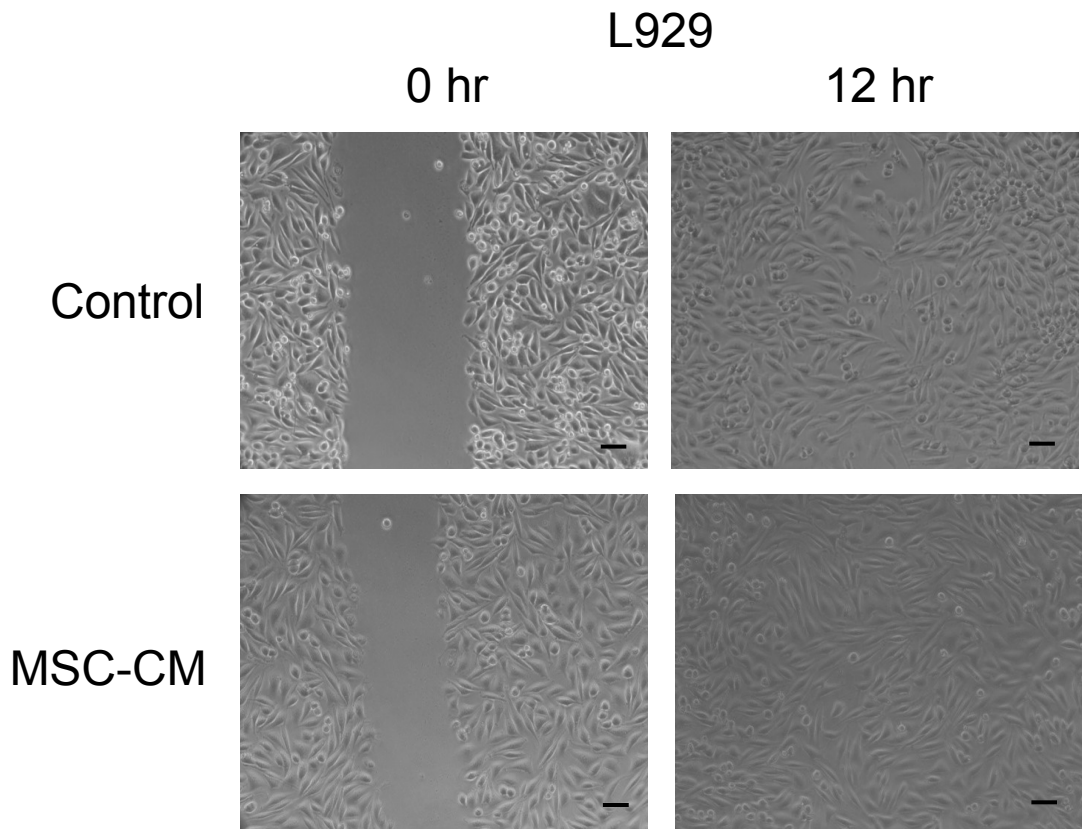
Figure 5.5 Scratch-wound closure by L929 fibroblasts is not enhanced by MSC-CM on fibronectin. Scratch-wound closure by L929 fibroblasts on fibronectin was not markedly affected by MSC conditioned medium, showing a very slight enhancement compared to unconditioned medium. Representative phase contrast images are shown of single cell type (L929) scratch assays immediately following the scratch and 12 hours thereafter. Original magnification is x10 (bar = 10μm).
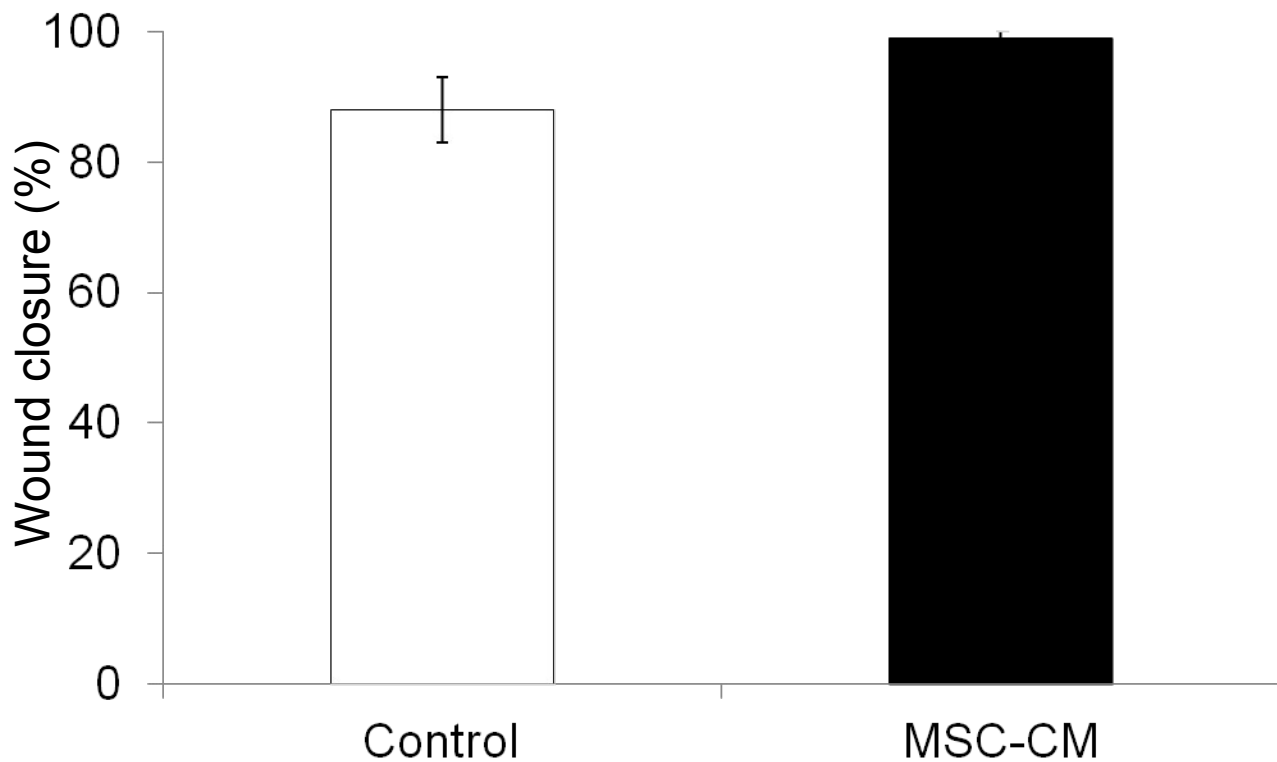
Figure 5.6 Scratch-wound closure by L929 fibroblasts in MSC-CM on fibronectin.
After 12 hours L929 fibroblasts on fibronectin had reached 88% (±5%) closure in
unconditioned medium, compared to 99% (±2%) closure in MSC conditioned medium.
Data shown are means ± SEM. No significant differences were found between results by
Mann Whitney U test.
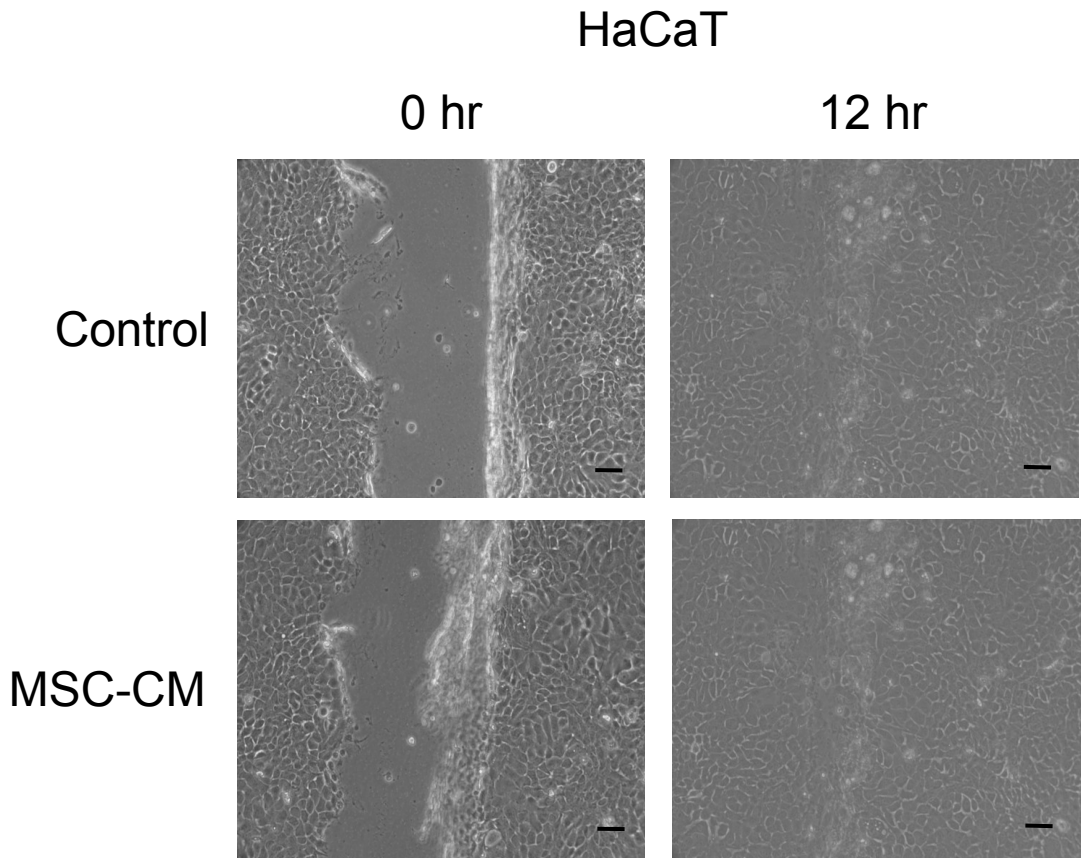
Figure 5.7 HaCaT keratinocytes on fibronectin appeared to close scratch wounds at a similar rate in MSC conditioned medium and in unconditioned medium. Representative phase contrast images are shown of single cell type (HaCaT) scratch assays immediately following the scratch and 12 hours thereafter. Original magnification is x10 (bar = 10µm).
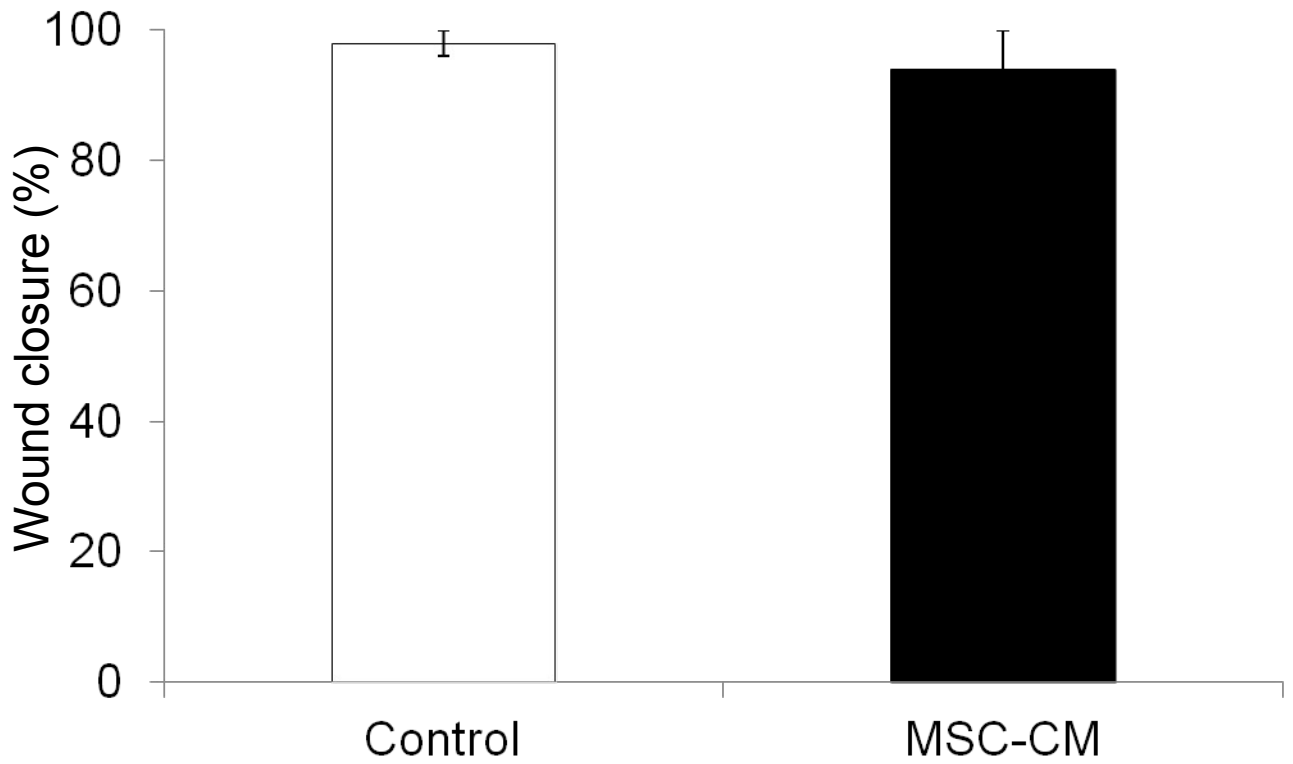
Figure 5.8 Scratch-wound closure by HaCaT keratinocytes in MSC-CM on fibronectin. After 12 hours HaCaT keratinocytes on fibronectin had reached 98% (±2%) closure in unconditioned medium, compared to 94% (±6%) closure in MSC conditioned medium. Data shown are means ± SEM. No significant differences were found between results by Mann Whitney U test.

5.4: The effects of coating tissue culture plates with MSC-CM on L929 fibroblasts and HaCaT keratinocytes.

L929 fibroblasts closed scratch wounds on serum free MSC-CM coated tissue culture plates faster than on unconditioned serum free medium-coated plates (Figure 5.9). Hence, after 6 hours post scratching, the degree of scratch wound closure by L929 fibroblasts on unconditioned medium-coated tissue culture plastic had reached 41% (±9%) compared to 54% (±6%) on MSC-CM. After 12 hours, L929 fibroblasts on unconditioned medium-coated tissue culture plastic had reached 70% (±13%) scratch wound closure compared to 83% (±4%) on MSC-CM coated plates (Figure 5.10). These differences were not significant, but came close to significance at the 12 hour time point (p=0.057 *Mann Whitney U test*).

HaCaT keratinocyte scratch-wounds closed at a similar rate on culture plates coated in (serum free) unconditioned medium and MSC-CM. In both cases, scratch wound closure was near to completion within 6 hours (Figure 5.11). Hence, after 6 hours post-scratching, HaCaT keratinocytes on unconditioned medium-coated tissue culture plastic had reached 84% (±6%) compared to 88% (±4%) on MSC-CM, respectively. After 12 hours post-scratching, the degree of scratch-wound closure on unconditioned medium-coated tissue culture plastic had reached 96% (±1%), compared to 98% (±1%) on MSC-CM, respectively (Figure 5.12). The difference between these values was not statistically significant (p>0.05 *Mann Whitney U test*).
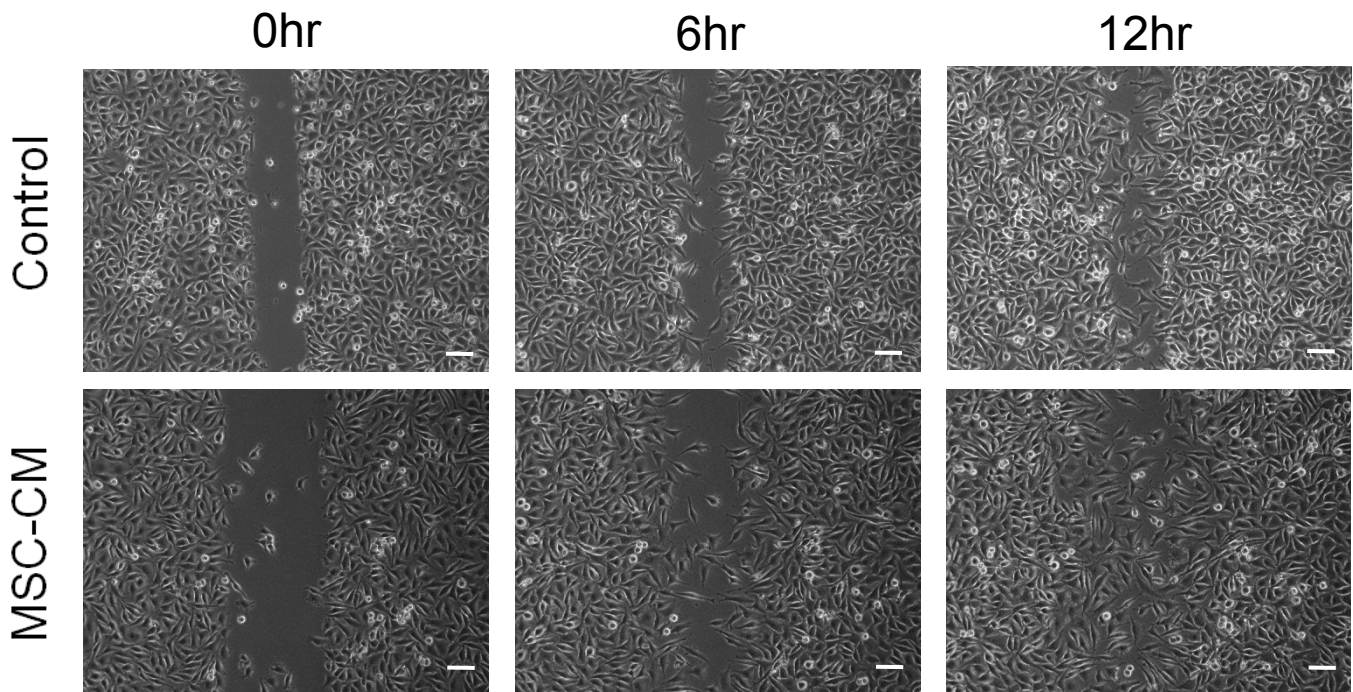
Figure 5.9 L929 fibroblasts on MSC-CM coated tissue culture plastic closed scratch wounds faster than on plastic coated in unconditioned medium. Representative phase contrast images are shown of single cell type (L929) scratch assays immediately following the scratch and 6 and 12 hours thereafter. Original magnification is x10 (bar = 10μm).
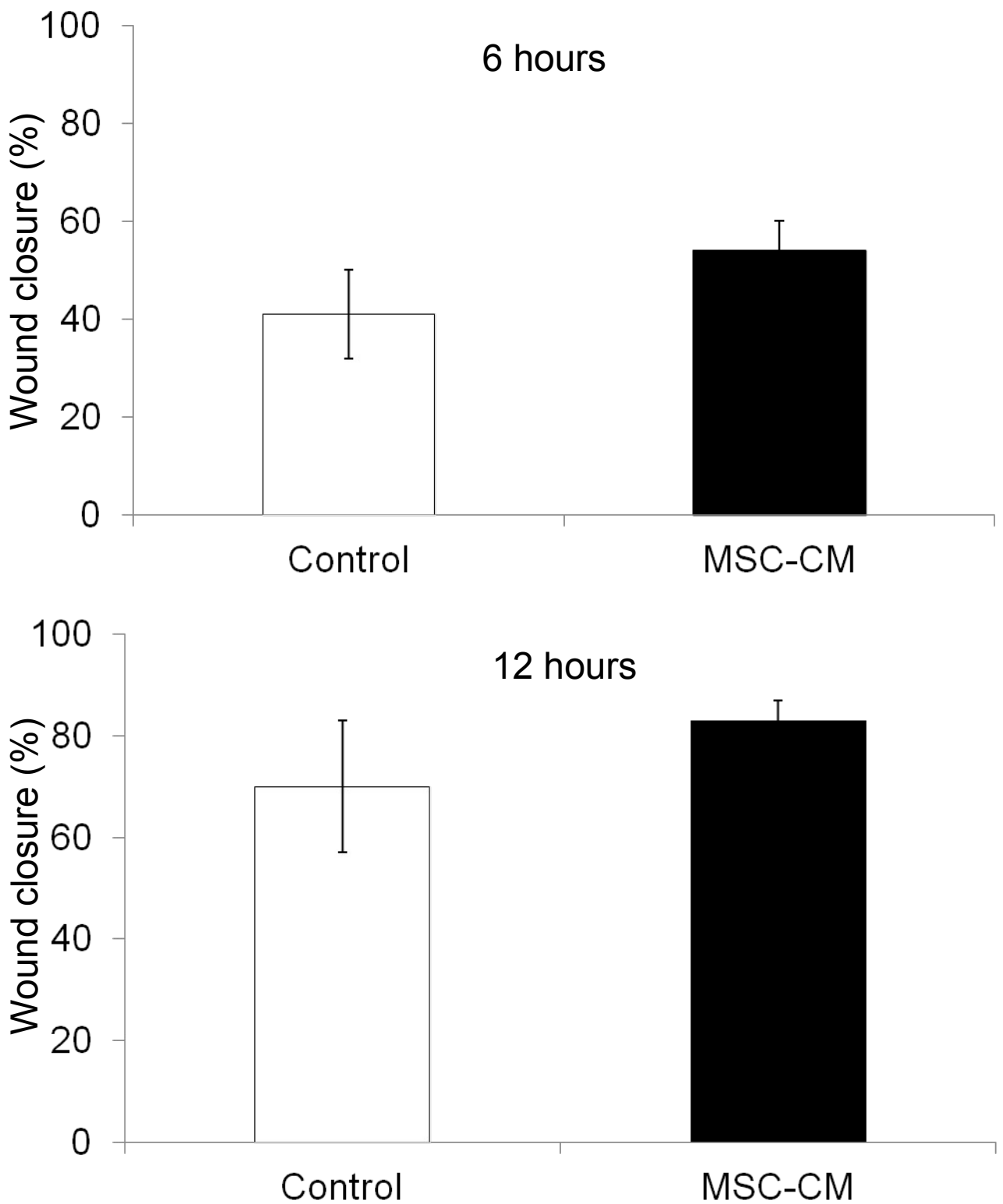
Figure 5.10 Scratch-wound closure by L929 fibroblasts on MSC-CM coated plates. After 6 hours L929 fibroblasts on unconditioned medium-coated tissue culture plastic had reached 41% (±9%), compared to 54% (±6%) on MSC-CM. After 12 hours L929 fibroblasts on unconditioned medium-coated tissue culture plastic had reached 70% (±13%), compared to 83% (±4%) on MSC-CM. Data shown are means ± SEM. No significant differences were found between results, although Control vs. MSC-CM was near significant (p=0.057) by Mann Whitney U test.

HaCaT

	0hr	6hr	12hr
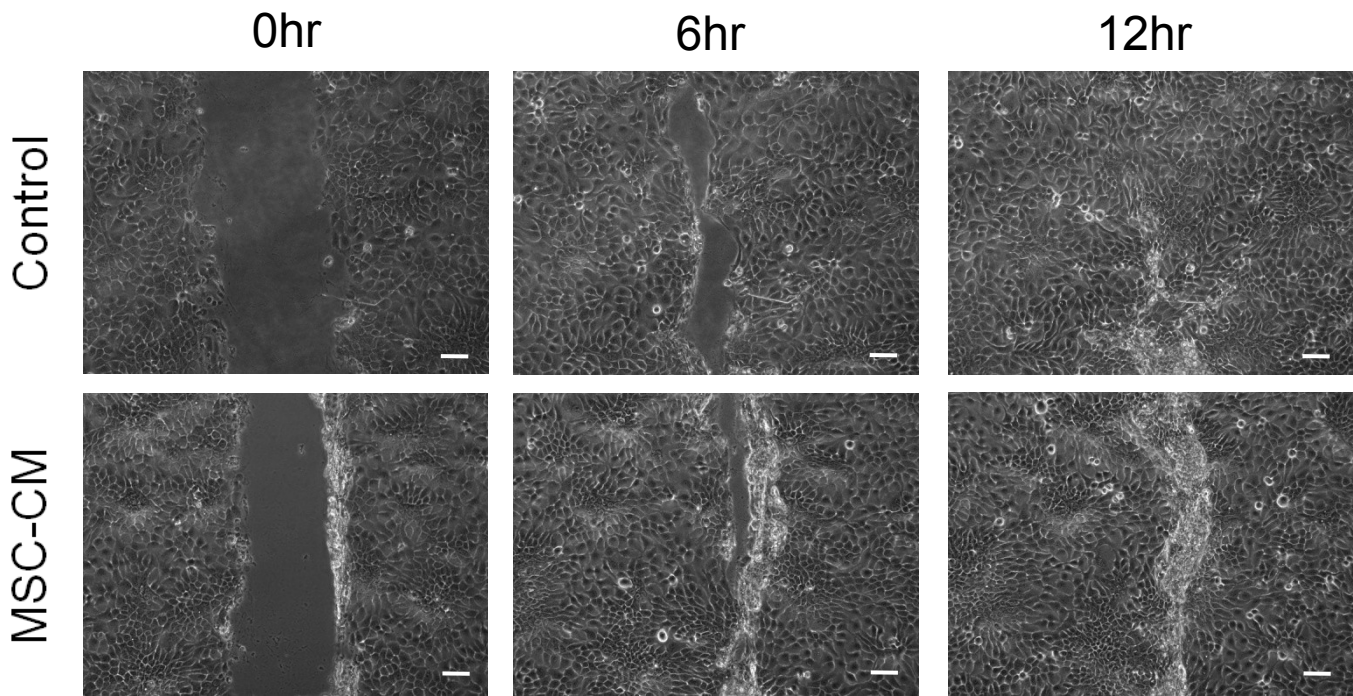
Figure 5.11 HaCaT keratinocytes on MSC-CM coated tissue culture plastic closed scratch wounds at a similar rate to cells on plastic coated in unconditioned medium. Representative phase contrast images are shown of single cell type (HaCaT) scratch assays immediately following the scratch and 6 and 12 hours thereafter. Original magnification is x10 (bar = 10μm).
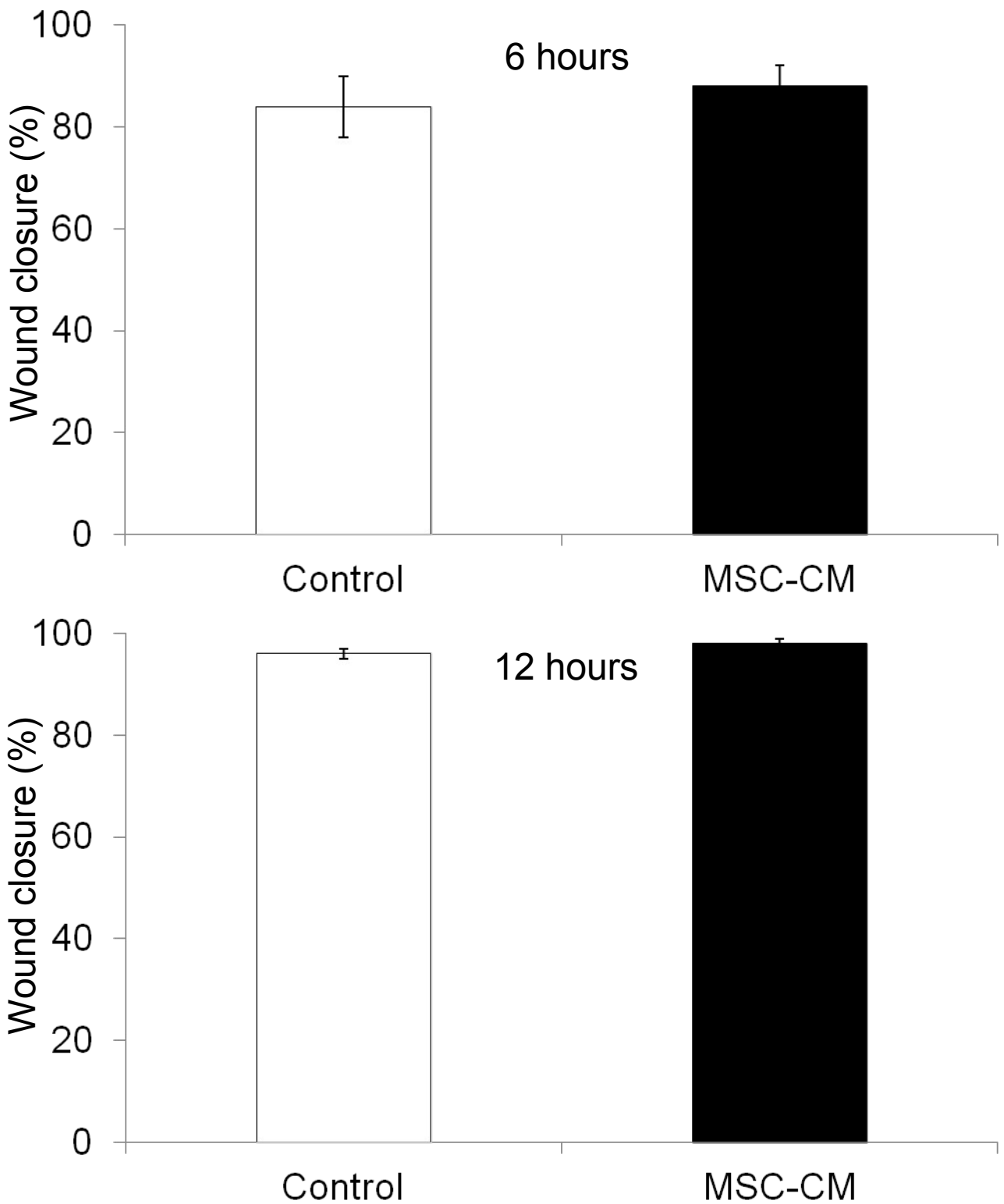
Figure 5.12 Scratch-wound closure by HaCaT keratinocytes on MSC-CM coated plates. After 6 hours HaCaT keratinocytes on unconditioned medium-coated tissue culture plastic had reached 84% (±6%), compared to 88% (±4%) on MSC-CM. After 12 hours HaCaT keratinocytes on unconditioned medium-coated tissue culture plastic had reached 96% (±1%), compared to 98% (±1%) on MSC-CM. Data shown are means ± SEM (No significant differences were found between results by Mann Whitney U test).

5.5: Soluble ECM proteins

L929 fibroblasts closed scratch wounds on uncoated tissue culture plates faster in the absence of exogenous ECM proteins than inthepresence of either decorin or fibronectin (Figure 5.13). Hence, after 12 hours post scratching, the degree of scratch wound closure by L929 fibroblasts in unconditioned medium had reached 98% (±3%) compared to 62% (±15%) in fibronectin supplemented medium and 47% (±16%) in decorin supplemented medium (Figure 5.14). These differences were not statistically significant (*ANOVA*).

Similarly, the presence of both soluble fibronectin and decorin within culture medium retarded the rate of scratch wound closure by HaCaT Keratinocytes, such that after 12 hours post scratching of scratch wound closure by L929 fibroblasts in unconditioned medium had reached 89% (±5%) compared to 18% (±6%) in fibronectin supplemented medium and 37% (±6%) in decorin supplemented medium (Figure 5.14). These differences were statistically significant (p<0.05 by *ANOVA*).
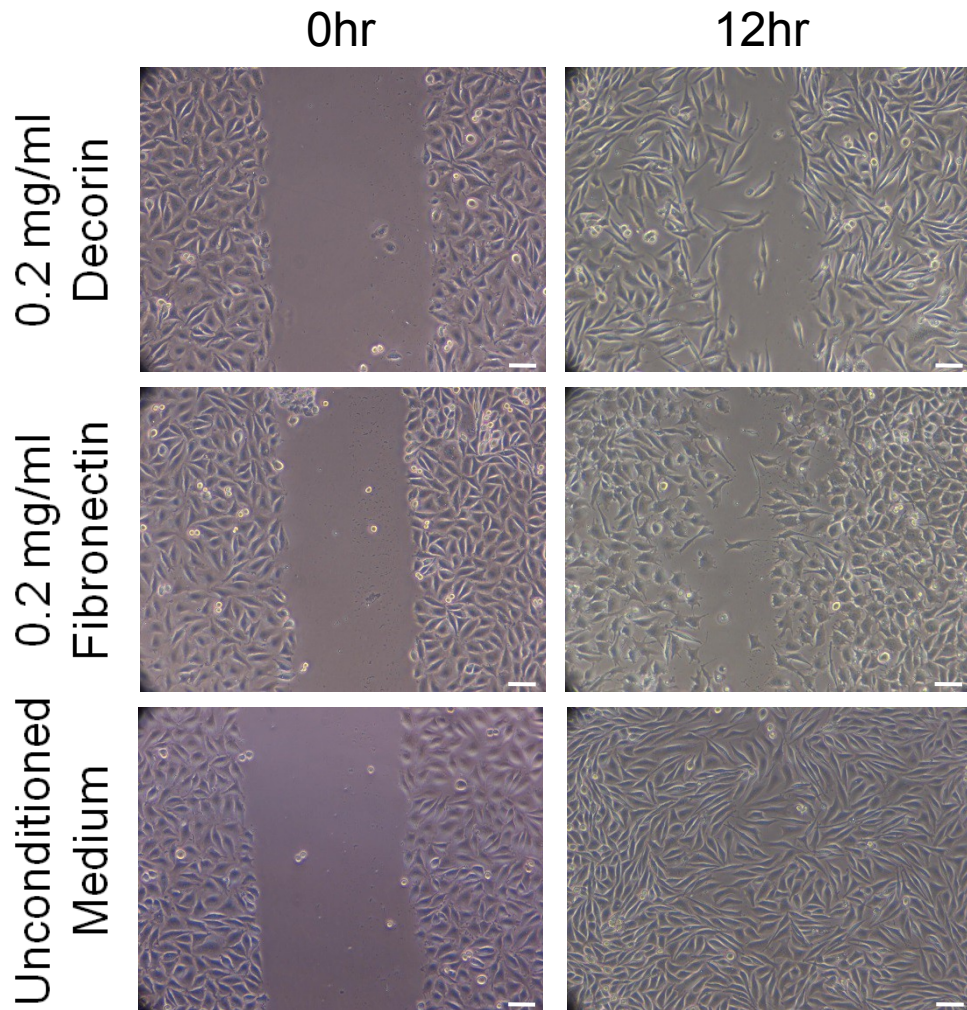
Figure 5.13. Soluble decorin and fibronectin reduced scratch wound closure by L929 fibroblasts compared to unsupplemented medium. Both ECM proteins at 0.2mg/ml were associated with a reduction in the rate of scratch wound closure by L929 fibroblasts. Representative phase contrast images are shown of single cell type (L929) scratch assays immediately following the scratch and 12 hours thereafter. Original magnification is x10 (bar = 10μm).
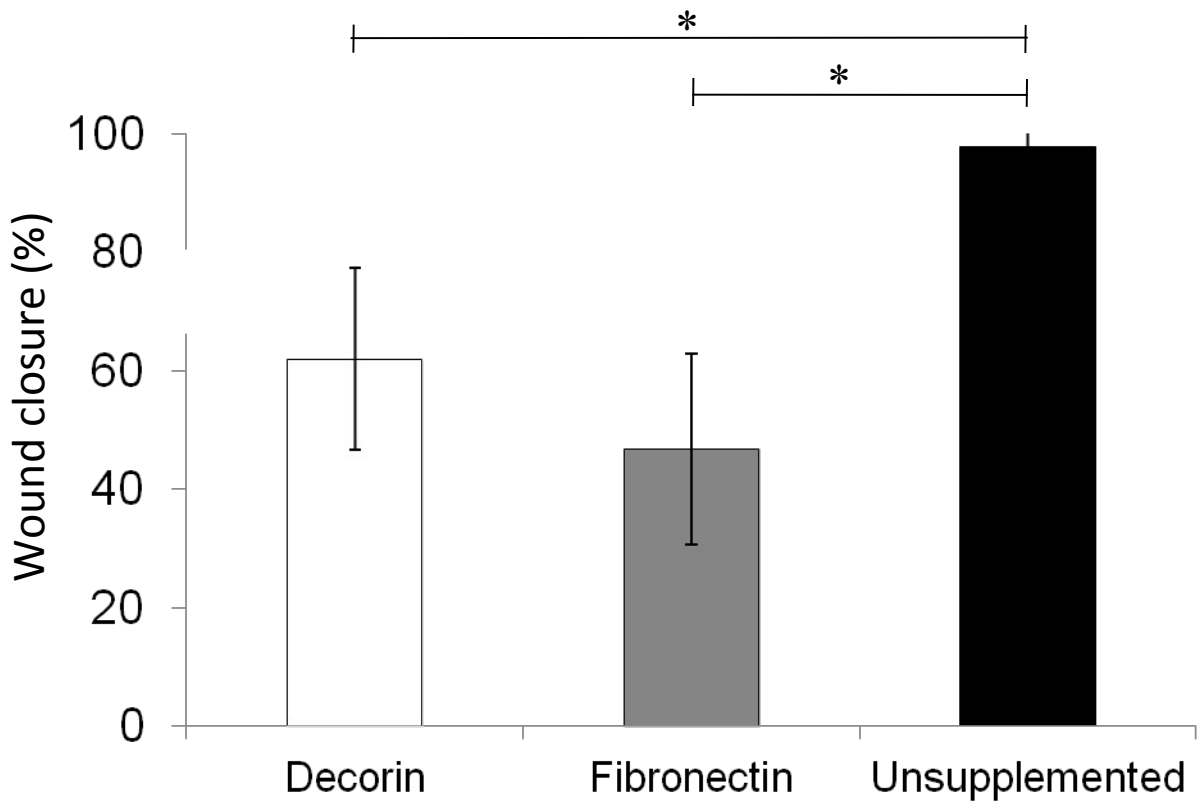
Figure 5.14. Scratch-wound closure by L929 fibroblasts in Decorin and fibronectin supplemented media. Twelve hours post-scratch, the extent of wound closure was 62% (±15%) for L929 fibroblasts in 0.2mg/ml decorin supplemented medium, 47% (±16%) for L929 fibroblasts in 0.2mg/ml fibronectin supplemented medium and 98% (±3%) for L929 fibroblasts in unsupplemented medium. Data shown are means ± SEM. There was a significant difference by ANOVA (p<0.05); (* denotes significance by Tukey's HSD).

HaCaT

	0hr	12hr
0.2 mg/ml Decorin		
0.2 mg/ml Fibronectin		
Unconditioned Medium		
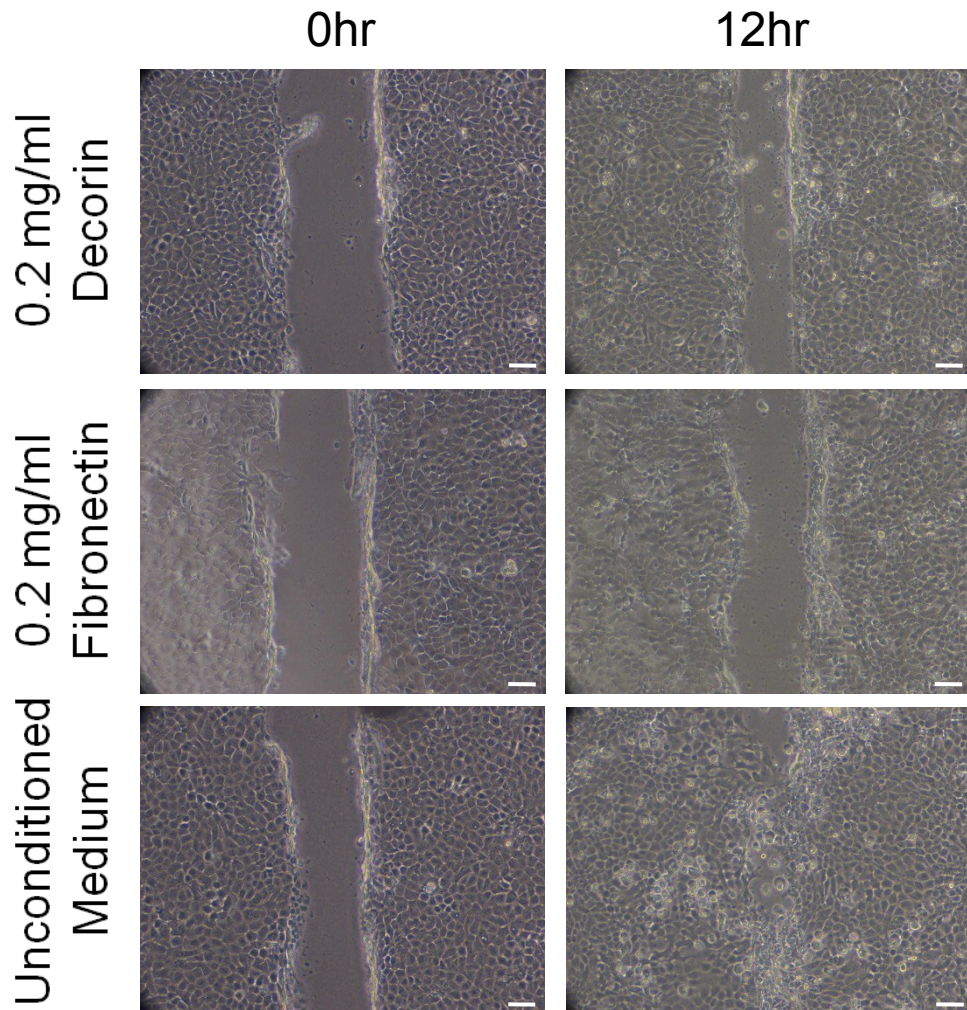
Figure 5.15. Scratch wound closure by HaCaT keratinocytes was retarded in the presence of soluble ECM proteins compared to unsupplemented medium. Both soluble decorin and fibronectin at 0.2mg/ml were associated with a reduction in the rate of scratch wound closure by HaCaT keratinocytes. Representative phase contrast images are shown of single cell type (HaCaT) scratch assays immediately following the scratch and 12 hours thereafter. Original magnification is x10 (bar = 10µm).
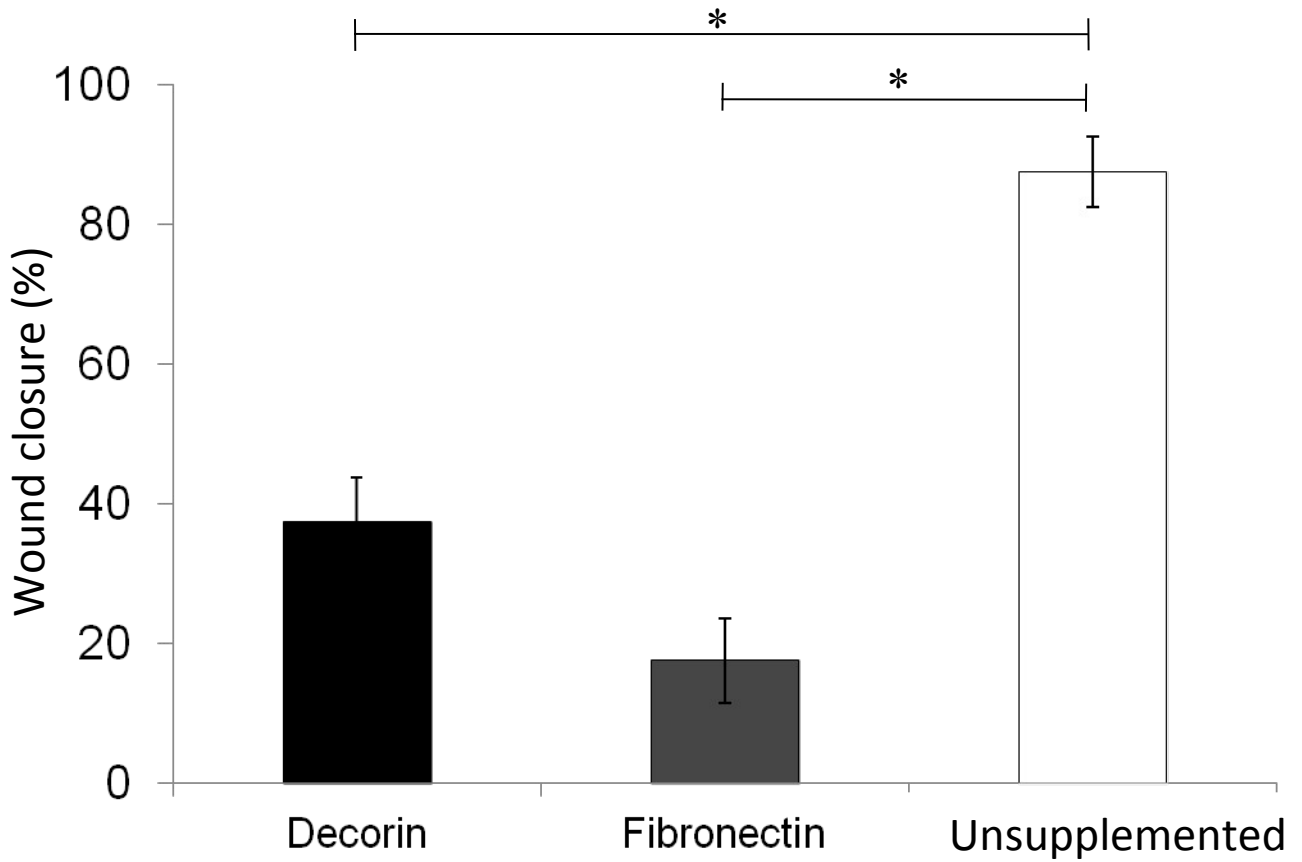
Figure 5.16. Scratch-wound closure by HaCaT keratinocytes in Decorin and fibronectin supplemented media. Twelve hours post-scratch, the extent of wound closure was 37% (±6%) for HaCaT keratinocytes in 0.2mg/ml decorin supplemented medium, 18% (±6%) for HaCaT keratinocytes in 0.2mg/ml fibronectin supplemented medium and 89% (±5%) for HaCaT keratinocytes in unsupplemented medium. Data shown are means ± SEM. There was a significant difference by ANOVA ($p < 0.05$); (* denotes significance by Tukey's HSD).

5.5: Discussion

Cell motility in wound healing is partially dependent upon the remodelling of the ECM (Gailit & Clark, 1996) as well as the expression of various growth factors (Moulin, 1995). The ECM protein fibronectin and the growth factor TGF-β1 are both secreted by MSC, and are also present during cutaneous wound healing *in vivo.* In Chapter 4, coating tissue culture plates with fibronectin was shown to enhance the rate of both L929 fibroblast and HaCaT keratinocyte migration into scratch-wounds, compared to their rates of migration on type I collagen. TGF-β1 was also shown to enhance the migration of L929 fibroblasts, but to inhibit the migration of HaCaT keratinocytes on type I collagen. As MSC were shown to secrete fibronectin and also TGF-β1 (in Chapter 3), this set of experiments investigated the effects of both of these MSC-secreted proteins in combination.

Whilst fibronectin and TGF-β1 were each shown to enhance L929 fibroblast migration individually, the combination of TGF-β1 supplemented media with fibronectin-coated tissue culture plates did not result in any further enhancement of L929 fibroblast migration compared to fibronectin in the absence of TGF-β1. However, the rate of scratch-wound closure by L929 fibroblasts in the presence of both TGF-β1 and fibronectin was somewhat greater than in the presence of TGF-β1 and type I collagen. This, along with the greater enhancement of L929 fibroblast scratch wound closure by fibronectin than TGF-β1 compared to their respective controls, suggests that fibronectin may have played a greater role than TGF-β1 in the improved rate of L929 fibroblast migration observed in the presence of MSC-CM. Interestingly, as well as containing fibronectin, MSC-CM has been shown to up-regulate the deposition of fibronectin and other ECM components such as elastin and type I collagen by fibroblasts (Jeon *et al,* 2010). As fibronectin improved the

migration of both L929 fibroblasts (and, indeed, HaCaT keratinocytes), this trophic activity would be expected to further encourage the potential use of MSC-CM in the treatment of cutaneous wounds.

TGF-β1 treatment significantly inhibited the migration of HaCaT keratinocytes on fibronectin-coated tissue culture plates. This matches the observations of the previous chapter, wherein TGF-β1 also inhibited the rate of HaCaT keratinocyte migration upon type I collagen-coated plates. The effects of TGF-β1 on keratinocytes during wound healing are somewhat uncertain, and published investigations into the problem have yielded contradictory results. Studies have reported a TGF-β1 mediated enhancement of keratinocyte migration *in vitro* using both transwell migration assays (Decline *et al*, 2003, Decline and Rouselle, 2000) and using time-lapse video microscopy (Sutherland *et al,* 2005), and the addition of a TGF-β1 neutralising antibody to murine keratinocyte cultures significantly inhibited keratinocyte migration (Stepp *et al,* 2007). Conversely, other studies have suggested that impaired TGF-β1 signal transduction results in accelerated wound healing and re-epithelialisation *in vivo* (Ashcroft *et al,* 1999, Hosokawa *et al*, 2005). As previously suggested in Chapter four, the ability of TGF-β1 to drive HaCaT keratinocytes towards terminal differentiation (Bushke *et al,* 2011) may contribute to the inhibitory effect of TGF-β1 on HaCaT keratinocyte migration on fibronectin as well as on type I collagen observed in this investigation, i.e. the keratinocytes would become less migratory as they begin to form a full and mature epithelial layer.

MSC-CM had no discernible effect upon L929 fibroblast scratch-wound closure on fibronectin-coated tissue culture plates compared to unconditioned (control) medium. This was in sharp contrast to those scratch assays performed on type I collagen-coated tissue culture plastic, where MSC-CM significantly improved

the rate of L929 fibroblast scratch-wound closure compared to unconditioned medium (Chapter 3). The rate of L929 fibroblast scratch-wound closure on fibronectin in both unconditioned medium and MSC-CM was similar to that on type I collagen in MSC-CM, and all of these were similarly greater than those in unconditioned medium on type I collagen. Therefore, it seems reasonable to suggest that the majority of the MSC-CM mediated enhancement of L929 fibroblast scratch-wound closure may be due to the effects of fibronectin. This hypothesis is supported by the previous observation that TGF-β1, which was the only other MSC-CM component examined that enhanced L929 fibroblast migration, had no further stimulatory effect upon L929 fibroblasts in the presence of fibronectin. Similarly, HaCaT keratinocyte scratch-wounds did not close any faster in MSC-CM compared to unconditioned medium when these assays were performed on fibronectin-coated tissue culture plates. As fibronectin was the only component of MSC-CM that had any stimulatory effect upon HaCaT keratinocyte migration when applied individually, and fibronectin-coating alone was associated with a similar rate of HaCaT scratch-wound closure to that seen in the presence of MSC-CM, this seems to suggest that the ability of MSC-CM to enhance HaCaT keratinocyte scratch-wound closure may also be dependent upon fibronectin as a major contributory factor.

Blocking antibodies for integrin receptors for fibronectin, such as α5β1 and/or αVβ6, could be used to test the hypothesis that fibronectin as an ECM substratum is an essential mediator of MSC-CM enhancement of L929 fibroblasts and HaCaT keratinocyte scratch-wound closure, i.e. if the blocking of the integrin receptors for fibronectin resulted in a diminished response to MSC-CM, this could confirm the essentiality of fibronectin to the ability of MSC-CM to stimulate skin cell migration via cell-matrix interactions and hence enhance wound healing *in vitro*.

In Chapter 4, coating tissue culture plates with fibronectin was shown to enhance L929 fibroblast and HaCaT keratinocyte migration compared to when the culture plates were coated with type I collagen. Thus it was hypothesised that the enhancement of L929 fibroblast and HaCaT keratinocytes migration seen in MSC-CM versus unconditioned medium was due to MSC-secreted fibronectin becoming deposited upon the culture plate surface and acting in a similar way to the fibronectin-coated plates used in Chapter 4. To investigate this hypothesis, tissue culture plates were coated in MSC-CM in the same manner as with fibronectin and type I collagen previously, and washed before cells were introduced in order to remove any non-bound growth factors or cytokines that may influence cell behaviour, hence leaving behind only that portion of the MSC secretome that would bind to tissue culture plastic. L929 fibroblast scratch-wound closure was faster on tissue culture plates that were coated in MSC-CM compared with those coated with unconditioned medium, although not to the same degree as was observed in experiments using whole MSC-CM, whilst HaCaT keratinocytes closed scratch-wounds at a similar rate in MSC-CM coated culture plates or those coated with unconditioned medium. This partial enhancement of L929 fibroblast migration, and the lack of an observable response by HaCaT keratinocytes, suggests that, whilst the result presented in this chapter imply that there may be an important role for fibronectin in the MSC-CM mediated enhancement of scratch-wound closure by both cell types, the portion of MSC-CM that deposits upon the tissue culture surface is not entirely responsible for the effects of MSC-CM on L929 fibroblasts, and may not significantly contribute to HaCaT keratinocyte migration at all. Immuno-staining of MSC-CM coated tissue culture plastic for MSC-secreted ECM proteins such as type I collagen, decorin and fibronectin, along with other secretome components, would help elucidate which

factors were present in the surface-bound portion of MSC-CM. In addition, if the effects of MSC-CM are not dependent upon surface-bound proteins, yet fibronectin was seen to have a stimulatory effect upon both L929 fibroblast and HaCaT keratinocyte scratch-wound closure, then scratch assays performed upon these cell types using culture medium supplemented with fibronectin in solution compared to both MSC-CM and unconditioned medium, might have been expected to demonstrate whether or not fibronectin may be acting as a soluble stimulatory factor, influencing cell migration via a paracrine mechanism rather than simply acting as a more permissive substrate for cellular migration. The results of these experiments suggest that soluble fibronectin is not directly stimulatory to skin cell migration in this model system, as medium supplemented with fibronectin (and indeed decorin) was seen to result in a retardation of the rate of scratch wound closure by both L929 fibroblasts and HaCaT keratinocytes.

Chapter 6

The Effects of MSC Secreted Factors on Endothelial Cells

6.1: Aims and Background

Chapter 1 discussed how the effectiveness of wound healing, particularly for chronic wounds such as pressure ulcers, depends on a good vascular supply to the wound bed. Indeed, many potential therapies for severe or chronic cutaneous wounds fail as a result of poor vasculature (Laschke *et al*, 2006, Jain *et al,* 2005), with the obvious implication that strategies that improve blood vessel growth into the wound bed will promote wound healing. Chapters 3-5 demonstrated that MSC-CM were stimulatory to skin cells, specifically L929 fibroblasts and HaCaT keratinocytes, and then further examined which of the individual components of the MSC secretome identified by ELISA and mass spectrometry may be active in this role. However, the effects of MSC secreted factors on endothelial cells had not been examined, even though there is evidence to suggest that MSC are pro-angiogenic through their paracrine activity (Kinnaird *et al*, 2004, Beckermann *et al*, 2008, Zackarek *et al*, 2007) and that MSC are capable of endothelial differentiation (Oswald *et al*, 2004, Jazyayeri *et al*, 2008), although the engraftment into new vasculature has shown to be low *in vivo* (Tomita *et al*, 2002). Therefore, in this section of the study, the effects of MSC-CM were tested against an endothelial cell line, EaHy926 cells (Edgell *et al*, 1983). This analysis included assaying the effects of individual MSC-CM from 3 different donors on EaHy926 cell adhesion and migration on a range of ECM protein substrates, again using the scratch assay, along with further identification of individual components of the MSC secretome present in each donor.

6.2: The effects of MSC-CM upon EaHy-926 cell adherence and migration.

MSC-CM significantly enhanced the rate of scratch wound closure by EaHy-926 endothelial cells (Figures 6.1-6.2), such that after 6 hours post scratching, EaHy-926 endothelial cells in the presence of MSC-CM had closed scratch wounds by 35% (±2%), whilst cells in unconditioned (control) medium had only closed the scratch wounds by 20% (±1%). After 12 hours post scratching, EaHy-926 endothelial cells had closed scratch wounds by 56% (±3%), in MSC-CM compared with cells in unconditioned (control) medium, which had only closed scratch wounds by 30% (±3%). In both cases, these differences between the extent of scratch wound closure in MSC-CM versus unconditioned (control) medium were significant (*=p<0.05 by Mann Whitney U test).

No similar enhancement in scratch wound closure was observed when MSC-CM was used to coat tissue culture plates to form an ECM substrate, rather than as culture medium (Figures 6.3-6.4). Hence, at 6 hours post scratching EaHy-926 endothelial cells had closed scratch wounds by a similar degree in both MSC-CM coated and unconditioned (control) medium coated culture plates, at 24% (±2%) and 21% (±2%), respectively. Similarly, after 12 hours post scratching, the degree of scratch wound closure by EaHy-926 endothelial cells was 36% (±2%) in MSC-CM coated culture plates and 34% (±3%) in culture plates coated in unconditioned (control) medium. No significant differences were found between these values (p>0.05 *Mann Whitney U test*).

However, MSC-CM coating of culture plates did result in a significant increase in the degree of EaHy-926 cell spreading such that after 4 hours post-seeding the average cell area on MSC-CM coated culture plates was $1322\mu m^2$ ($\pm140\mu m^2$)

compared to 389µm^2 (±30µm^2) on culture plates coated with unconditioned (control) medium (Figure 6.5-6.6).
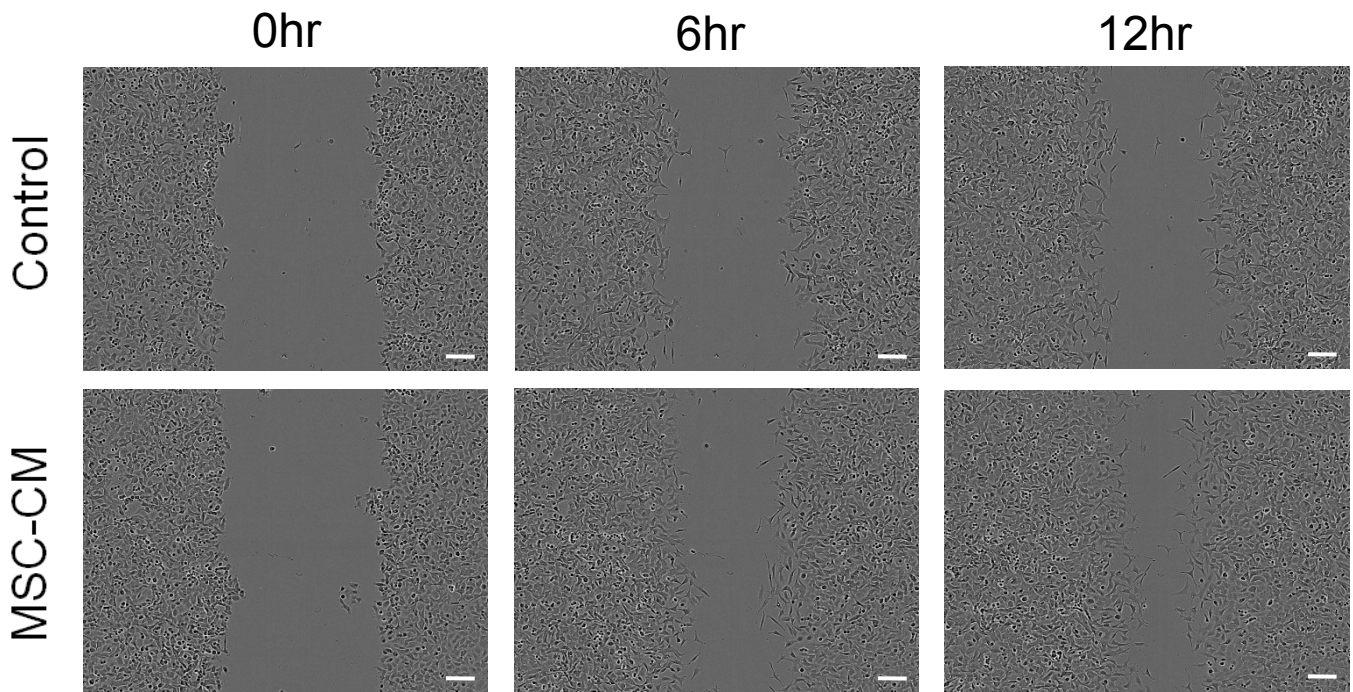
Figure 6.1 EaHy-926 endothelial cells closed scratch wounds faster in MSC-CM than in unconditioned medium. Representative phase contrast images are shown of single cell type (EaHy-926) scratch assays immediately following the scratch and 6 and 12 hours thereafter. Original magnification is x10 (bar = 100μm).
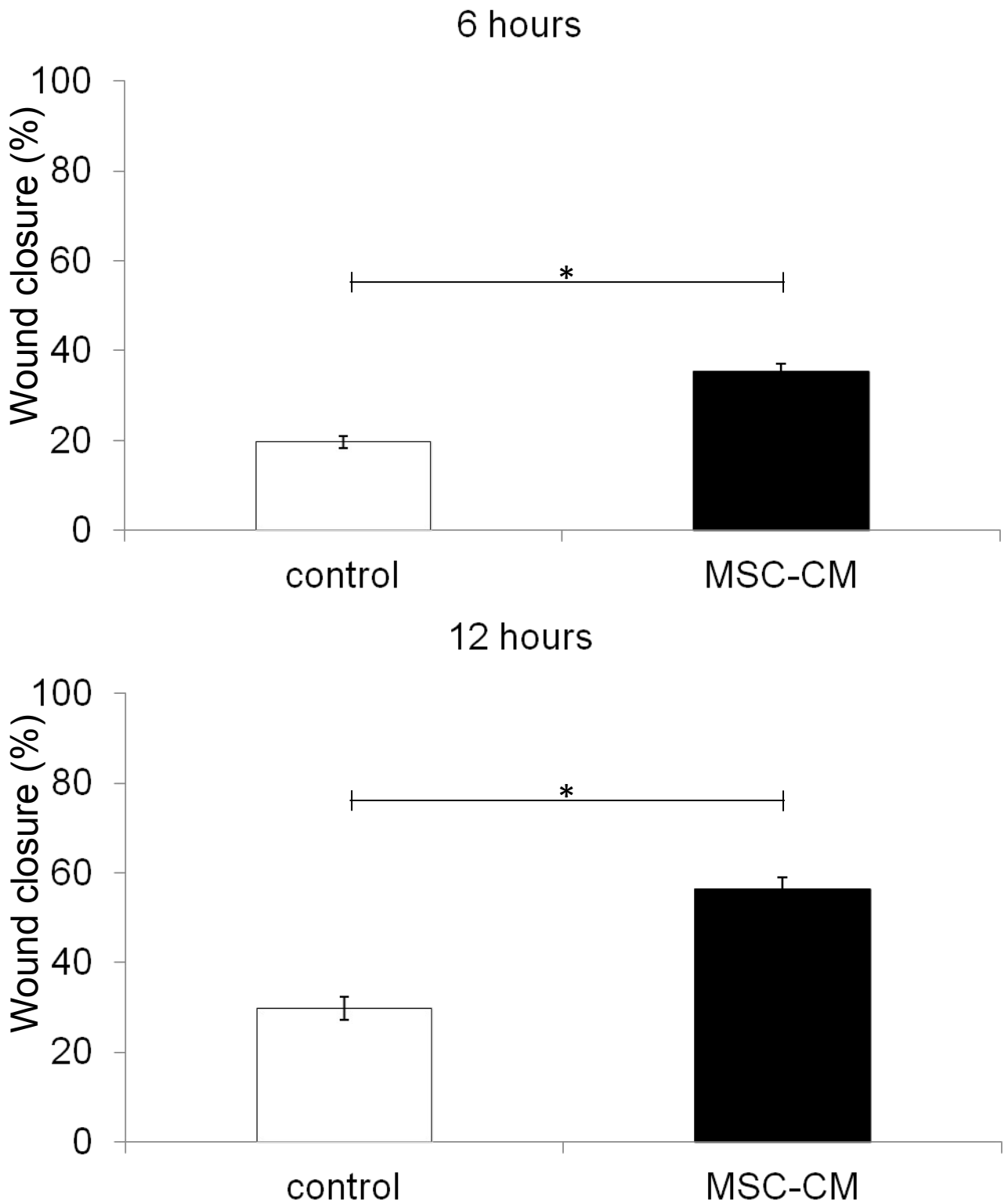
Figure 6.2 Scratch-wound closure by EaHy-926 endothelial cells in MSC-CM. After 6 hours EaHy-926 endothelial cells in unconditioned (control) medium had reached 20% (±1%), compared to 35% (±2%) in MSC-CM. After 12 hours EaHy-926 endothelial cells in unconditioned medium had reached 30% (±3%), compared to 56% (±3%) in MSC-CM. Data shown are means ± SEM. (* = p<0.05 by Mann Whitney U test).

EaHy-926

	0hr	6hr	12hr

Control
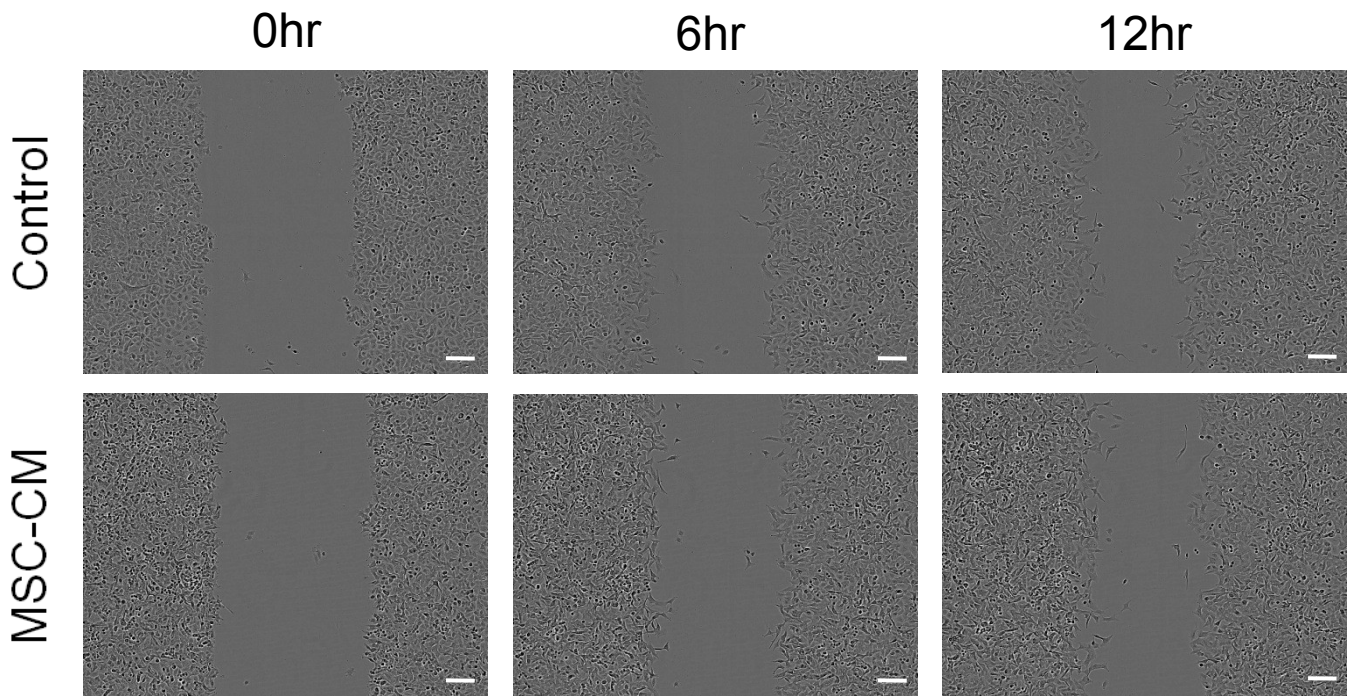
MSC-CM

Figure 6.3 EaHy-926 endothelial cells on MSC-CM coated tissue culture plates closed scratch wounds at a similar rate to cells on plates coated in unconditioned medium. Representative phase contrast images are shown of single cell type (EaHy-926) scratch assays immediately following the scratch and 6 and 12 hours thereafter. Original magnification is x10 (bar = 100μm).
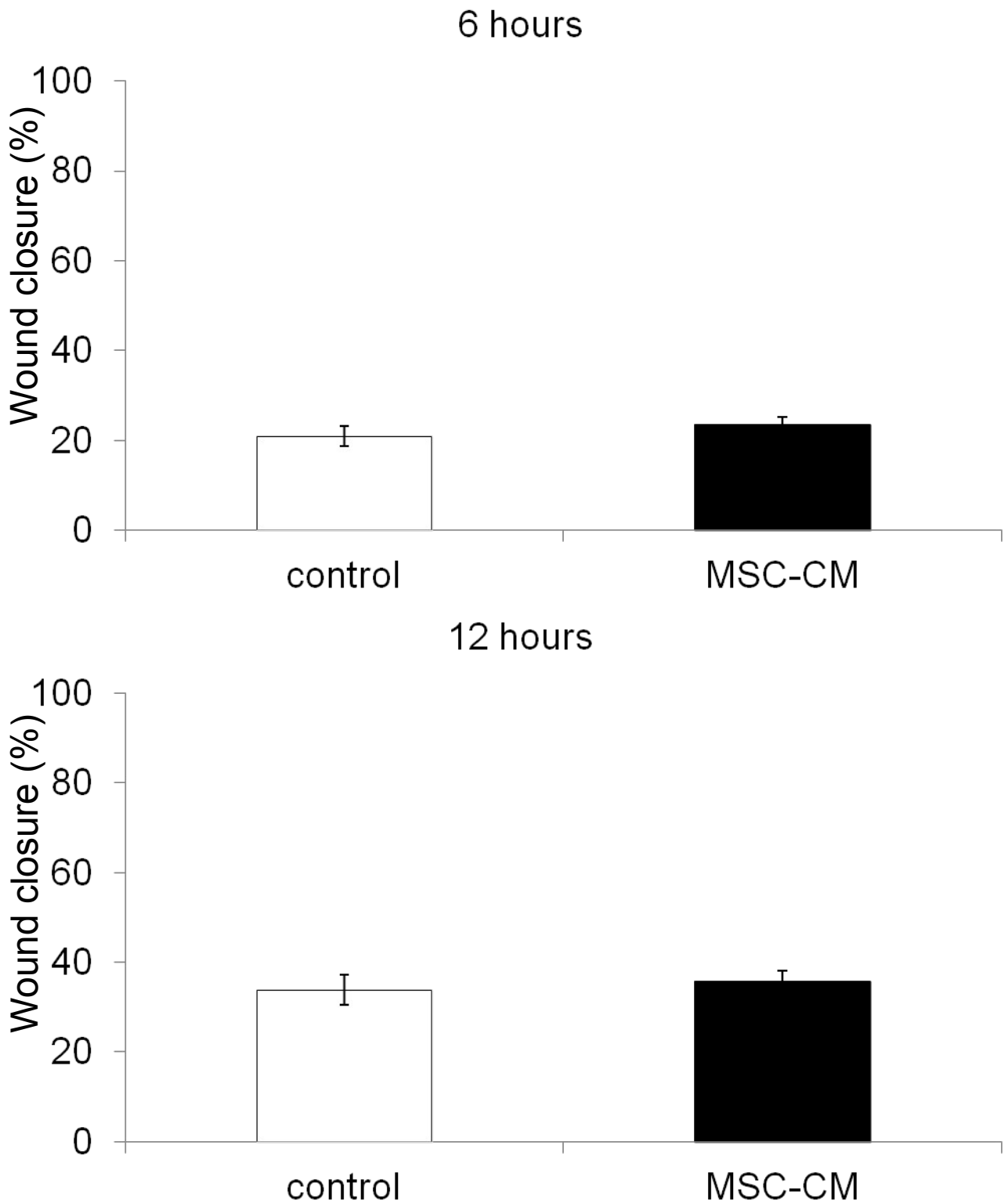
Figure 6.4 Scratch-wound closure by EaHy-926 endothelial cells on MSC-CM coated plates. After 6 hours EaHy-926 endothelial cells on unconditioned medium-coated tissue culture plastic had reached 21% (±2%), compared to 24% (±%) on MSC-CM. After 12 hours EaHy-926 endothelial cells on unconditioned medium-coated tissue culture plastic had reached 34% (±3%), compared to 36% (±2%) on MSC-CM. Data shown are means ± SEM (No significant differences were found between results by Mann Whitney U test).
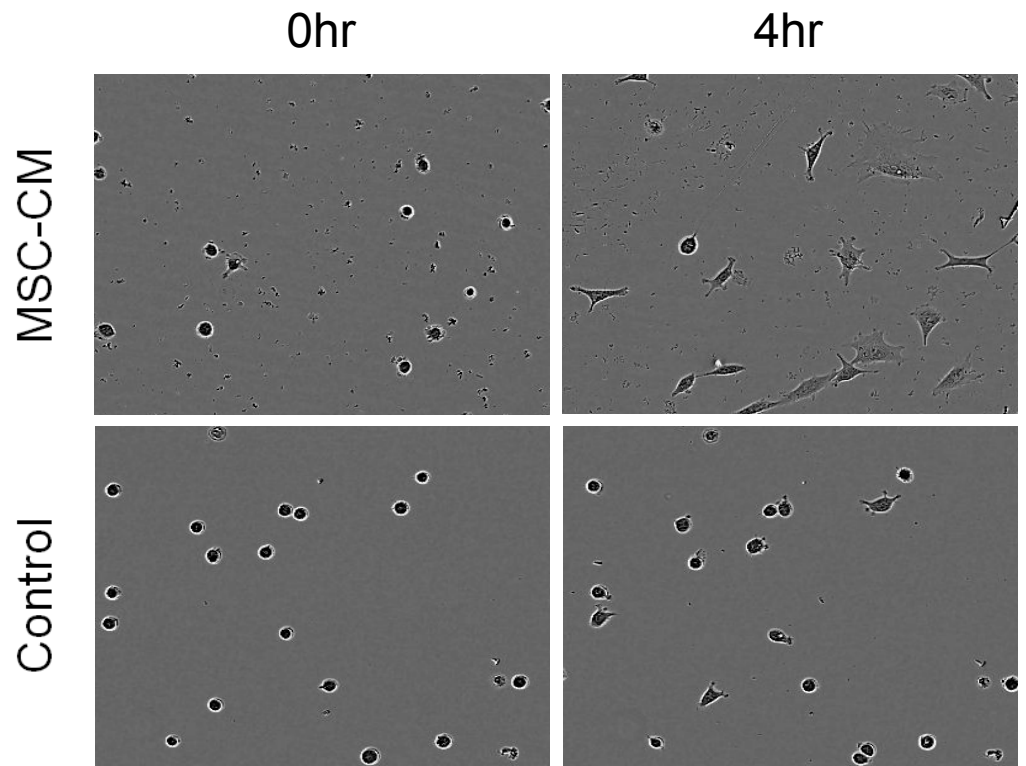
Figure 6.5 MSC-CM coating of culture plates influences EaHy-926 endothelial cell adherence and spreading. After 4 hours in culture EaHy-926 endothelial cells were observably more spread on culture plates coated with MSC-CM than on plates coated with unconditioned (control) medium. Representative phase contrast images are shown of EaHy-926 endothelial cells immediately following seeding or 4 hours thereafter.
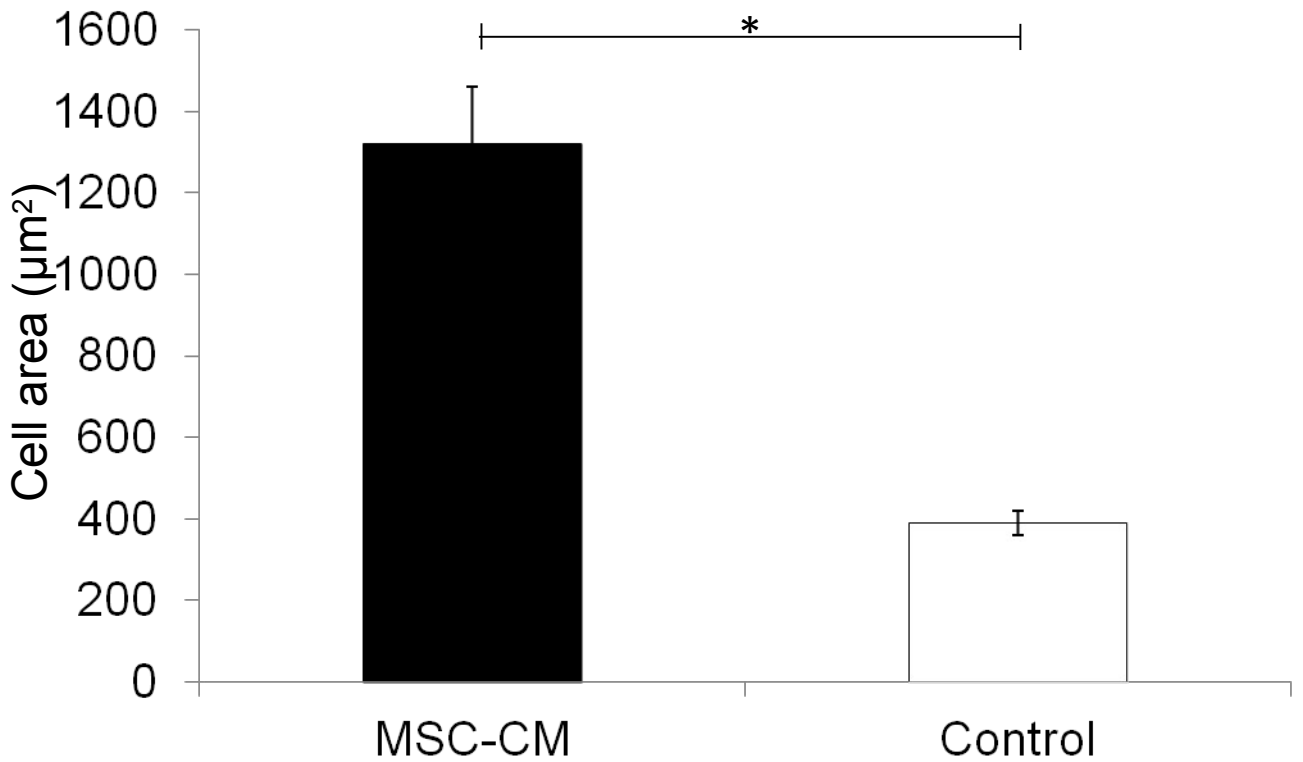
Figure 6.6 Cell areas on MSC-CM coated plates. After 4 hours in culture the average cell area was 1322μm² (±140μm²), for EaHy-926 endothelial cells on MSC-CM coated culture plates and 389μm² (±30μm²) for EaHy-926 endothelial cells on unconditioned (control) medium coated culture plates. Data shown are means ± SEM in relative units (*=p<0.05 Mann Whitney U test).

6.3: The ECM protein content of MSC-CM from 3 separate donors.

The MSC-CM, derived from n=3 donors, that demonstrated an enhancement of EaHy926 cell migration in scratch wound assays, and of cell adhesion when used to coat culture plates, was examined by MALDI/TOF/TOF mass spectrometry. All three MSC-CM were found to contain fibronectin, collagen type I, collagen type VI, and lumican, whilst cartilage oligomeric matrix protein (COMP) and SPARC were present in two out of three MSC-CM and laminin, decorin, heparan sulphate proteoglycan (HSPG) and IGFBP-7 were each only observed in one MSC-CM (Table 6.1). Hence, there was some similarity but also clear donor-donor variability in the ECM components of the MSC secretome. Experiments were therefore performed to examine the effects of some of the individual ECM components identified, particularly fibronectin, collagen type 1 and decorin, on EaHy926 cells, much as had been performed previously with L929 fibroblasts and HaCaT keratinocytes.

TABLE 6.1 PROTEINS DETECTED IN MSC CONDITIONED MEDIUM VIA MASS SPECTROMETRY (MALDI-TOF/TOF)

MSC-CM 1	MSC-CM 2	MSC-CM 3
Fibronectin	Fibronectin	Fibronectin
Collagen type I	Collagen type I	Collagen type I
Collagen type VI	Collagen type VI	Collagen type VI
Laminin	-	-
Cartilage oligomeric matrix protein	Cartilage oligomeric matrix protein	
Lumican	Lumican	Lumican
-	-	Decorin
-	-	HSPG
SPARC	-	SPARC
IGFBP-7	-	-

Table 6.1 Mass spectrometry of MSC-CM from 3 separate donors. MALDI-TOF/TOF mass spectrometry of MSC-CM detected variable protein content between media conditioned by MSC from three different patient donors.

6.4: The effects of ECM proteins on EaHy-926 endothelial cells.

EaHy-926 cells adhered more readily to fibronectin-coated culture plates than to culture plates coated in either decorin or collagen type I to the degree that after four hours post-seeding those cells in fibronectin coated plates had spread significantly further than cells in either collagen type I or decorin coated plates (Figures 6.7-6.8).

The coating of culture plates with these individual ECM proteins also affected the rate of migration of EaHy-926 cells in the presence and absence of MSC-CM (as culture medium), and as determined by scratch assays. Hence, in unconditioned (control) medium after both 6 and 12 hours post scratching, EaHy-926 cells in fibronectin coated plates were observably more advanced in closing the scratch wound areas than those cells in plates coated in either collagen type I or decorin (Figure 6.9). In these unconditioned (control) medium cultures, scratch wound closure by the EaHy-926 cells in fibronectin coated culture plates was 24% (±2%) after 6 hours post scratching, compared with 20% (±1%) in collagen type I coated culture plates and 19% (±1%) in decorin coated culture plates. After 12 hours post scratching in the same unconditioned (control) medium conditions, the extent of scratch wound closure in fibronectin, collagen type I and decorin coated culture plates was 35% (±4%), 26% (±2%), and 26% (±1%), respectively (Figure 6.10). .

Fibronectin was also the most favourable culture substrate for EaHy-926 cells in the presence of MSC-CM. However, MSC-CM enhanced scratch wound closure whichever of the ECM components had been used to coat the culture plates. Hence, at 6 hours post scratching, the extent of scratch wound closure in MSC-CM was 35% (±2%) (versus 24% (±2%) in control medium) on fibronectin coated culture plates, 32% (±1%) (versus 20% (±1%) in control medium) on collagen type I coated culture

plates, and 25% (±1%) (versus 19% (±1%) in control medium on decorin coated culture plates. A similar relationship between the effects of coating the culture plates with these ECM components and the effects of MSC-CM on EaHy926 scratch wound closure was observed at 12 hours post scratching (Figure 6.10).

In MSC-CM or unconditioned (control) medium, scratch wound closure by EaHy-926 cells was significantly enhanced in fibronectin coated culture plates compared to wound closure in decorin coated culture plates, but not collagen type I coated culture plates at 6 hours post scratching ($p<0.05$ by ANOVA). At 12 hours post scratching, scratch wound closure was significantly enhanced in fibronectin coated culture plates compared to both decorin or collagen type I coated culture plates ($p<0.05$ by ANOVA), in MSC-CM or unconditioned (control) medium. EaHy-926 scratch wound closure was significantly greater at both 6 and 12 hours post scratching, in MSC-CM compared to unconditioned (control) medium, irrespective of the ECM component used to coat the culture plates ($p<0.05$ by ANOVA).
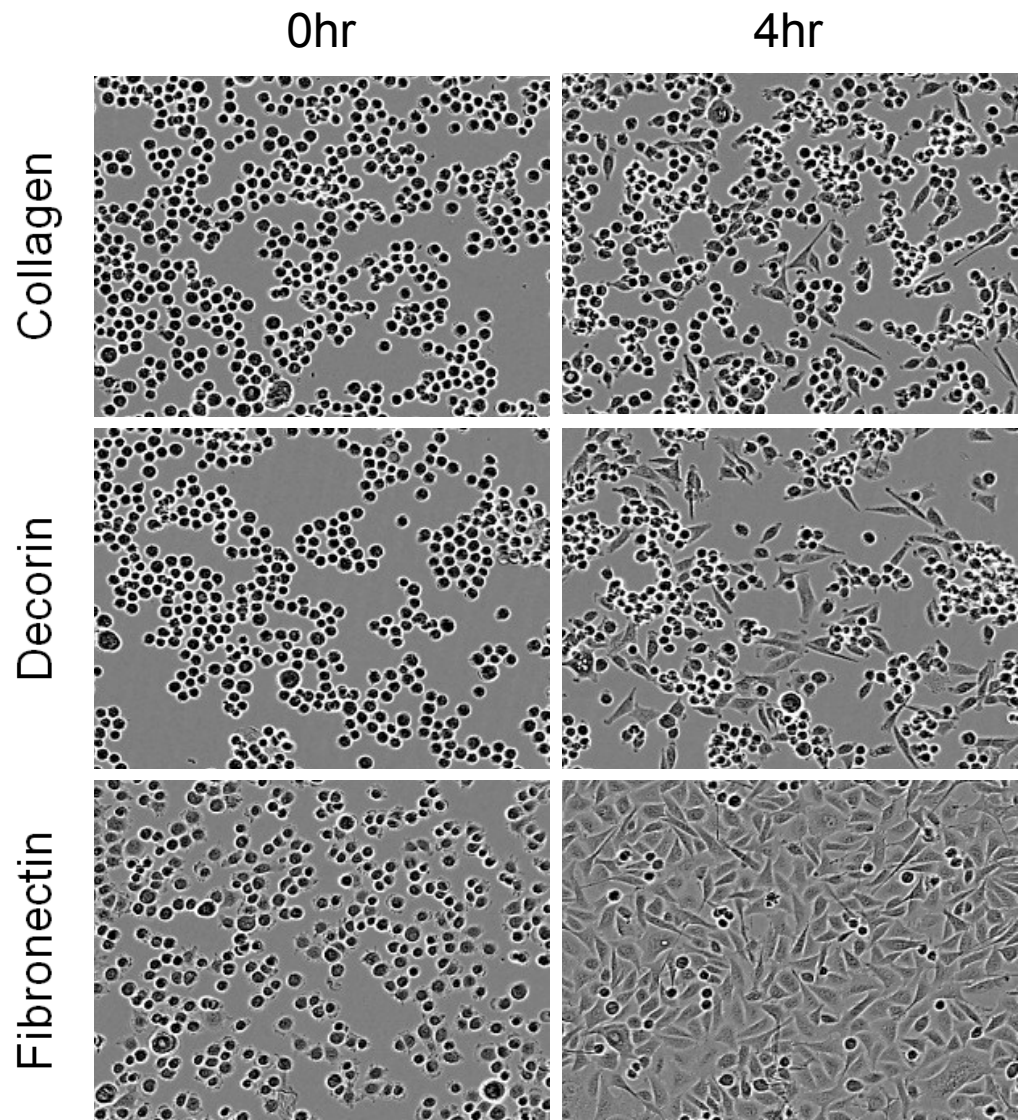
Figure 6.7 ECM protein coating of culture plates influences EaHy-926 endothelial cells adherence and spreading. After 4 hours in culture EaHy-926 endothelial cells were observably more spread on culture plates coated with fibronectin than on plates coated with type I collagen or decorin. Representative phase contrast images are shown of EaHy-926 endothelial cells immediately following seeding or 4 hours thereafter.
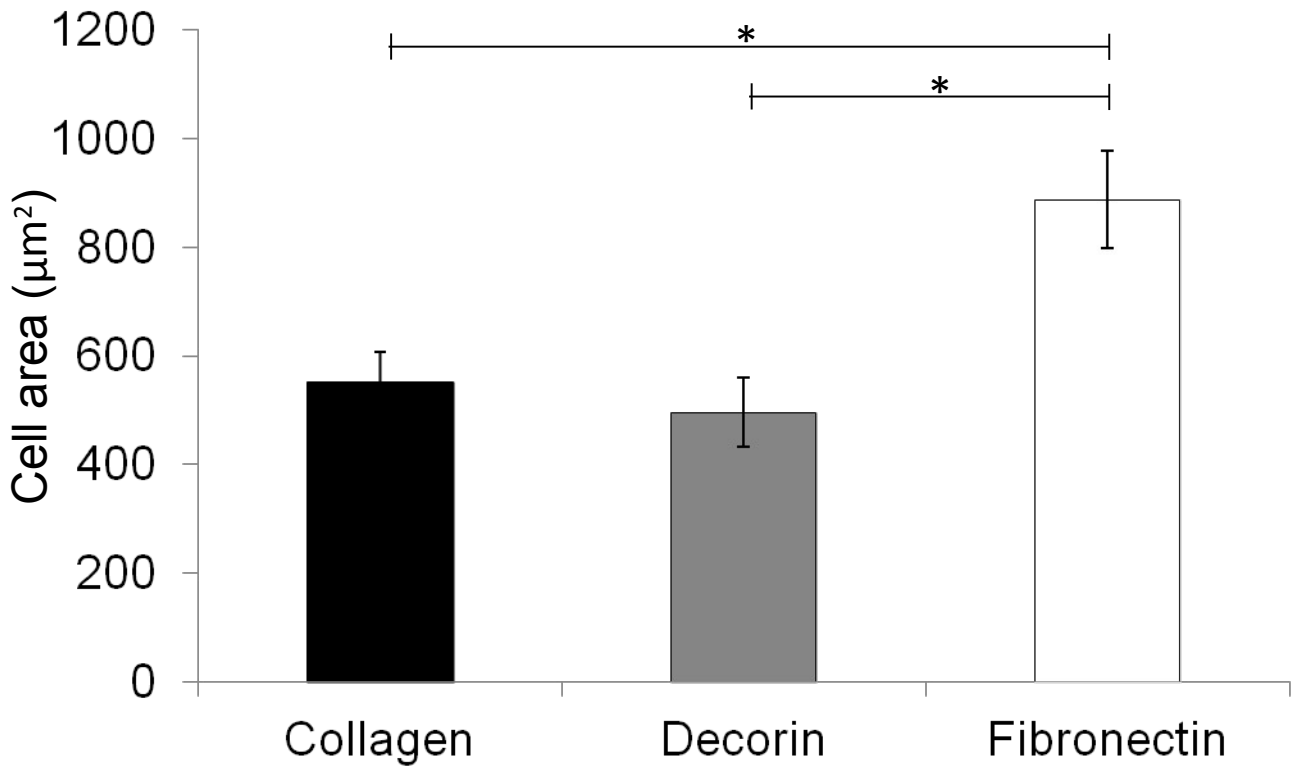
Figure 6.8 Cell areas on ECM proteins. After 4 hours in culture the average cell area was 551μm² (±58μm²), for EaHy-926 endothelial cells on type I collagen, 495μm² (±64μm²), for EaHy-926 endothelial cells on decorin and 887μm² (±90μm²), for EaHy-926 endothelial cells on fibronectin. Data shown are means ± SEM in relative units. There was a significant difference by ANOVA (p<0.05); (* denotes significance by Tukey's HSD).
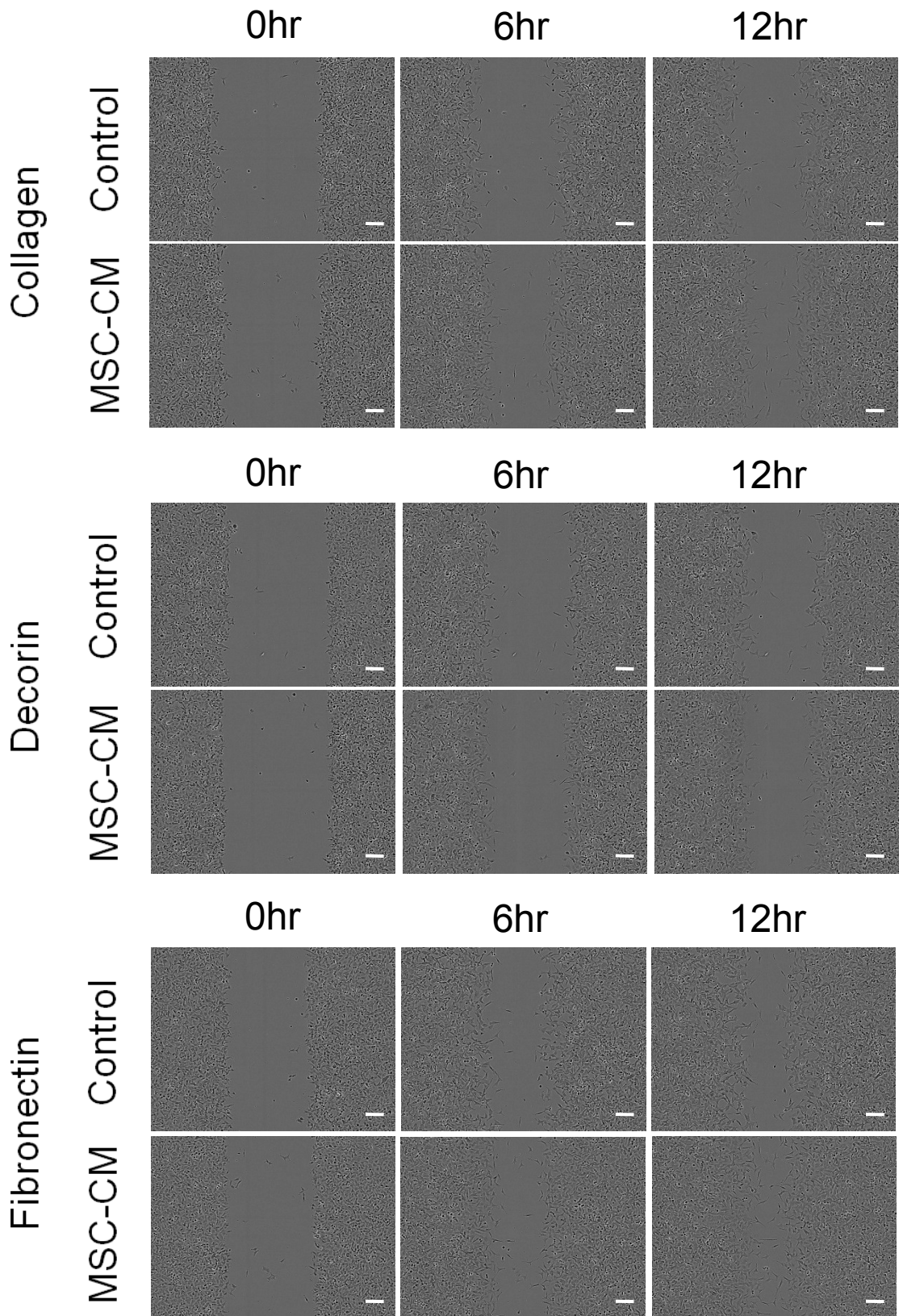
Figure 6.9 EaHy-926 endothelial cells closed scratch wounds faster in MSC-CM than in unconditioned medium on type I collagen, fibronectin, and decorin coated culture plates. Representative phase contrast images are shown of single cell type (EaHy-926) scratch assays immediately following the scratch and 6 and 12 hours thereafter. Original magnification is x10 (bar = 100μm).
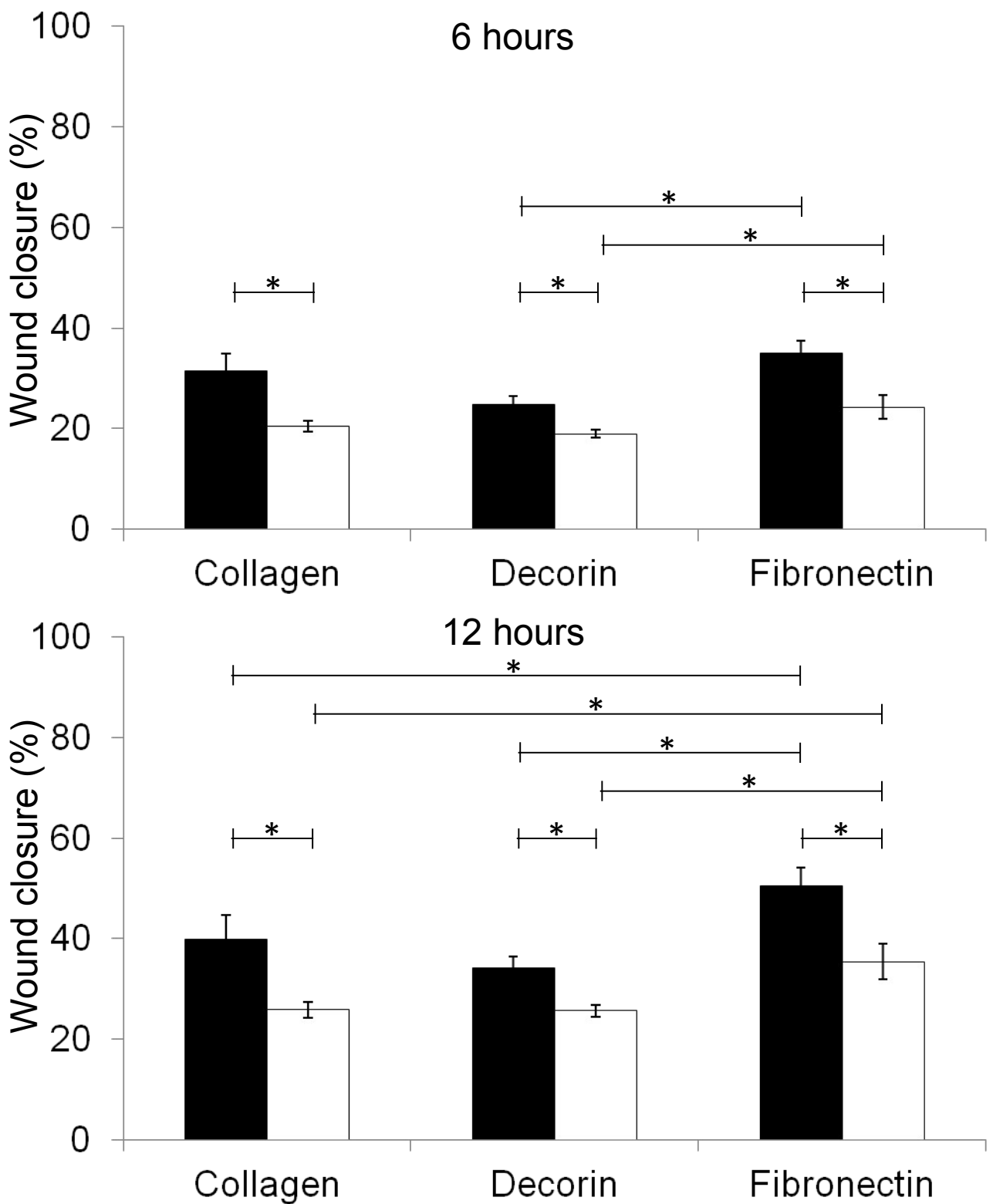
Figure 6.10 Scratch-wound closure by EaHy-926 endothelial cells in MSC-CM upon ECM protein coated culture plates. After both 6 hours and 12 hours EaHy-926 endothelial cells in MSC-CM (black bars) had closed scratch wounds by a significantly greater degree than those in unconditioned control medium (white bars). After 6 hours EaHy-926 endothelial cells in unconditioned medium on fibronectin coated culture plates had closed scratch wounds by a significantly greater degree than those on culture plates coated in decorin. By 12 hours post-scratching, EaHy-926 endothelial cells on plates coated in both collagen and fibronectin had closed scratch wounds by a significantly greater degree than those on decorin coated culture plates. Data shown are means ± SEM. There were significant differences by ANOVA ($p<0.05$); (* denotes significance by Tukey's HSD).

6.5: Discussion

In previous chapters MSC-CM has been shown to promote the migration of skin cells in an *in* vitro wound healing model, and the potentially beneficial individual factors within the 'whole' MSC-CM have been tested to elucidate their relative contribution to this effect. However, as described in Chapter one of this thesis, cutaneous wound healing *in vivo* is a complex process influenced not only by the migration of dermal and epidermal skin cells, but also by a host of cellular events including amongst others, angiogenesis; the formation of new vasculature within the wound area. If MSC can stimulate endothelial cells and contribute to angiogenesis, as the results presented in this thesis as well as numerous previous reports (Beckermann *et al,* 2008, Zacharek *et al*, 2007) suggest, this supports their potential use in the treatment of cutaneous wounds. Similarly, poor vascularisation of the wound bed has been implicated in the failure of both conventional skin grafts and tissue engineered skin substitutes. Hence, treatment with MSC along with or prior to skin grafting might be considered to improve the condition of the wound bed, increasing the likelihood of a successful graft. In this chapter, the effects of MSC-CM upon an endothelial cell line, EaHy-926, have been investigated using the scratch assay, as well as evaluating the effects of individual ECM proteins found in MSC-CM (by mass spectrometry).

In these experiments, MSC-CM was found to be stimulatory to EaHy-926 endothelial cell migration *in vitro*. This is similar to previous studies in which MSC-CM has been shown to stimulate angiogenesis *in vitro*. For example, Beckermann and co-workers observed enhanced sprouting of human vascular endothelial cells from spheroid cultures in collagen gels in the presence of MSC-CM (Beckermann *et al,* 2008), whilst another group have reported that MSC-CM enhanced the tubule

formation by murine endothelial cells in matrigel assays (Zacharek *et al*, 2007). Interestingly, one study reports that co-culture of MSC with endothelial cell tubules resulted in the degradation of capillary networks and the apoptosis of endothelial cells, whereas MSC-CM did not exhibit this anti-angiogenic effect (Otsu *et al*, 2008). This last finding supports the investigation of MSC-CM as a pro-angiogenic agent within this chapter, and hence of using MSC secreted factors to treat wounds as opposed to cell transplantation.

Mass spectrometry of MSC-CM revealed the presence of collagen types I and VI, as well as fibronectin and lumican in medium conditioned by each of the three MSC examined, and laminin, decorin, COMP, SPARC, heparan sulphate proteoglycan (HSPG) and IGFBP-1 in one or two but not all three of the MSC-CM samples. Of these ECM components, fibronectin, collagen and laminin are known to promote or support angiogenesis (Campbell *et al*, 2010). Fibronectin contains RGD protein motifs known to mediate angiogenesis by integrin receptor signalling. RGD motifs bind to α5β1 integrin receptors, amongst others, and these have been shown to be essential for the proper formation of vasculature in knock out mouse models *in vivo* (Yang *et al*, 1993, Goh *et al*, 1997, Francis *et al*, 2002). Similarly, the selective inhibition of α1β1 integrin receptors for collagen results in impaired angiogenesis in *ex vivo* chorioallantoic membrane (CAM) assays (Marcinkiewicz *et al*, 2003). Laminin peptides have also been shown to be pro-angiogenic both *in vitro* (Malinda *et al*, 1999) and *in vivo* (Kibbey *et al*, 1992). Conversely decorin and lumican, another small leucine rich proteoglycan (SLRP), have been shown to inhibit angiogenesis. Decorin inhibits endothelial cell migration and tubule formation *in vitro* (Davies *et al*, 2001) and inhibits the pro-angiogenic effects of VEGF (Sulochanaet *et al*, 2005). Lumican interferes with α2β1 receptor activity and inhibits angiogenesis both *in vitro* and *in vivo* (Niewiarowska *et al*, 2011, Albig *et al*, 2007). As previously presented within this thesis, MSC-CM contains factors that are both stimulatory and inhibitory to cellular processes involved in wound healing, and the presence of decorin and lumican within the MSC secretome suggest that this is also the case for the effects of MSC-CM on endothelial cell migration. However, similar to the results shown in Chapter 3 using L929 fibroblasts and HaCaT keratinocytes, the net effect of 'whole' conditioned medium was stimulatory overall to EaHy-926 cells, suggesting that the

stimulatory factors present overcome any inhibitory effects of other factors also secreted by MSC.

Also similar to the results observed in scratch-wound assays using L929 fibroblasts presented in previous chapters within this thesis, fibronectin coating of tissue culture plates lead to an enhancement of EaHy-926 endothelial cell migration compared to either type I collagen or decorin. This suggests that fibronectin contributes to the MSC-CM mediated enhancement of endothelial cell migration. However, the addition of MSC-CM to endothelial cell scratch assays performed upon fibronectin coated culture plates (and indeed upon plates coated in collagen and decorin) resulted in a further enhancement of endothelial cell migration compared to unconditioned medium. This shows that whilst fibronectin contributes to the enhancement of endothelial cell migration, it may not be responsible for the entire effect. Further experiments investigating the effects of MSC secreted growth factors and cytokines individually, and in combination,, may reveal the relative contribution of MSC secreted factors to the enhancement of endothelial cell migration, as was investigated in Chapters 4-5 for L929 and HaCaT cells. For example, IL-8, shown to be secreted by MSC in Chapter 3 of this thesis, and in previous studies (Chen e*t al,* 2008), is known to promote angiogenesis *in vivo* (Waugh and Wilson 2008). MSC have also been consistently shown to secrete VEGF (Chen *et al*, 2008, Beckermann *et al,* 2008, Wu *et al*, 2007), an essential mediator of angiogenesis (reviewed extensively in Ferarra, 2009). Therefore, it seems reasonable to expect that these factors especially would be likely to contribute to the MSC-CM mediated enhancement of EaHy-926 endothelial cell migration and this warrants further investigation.

The next chapter will discuss in more detail the summary findings of this thesis and consider how these findings relate to the wider field, and how this work informs the use of the MSC secretome as a potential therapy for cutaneous wound healing.

Chapter 7

Discussion

7.1: Summary of Results

The results presented within this thesis have shown that the skin cell lines, L929 fibroblasts and HaCaT keratinocytes, representing the cellular portion of the dermis and epidermis, respectively, migrate *in vitro* to close a scratch wound, and that treatment with MSC-CM accelerates their closure of the wound. Proliferation of both cell types was enhanced by MSC-CM over 72 hours, but these proliferative increases were not statistically significant and were not within the time course of scratch wound closure. Therefore, it is reasonable to conclude that MSC secrete factors that enhance skin cell migration. Medium conditioned by either L929 fibroblasts or HaCaT keratinocytes failed to elicit any similar enhancement of the rate of migration of either cell type.

When analysed using ELISA and mass spectrometry, MSC-CM was found to contain cytokines and ECM components (notably fibronectin, collagen type I and decorin) that are known to play a part in cutaneous wound healing. These factors were individually applied to scratch wounds. TGF-β1 was found to enhance the migration of L929 fibroblasts, but slowed the migration of HaCaT keratinocytes. The other cytokines investigated, IL-6 and IL-8, either had no effect (IL-6) or inhibited the migration of both cell types (IL-8). The ECM protein, fibronectin, was used to coat the surface of the culture plates, and this significantly enhanced the adherence and migration of both cell types compared to collagen type I. Conversely decorin, a SLRP, inhibited the adherence of both cell types, and the migration of HaCaT keratinocytes; the inhibitory effect of decorin upon L929 fibroblasts was so severe as to prevent the assessment of the rate of migration under these conditions.

When two of the MSC secreted factors that were most stimulatory to scratch wound closure were examined in combination, i.e. TGF-β1 and fibronectin, the presence of TGF-β1 failed to elicit any further enhancement of the migration of L929 fibroblasts when compared with their rate of migration on fibronectin alone. Similar to the results observed using TGF-β1 supplemented medium on a collagen coated culture surface, TGF-β1 inhibited HaCaT keratinocyte migration upon fibronectin in a concentration-dependent manner up to a maximum inhibition of 47 percentile points (53% closure compared to 100% after 12 hours in culture) at 8ng/ml of TGF-β1. The addition of MSC-CM did not elicit any significant enhancement of the rate of migration of L929 fibroblasts on fibronectin coated culture surfaces. HaCaT keratinocyte migration was not significantly enhanced by MSC-CM in the presence fibronectin in this instance. MSC-CM was also used to coat culture surfaces prior to scratch-wounding. This MSC-CM coating lead to an enhancement of L929 fibroblast migration compared to that on surfaces coated with unconditioned culture medium, but had no observable effect upon HaCaT keratinocyte migration. The presence of EMC proteins (decorin and fibronectin) as supplements in growth medium reduced the rate of scratch wound closure by both L929 fibroblasts and HaCaT keratinocytes.

Similar to the effects of MSC-CM on L929 fibroblasts and HaCaT keratinocytes, MSC-CM enhanced the rate of migration of EaHy-926 endothelial cells on culture plates coated in either collagen type I, decorin, or fibronectin. Coating culture surfaces with MSC-CM also enhanced the adherence of EaHy-926 cells, as observed by the degree of cell spreading. Fibronectin coating of culture plates enhanced the rate of migration of EaHy-926 endothelial cells compared to either decorin or type I collagen, as well as their adherence to the culture surface.

7.2: How representative is the model system of cutaneous wound healing?

The majority of the results presented within this thesis were obtained using an *in vitro* model of wound healing, the scratch assay. Briefly, this model incorporated a confluent monolayer of cells grown upon collagen type I coated tissue culture plastic. The cell layer was then scored with a sterile point to produce a 'wound-area' and the cells were observed as they repopulated the scratch.

Cell lines were used in this assay to represent the major cellular components of the dermis and epidermis - L929 fibroblasts and HaCaT keratinocytes - along with wound vasculature using EaHy-926 cells. L929 is a sub-clone (number 929; Sanford *et al*, 1948) of a fibroblast cell line that was originally established by Earle and co-workers in the 1940s (WR Earle, 1943). L929 fibroblasts are capable of myofibroblast differentiation, as seen in human dermal fibroblasts in wounded skin *in vivo* (Nakamura, *et al*, 2004), but are murine in origin, and thus may differ markedly from human fibroblasts. Particulary relevant to this investigation, the receptors expressed by a mouse cell line may not recognise human cytokines such as those secreted by the human MSC used in these experiments. HaCaT is a spontaneously immortalised human keratinocyte cell line, (Boukamp *et al*, 1988). HaCaT cells have been shown to be capable of differentiation in organotypic co-cultures to form a multilayered, differentiated epidermis *in vitro* similar to that formed by normal human keratinocytes in living skin (Kehe et al, 1999). However, HaCaT keratinocytes have a reduced expression of receptors for keratinocyte growth factor (KGF) and granulocyte-macrophage colony-stimulating factor (GM-CSF) compared to normal human keratinocytes, which results in delayed formation of a multilayered epithelium and their incomplete differentiation (Maas-Szabowski *et al*, 2003, Stark *et al*, 2004). EaHy-926 cells are derived from a hybridoma of primary human vascular endothelial

cells with human lung carcinoma cells (Edgell *et al*, 1983), and as such may also differ from primary human endothelial cells. Additionally, the oncogenic transformation of cells may involve the activation of cells by autocrine growth factor stimulation.

Therefore, it is important to note that these cell lines may not entirely replicate the behaviour of primary human cells *in vivo* and that further work to validate the results are of clear benefit. However, the main purpose of these experiments was to use a consistent model of skin wound healing to assess the effects of MSC secreted factors. The use of cell lines, as opposed to primary fibroblasts, keratinocytes or endothelial cells, removed the possibility of inter-donor variability that these primary cells would likely present, such that the effects of the MSC-CM, which in itself was derived from primary normal human cells and was therefore likely to be variable, could be quantified independently of this confounding factor.

The use of an *in vitro* model, such as the 2-dimensional scratch wound assay, cannot accurately replicate the conditions of living, wounded skin. In addition to the cell types that have been used in this work, cutaneous wound healing *in vivo* is dependent upon numerous other cell types, i.e. neutrophils and macrophages for the removal of foreign material and potential pathogens, Langerhans cells for immune surveillance, neural cells for re-innervation within the wound area, melanocytes, sweat glands, and all the components of hair follicles. Furthermore, circulatory and haemostatic factors such as thrombus formation, immune and inflammatory events, i.e. complement activation, and a complex microenvironment involving numerous and temporally variable ECM proteins, degradatory enzymes, and trophic factors are all aspects of the normal wound healing process that are unrepresented within this model system. These conditions could be more accurately replicated in experiments

undertaken using animal models, but due to the associated cost, ethical considerations and a perceived need for consistency in order to analyse potentially variable MSC, an *in vitro* methodology has been preferred for the work presented within this thesis.

The results presented within this thesis support the hypothesis that MSC-CM can stimulate a response from the cell populations present within skin that may enhance processes associated with cutaneous wound healing. Reepithelialisation, leading to the re-establishment of the barrier function of skin, is dependent upon the migration of keratinocytes into the wound area, migration of fibroblasts is associated with the contraction of wound margins, and the recruitment of endothelial cells is required for the vascularisation of a wound area, or the bed in which a graft may be applied. The data presented in this thesis suggest that MSC secretions would enhance each of these activities. In addition, the numerous factors detected within MSC-CM in this study are known to play significant roles within *in vivo* wound healing. Therefore, this body of work supports the hypothesis that MSC-secreted factors may be beneficial to wound healing. However, further study is required using primary human responder cells or in vivo models in order to verify this conclusion.

7.3: What are the advantages of using MSC secreted components?

Mesenchymal stem cells have shown potential to assist in the repair of numerous damaged tissues, either through their differentiation potential or paracrine activity. Several studies have demonstrated that MSC can enhance cutaneous wound healing (Sasaki *et al,* 2008, Falanga *et al,* 2007, Vojtassák *et al,* 2006) and MSC secreted factors can elicit this enhancement in the absence of the MSC themselves (Chen *et al,* 2008, Kim *et al,* 2007). The results presented within this thesis support the interpretation that it is the paracrine activity of MSC that is effective in skin wound healing. This has important applications to the nature of the therapeutic use of MSC. Whilst, thus far, clinical trials involving MSC transplantation into human patients have demonstrated safety (Ghannam *et al,* 2010, Centeno *et al,* 2009, Tarte *et al,* 2009), reports exist that suggest MSC are capable of undergoing spontaneous malignant transformation *in vitro* (Rubio *et al,* 2005, Rubio *et al,* 2008, Rosland *et al,* 2009) and can form solid tumours *in vivo* (Wang *et al,* 2005, Li *et al,* 2007). The possible malignant transformation of human MSC remains a topic of some debate and two of the aforementioned papers were since retracted by multiple of the original authors following the identification of cross-contamination of MSC cultures with tumour cell lines (De la Fuente *et al,* 2010, Torsvick *et al,* 2010). Human MSC transformation appears to be something of a rarity stemming from exceptional periods in culture (Lazennec and Jorgensen, 2008). Nonetheless, the possibility of such malignancy arising from MSC culture raises a serious caveat regarding the clinical use of MSC. If, as these results and other previous reports suggest, the beneficial effects of MSC may be harnessed from their secreted components without the need to transplant living cells, then this would circumvent the question of spontaneous malignant MSC transformation and the associated risk to patients.

The results presented within this thesis support the hypothesis that MSC-CM can stimulate a response from the cell populations present within skin that may enhance processes associated with cutaneous wound healing. Reepithelialisation, the essential the re-establishment of the barrier function of skin, is dependent upon the migration of keratinocytes into the wound area. The migration of fibroblasts is associated with the contraction of wound margins, and the recruitment of endothelial cells is required for the vascularisation of a wound area, or the bed in which a graft may be applied. In addition to the reported effects of MSC-CM upon the cell lines, the numerous factors detected within MSC-CM in this study are known to play significant roles within *in vivo* wound healing and have in many instances been shown to stimulate cell responses in *in vitro* models by other investigations referred to throughout this thesis. This body of work, to which this thesis contributes, supports the hypothesis that MSC-secreted factors may be beneficial to wound healing in the absence of the cells themselves.

7.4: Why investigate co-cultures of L929 fibroblasts and HaCaT keratinocytes?

Beginning with the initial development of skin, the behaviour of the dermal and epidermal cells that make up the organ are intrinsically liked to one another. Intracellular signalling between the mesenchymal and epithelial cells (via TGF-β, BMP and Notch) determines the formation of the epidermis, hair follicles and sebaceous glands from epithelial precursors (Fuchs and Horsley, 2008). This interaction continues and is essential for both the maintenance of skin homoeostasis and the process of skin wound healing. Keratinocytes have been shown to modulate the production and degradation of collagen by dermal fibroblasts through TNF-α and IL-1 signalling and the regulation of MMP expression (Tandara and Mustoe, 2011), and fibroblasts have been shown to profoundly influence keratinocyte proliferation and differentiation as well as their deposition of basement proteins (El Ghalbzouri e*t al* 2002). Paracrine interaction between dermal and epidermal cell types has been shown to affect their behaviour in *in vitro* models of skin wound healing. In fibroblast and keratinocyte co-culture experiments, fibroblasts were shown to up regulate the expression of IL-1 receptor compared to mono-cultures, whilst keratinocytes showed increased expression of IL-1. Similarly keratinocytes in co-culture up regulated KGF receptor whilst fibroblasts increased their expression of KGF (Maas-Szabowski *et al*, 2000). The presence of both cell types lead to enhanced cell migration and proliferation. Observing the effects of this interaction *in vitro*, Maas-Szabowski and co-workers suggested that epidermal tissue regeneration in organotypic co-cultures is regulated by keratinocyte derived interleukin-1 signalling, which induces keratinocyte growth factor expression in co-cultured fibroblasts. Similarly, as previously mentioned, the enhancement of skin wound healing by IL-6 observed *in vivo* was shown *in vitro* to be dependent on paracrine interactions between fibroblasts and keratinocytes, as IL-6 induced the secretion of keratinocyte-stimulating factors by

fibroblast cells, whilst having no effect on keratinocyte mono-cultures (Gallucci *et al,* 2004).

The MSC-CM mediated *in vitro* enhancement of skin wound healing demonstrated within Chapter 3 of this thesis was observed in both fibroblasts and keratinocytes. The migration of both of these cell types is essential for effective *in vivo* wound healing, as fibroblasts move into the wounded skin from surrounding undamaged tissue and contract the wound margins, reducing the area, whilst keratinocytes migrate across granulation tissue and new ECM to re-epithelialise the wound surface (Sorrell & Caplan 2004). As these processes are directly related (fibroblast migration contributes to reducing the area that needs covering by migrating keratinocytes), it seems reasonable to speculate as to whether enhancing the migration of either cell type individually would lead to the other becoming the limiting factor to the overall rate of wound healing. By this argument, the enhancement of the rate of migration of both fibroblasts *and* keratinocytes (as was seen in this *in vitro* model) might contribute further to the healing of cutaneous wounds than an enhancement of the migration of either cell type individually.

7.5: The influence of MSC secreted cytokines on wound healing

Of the MSC-secreted cytokines investigated within this thesis, some displayed little or no enhancement of skin wound healing, and indeed appeared to be actively inhibitory to the migration of L929 fibroblasts and/or HaCaT keratinocytes. This inhibitory activity may have unwelcome implications for the use of MSC-CM to treat skin wounds clinically, as impaired fibroblast and keratinocyte migration would likely limit the rate of wound healing. However, it is important to note that the migration of these cells is only one important aspect in the complex process of cutaneous wound repair and that the overall wound healing activity of the MSC-secreted cytokines may well differ *in vivo* through their effects on other aspects of the healing process. For example, IL-8 was shown to inhibit L929 fibroblast scratch wound closure significantly, and to also inhibit scratch wound closure by HaCaT keratinocytes, albeit to a lesser degree. Despite this finding, suggesting an inhibitory activity for the chemokine, IL-8 is thought to play a role in numerous stages of wound healing, essentially including chemoattraction of neutrophils (Baggolini *et al.,* 1994, Schroder *et al.,* 1993). Overall IL-8 expression reaches peak levels within one day of wound occurrence and correlates with the rapid influx of neutrophils to the wound area, along an increasing IL-8 concentration gradient (Engelhardt *et al.,* 1998). Initially expressed by skin cells in response to PDGF, IL-8 is subsequently secreted by neutrophils, further stimulating neutrophil recruitment (Clark, 1993). This increased expression of IL-8 normally resolves within 4 days of wound healing, often corresponding with the complete reepithelialisation of normal wounds (Engelhardt *et al.,* 1998). Contrary to the current findings, IL-8 has been shown to be involved in the stimulation of keratinocyte migration and proliferation (Rennekamff *et al.,* 1997, 2000). Topical application of IL-8 enhanced the rate of reepithelialisation and reduced the degree of contracture in *in vivo* wounds, despite having no effect upon the migration of cultured

keratinocytes *in vitro* (Rennekampff *et al.,* 2000). In contrast, excessive IL-8 is associated with non-healing wounds, and has been shown to retard the proliferation of keratinocytes and to impair the contractile activity of dermal fibroblasts *in vitro* (Iocono *et al.,* 2000). Diminished expression of IL-8 is associated with the scarless wound healing characteristic of foetal wounds (Liechty *et al.,* 1998), whereas a topical application of IL-8 has been shown to reduce wound contracture and *in vivo* as is consistent with the aforementioned *in vitro* study by Ionoco and co workers (Rennekampff *et al.,* 2000).

IL-8 is known to promote angiogenesis *in vivo* (Waugh and Wilson, 2008). As the vascularisation of the wound area is also an important factor in successful wound healing, and, indeed, a lack of neo-vasculature is characteristic of non-healing 'chronic' wounds, it is possible that the presence of IL-8 in MSC-CM may contribute to the overall wound healing effects of MSC secreted factors *in vivo* through its angiogenic activity. There exist various techniques available for the investigation of this hypothesis, including *ex vivo* angiogenesis models, e.g. the chick CAM assay (Okamoto *et al.,* 1988, Ribatti *et al.,* 2011), in *vitro assays*, e.g. tubule formation in Matrigel (Khoo *et al.,* 2011), as well as the use of *in vivo* wound healing models, e.g. following the creating of defined skin wounds in rodents or larger bodied animals.

Hence, in clinical wound healing, MSC secreted IL-8 could have particular and important applications, e.g. in promoting angiogenesis to increase the success of skin grafts and following the application of tissue engineered constructs, as well as enhancing the proliferation and migration of keratinocytes, thereby accelerating reepithelialisation. However, such potential advantages must be balanced with a consideration of the aforementioned inhibitory actions of IL-8 upon wound contraction and its association, in excess, with non-healing wounds.

Similarly, IL-6 did not elicit any enhancement of skin wound healing in these experiments, but as mentioned in Chapter 4, has been shown to induce fibroblasts to produce factors capable of stimulating keratinocyte migration (Gallucci *et al*, 2004). This being the case, it seems reasonable to suggest that the presence of IL-6 in MSC-CM might contribute to skin wound healing in an *in vivo* scenario where both cell types are present, yet not appear to influence an *in vitro* assay such as this one, using single cell cultures. MCP-1 and RANTES, which were secreted cytokines both found in MSC-CM by ELISA, were not investigated using this model, as they were not expected to influence L929 fibroblast or HaCaT keratinocyte behaviour. Rather, these factors are thought to influence cutaneous wound healing *in vivo* by attracting macrophages and other immune cells to the wound site, that were not used in the model system (Dipietro *et al*, 2001).

Transforming Growth Factor (TGF)-β1 marginally enhanced the migration of L929 fibroblasts on collagen coated culture surfaces, but had no effect on their migration on fibronectin coated surfaces. TGF-β1 also inhibited the rate of migration of HaCaT keratinocytes. Cytokines can often induce different effects when present in different combinations, but if this is indeed the same effect that TGF-β1 has when present in MSC-CM, it stands to reason that another factor or combination of factors within the MSC secretome may stimulate HaCaT keratinocyte migration sufficiently to ameliorate this inhibitory effect, resulting in the overall enhancement of HaCaT keratinocyte migration seen in the presence of 'whole' MSC-CM.

Although not represented in this model system, scarring is an important aspect of cutaneous skin wound healing. The balance of growth factors within the wound milieu is especially relevant to the degree of scarring that remains after wound closure *in vivo*. Specifically, the balance of TGF-β1 to TGF-β3 appears to influence scar

formation, with the scarless wound healing associated with foetal skin repair being characterised by a reduction in the former, and an increase in the latter. Similarly, the addition of exogenous TGF-β3, or the neutralisation of TGF-β1 has been shown to reduce scarring in adult rodents (Shah *et al*, 1994, Shah *et al*, 1995). With this in mind, there may be a possibility that TGF-β1 present within MSC-CM could contribute to more severe scarring if used to treat wounds clinically. In many cases this would be undesirable, especially in the case of wounds that occur over joints and following severe burns, as these are prone to contractures that in addition to being aesthetically unpleasant can be physically disabling. However, in the case of non-healing chronic wounds it may be that overcoming the impaired healing process and achieving the complete closure of a persistent wound could render the degree of scarring a secondary concern. Conversely, it could be possible that the addition of exogenous TGF-β3 to MSC-CM (or incorporated into an MSC-CM derived therapeutic agent) might allow for the balancing of these growth factors in such a way as to reduce or even eliminate excessive scarring following wound healing, or the contracture often seen around the margins of autologous skin grafts or tissue engineered constructs.

7.6 The influence of MSC secreted extracellular matrix on wound healing

The four MSC-CM analysed by MALDI-TOF/TOF mass spectrometry showed a degree of variation in the detectable ECM components, and whilst collagen type I, collagen type VI and fibronectin were detected in each, collgen type V, collagen Type XII and laminin were only detected in 1/4 samples, COMP and IGFBP-7 in 2/4 samples, Lumican and SPARK in 3/4 samples each. These different compositions of MSC-CM might go some way to explaining the degree of variability between individual MSC-CM and their effects upon skin cell behaviour within the models described in this thesis. Of the MSC secreted ECM components examined, fibronectin appeared to have the greatest beneficial effect, whereas decorin was inhibitory. Coating culture surfaces with fibronectin significantly enhanced L929 fibroblasts ability to adhere to the surface, and also enhanced the rate of migration of these cells into the wound area. The degree of enhancement of L929 migration seen in the presence of fibronectin was equivalent to the enhancement by MSC-CM, and indeed neither the addition of exogenous TGF-β1 nor the addition of 'whole' MSC-CM to scratch wounds performed upon fibronectin coated culture surfaces managed to elicit any further enhancement of L929 fibroblast migration. Similarly, HaCaT keratinocytes closed scratch wounds at a similar rate in MSC-CM or unconditioned medium when upon fibronectin coated culture surfaces. This suggests that the MSC-CM mediated enhancement of scratch wound closure described in Chapter 3 may be mostly due to the presence of fibronectin within the MSC secretome. This is in agreement with a previous report showing that a topical application of fibronectin enhanced wound healing *in vivo* in rodents (Kwon *et al,* 2007). It would be of enormous interest to compare the effects of topical fibronectin, MSC-CM and, perhaps MSC (i.e. the cells themselves), upon cutaneous wound healing *in vivo*. The incorporation of MSC into such a comparative study would allow the contribution of

any engraftment and/or differentiation of these cells into skin tissues, or effects driven by direct contact between MSC and the local skin cell populations, to be taken into consideration. This will also inform our knowledge of the efficacy of MSC cell transplantation, compared with that of an application of MSC-CM or fibronectin.

It is possible that the influence of fibronectin upon cutaneous wound healing might be somewhat lessened in the case of chronic wounds, where the over-expression of proteolytic enzymes may lead to its degradation before any beneficial effects can be conferred. That said, the various protein domains that comprise fibronectin are known to influence a range of cell functions including cell adhesion, cell migration, cell proliferation, cell differentiation, chemotaxis, tissue-remodeling and overall wound healing (Grinnell, 1984, Pankov and Yamada, 2002). In one recent study, a recombinant protein comprising two fibronectin derived adhesion motifs for integrins, Pro-His-Ser-Arg-Asn (PHSRN) and Arg-Gly-Asp (RGD) was reported to improve fibroblast and keratinocyte migration and adherence *in vitro*, as well as enhancing skin wound healing *in vivo* in rabbits (Jung *et al*, 2007). Therefore, the nature and/or degree of any proteolytic digestion, the location of cleavage sites, and the resulting breakdown products that are generated might influence the effects of fibronectin upon cutaneous wound healing in the presence of the proteinases that are over-expressed in chronic wounds.

The inhibitory effect of decorin on fibroblasts and keratinocytes seen in these investigations may be of relevance *in vivo*. Decorin binds to both collagen type I, and is upregulated in wound healing (Yeo *et al*, 1991). As discussed in Chapter 4, previous studies suggest variable effects of decorin, on skin cells and on overall wound healing (Merle *et al*, 1997, Schmidt *et al*, 1987, Järveläinen *et al*, 2006). This suggests that decorin is involved in processes that affect cutaneous wound healing and

that the nature of this influence warrants further study. However, in the context of 'whole' MSC-CM the influence of potentially inhibitory factors does not prevent an overall enhancement of the rate of wound healing.

The results observed in experiments involving both soluble and surface bound fibronectin and decorin suggest a regulatory role for each molecule in the wound healing response, and possibly a competitive adhesion blocking affect in the case of soluble fibronectin. These data seem to show that neither meolecule accounts for the effects of MSC-CM observed *in vitro,* although fibronectin may contribute to some degree.

7.7 The effects of MSC secreted factors on endothelial cells

Angiogenesis, the formation of new vasculature, depends on endothelial cell migration and the actions of endothelial cell chemotactic factors (Folkman and Shing, 1992, Lanza, *et al*, 2007, Ferrara, 2009, Waugh and Wilson, 2008), and ECM proteins (Campbell *et al,* 2010). Many of these pro-angiogenic factors have been found to be present within the MSC secretome, both within this thesis,e.g. IL-8, collagens, fibronectin and laminin, and in previous studies, e.g. VEGF (Chen et al., 2008). VEGF was not detected in the current study either by ELISA or using MALDI-TOF/TOF; this may have been due to differences in experimental protocol, e.g. in the generation of the MSC CM or limitations of the assay techniques used. As described previously, angiogenesis is an important feature of skin wound healing. Therefore, this thesis has investigated the effects of MSC secreted factors upon the adhesion and migration of EaHy-926 cells, an endothelial cell line (Edgell *et al*, 1983). These experiments showed that MSC-CM enhanced both the rate of endothelial cell migration and the adherence of these cells to their culture surface, and that this effect was in part, but not entirely, mediated by the presence of fibronectin within the MSC secretome, as detected by MALDI/TOF/TOF mass spectrometry. Other studies have also highlighted a role for fibronectin in stimulating angiogenesis (Yang *et al,* 1993, Goh *et al,* 1997, Francis *et al,* 2002), demonstrating that RGD peptides within fibronectin can trigger integrin receptors that mediate the angiogenic actions of endothelial cells. The effects of MSC-CM upon endothelial cell migration were not entirely reproduced by fibronectin, as suggested by the further enhancement of EaHy-926 endothelial cell migration by MSC-CM, compared to unconditioned medium, in the presence of exogenous fibronectin. Interleukin (IL)-8, VEGF, and laminin, also,

have all been shown to be stimulatory to endothelial cells (Malinda *et al*, 1999, Kibbey *et al*, 1992, Ferrara, 2009, Waugh and Wilson, 2008). Investigations presented within Chapters 3 and 6 of this thesis as well as other studies (Chen *et al,* 2008, Beckermann *et al,* 2008, Wu *et al*, 2007) have found these factors to be present within MSC-CM. It seems likely that some or all of these known mediators of angiogenesis might contribute to the effects of MSC-CM upon EaHy926 endothelial cells.

In addition to insufficient vascularisation of wound beds contributing to the failure of grafts used to treat cutaneous wounds, any engineered skin tissue constructs containing living cells are limited to a $3mm^3$ volume in the absence of vasculature if the cells are to be maintained by the diffusion of nutrition from the surrounding tissues (Folkman and Hochberg, 1973). If the incorporation of MSC or MSC-CM derived factors into tissue engineered skin constructs could stimulate the formation of new vasculature into the graft, this would increase the amount of viable engineered tissue that could be implanted, potentially enhancing the effectiveness of tissue engineering strategies for cutaneous wound healing. It is has also been shown that as well as MSC secreting fibronectin and collagen (ECM proteins that promote angiogenesis), the presence of MSC supports the survival of blood vessels formed within fibronectin and collagen rich environments (Koike *et al*, 2004).

Overall, the data presented here supports the hypothesis that MSC may stimulate the formation of new vasculature, and that this may be an important aspect of MSC-mediated enhancement of wound healing. These findings also lends further support to the potential use of MSC as a clinical therapeutic agent for the treatment of severe or chronic cutaneous wounds, or in conjunction with conventional or tissue engineered skin grafts.

7.8: Conclusion

The results presented within this thesis demonstrate an MSC-CM mediated enhancement of skin cell migration, consistent with previous reports that MSC secreted factors promote skin wound healing, and reveal a range of components of the MSC secretome that may contribute to this effect. In particular, fibronectin when present as a substratum for cells appeared to be beneficial, stimulating scratch wound closure by all cell types investigated, although it's presence as a soluble factor in culture medium had no beneficial effects upon scratch closure. This work is clearly limited to a simple model wound healing and cell migration, the scratch assay. As such the results presented herein are not necessarily representative of the full spectrum of *in vivo* processes involved in wound healing, but, nonetheless, the study reveals specific effects of MSC-CM and its constituent components upon the specific aspects of wound healing that are modelled by this system. Additionally, the experiments presented in this thesis were performed independently either twice and the data pooled, or only once but using three individual donor's MSC cultures. Therefore further independent experimentation is required to establish the reproducibility of these findings. The study is further limited by the use of transformed cell lines to model the behaviour of primary cells *in vivo*, and particularly by the use of a murine transformed cell line in a system that is otherwise largely composed of human cells or derived factors. Whilst the cell lines used will not be fully representative of the behaviour of untransformed cells, and indeed may show limited responsiveness to stimulatory factors for this reason, their use did allow for a more consistent evaluation of the potentially variable factor, MSC-CM. which would not necessarily have been the case using normal human fibroblasts and keratinocytes.

Further work is now required to establish that normal human skin cells respond to MSC secreted factors in a similar manner and to identify which factors contribute to this stimulatory effect and the precise mechanisms involved. To validate these results, as well as future factors of interest, it would be advantageous to develop more sophisticated *in vitro* models of wound healing or examine *in vivo.*

Pursuant to the eventual goal of MSC-derived therapies of skin wound healing, future investigation should also attempt to evaluate the most effective method of delivering this beneficial effect within a clinical context. Topical applications of MSC-CM, or of selected stimulatory factors, to a wound site may be effective, but equally, the delivery of living cells within biomaterial scaffolds, potentially acting as a 'cytokine factory,' might also enhance wound healing. A comparison of the efficacy of a range of such methods would inform the clinical utilisation of the ability of MSC derived factors to stimulate cutaneous wound healing.
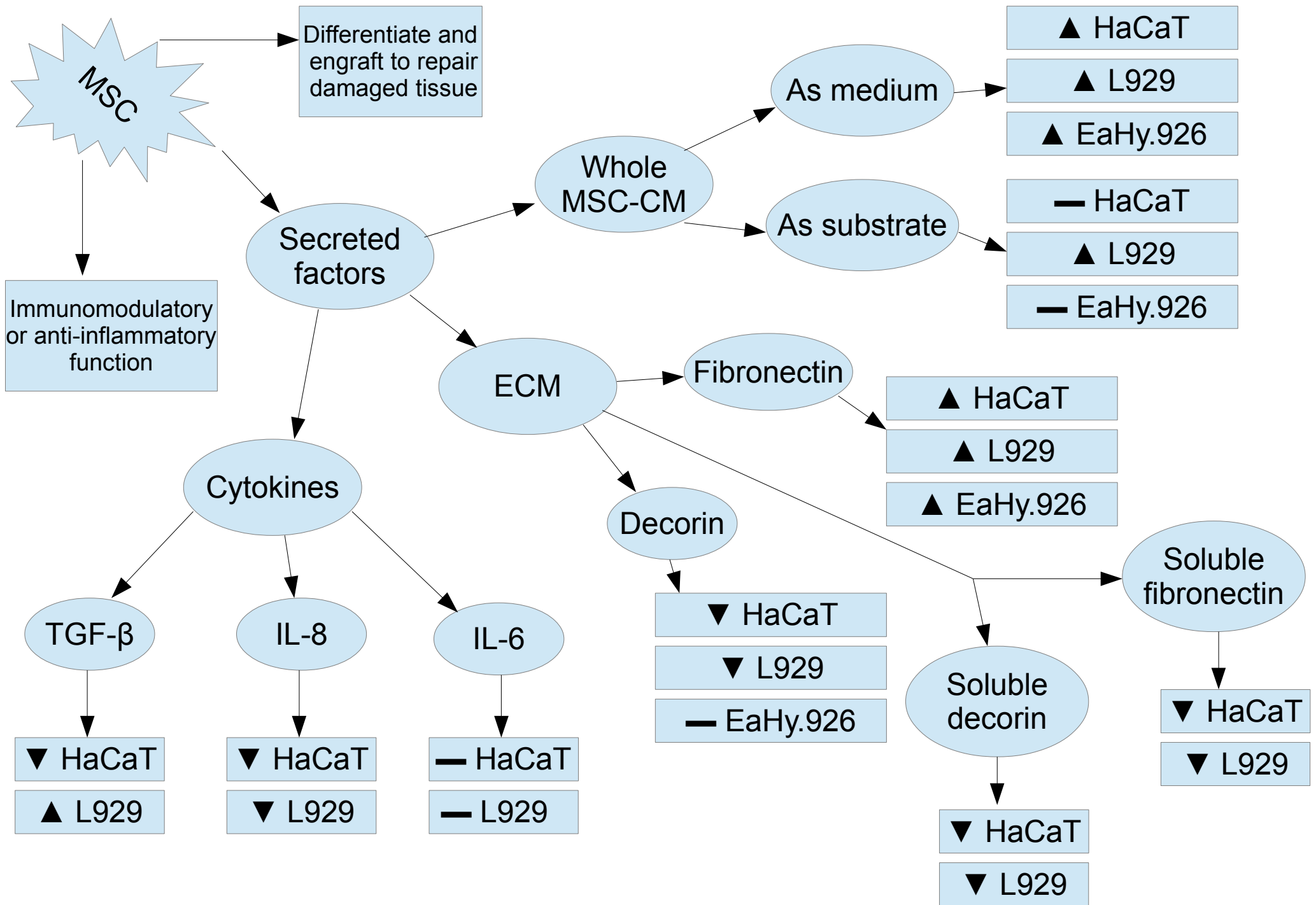
Summary model diagram.

Representative illustration summarizing the effects of MSC-CM, and MSC-secreted cytokines and ECM proteins upon the experimental cell lines under various test conditions as investigated within this thesis. ▲ represents a stimulatory effect,▼ represents an inhibition, ━ represents no observable/significant effect.

References

Agren MS, Steenfos HH, Dabelsteen S, Hansen JB, Dabelsteen E. Proliferation and mitogenic response to PDGFBB of fibroblasts isolated from chronic venous leg ulcers is ulcerage dependant. *J Invest Dermatol* 1999;112:4639.

Albig AR, Roy TG, Becenti DJ, Schiemann WP. (2007) Transcriptome analysis of endothelial cell gene expression induced by growth on matrigel matrices: identification and characterization of MAGP-2 and lumican as novel regulators of angiogenesis. Angiogenesis 10(3):197–216

Alemdaroglu C, Degim Z, Celebi N, Sengezer M, Alomeroglu M, Nacar A. Investigation of epidermal growth factor containing liposome formulation effects on burn wound healing. *J Biomed Mater Res A.* 2008;85(1):271-83.

Alemdaroglu C, Degim Z, Celebi N, Zor F, Ozturk S, Erdogan D. An investigation on burn wound healing in rats with chitosan gel formulation containing epidermal growth factor. *Burns.* 2006;32(3):319-27.

Altman SA, Randers L, Rao G. Comparison of trypan blue dye exclusion and fluorometric assays for mammalian cell viability determinations. Biotechnol Prog. 1993 Nov-Dec;9(6):671-4.

Arthur A, Zannettino A, Gronthos S. The therapeutic applications of multipotential mesenchymal/stromal stem cells in skeletal tissue repair. *J Cell Physiol* 2009; 218: 237-245

Asari S, Itakura S, Ferreri K, Liu CP, Kuroda Y, Kandeel F, Mullen Y: Mesenchymal stem cells suppress B-cell terminal diff erentiation. *Exp Hematol* 2009, 37:604-615.

Ashcroft GS, Yang X, Glick AB, Weinstein M, Letterio JL, Mizel DE, Anzano M, Greenwell-Wild T, Wahl SM, Deng, C. Mice lacking Smad3 show accelerated wound healing and an impaired local inflammatory response. *Nat. Cell Biol. 1999;* 1, 260-266.

Au P, Tam J, Fukumura D, Jain RK. Bone marrow-derived mesenchymal stem cells facilitate engineering of long-lasting functional vasculature. Blood. 2008;111:4551-4558.

Augello A, Tasso R, Negrini SM, Cancedda R, Pennesi G. Cell therapy using allogeneic bone marrow mesenchymal stem cells prevents tissue damage in collagen-induced arthritis. Arthritis Rheum. 2007;56(4):1175–86.

Bae KS, Park JB, Kim HS, Kim DS, Park JD , and Kang SJ. Neuron-Like Differentiation of Bone Marrow-Derived Mesenchymal Stem Cells. Yonsei Med J 52(3):401-412, 2011

Baglioni S, Francalanci M, Squecco R, Lombardi A, Cantini G, Angeli R, Gelmini S, Guasti D, Benvenuti S, Annunziato F, Bani D, Liotta F, Francini F, Perigli G, Serio M, Luconi M. Characterization of human adult stem-cell populations isolated from visceral and subcutaneous adipose tissue. *FASEB J* 23(10):3494-505, 2009.

Bajada S, Harrison PE, Ashton BA, Cassar-Pullicino VN, Ashammakhi N, Richardson JB. Successful treatment of refractory tibial nonunion using calcium sulphate and bone marrow stromal cell implantation. J Bone Joint Surg Br. 2007; 89:1382-6.

Bang OY, Lee JS, Lee PH, Lee G. Autologous mesenchymal stem cell transplantation in stroke patients. Ann Neurol. 2005; 57:874-82.

Bao P, Kodra A, Tomic-Canic M, Golinko MS, Ehrlich HP, Brem H. The role of vascular endothelial growth factor in wound healing. *J Surg Res*. 2009;153(2):347-58.

Barrientos S, Stojadinovic O, Golinko MS, Brem H, Tomic-Canic M, Growth factors and cytokines in wound healing. Wound Repair Regen 2008; 16:585–601.

Bartholomew A, Patil S, Mackay A, Nelson M, Buyaner D, Hardy W, Mosca J, Sturgeon C, Siatskas M, Mahmud N, Ferrer K, Deans R, Moseley A, Hoff man R, Devine SM: Baboon mesenchymal stem cells can be genetically modified to secrete human erythropoietin in vivo. *Hum Gene Ther* 2001, 12:1527-1541.

Bartholomew A, Sturgeon C, Siatskas M, Ferrer K, McIntosh K, Patil S, *et al*. Mesenchymal stem cells suppress lymphocyte proliferation in vitro and prolong skin graft survival in vivo. Exp Hematol. 2002; 30(1):42–8.

Basu A, Kligman LH, Samulewicz SJ, Howe CC. Impaired wound healing in mice deficient in a matricellular protein SPARC (osteonectin, BM-40). BMC Cell Biology 2001, 2:15

Baxter MA, Wynn RF, Jowitt SN et al. Study of telomere length reveals rapid aging of human marrow stromal cells following in vitro expansion. Stem Cells 2004;22:675–682.

Bayat, A., McGrouther, D., & Ferguson, M. Skin scarring. BMJ 326, 88-92. 11-1-2003.

Bianco P, Gehron Robey P. Marrow stromal stem cells. J Clin Invest 2000;105:1663–1668.

Bianco, P., Robey, P. G., and Simmons, P. J. (2008). Mesenchymal stem cells: revisiting history, concepts, and assays. Cell Stem Cell *2*, 313–319.

Borges, J., Tegtmeier, F., Padron, N., Mueller, M., Lang, E., & Stark, G. Chorioallantoic Membrane Angiogenesis Model for Tissue Engineering: A New Twist on a Classic Model. Tissue Engineering 9, 441-450. 2003.

Boukamp P, Dzarlieva-Petrusevska RT, Breitkreuz D, Hornung J, Markham A, Fusenig NE. Normal keratinization in a spontaneously immortalized aneuploid human keratinocyte cell line. *J. Cell Biol* 1988; 106: 761-771.

Boukamp P, Popp S, Altmeyer S, Hülsen A, Fasching C, Cremer T, Fusenig NE. Sustained nontumorigenic phenotype correlates with a largely stable chromosome content during long-term culture of the human keratinocyte line HaCat. *Genes, Chromosomes and Cancer*;1997,19: 201-214.

Boukamp P, Petrussevska RT, Breitkreutz D, Hornung J, Markham A, Fusenig NE Normal keratinization in a spontaneously immortalized aneuploid human keratinocyte cell line. J Cell Biol. 1988 Mar;106(3):761-71.

Bradshaw AD, Reed MJ, and Sage EH. SPARC-null mice exhibit accelerated cutaneous wound closure. J. Histochem Cytochem 2002, 50(1):1-10

Brown GL, Nanney LB, Griffen J, et al. Enhancement of wound healing by topical treatment with epidermal growth factor. *N Engl J Med.* 1989;321(2):76-9.

Bullock, A., Higham, M., & MacNeil, S. Use of human fibroblasts in the development of a xenobiotic free culture and delivery system for human keratinocytes. Tissue Eng. 2006 Feb; 12(2):245-55

Buschke S, Stark HJ, Cerezo A, Prätzel-Wunder S, Boehnke K, Kollar J, Langbein L, Heldin CH, Boukamp P. A decisive function of transforming growth factor-β/Smad signaling in tissue morphogenesis and differentiation of human HaCaT keratinocytes. Mol Biol Cell. 2011 Mar;22(6):782-94.

Can A, and Karahuseyinoglu S. Concise review: human umbilical cord stroma with regard to the source of fetus derived stem cells. Stem Cells 2007; 25, 2886.

Cao C, Dong Y: Study on culture and in vitro osteogenesis of blood derived human mesenchymal stem cells. Zhongguo Xiu Fu Chong Jian Wai Ke Za Zhi 2005, 19:642-647.

Caplan, A.I. (2007). Adult mesenchymal stem cells for tissue engineering versus regenerative medicine. J Cell Physiol *213*, 341–347.

Caplan, A. I., and Dennis, J. E. (2006) Mesenchymal stem cells as trophic mediators. *J. Cell. Biochem.* 98, 1076–1084

Casiraghi F, Azzollini N, Cassis P, Imberti B, Morigi M, Cugini D, Cavinato RA, Todeschini M, Solini S, Sonzogni A, Perico N, Remuzzi G, Noris M: Pretransplant infusion of mesenchymal stem cells prolongs the survival of a semi-allogeneic heart transplant through the generation of regulatory T cells. *J Immunol* 2008, 181:3933-3946.

Cei S, Kandler B, Fugl A, Gabriele M, Hollinger JO, Watzek G, et al. Bone marrow stromal cells of young and adult rats respond similarly to platelet-released supernatant and bone morphogenetic protein-6 in vitro. J Periodontol 2006;77:699–706.

Centeno CJ, Schultz JR, Cheever M, Robinson B, Freeman M, Marasco W: Safety and complications reporting on the re-implantation of culture expanded mesenchymal stem cells using autologous platelet lysate technique. *Curr Stem Cell Res Ther* 2009, Dec 2.

Chen WY, Abatangelo G. Functions of hyaluronan in wound repair. Wound Repair Regen. 1999 Mar-Apr;7(2):79-89.

Chen LB, Jiang XB, Yang L. Differentiation of rat marrow mesenchymal stem cells into pancreatic islet beta-cells. *World J Gastroenterol* 2004; 10: 3016-3020

Chen L, Tredget EE, Wu PYG, Wu Y. Paracrine Factors of Mesenchymal Stem Cells Recruit Macrophages and Endothelial Lineage Cells and Enhance Wound Healing. PLoS ONE. 2008; 3: e1886.

Choi YH, Burdick MD, Strieter RM. Human circulating fibrocytes have the capacity to differentiate osteoblasts and chondrocytes. *Int J Biochem Cell Biol* 2010; 42: 662-671

Clark RA, Ghosh K & Tonnesen MG. Tissue engineering for cutaneous wounds. *J Invest Dermatol.* 2007;127, 1018–1029.

Clark RAF: Basics of cutaneous wound repair. *J Dermatol Surg Oncol.* 1993; 19:693–706

Collins, TJ. Image J for microscopy. Biotechniques. 2007; 43(Suppl.1):25-30

Consortium for spinal cord medicine. Pressure ulcer prevention and treatment following spinal cord injury: a clinical practical guideline for health-care professionals. 1-94. 24-8-2007.

Cooper DM, Yu EZ, Hennessey P, Ko F, Robson MC. Determination of endogenous cytokines in chronic wounds. Ann Surg 1994; 219:68892.

Cory AH, Owen TC, Barltrop JA, Cory JG. Use of an aqueous soluble tetrazolium/formazan assay for cell growth assays in culture. Cancer Commun. 1991; 3:207-12

Coulomb B, Friteau L, Baruch J, Guilbaud J, Chretien Marquet B, Glicenstein J, Lebreton-Decoster C, Bell E & Dubertret L. Advantage of the presence of living dermal fibroblasts within in vitro reconstructed skin for grafting in humans. *Plast Reconstr Surg.* 1998;101,1891–1903.

Davies CL, Melder RJ, Munn LL, Mouta-Carreira C, Jain RK, Boucher Y: Decorin inhibits endothelial migration and tube-like structure formation: role of thrombospondin-1. Microvasc Res 2001; 62: 26–42.

Deans RJ, Moseley AB. Mesenchymal stem cells: Biology and potential clinical uses. Exp Hematol 2000;28:875–884.

Decline, F., Okamoto, O., Mallein-Gerin, F., Helbert, B., Bernaud, J., Rigal, D. and Rousselle, P. Keratinocyte motility induced by TGF_1 is accompanied by dramatic changes in cellular interactions with laminin 5. *Cell Motil. Cytoskeleton 2003;* 54, 64-80.

Decline F, Rousselle P. Keratinocyte migration requires alpha2beta1 integrin-mediated interaction with the laminin 5 gamma2 chain. Cell Sci. 2001 Feb;114(Pt 4):811-23.

De la Fuente R, Bernard A, Garcia-Castro J, Martin MC, Cigudosa JC. Retraction: Spontaneous Human Adult Stem Cell Transformation. *Cancer Res* 2010;70:6682.

Deng W, Han Q, Liao L, Li C, Ge W, Zhao Z, You S, Deng H, Murad F, Zhao RCH. Engrafted bone marrow-derived Flk-1+ mesenchymal stem cells regenerate skin tissue. Tissue Eng 2005;11:110–119.

Deodato B, Arsic N, Zentilin L, et al. Recombinant AAV vector encoding human VEGF165 enhances wound healing. *Gene Ther.* 2002;9(12):777-85.

De Ugarte DA, Alfonso Z, Zuk PA, Elbarbary A, Zhu M, Ashjian P, Benhaim P, Hedrick MH, Fraser JK: Differential expression of stem cell mobilization associated molecules on multi-lineage cells from adipose tissue and bone marrow. Immunol Lett 2003, 89:267-270.

Dezawa M, Hoshino M, Ide C. Treatment of neurodegenerative diseases using adult bone marrow stromal cell derived neurons. Expert Opin Biol Ther 2005;5:427-35.

Dinsdale SM. Decubitus ulcers in swine: light and electron microscopy study of pathogenesis. Arch Phys Med Rehabil. 1973 Feb;54(2):51-6

Di Nicola M, Carlo-Stella C, Magni M, Milanesi M, Longoni PD, Matteucci P, et al. Human bone marrow stromal cells suppress T-lymphocyte proliferation induced by cellular or nonspecific mitogenic stimuli. Blood. 2002; 99(10):3838–43.

Dipietro LA, Reintjes MG, Low QE, Levi B, Gamelli RL. Modulation of macrophage recruitment into wounds by monocyte chemoattractant protein-1. Wound Repair Regen 2001; 9:28–33.

Djouad F, Charbonnier LM, Bouffi C, Louis-Plence P, Bony C, Apparailly F, Cantos C, Jorgensen C, Noel D: Mesenchymal stem cells inhibit the differentiation of dendritic cells through an interleukin-6-dependent mechanism. *Stem Cells* 2007, 25:2025-2032.

Dominici M, Le Blanc K, Mueller I, Slaper-Cortenbach I, Marini F, Krause D, Deans R, Keating A, Prockop Dj, Horwitz E. Minimal criteria for defining multipotent mesenchymal stromal cells. The International Society for Cellular Therapy position statement. *Cytotherapy* 2006; 8: 315-317

Downey, D, Larabee, W, Voci, V, Pickart, L: Acceleration of wound healing using Glycyl-L-Histidyl-L-Lysyl-Cu (II). *Plastic Surg* 1985 48: 573–574,

Drexler HG, Uphoff CC. Mycoplasma contamination of cell cultures: Incidence, sources, effects, detection, elimination, prevention. Cytotechnology. 2002 Jul;39(2):75-90.

Dunlevy JR, Couchman JR. Interleukin-8 induces motile behavior and loss of focal adhesions in primary fibroblasts. J Cell Sci. 1995 Jan;108 (Pt 1):311-21.

Earle WR, Schilling EL, Stark TH, Straus NP, Brown MF & Sbelton E. Production of malignancy in vitro. 4. The mouse fibroblast cultures and changes seen in the living cells. J. Nat. Cancer Inst. 1943; 4:165-212.

Edgell CJ, McDonald CC, Graham JB. Permanent cell line expressing human factor VIII-related antigen established by hybridization. *Proc Natl Acad Sci USA*. 1983 Jun;80(12):3734-7.

Edmonson SR, Thumiger SP, Werther GA, Wraight CJ. Epidermal Homeostasis: The Role of the Growth Hormone and Insulin-Like Growth Factor Systems. Endocrine Reviews 2003; 24:737–764

Ehrenreich, M. & Ruszczak, Z. Update on Tissue-Engineered Biological Dressings. Tissue Engineering 12, 2407-2424. 2006.

Einhorn TA. Enhancement of fracture healing. *Instr Course Lect* 1996; 45: 401-416

El Ghalbzouri A, Gibbs S, Lamme E, et al. Effect of fibroblasts on epidermal regeneration. *Br J Dermatol*. 2002;147:230–243.

Engelhardt E, Toksoy A, Goebeler M, Debus S, Brocker EB, and Gillitzer R. Chemokines IL-8, GROalpha, MCP-1, IP-10, and Mig are sequentially and differentially expressed during phase-specific infiltration of leukocyte subsets in human wound healing. *Am J Pathol.* 1998;153: 1849–1860.

Falanga V, Iwamoto S, Chartier M, Yufit T, Butmarc J, Kouttab N, Shrayer D, Carson P. Autologous bone marrow-derived cultured mesenchymal stem cells delivered in a fibrin spray accelerate healing in murine and human cutaneous wounds. Tissue Eng. 2007; 13:1299-312.

Fathke C, Wilson L, Hutter J, Kapoor V, Smith A, Hocking A, Isik F. Contribution of bone marrow derived cells to skin: collagen deposition and wound repair. Stem Cells 2006;22:812–822.

Ferguson, M W J. O'Kane, S. Scar-free healing: from embryonic mechanisms to adult therapeutic intervention. Philos Trans R Soc Lond B Biol Sci. 2004 May 29; 359(1445): 839–850.

Ferrara N. VEGF-A: a critical regulator of blood vessel growth. Eur Cytokine Netw. 2009 Dec;20(4):158-63.

Firth JD, Uitto VJ, Putnins EE. Mechanical induction of an epithelial cell chymase associated with wound edge migration. J Biol Chem. 2008 Dec 12;283(50):34983-93.

Francis SE, Goh KL, Hodivala-Dilke K, Bader BL, Stark M, Davidson D, Hynes RO. "Central roles of $\alpha5\beta1$ integrin and fibronectin in vascular development in mouse embryos and embryoid bodies," Arteriosclerosis, Thrombosis, and Vascular Biology, vol. 22, no. 6, pp. 927–933, 2002.

Frank, C., Bayoumi, I., & Westendorp, C. Approach to infected skin ulcers. Canadian Family Physician 51, 1352-1359. 2005.

Friedenstein,A.J. (1980). Stromal mechanisms of bone marrow: cloning in vitro and retransplantation in vivo. Haematol Blood Transfus 25, 19–29.

Friedenstein, A.J., Chailakhjan, R.K., and Lalykina, K.S. (1970). The development of fibroblast colonies in monolayer cultures of guinea-pig bone marrow and spleen cells. Cell Tissue Kinet 3, 393–403.

Friedenstein AJ, Gorskaja JF, Kulagina NN: Fibroblast precursors in normaland irradiated mouse hematopoietic organs. Exp Hematol 1976, 4:267-274.

Fu L, Zhu L, Huang Y, Lee TD, Forman SJ, Shih CC: Derivation of neural stem cells from mesenchymal stemcells: evidence for a bipotential stem cell population. *Stem Cells Dev* 2008, 17(6):1109-1121.

Fuchs E, Cleveland DW. A structural scaffolding of intermediate filaments in health and disease. *Science*,1998;279 (5350): 514–9

Fuchs E, Horsley V. More than one way to skin... *Genes Dev*. 2008 Apr 15;22(8):976-85

Fujii M, Takeda K, Imamura T, Aoki H, Sampath TK, Enomoto S, et al. Roles of bone morphogenetic protein type I receptors and Smad proteins in osteoblast and chondroblast differentiation. Mol Biol Cell 1999;10:3801–3813.

Fujita T, Azuma Y, Fukuyama R, Hattori Y, Yoshida C, Koida M, Ogita K, Komori T. Runx2 induces osteoblast and chondrocytes differentiation and enhances their migration by coupling with PI3K-Akt signaling. *J Cell Biol* 2004; 166: 85-95

Gailit J, Clark RA. Studies in vitro on the role of alpha v and beta 1 integrins in the adhesion of human dermal fibroblasts to provisional matrix proteins fibronectin, vitronectin, and fibrinogen. J Invest Dermatol. 1996 Jan;106(1):102-8.

Galeano M, Deodato B, Altavilla D, et al. Effect of recombinant adeno-associated virus vector-mediated vascular endothelial growth factor gene transfer on wound healing after burn injury. *Crit Care Med.* 2003;31(4):1017-25.

Gallucci RM, Lee EG and Tomasek JJ. IL-6 Modulates Alpha-Smooth Muscle Actin Expression in Dermal Fibroblasts from IL-6-Deficient Mice. *Journal of Investigative Dermatology* (2006) 126, 561–568.

Gallucci RM, Sloan DK, Heck JM, Murray AR, O'Dell SJ. Interleukin 6 indirectly induces keratinocyte migration. J Invest Dermatol 2004; 122:764–72.

Gerdoni E, Gallo B, Casazza S, Musio S, Bonanni I, Pedemonte E, et al. Mesenchymal stem cells effectively modulate pathogenic immune response in experimental autoimmune encephalomyelitis. Ann Neurol.2007;61(3):219–27.

Ghalbzouri, A., Hensbergen, P., Gibbs, S., Kempenaar, J., Schors, R., & Ponec, M. Fibroblasts facilitate re-epithelialisation in wounded skin equivalents. Laboratory Investigation , 102-112. 2003.

Ghannam S, Bouffi ,Djouad F, Jorgensen C, and Noël, D. Immunosuppression by mesenchymal stem cells: mechanisms and clinical applications. *Stem Cell Research & Therapy* 2010, 1:2.

Ghazarian A, Garner WL, Ehrlich HP. Memory of past exposure to the chemokine IL-8 inhibits the contraction of fibroblast-populated collagen lattices. Exp Mol Pathol. 2000 Dec;69(3):242-7.

Glennie S, Soeiro I, Dyson PJ, Lam EW, Dazzi F. Bone marrow mesenchymal stem cells induce division arrest anergy of activated T cells. Blood. 2005; 105(7):2821–7.

Goh KL, Yang JT, and Hynes RO, "Mesodermal defects and cranial neural crest apoptosis in α5 integrin null embryos," *Development*, vol. 124, no. 21, pp. 4309–4319, 1997.

Greenhalgh DG. The role of apoptosis in wound healing. *Int J Biochem Cell Biol.* 1998;30(9):1019-30

Grey, J., Enoch, S., & Harding, K. ABC of wound healing Pressure ulcers. BMJ 332, 472-475. 25-9-2006.

Grinnell F. Fibronectin and wound healing. J Cell Biochem 1984;26:107-16

Gu TM, Niu XT, Guo H. Clinical observation on changes of fibroblast growth factor in burn wounds. *Zhongguo Xiu Fu Chong Jian Wai Ke Za Zhi.* 2000;14(5):261-3.

Gu K, Zhang L, Jin T, Rutherford RB. Identification of potential modifiers of Runx2/Cbfa1 activity in C2C12 cells in response to bone morphogenetic protein-7. Cells Tissues Organs 2004;176:28–40.

Haddow, D., Steele, D., Short, R., Dawson, R., & MacNeil, S. Plasma-polymerised surfaces for culture of human keratinocytes and transfer of cells to an *in vitro* wound bed model. J Biomed Mater Res , 80-87. 2001.

Harding, K., Morris, H., & Patel, G. Science, medicine, and the future Healing chronic wounds. BMJ 324, 160-163. 19-1-2002.

Hare JM, Traverse JH, Henry TD, Dib N, Strumpf RK, Schulman SP, Gerstenblith G, DeMaria AN, Denktas AE, Gammon RS, Hermiller JB Jr, Reisman MA, Schaer GL, Sherman W. A randomized, double-blind, placebo-controlled, dose-escalation study of intravenous adult human mesenchymal stem cells (prochymal) after acute myocardial infarction. *J Am Coll Cardiol* 2009; 54: 2277-2286

Hasan A, Murata H, Falabella A, Ochoa S, Zhou L, Badiavas E, et al. Dermal fibroblasts from venous ulcers are unresponsive to the action of transforming growth factorbeta 1. *J Dermatol Sci* 1997;16:5966.

Hass, R., Kasper, K., Bohm, S. and Jacobs, R. Different populations and sources of human mesenchymal stem cells (MSC): A comparison of adult and neonatal tissue-derived MSC Cell Communication and Signaling 2011, 9:12

Heldin CH,Westermark B. Mechanism of action and in vivo role of platelet-derived growth factor. *Physiol Rev.* 1999;79(4):1283-316.

Hoath, S. & Leahy, D. The organisiation of human epidermis: Functional epidermal units and Phi proportionality. Journal of Investigative Dermatology 121, 1440-1446. 24-6-2003.

Honmou O, Houkin K, Matsunaga T, Niitsu Y, Ishiai S, Onodera R, Waxman SG, Kocsis JD Intravenous administration of auto serum-expanded autologous mesenchymal stem cells in stroke. Brain. 2011 Jun;134(Pt 6):1790-807.

Horch, R., Kopp, J., Kneser, U., Beier, J., & Bach, A. Tissue engineering of cultured skin substitutes. J.Cell.Mol.Med. 9, 592-608. 30-8-2005.

Horwitz EM, Gordon PL, WKK Koo, Marx JC, Neel MD, McNall RY, Muul L, Hofmann T. Isolated allogeneic bone marrow-derived mesenchymal cells engraft and stimulate growth in children with osteogenesis imperfecta: Implications for cell therapy of bone. Proc Natl Acad Sci USA 2002; 99:8932– 8937.

Hosokawa, R., Urata, M. M., Ito, Y., Bringas, P., Jr and Chai, Y. Functional significance of Smad2 in regulating basal keratinocyte migration during wound healing. *J. Invest. Dermatol.* 2005;125, 1302-1309.

Iocono JA, Colleran KR, Remick DG, Gillespie BW, Ehrlich HP, and Garner WL. Interleukin-8 levels and activity in delayed-healing human thermal wounds. *Wound Repair Regen.* 2000; 8: 216–225.

Järveläinen H, Puolakkainen P, Pakkanen S, Brown EL, Höök M, Iozzo RV, Sage EH, Wight TN. A role for decorin in cutaneous wound healing and angiogenesis. Wound Repair Regen. 2006 Jul-Aug;14(4):443-52.

Jeon YK, Jang YH, Yoo DR, Kim SN, Lee SK, Nam MJ. Mesenchymal stem cells' interaction with skin: wound-healing effect on fibroblast cells and skin tissue. Wound Repair Regen. 2010 Nov-Dec;18(6):655-61

Jiang XX, Zhang Y, Liu B, Zhang SX, Wu Y, Yu XD, Mao N: Human mesenchymal stem cells inhibit differentiation and function of monocyte derived dendritic cells. *Blood* 2005, 105:4120-4126.

Jörn W, Kuhbier BW, Radtke Christine, Peter M, Vogt , Kasper Cornelia, Reimers Kerstin: Isolation, Characterization, Differentiation, and Application of Adipose-Derived Stem Cells. Adv Biochem Engin/Biotechnol 2010, 123:55-105.

Joseph J, Variathu KT, Mohanty M. Mediatory role of interleukin-6 in α-smooth muscle actin induction and myofibroblast formation around silicone tissue expander. *J Biomed Mater Res A*. 2013 Apr 24

Jung MY, Thapa N, Kim JE, Yang JD, Cho BC, Kim IS. Recombinant tetra-cell adhesion motifs supports adhesion, migration and proliferation of keratinocytes/fibroblasts, and promotes wound healing. Exp Mol Med. 2007 Oct 31;39(5):663-72.

Karahuseyinoglu S, Cinar O, Kilic E, Kara F, Akay GG, Demiralp DO, Tukun A, Uckan D, Can A. Biology of stem cells in human umbilical cord stroma: in situ and in vitro surveys. Stem Cells. 2007 Feb;25(2):319-31.

Kane CJ, Hebda PA, Mansbridge JN, Hanawalt PC. Direct evidence for spatial and temporal regulation of transforming growth factor beta 1 expression during cutaneous wound healing. J Cell Physiol. 1991 Jul;148(1):157-73.

Kaverina I, Straube A. Regulation of cell migration by dynamic microtubules. *Semin Cell Dev Biol.* 2011 Dec;22(9):968-74.

Katagiri T, Yamaguchi A, Komaki M, Abe E, Takahashi N, Ikeda T, et al. Bone morphogenetic protein-2 converts the differentiation pathway of C2C12 myoblasts into the osteoblast lineage. J Cell Biol 1994;127:1755–1766.

Kehe, K., Abend, M., Kehe, K., & Ridi, R. Tissue engineering with HaCat cells and a fibroblast cell line. Arch Dermatol Res 291, 600-605. 1999.

Kern S., Eichler H., Stoeve J., Kluter H., Bieback K. Comparative analysis of mesenchymal stem cells from bone marrow, umbilical cord blood, or adipose tissue. Stem Cells 2006; 24:1294-301

Khoo CP, Micklem K, Watt SM. A Comparison of Methods for Quantifying Angiogenesis in the Matrigel Assay In Vitro. Tissue Eng Part C Methods. 2011 Jun 8.

Kibbey MC, Grant DS, and Kleinman HK, "Role of the SIKVAV site of laminin in promotion of angiogenesis and tumor growth: an in vivo Matrigel model," *Journal of the National Cancer Institute*, vol. 84, no. 21, pp. 1633–1638, 1992.

Kim WS, Park BS, Sung JH, Yang JM, Park SB, Kwak SJ, Park JS. Wound healing effect of adipose-derived stem cells: a critical role of secretory factors on human dermal fibroblasts. J Dermatol Sci. 2007; 48:15-24.

Kinnaird T, Stabile E, Burnett MS, Lee CW, Barr S, Fuchs S, Epstein SE (2004) Marrow-derived stromal cells express genes encoding a broad spectrum of arteriogenic cytokines and promote in vitro and in vivo arteriogenesis through paracrine mechanisms. Circ Res 94:678–85

Koc ON, Gerson SL, Cooper BW, Dyhouse SM, Haynesworth SE, Caplan AI, Lazarus HM: Rapid hematopoietic recovery after co-infusion of autologous blood stem cells and culture-expanded marrow mesenchymal stem cells in advanced breast cancer patients receiving high-dose chemotherapy. *J Clin Oncol* 2000, 18:307-316.

Kolokol'chikova EG, Budkevich LI, Bobrovnikov AE, Badikova AK & Tumanov VP. Morphological changes in burn wounds after transplantation of allogenic fibroblasts. *Bull Exp Biol Med.* 2001;131, 89 –93.

Kopen GC, Prockop DJ, Phinney DG: Marrow stromal cells migrate throughout forebrain and cerebellum, and they differentiate into astrocytes after injection into neonatal mouse brains. *Proc Natl Acad Sci USA* 1999, 96(19):10711-10716.

Kozłowski L, Zakrzewska I, Tokajuk P, Wojtukiewicz MZ. Concentration of interleukin-6 (IL-6), interleukin-8 (IL-8) and interleukin-10 (IL-10) in blood serum of breast cancer patients. *Rocz Akad Med Bialymst*. 2003;48:82-4.

Krampera M, Cosmi L, Angeli R, Pasini A, Liotta F, Andreini A, Santarlasci V, Mazzinghi B, Pizzolo G, Vinante F, Romagnani P, Maggi E, Romagnani S, Annunziato F: Role for interferon-gamma in the immunomodulatory activity of human bone marrow mesenchymal stem cells. *Stem Cells* 2006, 24:386-398.

Krampera M, Glennie S, Dyson J, Scott D, Laylor R, Simpson E, et al. Bone marrow mesenchymal stem cells inhibit the response of naive and memory antigen-specific T cells to their cognate peptide. Blood. 2003;101(9):3722–9.

Kresse H, Schönherr E. Proteoglycans of the extracellular matrix and growth control. J Cell Physiol. 2001 Dec;189(3):266-74.

Kuroda R, Ishida K, Matsumoto T, Akisue T, Fujioka H, Mizuno K, Ohgushi H, Wakitani S, Kurosaka M. Treatment of a full-thickness articular cartilage defect in the femoral condyle of an athlete with autologous bone-marrow stromal cells. *Osteoarthritis Cartilage* 2007; 15: 226-231

Kwon AH, Qiu Z, Hirao Y. Topical application of plasma fibronectin in full-thickness skin wound healing in rats. Exp Biol Med (Maywood). 2007 Jul;232(7):935-41.

Lauer, G., Sollberg, S., Cole, M., Flamme, I., Stürzebecher, J., Mann, K., Krieg, T., & Eming, S. Expression and proteolysis of vascular endothelieal growth factor is increased in chronic wounds. Journal of Investigative Dermatology 115, 12-18. 25-4-2000.

Lauffenburger, D.A., Horwitz, A.F. Cell migration: a physically integrated molecular process. Cell 1996; 84:359–369.

Lazennec G and Jorgensen C. Concise review: adult multipotent stromal cells and cancer: risk or benefit? *Stem Cells*. 2008 June ; 26(6): 1387–1394.

Li H, Fan X, Kovi RC, et al. Spontaneous expression of embryonic factors and p53 point mutations in aged mesenchymal stem cells: a model of age-related tumorigenesis in mice. Cancer Res 2007;67:10889–10898.

Li Y, Fan J, Chen M, Li W, Woodley DT. Transforming growth factor-alpha: a major human serum factor that promotes human keratinocyte migration. J Invest Dermatol. 2006; 126:2096-105.

Liechty KW, Crombleholme TM, Cass DL, Martin B, AND Adzick NS. Diminished interleukin-8 (IL-8) production in the fetal wound healing response. *J Surg Res*. 1998; 77: 80–84.

Lindblad, W. J. 1998 Perspective article: collagen expression by novel cell populations in the dermal wound environment. Wound Repair Regen. 6, 186–193.

Liu TM, Martina M, Hutmacher DW, Hui JH, Lee EH, Lim B. Identification of common pathways mediating differentiation of bone marrow- and adipose tissue-derived human mesenchymal stem cells into three mesenchymal lineages. Stem Cells 2007; 25:750-60.

Lu LL, Liu YJ, Yang SG, Zhao QJ, Wang X, Gong W, Han ZB, Xu ZS, Lu YX, Liu D, Chen ZZ, Han ZC. Isolation and characterization of human umbilical cord mesenchymal stem cells with hematopoiesis-supportive function and other potentials. Haematologica 2006; 91, 1017.

Luckett-Chastain LR, Gallucci RM. Interleukin-6 (IL-6) modulates migration and matrix metalloproteinase function in dermal fibroblasts from IL-6KO mice. Br J Dermatol. 2009; 156:1163-71.

Maas-Szabowski N, Stark HJ, Fusenig NE. Keratinocyte growth regulation in defined organotypic cultures through IL-1-induced keratinocyte growth factor expression in resting fibroblasts. *J Invest Dermatol* 2000 Jun;114(6):1075-84.

Maas-Szabowski, N., Stärker, A., & Fusenig, N. Epidermal tissue regeneration and stromal interaction in HaCat cells is initiated by TGF-alpha. Journal of Cell Science 116, 2937-2948. 2003.

MacNeil, S. Progress and opportunities for tissue-engineered skin. Nature 445, 874-880. 22-2-2007.

Makino S, Fukuda K, Miyoshi S, Konishi F, Kodama H, Pan J, Sano M, Takahashi T, Hori S, Abe H, Hata J, Umezawa A, Ogawa S. Cardiomyocytes can be generated from marrow stromal cells in vitro. *J Clin Invest* 1999; 103: 697-705

Malgieri A, Kantzari E, Patrizi MP, Gambardella S. Bone marrow and umbilical cord blood human mesenchymal stem cells: state of the art. Int J Clin Exp Med. 2010 Sep 7;3(4):248-69.

Malinda KM, Nomizu M, Chung M, Delgado M, Kuratomi Y, Yamada Y, Kleinman HK, Ponce ML. "Identification of laminin $\alpha 1$ and $\beta 1$ chain peptides active for endothelial cell adhesion, tube formation, and aortic sprouting," *FASEB Journal*, vol. 13, no. 1, pp. 53–62, 1999.

Mansbridge, J. Commercial considerations in tissue engineering. J.Anat 209, 527-532. 23-7-2006.

Marcacci M, Kon E, Moukhachev V, Lavroukov A, Kutepov S, Quarto R, Mastrogiacomo M, Cancedda R. Stem cells associated with macroporous bioceramics for long bone repair: 6-to 7-year outcome of a pilot clinical study. *Tissue Eng* 2007; 13: 947-955

Marcinkiewicz C, Weinreb PH, Calvete JJ, Kisiel DG, Mousa SA, Tuszynski GP, Lobb RR, "Obtustatin: a potent selective inhibitor of $\alpha1\beta1$ integrin in vitro and angiogenesis in vivo," Cancer Research, vol. 63, no. 9, pp. 2020–2023, 2003.

Marionnet, C., Pierrard, C., Vioux-Chagnoleau, C., Sok, J., Asselineau, D., & Bernerd, F. Interaction between fibroblasts and keratinocytes in morphogenesis of dermal epidermal junction in a model of reconstructed skin. Journal of Investigative Dermatology 126, 971-979. 9-5-2006.

Markmann A, Hausser H, Schönherr E, Kresse H. Influence of decorin expression on transforming growth factor-beta-mediated collagen gel retraction and biglycan induction. *Matrix Biol*. 2000 Dec;19(7):631-6.

Marsh D. Concepts of fracture union, delayed union, and non-union. *Clin Orthop Relat Res* 1998; S22-S30

Marston, W. Dermagraft, a bioengineered human dermal equivalent for the treatment of chronic nonhealing diabetic foot ulcer. Expert Rev.Medical Devices 1, 21-31. 2004.

Mehlhorn AT, Schmal H, Kaiser S, Lepski G, Finkenzeller G, Stark GB, Südkamp NP. Mesenchymal stem cells maintain TGF-beta-mediated chondrogenic phenotype in alginate bead culture. *Tissue Eng* 2006; 12: 1393-1403

Merle B, Malaval L, Lawler J, Delmas P, Clezardin P. Decorin inhibits cell attachment to thrombospondin-1 by binding to a KKTR-dependent cell adhesive site present within the N-terminal domain of thrombospondin-1. J Cell Biochem. 1997 Oct 1;67(1):75-83.

Metcalfe, A. & Ferguson, M. Tissue engineering of replacement skin: the crossroads of biomaterials, wound healing, embryonic development, stem cells and regeneration. J.R.Soc.Interface 4, 413-437. 5-12-2007.

Miao Z, Jin J, Chen L, Zhu J, Huang W, Zhao J, Qian H, Zhang X. Isolation of mesenchymal stem cells from human placenta: comparison with human bone marrow mesenchymal stem cells. Cell Biol Int 2006; 30:681-7.

Michel G, Kemeny L, Peter RU, Beetz A, Ried C, Arenberger P, Ruzicka T. Interleukin-8 receptor-mediated chemotaxis of normal human epidermal cells. FEBS Lett 1992; 305:241–3

Michalik L, Auwerx J, Berger JP, Chatterjee VK, Glass CK, Gonzalez FJ, Grimaldi PA, Kadowaki T, Lazar MA, O'Rahilly S, Palmer CN, Plutzky J, Reddy JK, Spiegelman BM, Staels B, Wahli W (2006). "International Union of Pharmacology. LXI. Peroxisome proliferator-activated receptors". *Pharmacol. Rev.* 58 (4): 726–41.

Miyahara Y, Nagaya N, Kataoka M, Yanagawa B, Tanaka K, Hao H, Ishino K, Ishida H, Shimizu T, Kangawa K, Sano S, Okano T, Kitamura S, Mori H. Monolayered

mesenchymal stem cells repair scarred myocardium after myocardial infarction. *Nat Med* 2006; 12: 459-465

Montesano R, Vassalli JD, Baird A, Guillemin R, Orci L. Basic fibroblast growth factor induces angiogenesis in vitro. *Proc Natl Acad Sci U S A.* 1986;83(19):7297-301.

Montzka K, Lassonczyk N, Tschöke B, Neuss S, Führmann T, Franzen R, Smeets R, Brook G and Wöltje M. Neural differentiation potential of human bone marrow-derived mesenchymal stromal cells: misleading marker gene expression *BMC Neuroscience* 2009, 10:16

Morley SM, D'Alessandro M, Sexton C, Rugg EL, Navsaria H, Shemanko CS, Huber M, Hohl D, Heagerty AI, Leigh IM, Lane EB. Generation and characterization of epidermolysis bullosa simplex cell lines: scratch assays show faster migration with disruptive keratin mutations. Br J Dermatol. 2003 Jul;149(1):46-58.

Moscoso I, Centeno A, López E, Rodriguez-Barbosa JI, Santamarina I, Filgueira P, Sánchez MJ, Domínguez-Perles R, Peñuelas-Rivas G, Domenech N. Differentiation "in vitro" of primary and immortalized porcine mesenchymal stem cells into cardiomyocytes for cell transplantation. *Transplant Proc* 2005; 37: 481-482

Moulin V. Growth factors in skin wound healing. Eur J Cell Biol. 1995 Sep;68(1):1-7.

Mulder, G, Patt, L, Sanders, L, Rosenstock, J, Altman, M, Hanley, M, Duncan, G: Enhanced healing of ulcers in patients with diabetes by topical treatment with glycyl-L-histidyl-L-lysine copper. *Wound Rep Reg* 1994 2: 259–269,

Muhlhauser J, Merrill MJ, Pili R, et al. VEGF165 expressed by a replication-deficient recombinant adenovirus vector induces angiogenesis in vivo. *Circ Res.* 1995;77(6):1077-86.

Nakamura M, Takahashi T, Matsumoto T, Akiba Y, Matsui H, Tsuchimoto K, Ishii H, Yamada H. Expression of leptin in two-layered culture of gastric mucous cells and fibroblasts: effect of Helicobacter pylori attachment. Aliment Pharmacol Ther. 2004 Jul;20 Suppl 1:125-30.

Nam HJ, Park YY, Yoon G, Cho H, Lee JH. Co-treatment with hepatocyte growth factor and TGF-beta1 enhances migration of HaCaT cells through NADPH oxidase-dependent ROS generation. Exp Mol Med. 2010 Apr 30;42(4):270-9.

Nemeth K, Leelahavanichkul A, Yuen PS, Mayer B, Parmelee A, Doi K, Robey PG, Leelahavanichkul K, Koller BH, Brown JM, Hu X, Jelinek I, Star RA, Mezey E: Bone marrow stromal cells attenuate sepsis via prostaglandin E2-dependent reprogramming of host macrophages to increase their interleukin-10 production. *Nat Med* 2009, 15:42-49.

Niewiarowska J, Brézillon S, Sacewicz-Hofman I, Bednarek R, Maquart FX, Malinowski M, Wiktorska M, Wegrowski Y, Cierniewski CS. Lumican inhibits angiogenesis by interfering with $\alpha2\beta1$ receptor activity and downregulating MMP-14 expression. Thromb Res. 2011 Jul 11.

Nissen NN, Polverini PJ, Gamelli RL, DiPietro LA. Basic fibroblast growth factor mediates angiogenic activity in early surgical wounds. *Surgery.* 1996;119(4):457-65.

Nissen NN, Polverini PJ, Koch AE, Volin MV, Gamelli RL, DiPietro LA. Vascular endothelial growth factor mediates angiogenic activity during the proliferative phase of wound healing. *Am J Pathol.*1998;152(6):1445-52.

Nousbeck J, Sarig O, Avidan N, Indelman M, Bergman R, Ramon M, Enk CD, Sprecher E. Insulin-Like Growth Factor-Binding Protein 7 Regulates Keratinocyte Proliferation, Differentiation and Apoptosis. J Invest Dermatol. 2009 Aug 27.

Oishi K, Noguchi H, Yukawa H, Hayashi S. Differential ability of somatic stem cells. *Cell Transplant* 2009; 18: 581-589

Okamoto T, Oikawa S, Toyota T, Goto Y. Angiogenesis factors in ocular tissues of normal rabbits on chorioallantoic membrane assay. Tohoku J Exp Med. 1988 Jan;154(1):63-70.

Oreffo RO, Kusec V, Romberg S, Triffitt JT. Human bone marrow osteoprogenitors express estrogen receptor-alpha and bone morphogenetic proteins 2 and 4 mRNA during osteoblastic differentiation. *J Cell Biochem* 1999; 75: 382-392

Oswald J, Boxberger S, Jorgensen B, Feldmann S, Ehninger G, Bornhauser M, Werner C (2004) Mesenchymal stem cells can be differentiated into endothelial cells *in vitro*. Stem Cells 22: 377-384.

Pankov R, Yamada KM. Fibronectin at a glance. J Cell Sci 2002;115:3861-3

Papapetropoulos A, Pyriochou A, Altaany Z, et al. Hydrogen sulfide is an endogenous stimulator of angiogenesis. *Proc Natl Acad Sci U S A.* 2009;106(51):21972-7.

Pittenger MF, Mackay AM, Beck SC, Jaiswal RK, Douglas R, Mosca JD, Moorman MA, Simonetti DW, Craig S, Marshak DR: Multilineage potential of adult human mesenchymal stem cells. Science 1999, 284:143-147.

Postlethwaite AE, Keski-Oja J, Moses HL, Kang AH. Stimulation of the chemotactic migration of human fibroblasts by transforming growth factor beta. J Exp Med. 1987; 165:251-6.

Price RD, Das-Gupta, V, Harris PA, Leigh IM & Navsaria HA. The role of allogenic fibroblasts in an acute wound healing model. *Plast Reconstr Surg.* 2004;113, 1719–1729.

Prockop, D.J. (1997). Marrow stromal cells as stem cells for nonhematopoietic tissues. Science *276*, 71–74.

Prockop DJ. "Stemness" does not explain the repair of many tissues by mesenchymal stem/multipotent stromal cells (MSCs). Clin Pharmacol Ther 2007; 82:241–243.

Rastegar F, Shenaq D, Huang J, Zhang W, Zhang BQ, He BC, Chen L, Zuo GW, Luo Q, Shi Q, Wagner ER, Huang E, Gao Y, Gao JL, Kim SH, Zhou JZ, Bi Y, Su Y, Zhu G, Luo J, Luo X, Qin J, Reid RR, Luu HH, Haydon RC, Deng ZL, He TC. Mesenchymal stem cells: Molecular characteristics and clinical applications. *World J Stem Cells* 2010 August 26; 2(4): 67-80.

Reddy, M., Gill, S., & Rochon, P. Preventing Pressure Ulcers: A Systematic Review. JAMA 296, 974-984. 2006.

Reed MJ, Puolakkainen P, Lane TF, Dickerson D, Bornstein P, Sage EH: Differential expression of SPARC and thrombospondin 1 in wound repair: immunolocalization and in situ hybridization. J Histochem Cytochem 1993; 41:1467-1477

Ren G, Zhang L, Zhao X, Xu G, Zhang Y, Roberts AI, Zhao RC, Shi Y: Mesenchymal stem cell-mediated immunosuppression occurs via concerted action of chemokines and nitric oxide. *Cell Stem Cell* 2008, 2:141-150.

Rennekampff HO, Hansbrough JF, Kiessig V, Dore C, Sticherling M, and Schröder JM. Bioactive interleukin-8 is expressed in wounds and enhances wound healing. *J Surg Res* 2000; 93: 41–54.

Rennekampff HO, Hansbrough JF, Woods V JR, Dore C, Kiessig V, and Schröder JM. Role of melanoma growth stimulatory activity (MGSA/gro) on keratinocyte function in wound healing. *Arch Dermatol Res* 1997; 289: 204–212.

Ribatti D, Presta M, Vacca A, Ria R, Giuliani R, Dell'Era P, Nico B, Roncali L, and Dammacco F. Human Erythropoietin Induces a Pro-Angiogenic Phenotype in Cultured Endothelial Cells and Stimulates Neovascularization In Vivo. *Blood.* 1999 Apr 15;93(8):2627-36

Ribatti D, Ranieri G, Nico B, Benagiano V, Crivellato E. Tryptase and chymase are angiogenic in vivo in the chorioallantoic membrane assay. Int J Dev Biol. 2011;55(1):99-102.

Rissmann A, Pieper S, Adams I, Brune T, Wiemann D, Reinhold D. Increased blood plasma concentrations of TGF-beta1 and TGF-beta2 after treatment with intravenous immunoglobulins in childhood autoimmune diseases. *Pediatr Allergy Immunol.* 2009 May;20(3):261-5.

Robson MC. The role of growth factors in the healing of chronic wounds. Wound Repair Regen. 1997 Jan-Mar;5(1):12-7.

Romano Di Peppe S, Mangoni A, et al. Adenovirus-mediated VEGF(165) gene transfer enhances wound healing by promoting angiogenesis in CD1 diabetic mice. *Gene Ther.* 2002;9(19):1271-7.

Romanov YA, Darevskaya AN, Merzlikina NV, Buravkova LB. Mesenchymal stem cells from human bone marrow and adipose tissue: isolation, characterization, and differentiation potentialities. *Bull Exp Biol Med* 140(1):138-43, 2005.

Rosen ED, Spiegelman BM. Molecular regulation of adipogenesis. *Annu Rev Cell Dev Biol* 2000; 16: 145-171

Røsland GV, Svendsen A, Torsvik A, Sobala E, McCormack E, Immervoll H, Mysliwietz J, Tonn JC, Goldbrunner R, Lønning PE, Bjerkvig R, Schichor C. Long-term Cultures of Bone Marrow–Derived Human Mesenchymal Stem Cells Frequently Undergo Spontaneous Malignant Transformation. Cancer Res 2009; 69: (13).

Rubio D, Garcia-Castro J, Martin MC, et al. Spontaneous human adult stem cell transformation. Cancer Res 2005;65:3035–3039.

Rubio D, Garcia S, Paz MF, et al. Molecular characterization of spontaneous mesenchymal stem cell transformation. PLoS ONE 2008;3:e1398

Salcido, R., Popescu, A., & Ahn, C. Animal models in pressure ulcer research. Journal of Spinal Cord Medicine 30, 107-116. 1-12-2006.

Salem HK, Thiemermann C. Mesenchymal Stromal Cells: Current Understanding and Clinical Status. *Stem Cells* 2010;28:585–596

Sanchez-Ramos J, Song S, Cardozo-Pelaez F, Hazzi C, Stedeford T, Willing A, Freeman TB, Saporta S, Janssen W, Patel N, *et al.*: Adult bone marrow stromal cells differentiate into neural cells in vitro. *Exp Neurol* 2000, 164(2):247-256.

Sasaki M, Abe R, Fujita Y, Ando S, Inokuma D, Shimizu H. Mesenchymal Stem Cells Are Recruited into Wounded Skin and Contribute to Wound Repair by Transdifferentiation into Multiple Skin Cell Type. The Journal of Immunology, 2008; 180:2581 -2587

Sarugaser R, Lickorish, D, Baksh, D, Hosseini, MM, and Davies JE. Human umbilical cord perivascular (HUCPV) cells: a source of mesenchymal progenitors. Stem Cells 2005; 23, 220.

Sato K, Ozaki K, Oh I, Meguro A, Hatanaka K, Nagai T, Muroi K, Ozawa K: Nitric oxide plays a critical role in suppression of T-cell proliferation by mesenchymal stem cells. *Blood* 2007, 109:228-234.

Sato M, Sawamura D, Ina S, Yaguchi T, Hanada K, Hashimoto I. In vivo introduction of the interleukin 6 gene into human keratinocytes: induction of epidermal proliferation by the fully spliced form of interleukin 6, but not by the alternatively spliced form. Arch Dermatol Res 1999; 291:400–4.

Schaffler A, Buchler C: Concise review: adipose tissue-derived stromal cells–basic and clinical implications for novel cell-based therapies. Stem Cells 2007, 25:818-827.

Serini G, Bochaton-Piallat ML, Ropraz P, Geinoz A, Borsi L, Zardi L, Gabbiani G. The fibronectin domain ED-A is crucial for myofibroblastic phenotype induction by transforming growth factor-beta1. J Cell Biol. 1998 Aug 10;142(3):873-81.

Schmidt G, Robenek H, Harrach B, Glössl J, Nolte V, Hörmann H, Richter H, Kresse H. Interaction of small dermatan sulfate proteoglycan from fibroblasts with fibronectin. J Cell Biol. 1987 Jun;104(6):1683-91.

Schuleri KH, Amado LC, Boyle AJ, Centola M, Saliaris AP, Gutman MR, Hatzistergos KE, Oskouei BN, Zimmet JM, Young RG, Heldman AW, Lardo AC, Hare JM. Early improvement in cardiac tissue perfusion due to mesenchymal stem cells. *Am J Physiol Heart Circ Physiol* 2008; 294

Shah, M., Foreman, D. M. & Ferguson, M. W. J. 1994 Neutralising antibody to TGFβ-1,2, reduces scarring in adult rodents. *J. Cell Sci.* **107**, 1137–1157.

Shah, M., Foreman, D. M. & Ferguson, M. W. J. 1995 Neutralisation of TGFβ-1 and TGFβ-2 or exogenous addition of TGFβ-3 to cutaneous rat wounds reduces scarring. *J. Cell Sci.* 108, 985–1002.

Shen B, Wei A, Tao H, Diwan AD, Ma DD. BMP-2 enhances TGF-beta3-mediated chondrogenic differentiation of human bone marrow multipotent mesenchymal stromal cells in alginate bead culture. *Tissue Eng Part A* 2009; 15: 1311-1320

Shevchenko RV, Sibbons PD, Sharpe JR & James, SE. Use of a novel porcine collagen paste as a dermal substitute in full-thickness wounds. *Wound Repair Regen.* 2008;16, 198–207.

Shiota M, Heike T, Haruyama M, Baba S, Tsuchiya A, Fujino H, Kobayashi H, Kato T, Umeda K, Yoshimoto M, Nakahata T. Isolation and characterization of bone marrow-derived mesenchymal progenitor cells with myogenic and neuronal properties. *Exp Cell Res* 2007; 313: 1008-1023

Siméon A, Wegrowski Y, Bontemps Y, Maquart FX. Expression of glycosaminoglycans and small proteoglycans in wounds: modulation by the tripeptide-copper complex glycyl-L-histidyl-L-lysine-Cu(2+). J Invest Dermatol. 2000 Dec;115(6):962-8.

Smith AN, Willis E, Chan VT, Muffley LA, Isik FF, Gibran NS, and Hocking AM. Mesenchymal stem cells induce dermal fibroblast responses to injury. *Exp Cell Res*. 2010 January 1; 316(1): 48–54.

Soler PM, Wright TE, Smith PD, et al. In vivo characterization of keratinocyte growth factor-2 as a potential wound healing agent. *Wound Repair Regen.* 1999;7(3):172-8.

Sorrell, J. & Caplan, A. Fibroblast heterogeneity: more than skin deep. Journal of Cell Science 117, 667-675. 2004.

Sotiropoulou PA, Perez SA, Gritzapis AD, Baxevanis CN, Papamichail M: Interactions between human mesenchymal stem cells and natural killer cells. *Stem Cells* 2006, 24:74-85.

Spaggiari GM, Abdelrazik H, Becchetti F, Moretta L: MSCs inhibit monocyte derived DC maturation and function by selectively interfering with the generation of immature DCs: central role of MSC-derived prostaglandin E2. *Blood* 2009, 113:6576-6583.

Stanley AC, Park HY, Phillips TJ, Russakovsky V, Menzoian JO. Reduced growth of dermal fibroblasts from chronic venous ulcers can be eliminated with growth factors. *J Vasc Surg* 1997; 26:9949.

Stark, H.-J., Szabowski, A., Fusenig, N., & Maas-Szabowski, N. Organotypic cocultures as skin equivalents: a complex and sophisticated *in vitro* system. Biological Procedures Online , 55-60. 2004.

Stepp MA, Liu Y, Pal-Ghosh S, Jurjus RA, Tadvalkar G, Sekaran A, Losicco K, Jiang L, Larsen M, Li L, Yuspa SH. Reduced migration, altered matrix and enhanced TGFbeta1 signaling are signatures of mouse keratinocytes lacking Sdc1. J Cell Sci. 2007 Aug 15;120(Pt 16):2851-63.

Stevens, A. & Lowe, J. 1997, Human Histology, 2nd edn.

Strande LF, Foley ST, Doolin EJ & Hewitt CW. In vitro bioartificial skin culture model of tissue rejection and inflammatory/immune mechanisms. *Transplant Proc.* 1997;29, 2118–2119.

Sugama K, Suzuki K, Yoshitani K, Shiraishi K, Kometani T. Urinary excretion of cytokines versus their plasma levels after endurance exercise. *Exerc Immunol Rev*. 2013;19:29-48.

Sulochana KN, Fan H, Jois S, Subramanian V, Sun F, Kini RM, Ge R: Peptides derived from human decorin leucine-rich repeat 5 inhibit angiogenesis. J Biol Chem 2005; 280: 27935–27948.

Sun L, Akiyama K, Zhang H, Yamaza T, Hou Y, Zhao S, Xu T, Le A, Shi S: Mesenchymal stem cell transplantation reverses multiorgan dysfunction in systemic lupus erythematosus mice and humans. *Stem Cells* 2009, 27:1421-1432.

Sutherland J, Denyer M, Britland S. Motogenic substrata and chemokinetic growth factors for human skin cells. J Anat. 2005 Jul;207(1):67-78.

Tabera S, Perez-Simon JA, Diez-Campelo M, Sanchez-Abarca LI, Blanco B, Lopez A, Benito A, Ocio E, Sanchez-Guijo FM, Canizo C, San Miguel JF: The effect of mesenchymal stem cells on the viability, proliferation and differentiation of B-lymphocytes. *Haematologica* 2008, 93:1301-1309.

Tarte K, Gaillard J, Lataillade JJ, Fouillard L, Becker M, Mossafa H, Tchirkov A, Rouard H, Henry C, Splingard M, Dulong J, Monnier D, Gourmelon P, Gorin NC, Sensebe L: Clinical-grade production of human mesenchymal stromal cells: occurrence of aneuploidy without transformation. *Blood* 2009, Dec 23.

Tandara AA, Mustoe TA. MMP-and TIMP-secretion by human cutaneous keratinocytes and fibroblasts--impact of coculture and hydration. *J Plast Reconstr Aesthet Surg*. 2011 Jan;64(1):108-16.

Tendera M, Wojakowski W, Ruzyłło W, Chojnowska L, Kepka C, Tracz W, Musiałek P, Piwowarska W, Nessler J, Buszman P, Grajek S, Breborowicz P, Majka M, Ratajczak MZ. Intracoronary infusion of bone marrow-derived selected CD34+CXCR4+ cells and non-selected mononuclear cells in patients with acute STEMI and reduced left ventricular ejection fraction: results of randomized, multicentre Myocardial Regeneration by Intracoronary Infusion of Selected Population of Stem Cells in Acute Myocardial Infarction (REGENT) Trial. *Eur Heart J* 2009; 30: 1313-1321

Theerakittayakorn K, Bunprasert T. Differentiation Capacity of Mouse L929 Fibroblastic Cell Line Compare With Human Dermal Fibroblast. *World Academy of Science, Engineering and Technology*, 2011; 50: 373-376.

Tisato V, Naresh K, Girdlestone J, Navarrete C, Dazzi F. Mesenchymal stem cells of cord blood origin are effective at preventing but not treating graft-versus-host disease. Leukemia. 2007; 21(9):1992–9.

Tokcaer-Keskin Z, Akar AR, Ayaloglu-Butun F et al. Timing of induction of cardiomyocyte differentiation for in vitro cultured mesenchymal stem cells: A perspective for emergencies. Can J Physiol Pharmacol 2009;87:143–150.

Tominaga H, Maeda S, Miyoshi H, Miyazono K, Komiya S, Imamura T. Expression of osterix inhibits bone morphogenetic protein-induced chondrogenic differentiation of mesenchymal progenitor cells. J Bone Miner Metab 2009; 27: 36-45

Tomita S, Mickle DA, Weisel RD, Jia ZQ, Tumiati LC, Allidina Y, Liu P, Li RK. Improved heart function with myogenesis and angiogenesis after autologous porcine bone marrow stromal cell transplantation. J Thorac Cardiovasc Surg. 2002;123:1132–1140.

Tondreau T, Meuleman N, Delforge A, Dejeneffe M, Leroy R, Massy M, Mortier C, Bron D, Lagneaux L: Mesenchymal stem cells derived from CD133-positive cells in mobilized peripheral blood and cord blood: proliferation, Oct4 expression, and plasticity. Stem Cells 2005, 23:1105-1112.

Toriseva, M., Ala-aho, R., Karvinen, J., Baker, A., Marjomäki, V., Heino, J., & Kähäri, V. Collagenase-3 (MMP-13) enhances remodelling of three-dimensional collagen and promotes survival of human skin fibroblasts. Journal of Investigative Dermatology 127, 49-59. 17-8-2006.

Torsvik A, Røsland GV, Svendsen A, Molven A, Immervoll H, McCormack E, Lønning PE, Primon M, Sobala E, Tonn JC, Goldbrunner R, Schichor C, Mysliwietz

J, Lah TT, Motaln H, Knappskog S, Bjerkvig R. Spontaneous Malignant Transformation of Human Mesenchymal Stem Cells Reflects Cross-Contamination: Putting the Research Field on Track – Letter. Cancer Res; 70(15) August 1, 2010

Traggiai E, Volpi S, Schena F, Gattorno M, Ferlito F, Moretta L, Martini A: Bone marrow-derived mesenchymal stem cells induce both polyclonal expansion and differentiation of B cells isolated from healthy donors and systemic lupus erythematosus patients. *Stem Cells* 2008, 26:562-569.

Trento C, and Dazzi F. Mesenchymal stem cells and innate tolerance: biology and clinical applications. Swiss Med Wkly. 2010; 140: w13121

Tsai MS, Hwang SM, Chen KD, Lee YS, Hsu LW, Chang YJ, Wang CN, Peng HH, Chang YL, Chao AS, Chang SD, Lee KD, Wang TH, Wang HS, Soong YK. Functional network analysis of the transcriptomes of mesenchymal stem cells derived from amniotic Fluid, amniotic Membrane, cord blood, and bone marrow. Stem Cells 2007; 25: 2511-23.

Tuschil A, Lam C, Haslberger A, Lindley I. Interleukin-8 stimulates calcium transients and promotes epidermal cell proliferation. J Invest Dermatol 1992; 99:294–8.

Venkataramana NK, Kumar SK, Balaraju S, Radhakrishnan RC, Bansal A, Dixit A, Rao DK, Das M, Jan M, Gupta PK, Totey SM. Open-labeled study of unilateral autologous bone-marrow-derived mesenchymal stem cell transplantation in Parkinson's disease. *Transl Res* 155(2):62-70, 2009.

Vestal ML, Campbell JM. Tandem time-of-flight mass spectrometry. *Meth. Enzymol.* 402: 79–108, 2005.

Vojtassák J, Danisovic L, Kubes M, Bakos D, Jarábek L, Ulicná M, Blasko M. Autologous biograft and mesenchymal stem cells in treatment of the diabetic foot. Neuro Endocrinol Lett. 2006 Dec;27 Suppl 2:134-7.

Wakitani S, Imoto K, Yamamoto T, Saito M, Murata N, Yoneda M. Human autologous culture expanded bone marrow mesenchymal cell transplantation for repair of cartilage defects in osteoarthritic knees. *Osteoarthritis Cartilage* 2002; 10

Wakitani S, Mitsuoka T, Nakamura N, Toritsuka Y, Nakamura Y, Horibe S. Autologous bone marrow stromal cell transplantation for repair of full-thickness articular cartilage defects in human patellae: two case reports. *Cell Transplant* 2004; 13: 595-600

Wakitani S, Nawata M, Tensho K, Okabe T, Machida H, Ohgushi H. Repair of articular cartilage defects in the patellofemoral joint with autologous bone marrow mesenchymal cell transplantation: three case reports involving nine defects in five knees. *J Tissue Eng Regen Med* 2007; 1: 74-79

Wall, S., Bevan, D., Thomas, D., Harding, K., Edwards, D., & Patel, G. Differential expression of matrix metalloproteinases during impaired wound healing of the *diabetes* mouse. Journal of Investigative Dermatology 119, 91-98. 18-2-2002.

Walter MNM, Wright KT, Fuller HR, MacNeil S, Johnson WEB. Mesenchymal stem cell-conditioned medium accelerates skin wound healing: an in vitro study of fibroblast and keratinocyte scratch assays. Exp Cell Res. 2010 Apr 15;316(7):1271-81.

Wang Y, Huso DL, Harrington J, et al. Outgrowth of a transformed cell population derived fromnormal human BM mesenchymal stem cell culture. Cytotherapy 2005;7:509–519.

Waugh DJ, Wilson C. The interleukin-8 pathway in cancer. Clin Cancer Res. 2008 Nov 1;14(21):6735-41.

Werner S, Grose R. Regulation of wound healing by growth factors and cytokines. *Physiol Rev.* 2003;83(3):835-70.

Whitby, D. J. & Ferguson, M. W. 1991a Immunohistochemical localization of growth factors in fetal wound healing. Dev. Biol. 147, 207–215.

Whitby, D. J. & Ferguson, M. W. 1991b The extracellular matrix of lip wounds in fetal, neonatal and adult mice. Development 112, 651–668.

Woodbury D, Schwarz EJ, Prockop DJ, Black IB: Adult rat and human bone marrow stromal cells differentiate into neurons. *J Neurosci Res* 2000, 61(4):364-370.

Wright KT, Masri WE, Osman A, Roberts S, Trivedi J, Ashton BA, Johnson WE. The cell culture expansion of bone marrow stromal cells from humans with spinal cord injury: implications for future cell transplantation therapy. Spinal Cord. 2008 Dec;46(12):811-7.

Wu KH, Zhou B, Lu SH, Feng B, Yang SG, Du WT, Gu DS, Han ZC, Liu YL. In vitro and in vivo differentiation of human umbilical cord derived stem cells into endothelial cells. J Cell Biochem 2007;100, 608.

Wu Y, Chen L, Scott PG, Tredget EE. Mesenchymal stem cells enhance wound healing through differentiation and angiogenesis. Stem Cells. 2007; 25:2648-59.

Wu Y, Zhao RCH, Tredget EE. Concise Review: Bone Marrow-Derived Stem/Progenitor Cells in Cutaneous Repair and Regeneration. Stem Cells 2010;28:905–915.

Xia YP, Zhao Y, Marcus J, et al. Effects of keratinocyte growth factor-2 (KGF-2) on wound healing in an ischaemia-impaired rabbit ear model and on scar formation. *J Pathol.* 1999;188(4):431-8.

Yamada KM. Adhesive recognition sequences. J Biol Chem. 1991 Jul 15;266(20):12809-12.

Yamada KM, Clark RAF. Provisional matrix. In: Clark RAF, ed. The molecular and cellular biology of wound repair. 2nd ed. London: Plenum Press, 1996:5194.

Yang JT, Rayburn H, and Hynes RO, "Embryonic mesodermal defects in α5 integrin-deficient mice," *Development*, vol. 119, no. 4, pp. 1093–1105, 1993.

Yeh LC, Tsai AD, Lee JC. Osteogenic protein-1 (OP-1, BMP-7) induces osteoblastic cell differentiation of the pluripotent mesenchymal cell line C2C12. J Cell Biochem 2002;87:292–304.

Yeo TK, Brown L, Dvorak HF. Alterations in proteoglycan synthesis common to healing wounds and tumors. Am J Pathol. 1991 Jun;138(6):1437-50.

Yin J, Jin X, Beck S, Kang DH, Hong Z, Li Z, Jin Y, Zhang Q, Choi YJ, Kim SC, Kim H. In vitro myogenic and adipogenic differentiation model of genetically engineered bovine embryonic fibroblast cell lines. *Biotechnol Lett* 2010; 32: 195-202

Zachos TA, Shields KM, Bertone AL. Gene-mediated osteogenic differentiation of stem cells by bone morphogenetic proteins-2 or -6. J Orthop Res 2006;24:1279–1291.

Zambruno G, Marchisio PC, Marconi A, Vaschieri C, Melchiori A, Giannetti A, De Luca M. Transforming growth factor-beta 1 modulates beta 1 and beta 5 integrin receptors and induces the de novo expression of the alpha v beta 6 heterodimer in normal human keratinocytes: implications for wound healing. J Cell Biol. 1995 May;129(3):853-65.

Zappia E, Casazza S, Pedemonte E, Benvenuto F, Bonanni I, Gerdoni E, et al. Mesenchymal stem cells ameliorate experimental autoimmune encephalomyelitis inducing T-cell anergy. Blood. 2005;106(5):1755–61.

Zarnegar R, Michalopoulos GK. The many faces of hepatocyte growth factor: from hepatopoiesis to hematopoiesis. J Cell Biol. 1995 Jun;129(5):1177-80.

Zhang ZX, Guan LX, Zhang K, Zhang Q, Dai LJ. A combined procedure to deliver autologous mesenchymal stromal cells to patients with traumatic brain injury. Cytotherapy. 2008; 10:134-9.

Zheng Y, Du X, Wang W, Boucher M, Parimoo S, Stenn K. Organogenesis from dissociated cells: generation of mature cycling hair follicles from skin-derived cells. *J. Invest. Dermatol.* 2005;124:867–876.

Zhu W, Kim J, Cheng C, Rawlins BA, Boachie-Adjei O, Crystal RG, et al. Noggin regulation of bone morphogenetic protein (BMP) 2/7 heterodimer activity in vitro. Bone 2006;39:61–71.

Zuk PA, Zhu M, Ashjian P, De Ugarte DA, Huang JI, Mizuno H, Alfonso ZC, Fraser JK, Benhaim P, Hedrick MH: Human adipose tissue is a source of multipotent stem cells. Mol Biol Cell 2002, 13:4279-4295.

Appendixes

List of publications:

M.N.M. Walter, K.T. Wright, H.R. Fuller, S. MacNeil, W.E.B. Johnson. Mesenchymal stem cell-conditioned medium accelerates skin wound healing: An in vitro study of fibroblast and keratinocyte scratch assays. Experimental cell research 316; 1271-1281, 2010.
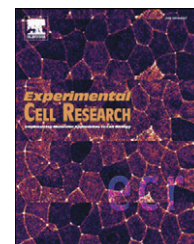
Research Article

Mesenchymal stem cell-conditioned medium accelerates skin wound healing: An *in vitro* study of fibroblast and keratinocyte scratch assays

M.N.M. Walter[a,b], K.T. Wright[a], H.R. Fuller[a], S. MacNeil[c], W.E.B. Johnson[b,*]

[a]Institute for Science and Technology in Medicine, Keele University RJAH Orthopaedic Hospital, Oswestry, SY10 7AG, UK
[b]School of Life and Health Science, Aston University, Aston Triangle, Birmingham, B4 7EJ, UK
[c]Kroto Research Institute and Centre for Nanoscience and Technology, Sheffield University, Sheffield, S1 2UE, UK

ARTICLE INFORMATION

ABSTRACT

We have used *in vitro* scratch assays to examine the relative contribution of dermal fibroblasts and keratinocytes in the wound repair process and to test the influence of mesenchymal stem cell (MSC) secreted factors on both skin cell types. Scratch assays were established using single cell and co-cultures of L929 fibroblasts and HaCaT keratinocytes, with wound closure monitored via time-lapse microscopy. Both in serum supplemented and serum free conditions, wound closure was faster in L929 fibroblast than HaCaT keratinocyte scratch assays, and in co-culture the L929 fibroblasts lead the way in closing the scratches. MSC-CM generated under serum free conditions significantly enhanced the wound closure rate of both skin cell types separately and in co-culture, whereas conditioned medium from L929 or HaCaT cultures had no significant effect. This enhancement of wound closure in the presence of MSC-CM was due to accelerated cell migration rather than increased cell proliferation. A number of wound healing mediators were identified in MSC-CM, including TGF-β1, the chemokines IL-6, IL-8, MCP-1 and RANTES, and collagen type I, fibronectin, SPARC and IGFBP-7. This study suggests that the trophic activity of MSC may play a role in skin wound closure by affecting both dermal fibroblast and keratinocyte migration, along with a contribution to the formation of extracellular matrix.

© 2010 Elsevier Inc. All rights reserved.

Introduction

Skin damage can occur as a result of burns, cuts, abrasions and ulcers to varying degrees of severity. If not repaired, any breach of the skin may compromise its barrier function and expose the body's tissues to microbial infections and mechanical damage. The healing of cutaneous wounds requires complex interactions between the dermal and epidermal cells, the extracellular matrix (ECM), and the nervous and vascular components of the damaged and surrounding skin [1,2]. In the course of wound healing, keratinocytes migrate from the basal population around the wound edge to cover the lesion and restore the barrier function of the skin and, once the wound area is covered, contact inhibition triggers their differentiation to a basal phenotype of stratified squamous keratinizing epidermal cells [2]. Also migrating into the wound site are dermal fibroblasts. The dermal fibroblasts differentiate into myofibroblasts in response to macrophage-derived cytokines such as TGF-β1, which is dependent on their contact with fibronectin [3]. The myofibroblasts also synthesise provisional ECM composed of fibronectin and hyaluronan and

---

* *Corresponding author.* School of Life and Health Science, Aston University, Aston Triangle, Birmingham, B4 7EJ, UK.
  E-mail address: w.e.johnson@aston.ac.uk (W.E.B. Johnson).

provide the motive force required for skin wound contraction [4]. As wound healing progresses, the myofibroblasts begin to die via apoptosis and are replaced by a second wave of dermal fibroblasts from the surrounding tissue, which produce a new collagenous ECM [5].

Mesenchymal stem cells are multipotent cells derived from a variety of tissues [6–8] which have been reported to have therapeutic potential following transplantation in humans with osteogenesis imperfecta [9], bone fracture [10], traumatic brain injury [11], stroke [12], amyotrophic lateral sclerosis [13], graft-versus-host disease [14,15], or myocardial infarction [16,17]. In injuries to skin, pre-clinical animal studies have shown that MSC transplantation enhances wound healing [18], and two reports have suggested that increased wound healing also occurs when MSC are applied to humans with acute wounds (after treatment for skin cancer) [19] or with lower extremity chronic skin wounds [19,20]. The mechanisms responsible for enhanced wound healing in the skin include the possible trans-differentiation of MSC to form cells of epidermal and dermal lineages [18,21], along with restorative paracrine effects of MSC synthesised growth factors [21]. However, despite evidence supporting the capacity of MSC to differentiate or trans-differentiate along a variety of cell lineages [22], the low levels of MSC engraftment after transplantation may indicate that their beneficial effects are more likely mediated via their secretion of soluble factors than via their long-term presence in repaired tissue [23]. For example, Chen et al. demonstrated that growth medium conditioned by murine bone marrow-derived MSC contained high levels of secreted cytokines and was sufficient to stimulate macrophage and endothelial migration and enhance cutaneous wound healing *in vivo* in Balb/C mice [24]. In other studies, Kim et al. have shown that adipose-derived MSC also stimulated human dermal fibroblasts via paracrine effects and significantly reduced the wound size and promoted re-epithelialisation in an *in vivo* model [25].

In this study, we have examined the effects of culture medium conditioned by human bone marrow-derived MSC on an *in vitro* skin wound healing model. We have used the scratch wound assay [26,27], wherein a confluent monolayer of L929 dermal fibroblasts and/or HaCaT keratinocytes was scored with a sterile point and the cells were observed using time-lapse microscopy as they repopulated the scratch area, effectively healing the wound. Through this analysis we have shown that MSC secreted factors in culture that stimulated L929 fibroblast and HaCaT keratinocyte migration to enhance wound closure. We have subsequently identified a number of targets present in MSC-CM that may bring about this effect. In addition, we report that MSC also synthesised several ECM proteins that may contribute directly to tissue formation in the wound healing response.

Materials and methods

Cell culture

The L929 dermal fibroblast cell line [28] and HaCaT keratinocyte cell line [29] were used as cell model systems, where stocks of both cell types were maintained under exponential growth in DMEM/F12 (Invitrogen, Paisley UK) culture medium, supplemented with 10% foetal calf serum (FCS) and antibiotics (penicillin/streptomycin — Invitrogen), at 37 °C and in a humidified atmosphere containing 5%

CO_2. Human MSC were derived from iliac crest biopsies and expanded in monolayer culture through passage II. The MSC characterisation that we have performed of these stromal cell populations at passage II–III has been described previously. In brief, these cells have been shown to be CD34 immunonegative, CD45 immunonegative and CD105 immunopositive by flow cytometry, and were capable of chondrogenic, osteoblastic and adipogenic differentiation using established protocols [30]. Conditioned medium was generated from MSC cultures in serum free DMEM/F12 medium supplemented with insulin, transferring, selenium (ITS-X, Invitrogen) and antibiotics when cultures were approximately 70% confluent, then removed after 72 h and all cellular debris were removed by filtration (0.2 μ filter). The number of MSC present in these MSC cultures was 698,500 (± 19,020) (mean ± SEM) per flask. Serum free conditioned medium (DMEM/F12/ with ITS-X) was similarly generated after 72 h from L929 and HaCaT cultures when approximately 70% confluent, which in both cases equated to greater than 1 million cells per flask.

Scratch wound assays

24 well tissue culture plates were collagen-coated by incubation in 0.2 mg/ml of collagen type I solution (Sigma, Dorset UK) for 2 h at 37 °C before rinsing with phosphate buffered saline (PBS, Invitrogen). In co-culture experiments, different cell types were distinguished by fluorescent tagging, using green and red linker kits (PKH26 or PKH67, Sigma). Each well was seeded with cells (keratinocytes, fibroblasts or both) to a final density of 100,000 cells per well (with co-cultures containing equal numbers of each cell type) and these were maintained at 37 °C and 5% CO_2 for 24 h to permit cell adhesion and the formation of a confluent monolayer. These confluent monolayers were then scored with a sterile pipette tip to leave a scratch of approximately 0.4–0.5 mm in width. Culture medium was then immediately removed (along with any dislodged cells). The removed medium was replaced with (i) a fresh serum supplemented culture medium (10% FCS), or (ii) with a fresh serum free culture medium, or (iii) with the conditioned medium which had been generated from MSC cultures under serum free conditions (MSC-CM) or L929-CM or HaCaT-CM, as described above. All scratch assays were performed in quadruplicate.

Microscopy, image capture and analysis

Wound closure was monitored by collecting digitised images at various time intervals after the scratch was performed until closure was either complete or no longer progressing. Digitised images were captured with an inverted microscope (Nikon Eclipse TS100, Nikon, Kingston-upon-Thames, UK) and digital camera (C4742-95, Hamamatsu photonics, Welwyn Garden City, Hertfordshire, UK) under phase or fluorescence. The digitised images were then analysed using Image-J software [31] to measure the width of the scratch at previously defined points along its length, i.e. at 0.01, 0.15, and 0.3 mm along the vertical axis of the image (which equated to the top, middle and bottom of the field of view). Digitised images were also obtained using the Cell IQ automated image capture system, (Chip-Man Technologies, Tampere, Finland) in which pre-selected fields were imaged using phase and red and green fluorescence microscopy on a continuous loop until wound closure was complete. Data has been presented as the

extent of wound closure, i.e. the percentage by which the original scratch width has decreased for each given time point. During these scratch assays L929 and HaCaT cell numbers were monitored using the Cell IQ automated cell counting and tracking protocol (Chip-Man Technologies).

Cell proliferation

The influence of MSC-CM on L929 and HaCaT cell proliferation was tested using the MTS (3-(4, 5-dimethylthiazol-2-yl)-5-(3-carboxymethoxyphenyl)-2-(4-sulfophenyl)-2H-tetrazolium) assay [32].
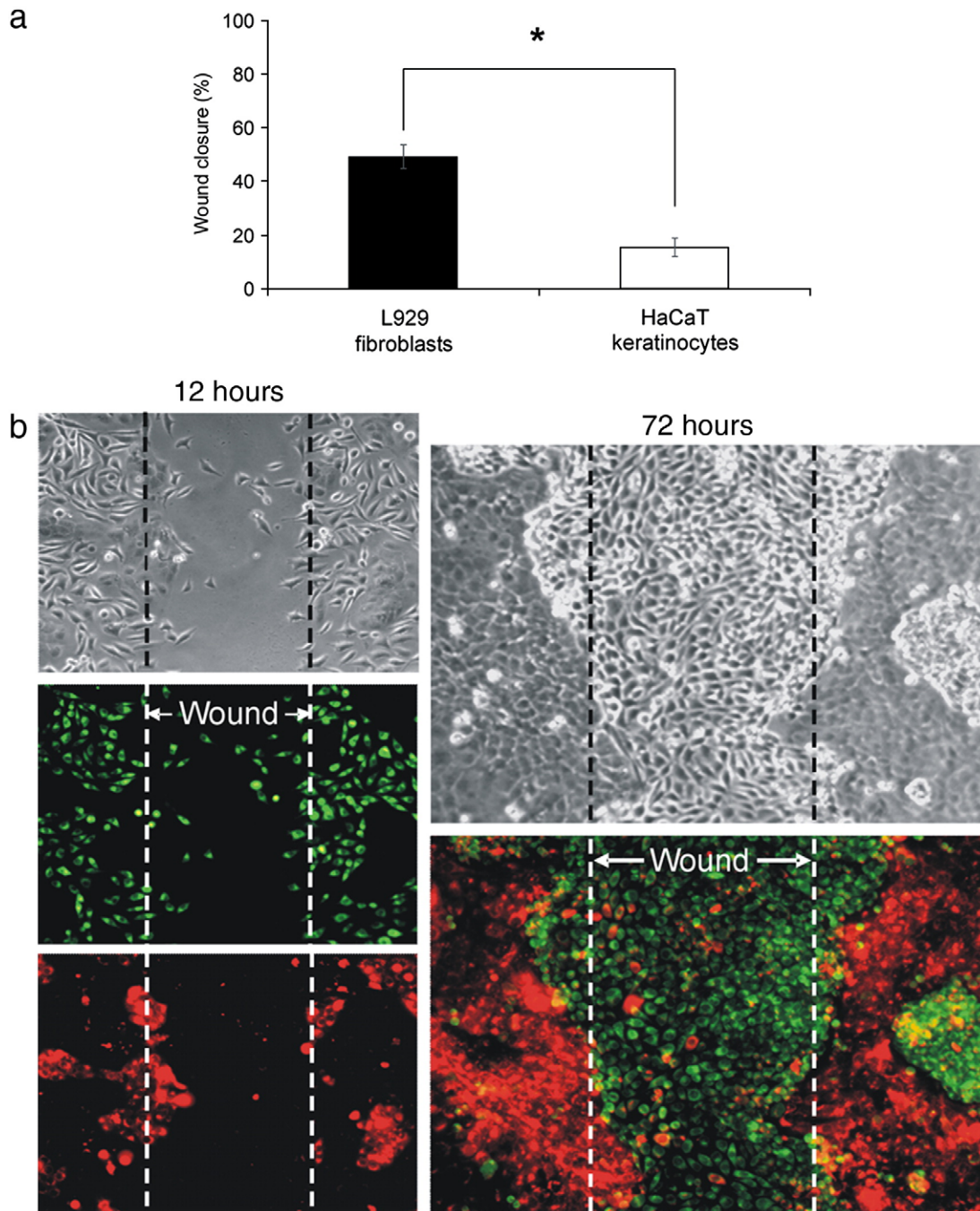
Fig. 1 – L929 dermal fibroblasts closed scratch assay wounds more rapidly than HaCaT keratinocytes. a) The extent of wound closure in scratch assays of L929 fibroblasts or HaCaT keratinocytes at 12 h in cultures with 10% FCS. Data shown are the means ($\pm$ SEM), *$p < 0.05$. b) In serum supplemented co-cultures, the L929 fibroblasts migrated into the "wound area" more rapidly than HaCaT keratinocytes when in co-cultures. Representative images are shown of the progression of wound closure at 12 h and 72 h, at which time the L929 fibroblasts (fluorescently-labelled green) can be seen to fill the wound area almost to the exclusion of the HaCaT keratinocytes (fluorescently-labelled red). Original magnification $\times$100.
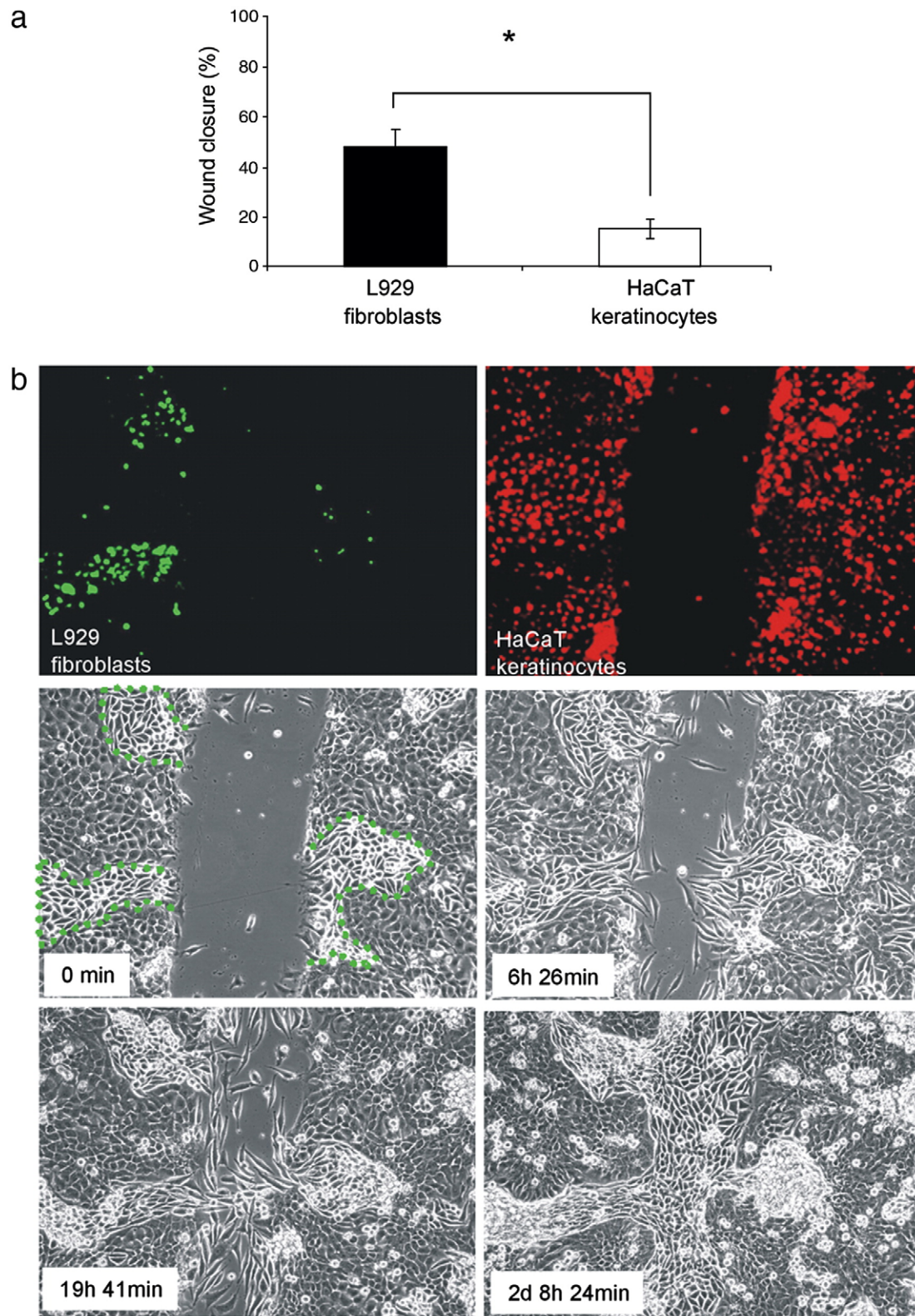
Fig. 2 – L929 dermal fibroblasts closed scratch assay wounds more rapidly than HaCaT keratinocytes in the absence of serum. a) The extent of wound closure in scratch assays of L929 fibroblasts or HaCaT keratinocytes at 12 h in cultures without serum supplementation. Data shown are means ± SEM, *$p < 0.05$. b) In serum free co-cultures, similar to the serum supplemented cultures, the L929 fibroblasts (fluorescently-labelled green) migrated into the "wound area" prior to the HaCaT keratinocytes (fluorescently-labelled red), such that at complete closure the fibroblasts appeared to fill the wound. Representative images are shown of the progression of wound closure throughout the time course of wound closure. Original magnification ×100.
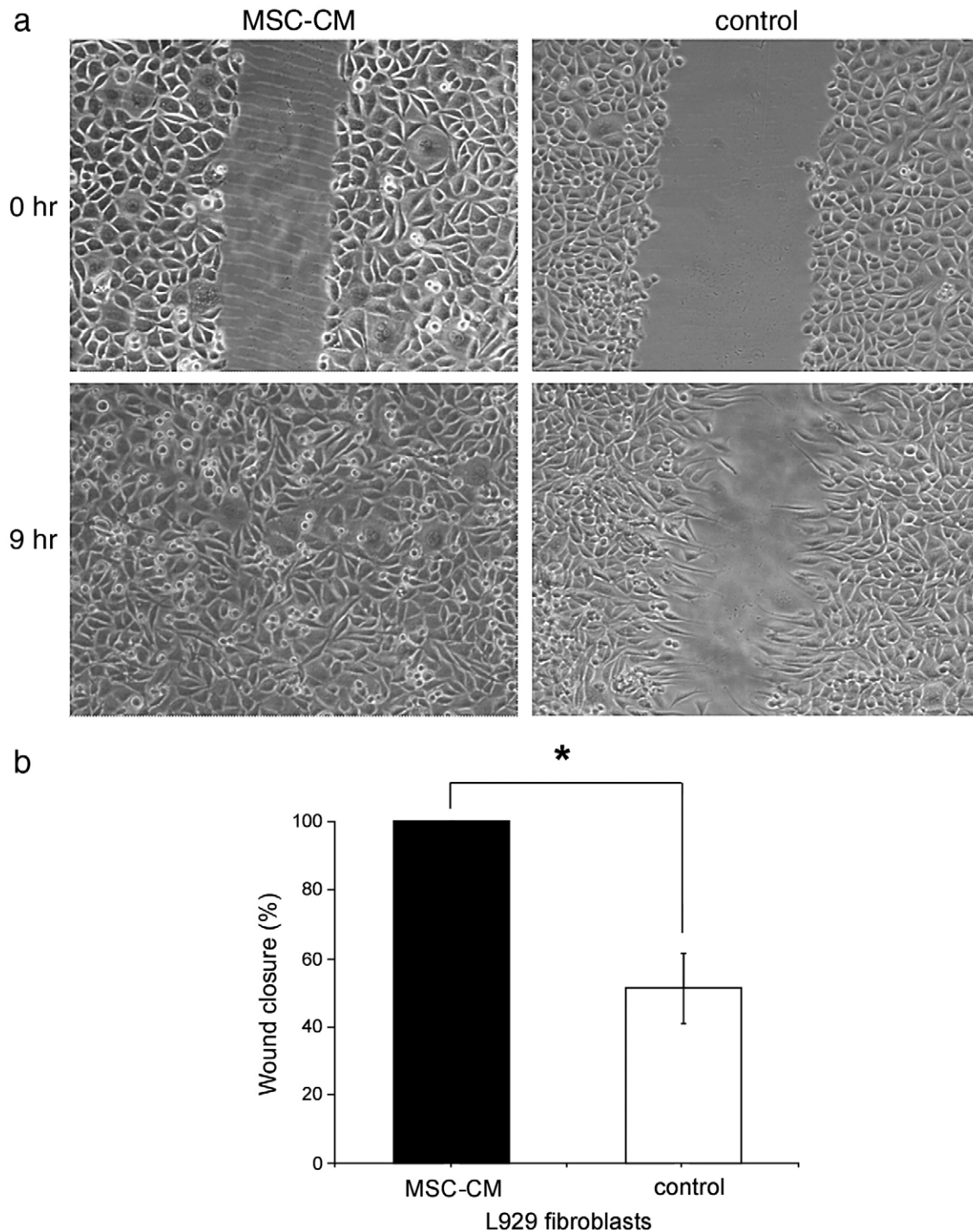
Fig. 3 – MSC-CM enhanced the rate of wound closure by L929 fibroblasts. a) Representative time-lapse images of L929 scratch assays immediately after the scratches had been made and then after 9 h in the presence of serum free MSC-CM versus control medium. In the presence of MSC-CM, wound closure was complete at this time. Original magnification ×100. b) There was a significant increase in the extent of wound closure in L929 scratch assays in MSC-CM compared with the control medium at 9 h. Data shown are means ± SEM, *$p < 0.05$.

Cells were seeded into 96 well plates in the DMEM/F12 culture medium containing 10% FCS at a seeding density of 10,000 cells per well, incubated for 2 h at 37 °C (to permit cell adhesion) and then washed repeatedly in serum free medium. Cells were then maintained in either serum free medium or in each of the three separate samples of MSC-CM (i.e. from 3 different donor MSC cultures). The relative number of viable cells present at the 24, 48 and 72 hour time-points following this treatment was subsequently determined by adding the MTS solution for 3 h, the absorbance was read at 490 nm. Each assay was performed with 5 replicate wells for each condition.
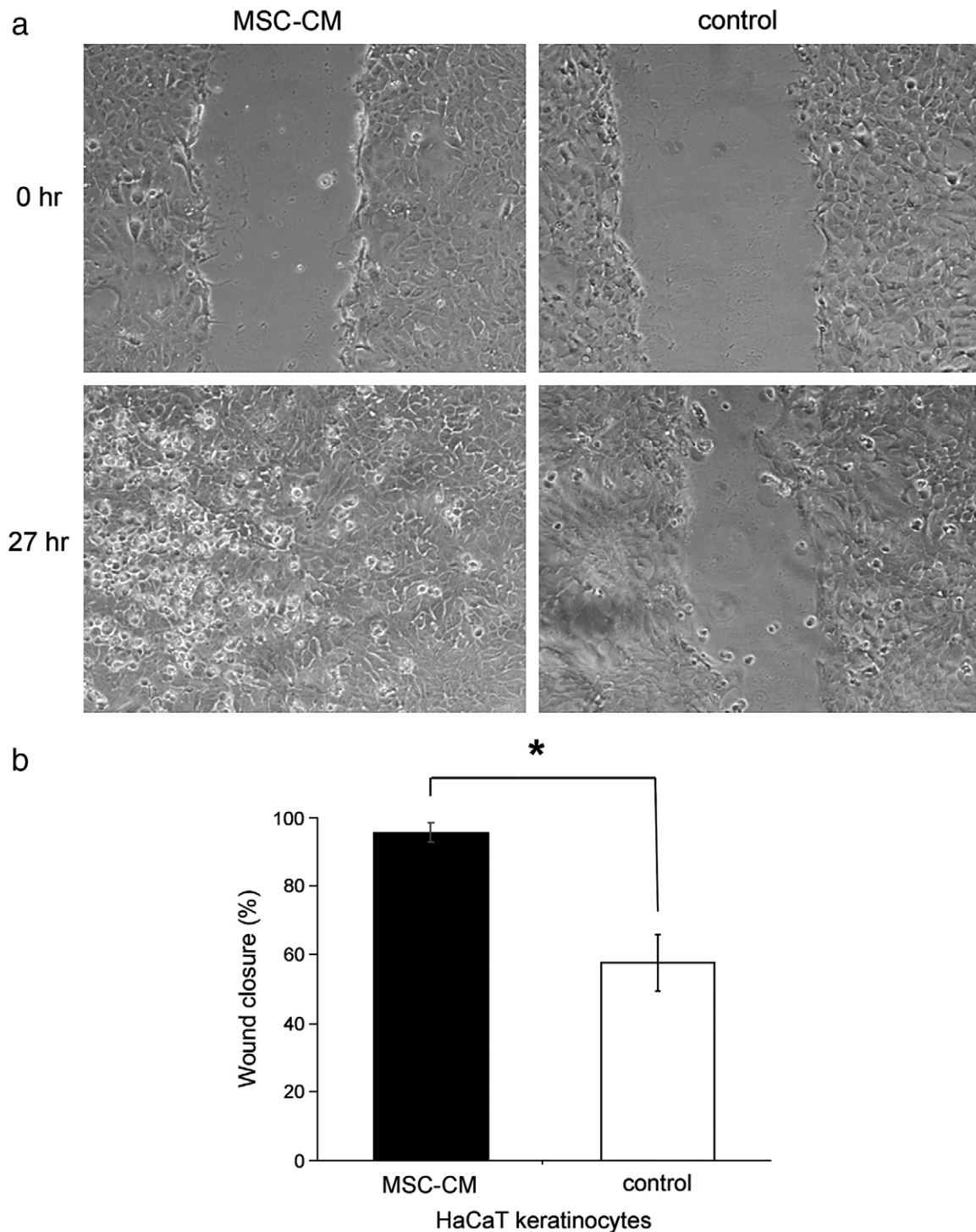
Fig. 4 – MSC-CM enhanced the rate of wound closure by HaCaT keratinocytes. a) Representative time-lapse images of HaCaT scratch assays immediately after the scratches had been made and then after 27 h in the presence of serum free MSC-CM versus control medium. In the presence of MSC-CM, wound closure was nearly complete at this time. Original magnification ×100. b) There was a significant increase in the extent of wound closure in HaCaT scratch assays in MSC-CM compared with the control medium at 27 h. Data shown are means ± SEM, *$p < 0.05$.

Analysis of MSC-CM content

Cytokines and matrix molecules in MSC-CM were analysed by commercial ELISA multi arrays (SA Biosciences, Frederick, MD, USA) according to the manufacturer's guidelines, and MALDI-TOF/ TOF mass spectrometry. For MALDI-TOF/TOF mass spectrometry, 2 ml of medium was incubated with 40 μl of Strataclean resin for 30 min at room temperature. Unbound supernatant was removed
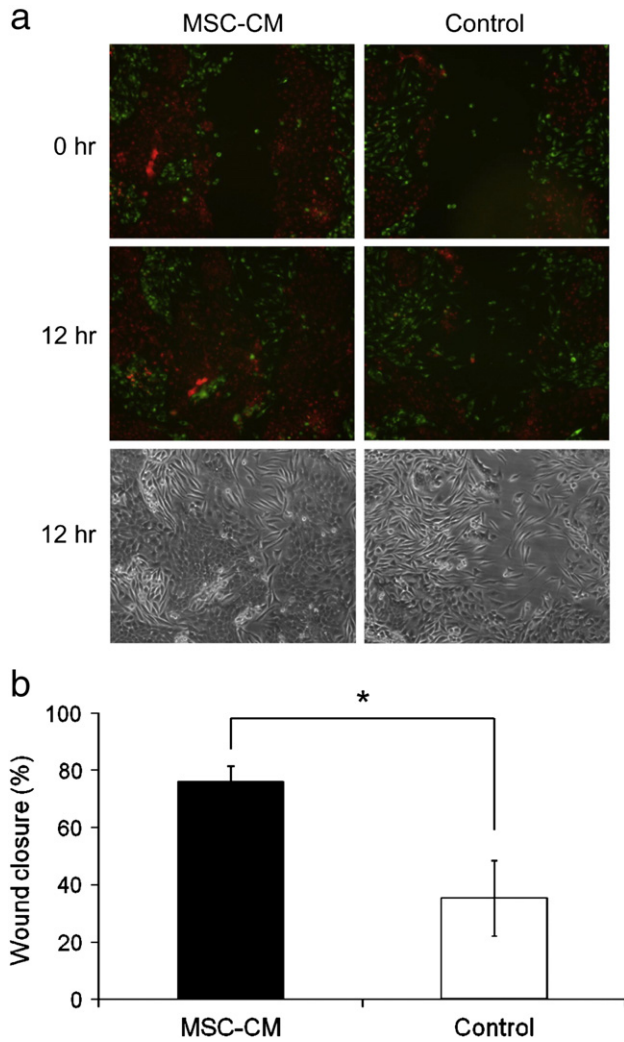
Fig. 5 – MSC-CM enhanced the rate of wound closure in L929 fibroblast and HaCaT keratinocyte co-cultures.
a) Representative images of scratch assays of L929 fibroblast (fluorescently-labelled green) and HaCaT keratinocyte (fluorescently-labelled red) co-cultures immediately after the scratches had been made (fluorescence images) and then after 12 h (fluorescence and phase images) in the presence of serum free MSC-CM versus control medium. Original magnification ×100. b) There was a significant increase in the extent of wound closure in L929 and HaCaT co-culture scratch assays in MSC-CM compared with the control medium at 12 h. Data shown are means ± SEM, $^*p < 0.05$.

over 40 min. The column was then washed in 100% B for a further 10 min. During the elution gradient, the sample was spotted at 10 second intervals using a Probot (Dionex) with α-cyano-4-hydroxycinnamic acid (CHCA) at 3 mg/ml (70% MeCN, 0.1% TFA) at a flow rate of 1.2 μl/min. Both MS and MS/MS analyses were performed on the fractionated peptides using an Applied Biosystems 4800 MALDI-TOF/TOF mass spectrometer (Applied Biosystems Inc., Foster City, CA, USA). The mass spectrometer was operated under control of 4000 Series Explorer v3.5.2 software (Applied Biosystems). Peak lists of MS and MS/MS spectra were generated using the 4000 Series Explorer v3.5.2 software after selective labelling of monoisotopic mass peaks. An automated
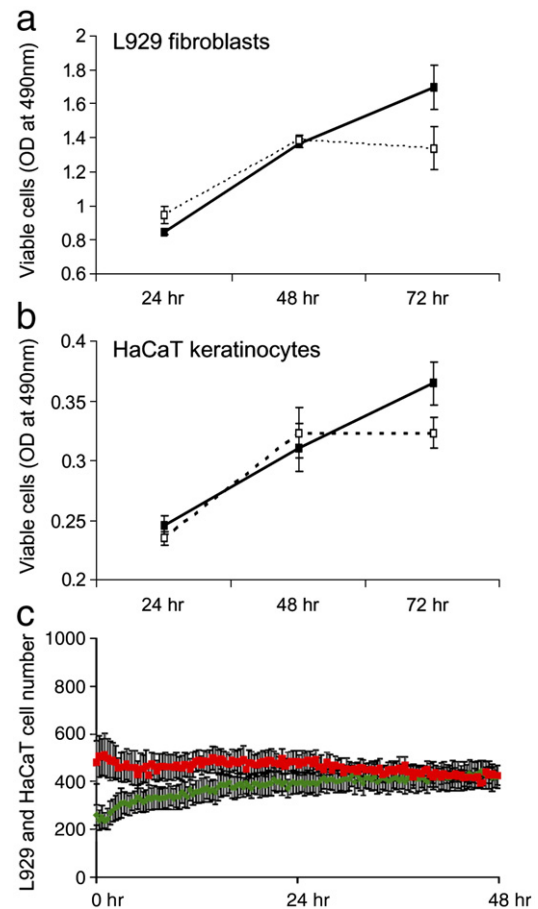
Fig. 6 – The influence of MSC-CM on L929 fibroblast and HaCaT keratinocyte cell proliferation/survival. Data shown indicates the viable cell number in L929 fibroblast (a) and HaCaT keratinocyte (b) cultures maintained in serum free MSC-CM (solid line) versus control medium (dotted line) over a 3 day time course. As shown, there was a non-significant increase in viable L929 and HaCaT cell number in MSC-CM after 72 h, which was beyond the time course for wound closure by each cell type in the presence of MSC-CM. (c) The number of L929 fibroblasts (green) and HaCaT keratinocytes (red) present in the field of view in L929: HaCaT co-culture scratch assays in MSC-CM. There was a slight, but non-significant increase in L929 cell numbers and no increase in HaCaT cell numbers over the course of wound closure. Data shown are means ± SEM.

and 1 μg of trypsin (porcine sequencing grade — Promega, Southampton, UK) was added to the resin/bound proteins and incubated overnight at 37 °C. The sample was centrifuged at 13,000 rpm for 5 min to recover the tryptic peptides. The tryptic peptides (20 μl) were first separated by liquid chromatography (Dionex Ultimate 3000, Dionex, Leeds, UK) on a Pepmap C18 column, 200 μm × 15 cm (Dionex) at a flow rate of 3 μl/min. The eluants used were: A. 0.05% TFA in water and B. 0.05% TFA in 100% acetonitrile. The gradient was run as follows: 5 min of isocratic pre-run at 100% A, followed by a linear gradient from 2 to 50% B

Fig. 7 – Growth factors and chemokines detected in MSC-CM by ELISA multi-array. Detectable levels of TGF-β1, IL-6, IL-8, MCP-1 and RANTES were seen in serum free MSC-CM. Relative cytokine levels have been expressed as arbitrary absorbance units normalised for MSC cell number. Data shown are means ± SEM.

database search was run using GPS Explorer v3.6 (Applied Biosystems). MASCOT was used as the search engine to search NCBInr database using the following search parameters: precursor ion mass tolerance of 50 ppm, fragment ion mass tolerance of 0.3 Da, the taxonomy was selected as human and oxidation of methionine residues was allowed as variable modifications. The identification criterion was at least 2 peptides by MS/MS with total ion score confidence intervals of at least 95%.

Statistical analysis

Data presented in this study are means ± standard error of the mean. These data were tested for normal distribution by Kolmogorov–Smirnov test using Analyse-it software. As all data were shown to be not normally distributed the non-parametric Mann–Whitney U test was used to determine significant differences between samples.

Results

In the presence of serum, L929 fibroblasts effected wound closure more rapidly than HaCaT keratinocytes in single cell type scratch assays. At 12 h when the extent of wound closure was 49% (±5%) for L929 scratch assays, the extent of closure for HaCaT scratch assays was only 15% (±3%) (Fig. 1a). Furthermore, complete wound closure of all scratches was seen in L929 cultures by 72 h, compared with only half of the scratches for HaCaT. In co-cultures, the L929 fibroblasts migrated faster than the HaCaT keratinocytes

to fill the scratch area. Hence, at 12 h the L929 cells were seen to have migrated further into the scratched areas than HaCaT cells, and by wound closure (72 h) the scratched areas were filled almost exclusively with L929 cells (Fig. 1b). L929 fibroblasts also closed scratch wounds significantly more rapidly than HaCaT keratinocytes under serum free conditions. Hence, at 12 h the extent of wound closure of serum free L929 scratch assays was 47% (±7%) compared with 16% (±4%) for wound closure of HaCaT scratch assays (Fig. 2a). In addition, in serum free L929: HaCaT co-culture scratch assays, the L929 cells were the first to migrate into the scratch and filled the area at wound closure (Fig. 2b).

When L929 fibroblast (Fig. 3) and HaCaT keratinocyte (Fig. 4) scratch assays were performed in MSC-CM which had been generated under serum free conditions, there was a significantly enhanced rate of wound closure for both cell types. Hence, when wound closure of L929 scratch assays was 51% (±10%) in serum free control medium (at the 9 hour time point in this set of experiments), it was 100% (±0%) in the presence of serum free MSC-CM. Similarly, when wound closure of HaCaT scratch assays was 57% (±8%) in serum free control medium (at the 27 hour time point in this set of experiments), it was 95% (±3%) in serum free MSC-CM. In contrast, neither L929-CM nor HaCaT-CM positively affected the rate of wound closure in scratch assays of either cell type at any time during the wound healing process. For example, when wound closure of L929 scratch assays was 48% (±7%) in serum free control medium (at 12 h in this set of experiments), it was only 43% (±8%) in L929-CM and only 42% (±17%) in HaCaT-CM. Similarly, when wound closure of HaCaT scratch assays was 15% (±4%) in serum free control medium (also at 12 h), it was only 14% (±8%) in L929-CM and 20% (±5%) in HaCaT-CM.

Scratch assay of L929 and HaCaT co-cultures closed significantly faster in the presence of serum free MSC-CM than in serum free control media (Fig. 5). Hence, after 12 h wound closure in L929:HaCaT co-culture scratch assays was 76% (±6%) in the presence of MSC-CM compared with 35% (±13%) in serum free control medium.

To address whether MSC-CM may have stimulated skin cell proliferation or survival in addition to cell migration during wound closure, L929 fibroblast and HaCaT keratinocyte cultures were established in 96 well plates in MSC-CM versus serum free control medium. The MTS assay was then performed to ascertain viable cell number. There was a non-significant, but marked increase in the number of L929 and HaCaT cells present at 72 h in MSC-CM versus control (Figs. 6a–b). However, no marked increases in viable cell number were seen for either cell type in the first 48 h, i.e. within the time frame of L929 and HaCaT wound closure in serum free MSC-CM. Cell proliferation was also monitored in L929:

Table 1 – Proteins detected in MSC conditioned medium via mass spectrometry (MALDI-TOF/TOF).			
Protein name	Accession number	Peptide count	Total ion score C.I.%
Collagen type I (alpha 1 chain)	gi22328092	16	100
Collagen type I (alpha 2 chain)	gi48762934	27	100
Collagen type V (alpha 2 chain)	gi16197600	3	100
Collagen type VI (alpha 1 chain	gi87196339	10	100
Collagen type XII (alpha 1 long isoform)	gi93141047	6	99.999
Fibronectin	gi4204943	8	99.999
Fibronectin (type III domain)	gi55667857	2	96.825
SPARC	gi2624793	3	96.613
Insulin-like growth factor binding protein 7	gi4504619	4	100

HaCaT co-cultures in situ using the Cell IQ image analysis system. This demonstrated firstly that in the presence of MSC-CM there was no overgrowth of L929 cells at the time point that the scratches were established, and secondly, that the increased rate of wound closure seen in MSC-CM compared to serum free control medium was not due to any marked increase in the rates of either L929 or HaCaT cell proliferation in situ (Fig. 6c).

MSC-CM was assayed to determine the presence of secreted cytokines or ECM components that may have influenced L929 fibroblast or HaCaT keratinocyte cell growth or migration. Detectable levels of interleukin (IL)-6, IL-8, transforming growth factor-β1 (TGF-β1), monocyte chemotactic protein-1 (MCP-1) and Rantes were found in the MSC-CM by ELISA (Fig. 7). In contrast, IL-1a, IL-1b, IL-4, IL-10, interferon-γ (IFN-γ), tumour necrosis factor-α (TNF-α), and growth regulated oncogene-α (Gro-A) were not detected. In addition, the ECM components collagen types I, V, VI and XII, and fibronectin were detected in MSC-CM by MALDI-TOF/TOF mass spectrometry, along with secreted protein acidic and rich in cysteine (SPARC) and insulin-like growth factor binding protein-7 (IGFBP-7) (Table 1).

Discussion

Cell migration is a rate limiting event in skin wound healing. Hence, the study of factors that influence dermal fibroblast and epidermal keratinocyte migration may help target therapies for improved cutaneous wound healing. In this set of investigations we have used the scratch assay to show that L929 fibroblasts migrated to effect wound closure more rapidly than HaCaT keratinocytes. In co-culture, the L929 fibroblasts were seen to fill the closed scratch almost entirely to the exclusion of the HaCaT keratinocytes, both in the presence or absence of serum supplementation. The chronology of cell migration into human cutaneous wounds is currently unclear. However, a recent study has suggested that dermal fibroblasts along with dermal microvascular endothelial cells may migrate into the wounded area prior to keratinocytes [33]. It was further suggested that dermal fibroblast migration is then halted as keratinocytes migrate to initiate re-epithelialisation, after which a further wave of fibroblast migration occurs during the tissue remodelling stage of wound healing. If this order of skin cell migration is correct, then the novel co-culture scratch assay we have reported here using L929 and HaCaT cell lines may prove useful for future studies of factors that influence cutaneous wound healing. The interaction of dermal fibroblasts and epidermal keratinocytes plays an important role in the healing process. Hence, the incorporation of both cell types in this co-culture model may be more representative of in vivo skin wound healing than the use of either cell type alone. A mix of L929 fibroblasts and HaCaT keratinocytes was evidently present in the scratch assays reported here. Whilst this differs significantly from the ordered separation into dermal and epidermal layers in undamaged skin, the usual compartmentalisation of these cell types is likely to be somewhat disrupted in cutaneous wounds.

The differences in healing rates we have seen in scratch assays of L929 or HaCaT cells as single cell types may simply be due to the fact that the L929 fibroblasts were murine in origin, whilst the HaCaT keratinocytes were human. Furthermore, L929 is derived from a tumour [28] whilst HaCaT is an immortalised cell line [29]. As such, these cells may differ in their behaviour from normal

human cells in vivo. However, both cell types have been utilised in previous studies as in vitro models of skin cell behaviour [34]. Their particular use in this study eliminates potential donor variations in primary skin cell cultures, which has thereby allowed for the development of a consistent model to assay the effects of MSC derived factors. Further study of primary human dermal fibroblasts and human epidermal keratinocytes, either singly or in co-culture, may help to validate the model.

A recent study by Smith et al. [35] demonstrated that co-culture of murine MSC with human dermal fibroblasts, where each cell type was separated in a modified Boyden chamber in the presence of bovine and equine serum, enhanced dermal fibroblast migration and proliferation. The response of the dermal fibroblasts included altered expression of genes involved in cell-matrix interactions. However, the MSC secreted factors which may have brought about these effects were not examined. We have similarly shown that conditioned medium obtained from serum free MSC cultures (MSC-CM) significantly promoted L929 fibroblast and HaCaT keratinocyte scratch wound closure compared with non-conditioned control medium. This stimulatory activity supports the application of MSC as a therapeutic agent in cutaneous wound healing. In addition, as we established serum free conditions in which to perform these experiments, we were able to identify a number of MSC secreted factors in MSC-CM that are known to promote cutaneous wound healing. TGF-β1 has diverse roles in cutaneous wound healing, including a stimulatory activity on re-epithelialisation, wound contracture, angiogenesis, scar formation and ECM deposition [36]. In particular, TGF-β1 stimulates increased cell migration in dermal fibroblasts [37] and keratinocytes [38]. Studies of knock-out mice have suggested that IL-6 forms an essential element of the normal cutaneous wound healing process by influencing dermal fibroblast migration [39], and has also been shown to stimulate keratinocyte migration [40] and proliferation [41], whilst IL-8 similarly promotes skin re-epithelialisation by increasing keratinocyte migration [42] and proliferation [43]. MCP-1 and RANTES may also function to promote dermal wound healing as a chemoattractant to cells of the immune system, particularly macrophages [44].

The increase in L929 and HaCaT cell number over the course of wound closure in co-culture scratch assays was non-significant for either cell type, both in control medium or in MSC-CM. This suggests that increased migration of these cells, as opposed to increased proliferation, was the main factor in the enhanced rate of wound closure in MSC-CM. In addition, MSC-CM was found to have little effect on L929 or HaCaT cell proliferation or survival, as assessed via the MTS assay. The moderate difference seen in the viable cell number present in MSC-CM compared with control medium at 72 h was at a time point outside of the time course of scratch wound closure in the presence of MSC-CM. Furthermore, there were no obvious differences in the adherence of L929 or HaCaT cells in MSC-CM or control medium in the scratch assays themselves. Therefore, the activity of MSC-CM on scratch wound closure may more readily be attributed to stimulation of increased fibroblast and keratinocyte cell migration, rather than on cell proliferation or survival. As described above, several of the MSC secreted growth factors and chemokines are likely targets for this stimulatory activity of cell migration in L929 and HaCaT scratch assays, although further experiments, e.g. with the use of neutralising antibodies are required to identify their precise activity.

The composition of the extracellular matrix (ECM) plays a major role in regulating cell migration [45] and a number of ECM components in MSC-CM were identified by mass spectrometry. Prominent amongst these are collagen type I and fibronectin, which are well-characterised stimulatory factors of fibroblast and keratinocyte cell adhesion and migration. However, as the tissue culture plates were already pre-coated in collagen type I, any additive effect from these ECM components in MSC-CM may have been small or negligible. Also detected was the extracellular glycoprotein SPARC (osteonectin/BM-40). Elevated levels of SPARC expression have been observed in cells at wound sites [46] and it has been demonstrated that the absence of SPARC is associated with impaired fibroblast migration [47]. Conversely, the absence of SPARC has also been shown to accelerate wound closure in SPARC-null mice [48], but this study suggested that this effect may have been due to an associated reduction in collagen content in the skin, which in turn leads to increased wound contractibility. Insulin-like growth factor binding proteins (IGFBP) play an important role in skin homeostasis, modulating IGF-mediated enhancement of dermal and epidermal cell migration, survival and proliferation [49]. In particular, IGFBP-7 has been shown to regulate the proliferation and survival of both HaCaT and primary human keratinocytes *in vitro* [50]. This suggests that IGFBP-7 in MSC-CM may have contributed to the increased wound closure seen in HaCaT keratinocyte scratch assays. However, further experiments that specifically target IGFBP-7 in MSC-CM are required to confirm such activity.

In summary, we have adapted an established *in vitro* model of skin wound healing; this was with a view to investigating the potential use of MSC for cell therapies of cutaneous wounds. The study has demonstrated that L929 fibroblasts and HaCaT keratinocytes bring about wound closure in scratch assays under serum and serum free conditions, where the L929 fibroblasts pioneered the wound healing process. We then used serum free scratch assays in order to dissect the response of the L929 fibroblasts and HaCaT keratinocytes to MSC secreted factors, and hence we have shown that MSC-CM stimulated wound closure for both cell types. Furthermore, we have identified a number of MSC secreted targets for this activity which can be tested using the model system. These studies provide a novel model system for the *in vitro* study of cell synthesised soluble factors that may influence skin wound healing and provide insight into the potential mechanisms whereby MSC transplantation is therapeutic.

Acknowledgment

REFERENCES

[1] K. Harding, H. Morris, G. Patel, Science, medicine, and the future: healing chronic wounds, BMJ 324 (2002) 160–163.

[2] A. Metcalfe, M. Ferguson, Tissue engineering of replacement skin: the crossroads of biomaterials, wound healing, embryonic development, stem cells and regeneration, J.R. Soc. Interface 4 (2007) 413–437.

[3] G. Serini, M. Bochotton-Pilliat, R. Ropraz, A. Geinoz, L. Borsi, L. Zardi, G. Gabiani, The fibronectin domain ED-A is crucial for myofibroblastic phenotype induction bt TGF-β1, J. Cell Biol. 3 (1998) 873–881.

[4] L. Germain, A. Jean, F.A. Auger, D. Garrel, Human wound healing fibroblasts have greater contractile properties than dermal fibroblasts, J. Surg. Res. 57 (1994) 268–273.

[5] J. Sorrell, A. Caplan, Fibroblast heterogeneity: more than skin deep, J. Cell Sci. 117 (2004) 667–675.

[6] S. Kern, H. Eichler, J. Stoeve, H. Kluter, K. Bieback, Comparative analysis of mesenchymal stem cells from bone marrow, umbilical cord blood, or adipose tissue, Stem Cells 24 (2006) 1294–1301.

[7] Z. Miao, J. Jin, L. Chen, J. Zhu, W. Huang, J. Zhao, H. Qian, X. Zhang, Isolation of mesenchymal stem cells from human placenta: comparison with human bone marrow mesenchymal stem cells, Cell Biol. Int. 30 (2006) 681–687.

[8] M.S. Tsai, S.M. Hwang, K.D. Chen, Y.S. Lee, L.W. Hsu, Y.J. Chang, C.N. Wang, H.H. Peng, Y.L. Chang, A.S. Chao, S.D. Chang, K.D. Lee, T.H. Wang, H.S. Wang, Y.K. Soong, Functional network analysis of the transcriptomes of mesenchymal stem cells derived from amniotic Fluid, amniotic Membrane, cord blood, and bone marrow, Stem Cells 25 (2007) 2511–2523.

[9] E.M. Horwitz, P.L. Gordon, W.K.K. Koo, J.C. Marx, M.D. Neel, R.Y. McNall, L. Muul, T. Hofmann, Isolated allogeneic bone marrow-derived mesenchymal cells engraft and stimulate growth in children with osteogenesis imperfecta: implications for cell therapy of bone, Proc. Natl. Acad. Sci. U. S. A. 99 (2002) 8932–8937.

[10] S. Bajada, P.E. Harrison, B.A. Ashton, V.N. Cassar-Pullicino, N. Ashammakhi, J.B. Richardson, Successful treatment of refractory tibial nonunion using calcium sulphate and bone marrow stromal cell implantation, J. Bone Joint Surg. Br. 89 (2007) 1382–1386.

[11] Z.X. Zhang, L.X. Guan, K. Zhang, Q. Zhang, L.J. Dai, A combined procedure to deliver autologous mesenchymal stromal cells to patients with traumatic brain injury, Cytotherapy 10 (2008) 134–139.

[12] O.Y. Bang, J.S. Lee, P.H. Lee, G. Lee, Autologous mesenchymal stem cell transplantation in stroke patients, Ann. Neurol. 57 (2005) 874–882.

[13] I. Ferrero, L. Mazzini, D. Rustichelli, M. Gunetti, K. Mareschi, L. Testa, N. Nasuelli, G.D. Oggioni, F. Fagioli, Bone marrow mesenchymal stem cells from healthy donors and sporadic amyotrophic lateral sclerosis patients, Cell Transplant. 17 (2008) 255–266.

[14] O. Ringdén, M. Uzunel, I. Rasmusson, M. Remberger, B. Sundberg, H. Lönnies, H.U. Marschall, A. Dlugosz, A. Szakos, Z. Hassan, B. Omazic, J. Aschan, L. Barkholt, K. Le Blanc, Mesenchymal stem cells for treatment of therapy-resistant graft-versus-host disease, Transplantation 81 (2006) 1390–1397.

[15] I. Müller, S. Lymperi, F. Dazzi, Mesenchymal stem cell therapy for degenerative inflammatory disorders, Curr. Opin. Organ Transplant. 13 (2008) 639–644.

[16] S.L. Chen, W.W. Fang, F. Ye, Y.H. Liu, J. Qian, S.J. Shan, J.J. Zhang, R.Z. Chunhua, L.M. Liao, S. Lin, J.P. Sun, Effect on left ventricular function of intracoronary transplantation of autologous bone marrow mesenchymal stem cell in patients with acute myocardial infarction, Am. J. Cardiol. 94 (2004) 92–95.

[17] D.G. Katritsis, P.A. Sotiropoulou, E. Karvouni, I. Karabinos, S. Korovesis, S.A. Perez, E.M. Voridis, M. Papamichail, Transcoronary transplantation of autologous mesenchymal stem cells and endothelial progenitors into infarcted human myocardium, Catheter. Cardiovasc. Interv. 65 (2005) 321–329.

[18] M. Sasaki, R. Abe, Y. Fujita, S. Ando, D. Inokuma, H. Shimizu, Mesenchymal stem cells are recruited into wounded skin and contribute to wound repair by transdifferentiation into multiple skin cell type, J. Immunol. 180 (2008) 2581–2587.

[19] V. Falanga, S. Iwamoto, M. Chartier, T. Yufit, J. Butmarc, N. Kouttab, D. Shrayer, P. Carson, Autologous bone marrow-derived cultured mesenchymal stem cells delivered in a fibrin spray accelerate healing in murine and human cutaneous wounds, Tissue Eng. 13 (2007) 1299–1312.

[20] J. Vojtassák, L. Danisovic, M. Kubes, D. Bakos, L. Jarábek, M. Ulicná, M. Blasko, Autologous biograft and mesenchymal stem cells in

treatment of the diabetic foot, Neuro Endocrinol. Lett. 27 (Suppl 2) (2006 Dec) 134–137.

[21] Y. Wu, L. Chen, P.G. Scott, E.E. Tredget, Mesenchymal stem cells enhance wound healing through differentiation and angiogenesis, Stem Cells 25 (2007) 2648–2659.

[22] T.M. Liu, M. Martina, D.W. Hutmacher, J.H. Hui, E.H. Lee, B. Lim, Identification of common pathways mediating differentiation of bone marrow- and adipose tissue-derived human mesenchymal stem cells into three mesenchymal lineages, Stem Cells 25 (2007) 750–760.

[23] D.J. Prockop, "Stemness" does not explain the repair of many tissues by mesenchymal stem/multipotent stromal cells (MSCs), Clin. Pharmacol. Ther. 82 (2007) 241–243.

[24] L. Chen, E.E. Tredget, P.Y.G. Wu, Y. Wu, Paracrine factors of mesenchymal stem cells recruit macrophages and endothelial lineage cells and enhance wound healing, PLoS ONE 3 (2008) e1886.

[25] W.S. Kim, B.S. Park, J.H. Sung, J.M. Yang, S.B. Park, S.J. Kwak, J.S. Park, Wound healing effect of adipose-derived stem cells: a critical role of secretory factors on human dermal fibroblasts, J. Dermatol. Sci. 48 (2007) 15–24.

[26] R. DeBiasio, G.R. Bright, L.A. Ernst, A.S. Waggoner, D.L. Taylor, Five-parameter fluorescence imaging: wound healing of living Swiss 3T3 cells, J. Cell Biol. 105 (1987) 1613–1622.

[27] M. Fronza, B. Heinzmann, M. Hamburger, S. Laufer, I. Merfort, Determination of wound healing effect of *Calendula* extracts using the scratch assay with 3T3 fibroblasts, J. Ethnopharmacol. 126 (2009) 463–467.

[28] W.R. Earle, E.L. Schilling, T.H. Stark, N.P. Straus, M.F. Brown, E. Sbelton, Production of malignancy in vitro. 4. The mouse fibroblast cultures and changes seen in the living cells, J. Nat. Cancer Inst. 4 (1943) 165–212.

[29] P. Boucamp, R.T. Petrussevska, D. Breitkreuz, J. Hornung, A. Markham, N.E. Fusenig, Normal keratinization in a spontaneously immortalized aneuploid human keratinocyte cell line, J. Cell Biol. 106 (1988) 761–771.

[30] K.T. Wright, W.E. Masri, A. Osman, S. Roberts, J. Trivedi, B.A. Ashton, W.E. Johnson, The cell culture expansion of bone marrow stromal cells from humans with spinal cord injury: implications for future cell transplantation therapy, Spinal Cord 46 (2008) 811–817.

[31] T.J. Collins, Image J for microscopy, Biotechniques 43 (Suppl.1) (2007) 25–30.

[32] A.H. Cory, T.C. Owen, J.A. Barltrop, J.G. Cory, Use of an aqueous soluble tetrazolium/formazan assay for cell growth assays in culture, Cancer Commun. 3 (1991) 207–212.

[33] K. Kehe, M. Abend, K. Kehe, R. Ridi, R.W. Peter, D. Beuningan, Tissue engineering with HaCaT cells and a fibroblast cell line, Arch. Dermatol. Res. 291 (1999) 600–605.

[34] B. Bandyopadhyay, J. Fan, S. Guan, Y. Li, M. Chen, D.T. Woodley, W. Li, A "traffic control" role for TGFbeta3: orchestrating dermal and epidermal cell motility during wound healing, J. Cell Biol. 172 (2006) 1093–1105.

[35] A.N. Smith, E. Willis, V.T. Chan, L.A. Muffley, F.F. Isik, N.S. Gibran, A.M. Hocking, Mesenchymal stem cells induce dermal fibroblast responses to injury, Exp. Cell Res. 316 (2010) 48–54.

[36] S. Barrientos, O. Stojadinovic, M.S. Golinko, H. Brem, M. Tomic-Canic, Growth factors and cytokines in wound healing, Wound Repair Regen. 16 (2008) 585–601.

[37] A.E. Postlethwaite, J. Keski-Oja, H.L. Moses, A.H. Kang, Stimulation of the chemotactic migration of human fibroblasts by transforming growth factor beta, J. Exp. Med. 165 (1987) 251–256.

[38] Y. Li, J. Fan, M. Chen, W. Li, D.T. Woodley, Transforming growth factor-alpha: a major human serum factor that promotes human keratinocyte migration, J. Invest. Dermatol. 126 (2006) 2096–2105.

[39] L.R. Luckett, R.M. Gallucci, Interleukin-6 (IL-6) modulates migration and matrix metalloproteinase function in dermal fibroblasts from IL-6KO mice, Br. J. Dermatol. 156 (2007) 1163–1171.

[40] R.M. Gallucci, D.K. Sloan, J.M. Heck, A.R. Murray, S.J. O'Dell, Interleukin 6 indirectly induces keratinocyte migration, J. Invest. Dermatol. 122 (2004) 764–772.

[41] M. Sato, D. Sawamura, T. Ina, T. Yaguchi, K. Hanada, I. Hashimoto, In vivo introduction of the interleukin 6 gene into human keratinocytes: induction of epidermal proliferation by the fully spliced form of interleukin 6, but not by the alternatively spliced form, Arch. Dermatol. Res. 291 (1999) 400–404.

[42] G. Michel, L. Kemeny, R.U. Peter, A. Beetz, C. Ried, P. Arenberger, T. Ruzicka, Interleukin-8 receptor-mediated chemotaxis of normal human epidermal cells, FEBS Lett. 305 (1992) 241–243.

[43] A. Tuschil, C. Lam, A. Haslberger, I. Lindley, Interleukin-8 stimulates calcium transients and promotes epidermal cell proliferation, J. Invest. Dermatol. 99 (1992) 294–298.

[44] L.A. Dipietro, M.G. Reintjes, Q.E. Low, B. Levi, R.L. Gamelli, Modulation of macrophage recruitment into wounds by monocyte chemoattractant protein-1, Wound Repair Regen. 9 (2001) 28–33.

[45] D.A. Lauffenburger, A.F. Horwitz, Cell migration: a physically integrated molecular process, Cell 84 (1996) 359–369.

[46] M.J. Reed, P. Puolakkainen, T.F. Lane, D. Dickerson, P. Bornstein, E.H. Sage, Differential expression of SPARC and thrombospondin 1 in wound repair: immunolocalization and in situ hybridization, J. Histochem. Cytochem. 41 (1993) 1467–1477.

[47] A. Basu, L.H. Kligman, S.J. Samulewicz, C.C. Howe, Impaired wound healing in mice deficient in a matricellular protein SPARC (osteonectin, BM-40), BMC Cell Biol. 2 (2001) 15.

[48] A.D. Bradshaw, M.J. Reed, E.H. Sage, SPARC-null mice exhibit accelerated cutaneous wound closure, J. Histochem. Cytochem. 50 (1) (2002) 1–10.

[49] S.R. Edmonson, S.P. Thumiger, G.A. Werther, C.J. Wraight, Epidermal homeostasis: the role of the growth hormone and insulin-like growth factor systems, Endocr. Rev. 24 (2003) 737–764.

[50] J. Nousbeck, O. Sarig, N. Avidan, M. Indelman, R. Bergman, M. Ramon, C.D. Enk, E. Sprecher, Insulin-like growth factor-binding protein 7 regulates keratinocyte proliferation, differentiation and apoptosis, J. Invest. Dermatol. 130 (2010) 378–387.

Appendix ii

MALDI-TOF/TOF Mass spectrometry of MSC-CM

MSC-1

Rank	Protein Name	Accession Number	Protein MW	Protein PI	Peptide Count	Total Ion Score	Total Ion Score C.I. %
1	alpha 2 type I collagen [Homo sapiens]	gi|48762934	129235.4	9.08	27	622.5189	100
2	Collagen, type I, alpha 1 [Homo sapiens]	gi|22328092	138925.6	5.7	16	431.0589	100
3	alpha 1 (I) chain propeptide	gi|180392	98494.94	6.47	11	247.0944	100
4	hypothetical protein [Homo sapiens]	gi|31873670	268733.5	5.36	18	235.1445	100
5	collagen, type VI, alpha 1 precursor [Homo sapiens]	gi|87196339	108462	5.26	10	158.2444	100
6	precursor polypeptide (AA -31 to 1139) [Homo sapiens]	gi|37465	129269.5	4.71	7	104.71	100
7	insulin-like growth factor binding protein 7 [Homo sapiens]	gi|4504619	29111.44	8.25	4	92.01	100
8	type V preprocollagen alpha 2 chain [Homo sapiens]	gi|16197600	128743.2	6.36	3	84.16	100
9	collagen, type XII, alpha 1 long isoform precursor [Homo sapiens]	gi|93141047	332940.5	5.38	6	80.47444	99.99992
10	actin, gamma 2 propeptide [Homo sapiens]	gi|4501889	41849.79	5.31	3	77.75	99.99985
11	fibronectin [Homo sapiens]	gi|4204943	41344.68	9.32	8	75.73443	99.99977
12	pro-alpha-1 collagen type 1 [Homo sapiens]	gi|179630	3768.75	4.66	3	75.41	99.99975
13	actin, gamma 1 propeptide [Homo sapiens]	gi|4501887	41765.79	5.31	3	72.69	99.99953
14	aldolase A [Homo sapiens]	gi|4557305	39395.3	8.3	3	40.92444	99.29309
15	Chain A, Crystal Structure Of Recombinant Human Triosephosphate Isomerase At 2.8 Angstroms Resoluti	gi|999892	26521.7	6.51	1	35.38	97.46599
16	fibronectin type III domain containing 1 [Homo sapiens]	gi|55667857	66828.44	6.55	2	34.4	96.82453
17	titin [Homo sapiens]	gi|1212992	2991589	6.35	10	34.26688	96.72569
18	Chain A, Bm-40, FsEC DOMAIN PAIR	gi|2624793	27054.1	5.53	3	34.12	96.61305
19	Chain A, The Crystal Structure Of Human Supernatant Protein Factor	gi|38492593	45895.12	7.92	3	33.11	95.72626
20	unnamed protein product [Homo sapiens]	gi|21750712	14218.59	10.58	1	32.1	94.60727
21	tumor necrosis factor	gi|339992	41974.87	4.9	2	31.3	93.51651
22	unnamed protein product [Homo sapiens]	gi|16552261	47458.89	5.01	4	30.69	92.5388
23	heparan sulfate proteoglycan perlecan [Homo sapiens]	gi|11602963	466304.2	6.03	4	29.96	91.17309
24	alpha2-HS glycoprotein [Homo sapiens]	gi|2521981	35640.84	5.2	1	29.4	89.95827
25	BIGH3 [Homo sapiens]	gi|2996636	56311.16	6.97	2	28.91	88.75891
26	vimentin [Homo sapiens]	gi|5030431	41537.03	4.82	4	28.17	86.67066
27	HCNP [Homo sapiens]	gi|9295341	98809.95	8.16	2	27.65444	84.99056
28	hypothetical protein [Homo sapiens]	gi|31874769	35774.97	8.51	3	27.53444	84.57006

29	KIAA0434 [Homo sapiens]	gi|2662149	170583.5	8.48	3	27.5	84.4472
30	unnamed protein product [Homo sapiens]	gi|30076	100613.6	9.1	3	26.66	81.12841
31	thrombospondin 2 precursor [Homo sapiens]	gi|40317628	129907.8	4.62	5	26.23	79.16428
32	KIAA0959 protein [Homo sapiens]	gi|4589562	91698.93	6.26	1	25.28	74.06965
33	Nebulin	gi|19856971	772727.3	9.1	4	25.09444	72.93772
34	asparaginyl-tRNA synthetase [Homo sapiens]	gi|4758762	62902.61	5.9	1	24.85	71.37085
35	SPECC1 protein [Homo sapiens]	gi|29477171	79033.8	5.31	1	24.16	66.44104
36	Dombrock blood group carrier molecule [Homo sapiens]	gi|20385823	35883.5	9.24	3	24.06	65.65936
37	E3 ligase for inhibin receptor [Homo sapiens]	gi|30060232	289429.5	5.29	2	24.04	65.50085
38	alpha-1 (III) collagen [Homo sapiens]	gi|930045	96442.1	9.28	4	23.99	65.10135
39	FLJ00343 protein [Homo sapiens]	gi|21748542	281254.3	5.77	6	23.24	58.52289
40	Latent-transforming growth factor beta-binding protein 2 precursor (LTBP-2)	gi|41017299	194936	5.08	2	22.69	52.92304
41	zinc finger CCCH-type containing 12B [Homo sapiens]	gi|57471635	77506.44	8.66	1	22.41	49.78789
42	unnamed protein product [Homo sapiens]	gi|34535472	87569.53	6.82	2	21.86	43.00872
43	T-cell antigen receptor chain (VJC) [Mus musculus]	gi|296757	34266.33	8.31	1	21.78	41.94918
44	Na,K-ATPase alpha-4 subunit [Homo sapiens]	gi|17148771	8127.467	10.1	1	21.72	41.14159
45	CCNL1 [Homo sapiens]	gi|37182448	34668.16	11.43	1	21.65	40.18522
46	RU1 [Homo sapiens]	gi|6635353	98167.24	5.86	2	21.55	38.79198
47	TAGLN [Homo sapiens]	gi|49168456	22536.4	8.87	2	21.54	38.65088
48	immunoglobulin kappa chain [Homo sapiens]	gi|11137043	9962.874	6.48	2	20.97	30.04668
49	type II hair keratin 3 [Homo sapiens]	gi|7161767	54160.51	5.54	2	20.97	30.04665
50	hypothetical protein [Homo sapiens]	gi|21740227	55327.56	9.69	1	20.92444	29.30895
51	INT4 protein [Homo sapiens]	gi|14124974	88834.93	5.69	1	20.8	27.2541
52	kinesin family member 5B [Homo sapiens]	gi|4758648	109616.8	6.12	1	20.64	24.52406
53	lipocalin 9 [Homo sapiens]	gi|48717447	20272.04	5.72	1	20.64	24.52406
54	monocyte/macrophage serine-esterase 1 [Homo sapiens]	gi|1335304	55567.32	5.66	1	20.55	22.94363
55	Olfactory receptor 1N2	gi|38372758	35160.13	7.98	1	20.34	19.12609
56	RUN and SH3 domain containing 2 [Homo sapiens]	gi|55741719	161094.5	6.17	2	20.21	16.66862
57	kinase suppressor of ras 2 [Homo sapiens]	gi|34222393	93525.83	9.18	1	20.15	15.50938
58	EGF-like-domain, multiple 7 [Homo sapiens]	gi|15214507	29612.41	8.58	1	20.01444	12.83053
59	vinculin isoform meta-VCL [Homo sapiens]	gi|7669550	123721.8	5.5	2	19.95	11.52748
60	ZNF557 protein [Homo sapiens]	gi|12804323	42925.05	9.12	1	19.82	8.839124
61	p21 (CDKN1A)-activated kinase 3 [Pan troglodytes]	gi|57113963	62270.5	5.33	1	19.66	5.418004
62	Sam68-like phosphotyrosine protein beta [Homo sapiens]	gi|4091776	29340.57	9.59	2	19.53	2.544

| 63 | steerin2 protein [Homo sapiens] | gi|27526777 | 267948.1 | 9.15 | 6 | 19.12 | 0 |
| 64 | fusion protein [Homo sapiens] | gi|408993 | 11748.92 | 7.88 | 1 | 19 | 0 |

MSC-2

Rank	Protein Name	Accession Number	Protein PI	Peptide Count	Total Ion Score	Total Ion Score C.I. %
1	alpha 2 type I collagen precursor [Homo sapiens]	gi|48762934	9.08	31	1014.354	100
2	Collagen, type I, alpha 1 [Homo sapiens]	gi|22328092	5.7	12	296.8544	100
3	collagen, type VI, alpha 1 precursor [Homo sapiens]	gi|87196339	5.26	6	177.68	100
4	Transferrin [Homo sapiens]	gi|37747855	6.97	4	170.73	100
5	cartilage oligomeric matrix protein precursor [Homo sapiens]	gi|40217843	4.36	6	166.36	100
6	fibronectin precursor [Homo sapiens]	gi|31397	5.45	7	128.48	100
7	alpha 1 (I) chain propeptide [Homo sapiens]	gi|180392	6.47	7	127.82	100
8	hemopexin precursor [Homo sapiens]	gi|386789	6.57	5	104.61	100
9	Chain D, Human Insulin Hexamers With Chain B His Mutated To Tyr Complexed With Phenol	gi|5542375	5.41	3	87.31	100
10	tumor necrosis factor	gi|339992	4.9	3	83.9	99.99990815
11	actin, gamma 1 propeptide [Homo sapiens]	gi|4501887	5.31	3	81.66	99.99984616
12	albumin, isoform CRA_k [Homo sapiens]	gi|119626074	5.97	3	60.07	99.97781459
13	Chain B, Structural Properties Of The B25tyr-Nme-B26phe Insulin Mutant.	gi|61680182	6.9	2	56.38	99.9481119
14	Chain B, Nmr Structure Of Human Insulin Mutant His-B10-Asp, Val-B12- Aba, Pro-B28-Lys, Lys-B29-Pro,	gi|159163040	5.44	2	52.33	99.86815389
15	complement component 1, s subcomponent precursor [Homo sapiens]	gi|4502495	4.86	2	50.28	99.78861819
16	lumican	gi|642534	6.16	2	43.24	98.93077937
17	anti-colorectal carcinoma heavy chain [Homo sapiens]	gi|425518	6.22	1	42.94	98.85430864
18	immunoglobulin heavy chain constant region gamma 4 [Homo sapiens]	gi|12054078	7.16	1	39.22	97.301842

19	Chain B, Solution Structure Of The Monomeric [thr(B27)->pro,Pro(B28)- >thr] Insulin Mutant (Pt Insulin)	gi|159162548	6.9	2	39.15	97.25800066
20	EGF-containing fibulin-like extracellular matrix protein 1 precursor [Homo sapiens]	gi|9665262	4.95	1	31.23	83.01492202
21	putative [Homo sapiens]	gi|553734	9.79	1	30.24	78.66623425
22	prominin 1 isoform 2 [Homo sapiens]	gi|224994189	6.97	1	30.17	78.31958996
23	actin, beta-like 2 [Homo sapiens]	gi|63055057	5.39	3	26.53	49.87347235
24	tRNA isopentenylpyrophosphate transferase isoform 5 [Homo sapiens]	gi|58041802	8.93	1	26.41	48.46912528
25	PREDICTED: similar to microtubule-associated proteins 1A/1B light chain 3 [Homo sapiens]	gi|169183885	10.52	1	24.6	21.82507718
26	macrophin 1 isoform 4 [Homo sapiens]	gi|17426161	5.05	1	24.4	18.1407922
27	keratin 1 [Homo sapiens]	gi|7331218	8.16	1	22.96	0
28	KIAA0184 [Homo sapiens]	gi|1136428	6.99	1	22.54	0
29	biglycan [Homo sapiens]	gi|179433	6.83	1	22.5	0
30	unnamed protein product [Homo sapiens]	gi|21752990	8.35	1	22.47	0
31	HECT domain containing 3 [Homo sapiens]	gi|118835514	5.47	1	21.25 444	0
32	La ribonucleoprotein domain family member 2 isoform 1 [Homo sapiens]	gi|30061567	7.33	2	22.01	0
33	inter-alpha (globulin) inhibitor H4 isoform 1 precursor [Homo sapiens]	gi|31542984	6.51	1	21.61	0
34	hypothetical protein [Homo sapiens]	gi|21739834	5.64	1	21.29	0
35	insulin-like growth factor binding protein 6 [Homo sapiens]	gi|183894	8.15	1	21.19	0
36	heparan sulfate proteoglycan [Homo sapiens]	gi|184427	6.05	1	19.94	0
37	unnamed protein product [Homo sapiens]	gi|194388696	11.79	1	19.72	0
38	ATF6 [Homo sapiens]	gi|3953531	8.36	1	19.72	0
39	nucleobindin 1 variant [Homo sapiens]	gi|62897169	5.15	2	18.83	0
40	unnamed protein product [Homo sapiens]	gi|158256468	5.89	1	18.75	0
41	transcription factor ELYS [Homo sapiens]	gi|17298096	6.19	1	18.6	0
42	hypothetical protein [Homo sapiens]	gi|7018446	8.24	1	18.58	0
43	NIPSNAP2 protein [Homo sapiens]	gi|2769254	9.42	1	18.56	0
44	fms-related tyrosine kinase 4 isoform 2 precursor [Homo sapiens]	gi|103472027	5.89	1	18.53	0
45	nesprin-1 beta [Homo sapiens]	gi|17861386	5.13	2	18.50 444	0

46	unnamed protein product [Homo sapiens]	gi|21748720	6.68	1	18.41	0
47	Chain A, Crystal Structure Of Human Dna Ligase I Bound To 5'- Adenylated, Nicked Dna	gi|56967028	5.79	1	18.13	0
48	alpha-1 (III) collagen [Homo sapiens]	gi|930045	9.28	1	17.9	0
49	hypothetical protein, similar to (U32865) linotte protein [Drosophila melanogaster] [Homo sapiens]	gi|5102582	6.8	1	17.89	0
50	KIAA1973 protein [Homo sapiens]	gi|18916849	8.57	1	17.38	0

MSC-3

Rank	Protein Name	Accession Number	Protein PI	Peptide Count	Total Ion Score	Total Ion Score C.I. %
1	fibronectin precursor [Homo sapiens]	gi|31397	5.45	24	464.9989	100
2	RecName: Full=Collagen alpha-2(I) chain; AltName: Full=Alpha-2 type I collagen; Flags: Precursor	gi|124056488	9.08	18	328.4245	100
3	Chain A, Apo-Human Serum Transferrin (Non-Glycosylated)	gi|110590597	6.58	11	238.5689	100
4	Transferrin [Homo sapiens]	gi|37747855	6.97	11	230.89	100
5	hemopexin precursor [Homo sapiens]	gi|386789	6.57	9	210.81	100
6	keratin 1 [Homo sapiens]	gi|119395750	8.15	5	127.1689	100
7	Collagen, type I, alpha 1 [Homo sapiens]	gi|22328092	5.7	8	119.5844	100
8	Chain D, Human Insulin Hexamers With Chain B His Mutated To Tyr Complexed With Phenol	gi|5542375	5.41	2	79.27	99.99974
9	anti-colorectal carcinoma heavy chain [Homo sapiens]	gi|425518	6.22	2	75.7	99.9994
10	Chain B, Structural Properties Of The B25tyr-Nme-B26phe Insulin Mutant.	gi|61680182	6.9	2	51.32	99.83606
11	collagen, type VI, alpha 1 precursor [Homo sapiens]	gi|87196339	5.26	4	47.42	99.59758
12	Chain B, Solution Structure Of The Monomeric [thr(B27)->pro,Pro(B28)- >thr] Insulin Mutant (Pt Insulin)	gi|159162548	6.9	2	46.6	99.51395

13	lumican	gi|642534	6.16	2	39.01	97.20953
14	Chain B, Nmr Structure Of Human Insulin Mutant Ile-A2-Ala, His-B10- Asp, Pro-B28-Lys, Lys-B29-Pro, 15 Structures	gi|159162579	5.44	1	36.43	94.94552
15	Chain A, Structure Of A Novel Extracellular Ca2+-Binding Module In Bm-40(Slash)sparc(Slash)osteonec	gi|157833849	5.01	2	34.25	91.65019
16	albumin preproprotein [Homo sapiens]	gi|4502027	5.92	3	33.53	90.14454
17	Chain B, Orientation In Solution Of Mmp-3 Catalytic Domain And N- Timp-1 From Residual Dipolar Coup	gi|34811011	8.27	1	32.71	88.09644
18	KIAA0184 [Homo sapiens]	gi|1136428	6.99	1	30.79	81.47848
19	unnamed protein product [Homo sapiens]	gi|158255712	5.39	1	29.91	77.31824
20	tumor necrosis factor	gi|339992	4.9	1	29.51	75.12995
21	unnamed protein product [Homo sapiens]	gi|194388696	11.79	1	27.21	57.76458
22	ATF6 [Homo sapiens]	gi|3953531	8.36	1	27.21	57.76458
23	ankyrin repeat and SOCS box-containing protein 1 [Homo sapiens]	gi|94721248	8.55	1	27	55.67214
24	alpha2-HS glycoprotein [Homo sapiens]	gi|2521981	5.2	2	26.74	52.93731
25	biglycan [Homo sapiens]	gi|179433	6.83	2	26.65	51.95184
26	NOL1/NOP2/Sun domain family, member 4 [Homo sapiens]	gi|15680185	8.47	2	24.97 444	29.33038
27	insulin-like growth factor binding protein 7 [Homo sapiens]	gi|4504619	8.25	3	24.97	29.25809
28	putative [Homo sapiens]	gi|553734	9.79	1	24.75	25.58222
29	Ig gamma 2 H chain, BUR [human, Peptide Mutant, 348 aa]	gi|243169	6.22	1	24.41	19.52208
30	actin, gamma 1 propeptide [Homo sapiens]	gi|4501887	5.31	2	24.36	18.59021
31	hypothetical protein [Homo sapiens]	gi|7018446	8.24	1	23.35	0
32	chitinase 3-like 1 precursor [Homo sapiens]	gi|144226251	8.69	2	23.32	0
33	retinoic acid induced 16 [Homo sapiens]	gi|89337270	5.27	3	23.32	0
34	HECT domain containing 3 [Homo sapiens]	gi|118835514	5.47	1	21.40 444	0
35	enyol-CoA: hydratase/3-hydroxyacyl-CoA dehydrogenase [Homo sapiens]	gi|452045	9.22	1	22.12	0
36	nebulin isoform 3 [Homo sapiens]	gi|115527120	9.11	3	21.50 566	0
37	KIAA0368 protein [Homo sapiens]	gi|122937211	8.95	2	20.56	0
38	La ribonucleoprotein domain family, member 6 isoform 1 [Homo sapiens]	gi|37537710	8.39	1	20.13	0
39	malate dehydrogenase 1, NAD (soluble), isoform CRA_d	gi|119620368	7.62	1	19.86	0

	[Homo sapiens]					
40	kinesin family member 27 [Homo sapiens]	gi|30794488	6.9	2	19.00 444	0
41	Chain A, Gelatinase A (Full-Length)	gi|5822007	5.2	2	18.97	0
42	plasminogen activator inhibitor type 1, member 2 isoform b precursor [Homo sapiens]	gi|211904152	9.42	2	18.88	0
43	CALU [Homo sapiens]	gi|49456627	4.48	2	18.83	0
44	prominin 1 isoform 2 [Homo sapiens]	gi|224994189	6.97	1	18.7	0
45	insulin-like growth factor-binding protein [Homo sapiens]	gi|183116	9.03	1	18.48	0
46	fms-related tyrosine kinase 4 isoform 2 precursor [Homo sapiens]	gi|103472027	5.89	1	17.92	0
47	hypothetical protein, similar to (U32865) linotte protein [Drosophila melanogaster] [Homo sapiens]	gi|5102582	6.8	1	17.9	0
48	inter-alpha (globulin) inhibitor H4 isoform 1 precursor [Homo sapiens]	gi|31542984	6.51	2	17.61	0
49	apoptotic cysteine protease proMch4	gi|1498324	5.97	1	17.5	0
50	hCG1648444 [Homo sapiens]	gi|119602744	6.8	1	17.49	0
51	KiSS-1 metastasis-suppressor, isoform CRA_a [Homo sapiens]	gi|119611912	9.82	1	17.23	0
52	unnamed protein product [Homo sapiens]	gi|194385514	6.44	1	17.12	0
53	Hsp70 subfamily B suppressor 1-like protein isoform 3 [Homo sapiens]	gi|223633995	5.63	1	17.06	0
54	RecName: Full=Mucin-19; Short=MUC-19; Flags: Precursor	gi|193806311	4.95	2	17.04	0
55	NY-REN-62 antigen [Homo sapiens]	gi|5360129	7.79	1	16.13	0
56	cyclic nucleotide-gated cation channel [Homo sapiens]	gi|4261908	8.58	1	15.85	0
57	hCG1784572 [Homo sapiens]	gi|119583243	6.13	1	15.84	0
58	unnamed protein product [Homo sapiens]	gi|34531210	9.18	1	15.83	0
59	mitogen-activated protein kinase 8 isoform JNK1 alpha2 [Homo sapiens]	gi|20986523	6.43	2	15.73	0
60	tubby like protein 4 isoform 2 [Homo sapiens]	gi|55953102	6.02	1	15.4	0
61	PREDICTED: transmembrane protein 46-like [Homo sapiens]	gi|169215850	11.24	2	15.16	0
62	cytochrome P450, family 4, subfamily F, polypeptide 22 [Homo sapiens]	gi|158138530	8.95	1	14.94	0
63	hypothetical protein [Homo sapiens]	gi|21739834	5.64	1	14.69	0
64	uridine-cytidine kinase 1-like 1 [Homo sapiens]	gi|57863312	6.93	1	14.65	0
65	immunoglobulin variable region VL kappa domain [Homo	gi|51103549	5.69	1	14.64	0

	sapiens]					
66	hCG2028661 [Homo sapiens]	gi|119601280	11.79	1	14.54	0
67	plasma membrane Ca2+ pumping ATPase [Homo sapiens]	gi|190133	5.69	1	14.5	0
68	unnamed protein product [Homo sapiens]	gi|158258353	6.96	1	14.5	0
69	hCG1814189 [Homo sapiens]	gi|119602137	5.76	1	14.48	0
70	protein kinase LYK5, isoform CRA_f [Homo sapiens]	gi|119614694	7.05	1	14.46	0
71	beta-mannosidase [Homo sapiens]	gi|2145100	5.32	1	14.41	0
72	thyroid hormone receptor interactor 10, isoform CRA_a [Homo sapiens]	gi|119589466	5.84	1	14.4	0
73	5'-nucleotidase domain containing 3, isoform CRA_c [Homo sapiens]	gi|119618123	8.46	1	14.37	0
74	PREDICTED: similar to tropomyosin 3, gamma isoform 5 [Pan troglodytes]	gi|114559859	4.72	2	14.33	0
75	keratin associated protein 19-3 [Homo sapiens]	gi|119630302	11.92	1	14.32	0
76	Chain A, Crystal Structure Of The Ubc Domain Of Baculoviral Iap Repeat-Containing Protein 6	gi|171849089	6.8	1	14.12	0
77	retinoblastoma-binding protein 6 isoform 1 [Homo sapiens]	gi|33620769	9.65	1	13.95	0
78	astrotactin 2 isoform b [Homo sapiens]	gi|46488917	5.63	1	13.85	0
79	hypothetical protein [Homo sapiens]	gi|193227749	9.57	1	13.85	0
80	immunoglobulin heavy chain variable region [Homo sapiens]	gi|13487739	9.38	1	13.74	0
81	vacuolar protein sorting 13B (yeast), isoform CRA_b [Homo sapiens]	gi|119612193	6.23	2	13.7	0
82	BIGH3 [Homo sapiens]	gi|3282161	8.91	1	13.7	0
83	unnamed protein product [Homo sapiens]	gi|158254782	6.34	1	13.68	0
84	KIAA0863 protein [Homo sapiens]	gi|40788964	9.44	1	13.66	0
85	Chain B, Crystal Structure Of Protein Phosphatase 2a (Pp2a) Holoenzyme With The Catalytic Subunit Carboxyl Terminus Truncated	gi|122921195	6.27	2	13.62	0
86	regulatory factor X domain containing 2 [Homo sapiens]	gi|148613886	6.14	1	13.59	0
87	unnamed protein product [Homo sapiens]	gi|158256468	5.89	1	13.57	0
88	prickle homolog 1 [Homo sapiens]	gi|222136678	5.84	1	13.47	0
89	R29893_1 [Homo sapiens]	gi|2887499	9.95	1	13.4	0
90	RNA binding motif protein 6 [Homo sapiens]	gi|5032033	5.93	1	13.27	0
91	tRNA aspartic acid methyltransferase 1 variant 5 [Homo sapiens]	gi|167887558	9.3	1	13.19	0
92	unnamed protein product [Homo sapiens]	gi|21758244	9.6	1	13.15	0

93	tropomyosin (227 AA) [Homo sapiens]	gi|825723	4.77	1	13.08	0
94	rcTPM3 [Homo sapiens]	gi|83674986	4.77	1	13.08	0
95	beta chain HLA-DQ molecule [Homo sapiens]	gi|2654381	7.98	1	13.02	0
96	RNF3A-2 [Homo sapiens]	gi|33150610	8.77	1	12.75	0
97	tetratricopeptide repeat domain 4 [Homo sapiens]	gi|56204887	7.95	1	12.7	0
98	keratin 8 [Homo sapiens]	gi|4504919	5.52	2	12.69	0
99	unnamed protein product [Homo sapiens]	gi|21752990	8.35	1	12.57	0
100	immunoglobulin heavy chain variable region [Homo sapiens]	gi|70798061	9.26	1	12.55	0

MSC-4

Rank	Protein Name	Accession Number	Protein PI	Peptide Count	Total Ion Score	Total Ion Score C.I. %
1	alpha 2 type I collagen precursor [Homo sapiens]	gi|48762934	9.08	37	1523.264	100
2	Collagen, type I, alpha 1 [Homo sapiens]	gi|22328092	5.7	27	952.089	100
3	fibronectin precursor [Homo sapiens]	gi|31397	5.45	20	612.2056	100
4	alpha 1 (I) chain propeptide [Homo sapiens]	gi|180392	6.47	21	550.1378	100
5	hypothetical protein [Homo sapiens]	gi|51476364	5.77	18	496.0657	100
6	collagen, type VI, alpha 1 precursor [Homo sapiens]	gi|87196339	5.26	8	220.09	100
7	Transferrin [Homo sapiens]	gi|37747855	6.97	5	203.5	100
8	Chain A, Apo-Human Serum Transferrin (Non-Glycosylated)	gi|110590597	6.58	5	202.3244	100
9	cartilage oligomeric matrix protein precursor [Homo sapiens]	gi|40217843	4.36	4	178.18	100
10	hemopexin precursor [Homo sapiens]	gi|386789	6.57	6	168.28	100
11	keratin 1 [Homo sapiens]	gi|7331218	8.16	3	164.5044	100
12	collagen, type II, alpha 1 (primary osteoarthritis, spondyloepiphyseal dysplasia, congenital), isof	gi|119578373	8.49	5	104.08	100
13	plasminogen activator inhibitor type 1, member 2 isoform b precursor [Homo sapiens]	gi|211904152	9.42	2	101.2	100
14	transferrin	gi|553788	6	4	97.67	100
15	actin, gamma 1 propeptide [Homo sapiens]	gi|4501887	5.31	2	97.66	100
16	alpha-1 (III) collagen [Homo sapiens]	gi|930045	9.28	2	90.28444	100
17	cathepsin B preproprotein [Homo sapiens]	gi|4503139	5.88	2	83.06	99.99988
18	Chain D, Human Insulin Hexamers With Chain B His Mutated	gi|5542375	5.41	2	80.44	99.99979

	To Tyr Complexed With Phenol					
19	Chain A, Gelatinase A (Full-Length)	gi|5822007	5.2	2	78.98	99.9997
20	decorin [Homo sapiens]	gi|181519	8.77	2	77.09 444	99.99954
21	unnamed protein product [Homo sapiens]	gi|158255712	5.39	2	76.91	99.99952
22	unnamed protein product [Homo sapiens]	gi|189054552	5.92	3	74.51	99.99917
23	tumor necrosis factor	gi|339992	4.9	3	63.86	99.99034
24	actin, beta-like 2 [Homo sapiens]	gi|63055057	5.39	2	62.96	99.98811
25	heparan sulfate proteoglycan [Homo sapiens]	gi|184427	6.05	2	60.56	99.97934
26	fibrillin	gi|306746	4.81	1	59.89	99.97589
27	lumican	gi|642534	6.16	2	57.45	99.95772
28	inter-alpha (globulin) inhibitor H4 isoform 1 precursor [Homo sapiens]	gi|31542984	6.51	1	55.35	99.93143
29	Chain B, Structural Properties Of The B25tyr-Nme-B26phe Insulin Mutant.	gi|61680182	6.9	2	55.08	99.92703
30	Keratin 77 [Homo sapiens]	gi|113414871	5.63	2	54.06 444	99.90781
31	insulin-like growth factor binding protein 6 [Homo sapiens]	gi|183894	8.15	1	50.85	99.80674
32	hypothetical protein [Homo sapiens]	gi|57997569	5.89	2	49.91	99.76004
33	pro-alpha-1 collagen type 1 [Homo sapiens]	gi|179631	5.15	3	48.75	99.68658
34	Chain B, Solution Structure Of The Monomeric [thr(B27)->pro,Pro(B28)- >thr] Insulin Mutant (Pt Insulin)	gi|159162548	6.9	2	45.58	99.34967
35	actin, gamma 2 propeptide [Homo sapiens]	gi|4501889	5.31	2	41.92	98.48946
36	unnamed protein product [Homo sapiens]	gi|16552261	5.01	2	41.92	98.48946
37	collagen, type XII, alpha 1 long isoform precursor [Homo sapiens]	gi|93141047	5.38	1	41.24	98.23342
38	Chain A, Structure Of A Novel Extracellular Ca2+-Binding Module In Bm-40(Slash)sparc(Slash)osteonec	gi|157833849	5.01	3	40.64	97.9717
39	Chain B, Nmr Structure Of Human Insulin Mutant Ile-A2-Ala, His-B10- Asp, Pro-B28-Lys, Lys-B29-Pro, 15 Structures	gi|159162579	5.44	1	34.24	91.14614
40	anti-colorectal carcinoma heavy chain [Homo sapiens]	gi|425518	6.22	1	33.32	89.05708
41	hypothetical protein [Homo sapiens]	gi|60219224	8.43	2	31.13	81.88106
42	CALU [Homo sapiens]	gi|49456627	4.48	2	30.5	79.05246
43	KIF27B [Homo sapiens]	gi|30025501	6.39	2	28.05 888	63.25104
44	keratin 10 [Homo sapiens]	gi|623409	5.01	1	27.65	59.62309

45	unnamed protein product [Homo sapiens]	gi|194388696	11.79	1	27.35	56.73537
46	ATF6 [Homo sapiens]	gi|3953531	8.36	1	27.35	56.73537
47	complement component 1, s subcomponent precursor [Homo sapiens]	gi|4502495	4.86	1	26.02	41.23308
48	EGF-containing fibulin-like extracellular matrix protein 1 precursor [Homo sapiens]	gi|9665262	4.95	1	25.79	38.03693
49	insulin-like growth factor binding protein 7 [Homo sapiens]	gi|4504619	8.25	3	25.29	30.47629
50	cadherin-like 23 [Homo sapiens]	gi|55958988	4.5	2	25.26	29.99437
51	Chain A, Crystal Structure Of Staurosporine Bound To Map Kap Kinase 2	gi|38492554	8.87	2	25.25	29.83298
52	ABT1-associated protein [Homo sapiens]	gi|18093112	5.01	1	25.21 678	29.29423
53	hypothetical protein [Homo sapiens]	gi|12052734	5.68	1	25.12	27.70089
54	immunoglobulin superfamily containing leucine-rich repeat variant [Homo sapiens]	gi|62898095	5	1	24.98	25.33225
55	fms-related tyrosine kinase 4 isoform 2 precursor [Homo sapiens]	gi|103472027	5.89	1	24.56	17.75054
56	putative [Homo sapiens]	gi|553734	9.79	1	24.46	15.8347
57	RecName: Full=Protein FAM90A1	gi|158564039	9.66	3	24.31 444	12.96598
58	RecName: Full=Mucin-19; Short=MUC-19; Flags: Precursor	gi|193806311	4.95	1	23.36	0
59	KIAA0611 protein [Homo sapiens]	gi|3327036	8.36	2	23.01	0
60	trypsin inhibitor [Homo sapiens]	gi|33985	6.58	2	22.72	0
61	hypothetical protein [Homo sapiens]	gi|21739834	5.64	1	22.51	0
62	hypothetical protein LOC340533 [Homo sapiens]	gi|56711286	6.03	1	22.26	0
63	prominin 1 isoform 2 [Homo sapiens]	gi|224994189	6.97	1	22.01	0
64	Chain O, Crystal Structure Of Anthrax Edema Factor (Ef) In Complex With Calmodulin In The Presence Of 10 Millimolar Exogenously Added Calcium Chloride	gi|66360499	4.05	1	21.38	0
65	Chain B, Orientation In Solution Of Mmp-3 Catalytic Domain And N- Timp-1 From Residual Dipolar Coup	gi|34811011	8.27	1	21.07	0
66	hCG33036, isoform CRA_b [Homo sapiens]	gi|119627063	6.07	2	19.9	0
67	dystonin isoform 1 [Homo sapiens]	gi|34577047	5.52	3	19.85 444	0
68	hypothetical protein [Homo sapiens]	gi|7018446	8.24	1	19.7	0
69	PRR7 protein [Homo sapiens]	gi|18203805	8.91	1	19.61	0
70	R29893_1 [Homo sapiens]	gi|2887499	9.95	1	19.51	0

71	KIAA0184 [Homo sapiens]	gi|1136428	6.99	1	19.29	0
72	tRNA aspartic acid methyltransferase 1 variant 5 [Homo sapiens]	gi|167887558	9.3	1	19.25	0
73	alpha2-HS glycoprotein [Homo sapiens]	gi|2521981	5.2	1	19.25	0
74	nebulin [Homo sapiens]	gi|806562	9.1	1	18.07 444	0
75	testis-specific bromodomain protein [Homo sapiens]	gi|46399198	9.05	1	19.14	0
76	immunoglobulin heavy chain variable region [Homo sapiens]	gi|70798061	9.26	1	18.84	0
77	hypothetical protein - human	gi|2135416	8.69	2	18.78	0
78	NUCB1 protein [Homo sapiens]	gi|16041802	5.05	1	18.65	0
79	microtubule-associated protein 2 4R isoform; 4R-MAP2 [Homo sapiens]	gi|913854	10.17	1	18.45	0
80	cadherin 15 preproprotein [Homo sapiens]	gi|4826669	4.81	1	18.37	0
81	hCG27399, isoform CRA_c [Homo sapiens]	gi|119607856	6.46	2	18.35	0
82	unnamed protein product [Homo sapiens]	gi|158256468	5.89	1	18.16	0
83	sialic acid-binding Ig-like lectin 10 [Homo sapiens]	gi|15217166	9.16	1	18.1	0
84	tetratricopeptide repeat domain 4 [Homo sapiens]	gi|56204887	7.95	1	17.86	0
85	unnamed protein product [Homo sapiens]	gi|21751193	6.21	1	17.85	0
86	IGFBP5 [Homo sapiens]	gi|48145735	8.58	2	17.77	0
87	solute carrier organic anion transporter family, member 5A1 isoform 2 [Homo sapiens]	gi|225637477	8.5	1	17.77	0
88	c-myc intron-binding protein 1 [Homo sapiens]	gi|77997595	6.45	1	17.62	0
89	hCG1814189 [Homo sapiens]	gi|119602137	5.76	1	17.62	0
90	hypothetical protein FLJ20294, isoform CRA_f [Homo sapiens]	gi|119588408	6.66	2	17.56	0
91	unnamed protein product [Homo sapiens]	gi|35883	7.44	1	17.56	0
92	unnamed protein product [Homo sapiens]	gi|194385514	6.44	2	17.52	0
93	Chain B, Human Complement Component C3	gi|78101268	5.55	1	17.47	0
94	NOL1/NOP2/Sun domain family, member 4 [Homo sapiens]	gi|15680185	8.47	1	17.39	0
95	KiSS-1 metastasis-suppressor, isoform CRA_a [Homo sapiens]	gi|119611912	9.82	1	17.26	0
96	calcium-activated chloride channel protein 2 [Homo sapiens]	gi|5726289	5.31	1	17.07	0
97	unnamed protein product [Homo sapiens]	gi|14042878	4.78	2	16.7	0
98	ankyrin repeat and SOCS box-containing protein 1 [Homo sapiens]	gi|94721248	8.55	1	16.34	0
99	RecName: Full=Stromal interaction molecule 2; Flags:	gi|17369338	6.3	1	16.27	0

	Precursor					
100	C2 [Homo sapiens]	gi|15277207	6.44	1	16.02	0